Limestone DISTRICT SCHOOL BOARD

We're Putting Wellness First | We're Turning Innovation into Action | We're Committed to Collaboration

AGENDA – EDUCATION, POLICY AND OPERATIONS COMMITTEE

Wednesday, December 7, 2022
Limestone Education Centre
220 Portsmouth Avenue, Kingston, ON
Link: **https://bit.ly/LDSBEPOCDec7**

Public Meeting – 5:30 PM

Acknowledgement of Territory: "The Limestone District School Board is situated on the traditional territories of the Anishinaabe and Haudenosaunee. We acknowledge their enduring presence on this land, as well as the presence of Métis, Inuit, and other First Nations from across Turtle Island. We honour their cultures and celebrate their commitment to this land."

1. CALL TO ORDER

2. ADOPTION OF AGENDA

3. DECLARATION OF CONFLICT OF INTEREST

4. DELEGATION/PRESENTATION
- 4.1 **COVID, Influenza and Masks –** Dr. Dick Zoutman, MD, FRCPC, CCPE, C. Dir (Pages 2-147)

5. PRIVATE SESSION REPORT – Special Meeting of the Board, December 2, 2022.

6. REPORTS FOR INFORMATION
- 6.1 **School Visit Presentation -** Indigenous Student Trustee Kolosov
- 6.2 **School Climate Survey** – Associate Superintendent Gollogly (Pages 148-150)
- 6.3 **2021-2022 EQAO Results** –Superintendent Hedderson and Associate Superintendent Sartor (Pages 151-154)
- 6.4 **Director's Annual Report –** Director Burra (Pages 155-156)

7. REPORTS FOR ACTION

8. UNFINISHED BUSINESS - None at this time.

9. NEW BUSINESS - None at this time.

10. CORRESPONDENCE - None at this time.

11. NEXT MEETING – February 8, 2023

12. ADJOURNMENT

Dick Zoutman, MD, FRCPC, CCPE, C. Dir

November 30, 2022

Mr. Krishna Burra, Director
Mr. Bob Godkin, Vice Chair
Limestone District School Board
220 Portsmouth Avenue
Kington, Ontario
K7M 0G2

Via email to: mittons@limestone.on.ca

Dear Messrs. Burra and Godkin,

I am writing to request the opportunity to make a presentation to the Education, Policy, and Operations Committee of the Limestone District School Board (LDSB) at your meeting scheduled for December 7, 2022.

My purpose in meeting with you is to bring to the attention of the LDSB Trustees important new information that I feel would impact your decision making concerning the need for a Board wide policy on the wearing of masks for the prevention of COVID-19 caused by the SARS-CoV-2 virus, as well as the current severe wave of influenza.

I am appending to this letter the reference materials that you should refer to as you consider this important matter.

The points I wish to make and my reasons are as follows:

1. We are in the midst of a long drawn out crisis in health care in Ontario and locally in the Kingston region.

a. The recent wave of Respiratory Syncytial Virus (RSV) infections as well as influenza and the persistently high levels of COVID-19 throughout Ontario and the Kingston region have led to extraordinary numbers of children requiring hospital care. The volume of children in hospital emergency departments and in patient units are so high that most other health care services for children have been put on hold. Health care leaders across the province have correctly indicated that this is a crisis the likes of which have not been seen before.
b. In November in the Kingston region the number of hospitalizations from COVID-19 has reached its highest number all year after climbing steadily since August.
c. There have been repeated outbreaks in area hospitals.

2. The true numbers of COVID-19 infections occurring in Ontario and the Kingston region are very much higher than presented by the Ontario government and Public Health.

a. COVID-19 is spreading very intensely throughout the Kingston region.
b. Since the government of Ontario stopped most COVID-19 PCR testing in early January 2022 the number of reported cases of COVID-19 provincially and locally has severely underestimated the true value.
c. In late October Ontario's COVID-19 new cases peaked at just over 100,000 new cases per day according to COVID-19 Resources Canada. Yet, the province reported only 1,500 cases. The true number of cases is thus 66 times higher than what is reported. This number of cases is equivalent to what we experienced at the first peak of the then new mega-infectious Omicron variant in January 2022.
d. In the Kingston region KFLA Public Health is reporting a maximum of 29 new cases of COVID-19 per day in November. This translates to a peak of 1,914 new daily cases in November which is 6 times higher than our local Omicron peak was in late December 2021.

3. The health impacts for our children of influenza and COVID-19 infections are extremely serious and potentially long lasting

a. We are learning that COVID-19 virus infection persists in the body not unlike other serious viruses such as hepatitis B, HIV and papilloma virus to mention a few examples (Chertow D. Research Square. December 2021).
b. Long-COVID where the virus persists and causes symptoms in those that have had the infection is described to occur in 20-40% of cases.
c. Long-COVID is now confirmed to occur in children. Organs affected include the brain, lungs, heart, blood clots, kidneys, pancreas (diabetes), liver, reproductive system etc (Kompaniyets L. MMWR, August 2022).
d. There is evidence now for immunological injury from COVID-19 infections (Shuwa H. Med (NY) June 2021).

4. Similarly, the health impacts for the teachers and staff of the LDSB are serious and long lasting

a. Repeated COVID-19 infections increase the risks for many serious long term COVID-19 related consequences (Bowe B. Nature Medicine. November 2022).

5. Prevention of the spread of COVID-19 and influenza requires layers of protections

a. No one intervention by itself offers complete protection from acquiring COVID-19.
b. Vaccination reduces mortality from COVID-19 infection, especially in the elderly. It may also reduce the risk of long-COVID symptoms. Influenza vaccination likewise reduces the severity of influenza disease and mortality.
c. COVID-19 and influenza are significantly airborne infections. Meaning that the viruses travel long distances through indoor air spaces on air currents.
d. Therefore, improved in-door air quality with increased ventilation with fresh outdoor air and filtration through HEPA filters and exposure to far-ultraviolet light (222 nm) combined significantly reduce the amount of COVID-19 and influenza circulating in the air (Aldehheel M. Int J Env Res Pub Health. November 2022).

e. Masks, especially well fitting high quality masks known as N95 or KN95 respirators, reduce the risk of COVID-19 transmission by 83% (Andrejko KL. MMWR. February 2022).
f. The protective efficacy of N95/KN95 masks is likely higher when one takes into account that these masks prevent transmission from and to another person, ie in both directions.
g. These masks are now widely available and much less costly than they were at the outset of the pandemic.
h. In a recently published study from Boston, schools that continued with a masking policy for teachers, staff and students for a 15 week period longer than other regional schools from February 28, 2022 to the end of the school year, had 50% fewer cases of COVID-19 documented in the 294,084 students and 46,536 staff and teachers (Cowger TL. NEJM. November 2022).

6. **The Limestone District School Board has the legal obligation and authority to independently introduce and enforce a masking policy in the interests of student's well-being and safety of their staff and teachers.**

It is my submission to the LDSB Board that for the reasons stated above that a masking policy across all of LDSB is urgently needed. Public health units across Ontario and the Chief Medical Officer of Health are all strongly recommending wearing masks to prevent the spread of COVID-19, influenza and RSV. The Canadian Paediatric Society and the American Pediatric Association all recommend that children wear masks for the prevention of COVID-19. The levels of COVID-19 and influenza in Ontario and the Kingston region are extra-ordinary high and wearing a mask will have an important benefit to reduce transmission of these dangerous viruses and create a safer environment for everyone who places their trust in the Limestone District School Board.

Sincerely,

Dick Zoutman, MD, FRCPC, CCPE, C. Dir

References and Attachments:

1. Biography of Dr. Dick Zoutman
2. COVID-19 Resources Canada: https://covid19resources.ca/covid-hazard-index/
3. Chertow D et al SARS-CoV-2 infection and persistence throughout the human body and brain. Research Square. December 2021

4. Kompaniyets L et al. Post-COVID-19 symptoms and conditions among children and adolescents- United States, March 1, 2020 – January 31, 2022. MMWR, August 2022
5. Shuwa H et al Alterations in T and B cell function persist in convalescent COVID-19 patients. Med (NY) June 2021
6. Bowe B et al. Acute and post-acute sequelae associated with SARS-CoV-2 reinfection. Nature Medicine. November 2022
7. Aldehheel M. The Role of Portable Air Purifiers and Effective Ventilation in Improving Indoor Air Quality in University Classrooms. Int J Env Res Pub Health. November 2022
8. Andrejko KL et al. Effectiveness of Face Mask or Respirator Use in Indoor Public Settings for Prevention of SARS-CoV-2 Infection — California, February–December 2021. MMWR February 4, 2022.
9. Cowger TL et al. Lifting Universal Masking in Schools - Covid-19 Incidence among Students and Staff. NEJM. November 9, 2022.

Biography:

Dr. Dick Zoutman is the Past Inaugural Chief of Staff at the Scarborough Health Network and Past Chief of Staff at Quinte Health Care. Dick is Professor, in the Faculty of Medicine University of Toronto and in the Faculty of Health Sciences at Queen's University. He is a Fellow of the Royal College of Physicians of Canada, in Internal Medicine, Infectious Diseases, and Medical Microbiology. He is also the Past Chief of Infectious Diseases at the Kingston Health Sciences Center. The primary focus of his academic research has been the use of Quality Improvement Science in advancing health care quality and infectious diseases.
During the 2003 outbreak of SARS Dr. Zoutman chaired the Ontario SARS Scientific Advisory Committee responsible for advising the Ontario Government on management of the epidemic.
Dick was the founding Co-Chair of the Ontario Provincial Infectious Diseases Advisory Committee (PIDAC). Dr. Zoutman is a Fellow of the Center for the Study of Democracy and also has his Black Belt in Lean and Six Sigma for Health Care. He is a Canadian Certified Physician Executive and a Chartered Director with the Conference Board of Canada and the De Groote School of Business.

SARS-CoV-2 infection and persistence throughout the human body and brain

Daniel Chertow (chertowd@cc.nih.gov)
National Institutes of Health https://orcid.org/0000-0002-1675-1728

Sydney Stein
National Institutes of Health https://orcid.org/0000-0002-0259-4485

Sabrina Ramelli
National Institutes of Health

Alison Grazioli
National Institutes of Health

Joon-Yong Chung
NCI https://orcid.org/0000-0001-5041-5982

Manmeet Singh
National Institutes of Health

Claude Kwe Yinda
National Institute of Allergy and Infectious Diseases

Clayton Winkler
National Institutes of Health

James Dickey
National Institutes of Health

Kris Ylaya
National Cancer Institute

Sung Hee Ko
National Institutes of Health

Andrew Platt
National Institutes of Health

Peter Burbelo
8Dental Clinical Research Core, NIDCR, NIH https://orcid.org/0000-0003-1717-048X

Martha Quezado
National Institutes of Health

Stefania Pittaluga
NIH

Madeleine Purcell
University of Maryland School of Medicine

Vincent Munster

National Institute of Allergy and Infectious Diseases https://orcid.org/0000-0002-2288-3196

Frida Belinky
NIH

Marcos Ramos-Benitez
National Institutes of Health

Eli Boritz
National Institutes of Health

Daniel Herr
University of Maryland School of Medicine

Joseph Rabin
University of Maryland School of Medicine

Kapil Saharia
University of Maryland School of Medicine

Ronson Madathil
University of Maryland School of Medicine

Ali Tabatabai
University of Maryland School of Medicine

Shahabuddin Soherwardi
TidalHealth Peninsula Regional

Michael McCurdy
University of Maryland St. Joseph Medical Center https://orcid.org/0000-0001-5319-0475

Karin Peterson
National Institutes of Health

Jeffrey Cohen
National Institutes of Health

Emmie de Wit
National Institute of Allergy and Infectious Diseases https://orcid.org/0000-0002-9763-7758

Kevin Vannella
National Institutes of Health

Stephen Hewitt
National Cancer Institute, National Institutes of Health https://orcid.org/0000-0001-8283-1788

David Kleiner
National Cancer Institute https://orcid.org/0000-0003-3442-4453

Biological Sciences - Article

Keywords:

Posted Date: December 20th, 2021

DOI: https://doi.org/10.21203/rs.3.rs-1139035/v1

SARS-CoV-2 infection and persistence throughout the human body and brain

Authors:

Sydney R. Stein[1,2], Sabrina C. Ramelli[3], Alison Grazioli[4], Joon-Yong Chung[5], Manmeet Singh[6], Claude Kwe Yinda[6], Clayton W. Winkler[7], James M. Dickey[1,2], Kris Ylaya[5], Sung Hee Ko[8], Andrew Platt[1,2], Peter D. Burbelo[9], Martha Quezado[5], Stefania Pittaluga[5], Madeleine Purcell[10], Vincent J. Munster[6], Frida Belinky[8], Marcos J. Ramos-Benitez[1,2,11], Eli A. Boritz[8], Daniel L. Herr[12], Joseph Rabin[13], Kapil K. Saharia[14,15], Ronson J. Madathil[16], Ali Tabatabai[17], Shahabuddin Soherwardi[18], Michael T. McCurdy[19,17], NIH COVID-19 Autopsy Consortium^, Karin E. Peterson[7], Jeffrey I. Cohen[19], Emmie de Wit[6], Kevin M. Vannella[1,2], Stephen M. Hewitt[5], David E. Kleiner[5], Daniel S. Chertow[1,2*]

Affiliations:

1. Emerging Pathogens Section, Critical Care Medicine Department, Clinical Center, National Institutes of Health, Bethesda, MD, USA
2. Laboratory of Immunoregulation, National Institute of Allergy and Infectious Diseases, National Institutes of Health, Bethesda, MD, USA
3. Critical Care Medicine Department, Clinical Center, National Institutes of Health, Bethesda, MD, USA
4. Kidney Disease Section, Kidney Diseases Branch, National Institute of Diabetes and Digestive and Kidney Diseases, National Institutes of Health, Bethesda, MD, USA
5. Laboratory of Pathology, Center for Cancer Research, National Cancer Institute, National Institutes of Health, Bethesda, MD, USA

6. Laboratory of Virology, Division of Intramural Research, National Institute of Allergy and Infectious Diseases, National Institute of Health, Hamilton, MT, USA
7. Laboratory of Persistence Viral Diseases, Rocky Mountain Laboratories, National Institute of Allergy and Infectious Diseases, National Institute of Health, Hamilton, MT, USA
8. Vaccine Research Center, National Institute of Allergy and Infectious Diseases, National Institutes of Health, Bethesda, MD, USA
9. National Institute of Dental and Craniofacial Research, National Institutes of Health, Bethesda, MD, USA
10. University of Maryland School of Medicine, Baltimore, MD, USA
11. Postdoctoral Research Associate Training Program, National Institute of General Medical Sciences, National Institutes of Health, Bethesda, MD, USA
12. R Adams Cowley Shock Trauma Center, Department of Medicine and Program in Trauma, University of Maryland School of Medicine, Baltimore, MD, USA
13. R Adams Cowley Shock Trauma Center, Department of Surgery and Program in Trauma, University of Maryland School of Medicine, Baltimore, MD, USA
14. Department of Medicine, Division of Infectious Disease, University of Maryland School of Medicine, Baltimore, MD, USA
15. Institute of Human Virology, University of Maryland School of Medicine, Baltimore, MD, USA
16. Department of Surgery, Division of Cardiac Surgery, University of Maryland School of Medicine, Baltimore, MD, USA

17. Department of Medicine, Division of Pulmonary and Critical Care Medicine, University of Maryland School of Medicine, Baltimore, MD, USA
18. Hospitalist Department, TidalHealth Peninsula Regional, Salisbury, MD, USA
19. Division of Critical Care Medicine, Department of Medicine, University of Maryland St. Joseph Medical Center, Towson, MD, USA
20. Medical Virology Section, Laboratory of Infectious Diseases, National Institute of Allergy and Infectious Diseases, National Institutes of Health, Bethesda MD
^See Acknowledgements
*Corresponding author. Email: chertowd@cc.nih.gov

COVID-19 is known to cause multi-organ dysfunction[1-3] in acute infection, with prolonged symptoms experienced by some patients, termed Post-Acute Sequelae of SARS-CoV-2 (PASC)[4-5]. However, the burden of infection outside the respiratory tract and time to viral clearance is not well characterized, particularly in the brain[3,6-14]. We performed complete autopsies on 44 patients with COVID-19 to map and quantify SARS-CoV-2 distribution, replication, and cell-type specificity across the human body, including brain, from acute infection through over seven months following symptom onset. We show that SARS-CoV-2 is widely distributed, even among patients who died with asymptomatic to mild COVID-19, and that virus replication is present in multiple pulmonary and extrapulmonary tissues early in infection. Further, we detected persistent SARS-CoV-2 RNA in multiple anatomic sites, including regions throughout the brain, for up to 230 days following symptom onset. Despite extensive distribution of SARS-CoV-2 in the body, we observed a paucity of inflammation or direct viral cytopathology outside of the lungs. Our data prove that SARS-CoV-2 causes systemic infection and can persist in the body for months.

Main text:

Infection with severe acute respiratory syndrome coronavirus 2 (SARS-CoV-2), the causative agent of coronavirus disease 2019 (COVID-19), has well described pulmonary and extrapulmonary manifestations[1-3], including multiorgan failure and shock among severe and fatal cases. Some survivors experience Post-Acute Sequelae of SARS-CoV-2 (PASC) – also known as Long COVID—with cardiovascular, pulmonary, and neurological manifestations with or without functional impairment[4-5]. While autopsy studies of fatal COVID-19 cases support the ability of SARS-CoV-2 to infect multiple organs[3,7-12], extra-pulmonary organs often lack histopathological

evidence of direct virally-mediated injury or inflammation[10-14]. The paradox of extra-pulmonary infection without injury or inflammation raises many pathogen- and host-related questions. These questions include, but are not limited to: What is the burden of infection within versus outside of the respiratory tract? What cell types are infected across extra-pulmonary tissues, and do they support SARS-CoV-2 infection and replication? In the absence of cellular injury and inflammation in extra-pulmonary tissues, does SARS-CoV-2 persist, and if so, over what interval? Does SARS-CoV-2 evolve as it spreads to and persists in different anatomical compartments?

To inform these pathogen-focused questions and to evaluate for the presence or absence of associated histopathology in matched tissue specimens, we performed extensive autopsies on a diverse population of 44 individuals who died from or with COVID-19 up to 230 days following initial symptom onset. Our approach focused on timely, systematic, and comprehensive tissue sampling and preservation of adjacent tissue samples for complementary analyses. We performed droplet digital polymerase chain reaction (ddPCR) for sensitive detection and quantification of SARS-CoV-2 gene targets in all tissue samples collected. To elucidate SARS-CoV-2 cell-type specificity and validate ddPCR findings, we performed *in situ* hybridization (ISH) broadly across sampled tissues. Immunohistochemistry (IHC) was used to further validate cell-type specificity in the brain where controversy remains on the regional distribution and cellular tropism of SARS-CoV-2 infection. In all samples where SARS-CoV-2 RNA was detected by ddPCR, we performed qRT-PCR to detect subgenomic (sg)RNA, an assay suggestive of recent virus replication[15]. We confirmed the presence of replication-competent SARS-CoV-2 in extrapulmonary tissues by virus isolation in cell culture. Lastly, in six

individuals, we measured the diversity and anatomic distribution of intra-individual SARS-CoV-2 variants using high-throughput, single-genome amplification and sequencing (HT-SGS).

We categorized autopsy cases of SARS-CoV-2 infection as "early" (n=17), "mid" (n=13), or "late" (n=14) by illness day (D) at the time of death, being ≤D14, D15-D30, or ≥D31, respectively. We defined persistence as presence of SARS-CoV-2 RNA among late cases. Due to the extensive tissue collection, we analyzed and described the results in terms of grouped tissue categories as the following: respiratory tract; cardiovascular; lymphoid; gastrointestinal; renal and endocrine; reproductive; muscle, skin, adipose, & peripheral nerves; and brain.

Autopsy cohort overview

Between April 26, 2020 and March 2, 2021, we performed autopsies on 44 PCR-confirmed cases (Extended Data Fig. 1). SARS-CoV-2 seroconversion was detected in 38 of these cases (Supplementary Data 1); three early cases (P27, P36, P37) had not seroconverted and perimortem plasma was unavailable for the other three cases (P3, P4, P15). Extensive sampling of the brain was accomplished in 11 of the 44 cases (Fig. 1). The cohort was 29.5% female with a mean age of 59.2 years and was diverse across race and ethnicity (Extended Data Table 1). 95.5% of patients had at least one comorbidity, with hypertension (54.5%), obesity (52.3%), and chronic respiratory disease (34.1%) being most common. Patients presented to the hospital a mean of 9.4 days following symptom onset and were hospitalized a mean of 26.4 days. Overall, the mean interval from symptom onset to death was 35.2 days and the mean postmortem interval was 26.2 hours. 81.8% of patients required intubation with invasive mechanical ventilation, 22.7% received extracorporeal membrane oxygenation (ECMO) support, and 40.9% required renal replacement therapy. Vasopressors, systemic steroids, systemic anticoagulation, and

antibiotics were commonly administered (Extended Data Table 1). Individual patient-level demographic and clinical information can be found in Extended Data Table 2.

Widespread infection and persistence

SARS-CoV-2 RNA was detected in all 44 cases and across 79 of 85 anatomical locations and body fluids sampled (Extended Data Fig. 2, Supplementary Data 1). The highest burden of SARS-CoV-2 RNA (i.e., >100,000 N gene copies/ng RNA input) was detected in the respiratory tract of early cases (Figure 1), but we detected at least 100 N gene copies/ng RNA input from every tissue group besides reproductive tissues from multiple individuals among early cases. The mean SARS-CoV-2 N gene copies/ng RNA detected from tissues in each grouping among early cases are as follows: 9,210.10 across respiratory tissues; 38.75 across cardiovascular tissues; 30.01 across lymphoid tissues; 24.68 across gastrointestinal tissues; 12.76 across renal and endocrine tissues; 0.36 across reproductive tissues; 27.50 across muscle, peripheral nerve, adipose, and skin tissues; 57.40 across ocular tissues; and 32.93 across brain tissues (Extended Data Table 3).

With a few exceptions, the overall burden of SARS-CoV-2 RNA decreased by a log or more across tissue categories among mid cases, and further decreased among late cases. However, several mid and late cases had high levels (≥5 N gene copies/ng RNA input) detected among multiple tissues (Extended Data Fig. 2). Further, persistence of low-level SARS-CoV-2 RNA (0.0004 to <0.5 N gene copies/ng RNA input) was frequently detected across multiple tissue categories among all late cases, despite being undetectable in plasma (Extended Data Fig. 2, Supplementary Data 1). Notably, SARS-CoV-2 RNA was detected in the brains of all six late

158 cases and across most locations evaluated in the brain in five of these six, including P42 who
159 died at D230 (Fig. 1).
160 Overall, SARS-CoV-2 RNA was detected in respiratory tissue of 43/44 cases (97.7%);
161 cardiovascular tissue of 35/44 cases (79.5%); lymphoid tissue of 38/44 cases (86.4%);
162 gastrointestinal tissue of 32/44 (72.7%); renal and endocrine tissue of 28/44 cases (63.6%);
163 reproductive tissue in 17/40 cases (42.5%); muscle, skin, adipose, and peripheral nervous tissue
164 in 30/44 cases (68.2%); ocular tissue and humors of 22/28 cases (57.9%); and brain tissue in
165 10/11 cases (90.9%) (Extended Data Table 3).
166 We additionally detected SARS-CoV-2 sgRNA across all tissue categories,
167 predominately among early cases (14/17, 82.4%), as well as in plasma, pleural fluid, and vitreous
168 humor (Fig. 1, Extended Data Fig. 2, Supplementary Data 1). sgRNA was also detected in at
169 least one tissue of 61.5% of mid cases and 42.9% of late cases, including across three tissue
170 categories in a case at D99 (P20).
171 We isolated SARS-CoV-2 in cell culture from multiple pulmonary and extrapulmonary
172 tissues, including lung, bronchus, sinus turbinate, heart, mediastinal lymph node, small intestine,
173 and adrenal gland from early cases up to D7 (P19, P27, P32, P37; Supplementary Data 1).
174
175 **Intra-individual viral variant diversity**
176 We used HT-SGS to analyze SARS-CoV-2 spike gene variant sequences from a total of
177 46 tissues in six individuals. In five individuals from the early group, predominant spike
178 sequences were largely identical across tissues. In P27, P19, and P18, no non-synonymous virus
179 genetic diversity was detected in pulmonary and extrapulmonary sites despite a high depth of
180 single-molecule sampling (Extended Data Fig. 3). Thus, virus populations that were relatively

181 homogeneous had disseminated in these individuals without coding changes in spike. However,
182 we also noted important patterns of intra-individual virus diversity in several patients from the
183 early group. In P27, although all 4,525 inferred spike amino acid sequences were identical, two
184 virus haplotypes, each with a single synonymous substitution, were preferentially detected in
185 extrapulmonary sites including right and left ventricles and mediastinal LN. In P38, we observed
186 clear virus genetic differences between the lung lobes and the brain, with a D80F residue found
187 in 31/31 pulmonary but 0/490 brain sequences and a G1219V residue that was restricted to brain
188 minor variants. A similar distinction was observed between sequences from dura mater and other
189 sites in P36, albeit at very low sampling depth (n = 2 sequences) from dura mater. Overall, these
190 findings suggested no need for alterations in receptor utilization to permit extrapulmonary
191 dissemination of SARS-CoV-2, while also revealing genetic compartmentalization between
192 viruses in the lung lobes and those in extrapulmonary sites, including the brain.
193
194 **ISH reveals SARS-CoV-2 cellular tropism**
195 We validated our ddPCR results across all tissue categories via ISH for SARS-CoV-2
196 spike RNA across selected early, mid, and late cases (Supplementary Data 3). Overall, we
197 detected SARS-CoV-2 RNA via ISH in 36 distinct cell types across all sampled organs
198 (Extended Data Table 4, Supplementary Data 3). Spike RNA was detected throughout the
199 respiratory tract in early cases, as well as within the sinus turbinate, trachea, lungs, from late
200 cases (i.e., P33, P20, P42).
201 The heart contained spike RNA within myocytes, endothelium, and smooth muscle of
202 vessels of both early (P18, P19) and late (P3 & P42) cases. The pericardium demonstrated a
203 positive signal for spike RNA within fibroblasts of the stroma. Intimal cells of the aorta were

additionally found to contain spike RNA. Mononuclear leukocytes within the lymph node, spleen, and appendix of an early case (P19) contained spike RNA, as did colonic epithelium (Fig 2).

Epithelial cells along the intestinal tract in early cases (P16, P18, P19) contained viral RNA, as well as stratified squamous epithelium of the esophagus. Mononuclear leukocytes were again visualized with SARS-CoV-2 RNA in lymphoid aggregates and the interstitium of the small and large intestine, with infected cells still present in the colon of late cases (P33, P42). Kupffer cells, hepatocytes, and bile duct epithelium within the liver were additionally found to contain spike RNA.

Within the kidney, spike RNA could be visualized within parietal epithelium of Bowman's capsule, collecting duct cells, distal tubule cells, and glomerular endothelium. The adrenal glands contained spike RNA within endocrine cells. Endocrine follicular cells of the thyroid and glandular cells of the pancreas were also positive for spike RNA (Fig. 2). Among reproductive organs, spike RNA was visualized within Leydig and Sertoli cells of the testis, germ cells within the testicular tubules, endometrial gland epithelium, endometrial stromal cells, uterine smooth muscle cells, and stromal cells of the post-menopause ovary (Fig. 2).

Myocytes within skeletal muscle contained spike RNA in both early (P18) and late (P20) cases. In addition to the organ-specific cell type infection of SARS-CoV-2, endothelium, muscularis of atrial vessels, and Schwann cells were identified as infected throughout the body, and were similarly positive across early and late cases.

Spike RNA was found in neurons, glia and ependyma, as well as endothelium of vessels across all lobes of the brain of early, mid, and late cases. Within the cerebellum specifically,

neurons, Purkinje cells, and endothelium of vasculature also contained spike protein via IHC (Fig. 3).

COVID-19 histological findings

The histopathology findings from our cohort were similar to those reported in other case series (Extended Data Fig. 4). All but five cases were considered to have died from COVID-19 (Extended Data Table 5), and, of these, 37 (94.5%) had either acute pneumonia or diffuse alveolar damage at the time of death (Supplementary Data 2). Phases of diffuse alveolar damage showed clear temporal associations, with the exudative phase seen mainly within the first three weeks of infection and the fibrosing phase not seen until after a month of infection (Extended Data Fig. 5). Pulmonary thromboembolic complications, which were also likely related to SARS-CoV-2 infection, with or without infarction, were noted in 10 (23%) cases. Another finding likely related to SARS-CoV-2 infection included myocardial infiltrates in four cases, including one case of significant myocarditis[16] (P3). Some of the cases of microscopic ischemia appeared to be associated with fibrin-platelet microthrombi, and may therefore be related to COVID-19 thrombotic complications. Within the lymph nodes and spleen, we observed lymphodepletion and both follicular and paracortical hyperplasia.

Outside the lungs, histological changes were mainly related to complications of therapy or preexisting co-morbidities: mainly obesity, diabetes, and hypertension. Five cases had old ischemic myocardial scars and three had coronary artery bypass grafts in place. Given the prevalence of diabetes and obesity in our cohort, it was not surprising to find diabetic nephropathy (10 cases, 23%) or steatohepatitis (5 cases, 12%). One case was known to have chronic hepatitis C with cirrhosis, but the other cases of advanced hepatic fibrosis were likely

related to fatty liver disease, even if diagnostic features of steatohepatitis were not present. Hepatic necrosis (13 cases, 30%) and changes consistent with acute kidney injury (17 cases, 39%) were likely related to hypoxic-ischemic injury in these very ill patients.

In the examination of the 11 brains, we found few histopathologic changes, despite the evidence of substantial viral burden. Vascular congestion was an unusual finding that had an unclear etiology and could be related to the hemodynamic changes incurred with infection. Global hypoxic/ischemic change was seen in two cases, one of which was a juvenile (P36) with a seizure disorder who was found to be SARS-CoV-2 positive on hospital admission, but who likely died of seizure complications unrelated to viral infection.

Discussion

Here we provide the most comprehensive analysis to date of SARS-CoV-2 cellular tropism, quantification, and persistence across the body and brain, in a diverse autopsy cohort collected throughout the first year of the pandemic in the United States. Our focus on short post-mortem intervals, comprehensive approach to tissue collection, and preservation techniques – RNA*later* and flash freezing of fresh tissue – allowed us to detect and quantify viral levels with high sensitivity by ddPCR and ISH, as well as culture virus, which are notable differences compared to other studies.

We show SARS-CoV-2 disseminates across the human body and brain early in infection at high levels, and provide evidence of virus replication at multiple extrapulmonary sites during the first week following symptom onset. We detected sgRNA in at least one tissue in over half of cases (14/27) beyond D14, suggesting that prolonged viral replication may occur in extra-pulmonary tissues as late as D99. While others have questioned if extrapulmonary viral presence

is due to either residual blood within the tissue[8,17] or cross-contamination from the lungs during tissue procurement[8], our data rule out both theories. Only 12 cases had detectable SARS-CoV-2 RNA in a perimortem plasma sample, and of these only two early cases also had SARS-CoV-2 sgRNA in the plasma, which occurred at Ct levels higher than nearly all of their tissues with sgRNA. Therefore, residual blood contamination cannot account for RNA levels within tissues. Furthermore, blood contamination would not account for the SARS-CoV-2 sgRNA or virus isolated from tissues. Contamination of additional tissues during procurement, is likewise ruled out by ISH demonstrating widespread SARS-CoV-2 cellular tropism across the sampled organs, by IHC detecting viral protein in the brain, and by several cases of virus genetic compartmentalization in which spike variant sequences that were abundant in extrapulmonary tissues were rare or undetected in lung samples.

Using both ddPCR and sgRNA analysis to inform our selection of tissue for virus isolation and ISH staining allow us to describe a number of novel findings. Others[6,8-12,17] have previously reported SARS-CoV-2 RNA within the heart, lymph node, small intestine, and adrenal gland. We demonstrate conclusively that SARS-CoV-2 is capable of infecting and replicating within these tissues. Current literature has also reported absent or controversial expression of ACE2 and/or TMPRSS2 in several extrapulmonary tissues, such as the colon, lymphoid tissues, and ocular tissues, calling into question if these tissues can become infected by SARS-CoV-2[1-3]. However, we observed high levels of SARS-CoV-2 RNA and evidence of replication within these organs, as well as SARS-CoV-2 RNA via ISH in colonic mucosal epithelium and mononuclear leukocytes within the spleen, thoracic cavity lymph nodes, and GI lymphoid aggregates. We believe these ISH positive cells represent either infection or

phagocytized virus in resident macrophages. Further, we isolated virus from a mediastinal lymph node and ocular tissue from two early cases (P19, P32).

Our use of a single-copy sequencing approach for the SARS-CoV-2 spike allowed us to demonstrate homogeneous virus populations in many tissues, while also revealing informative virus variants in others. Low intra-individual diversity of SARS-CoV-2 sequences has been observed frequently in previous studies[18-20], and likely relates to the intrinsic mutation rate of the virus as well as lack of early immune pressure to drive virus evolution in new infections. It is important to note that our HT-SGS approach has both a high accuracy and a high sensitivity for minor variants within each sample, making findings of low virus diversity highly reliable[21]. The virus genetic compartmentalization that we observed between pulmonary and extrapulmonary sites in several individuals supports independent replication of the virus at these sites, rather than spillover from one site to another. Importantly, lack of compartmentalization between these sites in other individuals does not rule out independent virus replication, as independently replicating populations may share identical sequences if overall diversity is very low. It was also interesting to note several cases where brain-derived virus spike sequences showed non-synonymous differences relative to sequences from other tissues. These differences may indicate differential selective pressure on spike by antiviral antibodies in brain versus other sites, though further studies will be needed to confirm this speculation.

Our results collectively show while that the highest burden of SARS-CoV-2 is in the airways and lung, the virus can disseminate early during infection and infect cells throughout the entire body, including widely throughout the brain. While others have posited this viral dissemination occurs through cell trafficking[11] due to a reported failure to culture virus from blood[3,22], our data support an early viremic phase, which seeds the virus throughout the body

following pulmonary infection. Recent work by Jacobs et al.[22] in which SARS-CoV-2 virions were pelleted and imaged from COVID-19 patient plasma, supports this mechanism of viral dissemination. Although our cohort is primarily made up of severe cases of COVID-19, two early cases had mild respiratory symptoms (P28; fatal pulmonary embolism occurred at home) or no symptoms (P36; diagnosed upon hospitalization for ultimately fatal complications of a comorbidity), yet still had SARS-CoV-2 RNA widely detected across the body, including brain, with detection of sgRNA in multiple compartments. Our findings, therefore, suggest viremia leading to body-wide dissemination, including across the blood-brain barrier, and viral replication can occur early in COVID-19, even in asymptomatic or mild cases. Further, P36 was a juvenile with no evidence of multisystem inflammatory syndrome in children, suggesting infected children without severe COVID-19 can also experience systemic infection with SARS-CoV-2.

Finally, a major contribution of our work is a greater understanding of the duration and locations at which SARS-CoV-2 can persist. While the respiratory tract was the most common location in which SARS-CoV-2 RNA tends to linger, ≥50% of late cases also had persistence in the myocardium, thoracic cavity lymph nodes, tongue, peripheral nerves, ocular tissue, and in all sampled areas of the brain, except the dura mater. Interestingly, despite having much lower levels of SARS-CoV-2 in early cases compared to respiratory tissues, we found similar levels between pulmonary and the extrapulmonary tissue categories in late cases. This less efficient viral clearance in extrapulmonary tissues is perhaps related to a less robust innate and adaptive immune response outside the respiratory tract.

We detected sgRNA in tissue of over 60% of the cohort. While less definitive than viral culture[23,24], multiple studies have shown that sgRNA levels correlate with acute infection and can

be detected in respiratory samples of immunocompromised patients experiencing prolonged infection[24]. These data coupled with ISH suggest that SARS-CoV-2 can replicate within tissue for over 3 months after infection in some individuals, with RNA failing to clear from multiple compartments for up to D230. This persistence of viral RNA and sgRNA may represent infection with defective virus, which has been described in persistent infection with measles virus – another single-strand enveloped RNA virus—in cases of subacute sclerosing panencephalitis[25].

The mechanisms contributing to PASC are still being investigated; however, ongoing systemic and local inflammatory responses have been proposed to play a role[5]. Our data provide evidence for delayed viral clearance, but do not support significant inflammation outside of the respiratory tract even among patients who died months after symptom onset. Understanding the mechanisms by which SARS-CoV-2 persists and the cellular and subcellular host responses to viral persistence promises to improve the understanding and clinical management of PASC.

Main References:

1. Bourgonje, A. R. *et al*. Angiotensin-converting enzyme 2 (ACE2), SARS-CoV-2 and the pathophysiology of coronavirus disease 2019 (COVID-19). *J Pathol*. **251**(3), 228-248 (2020). https://doi.org/10.1002/path.5471.
2. Salamanna, F., Maglio, M., Landini. M. P., & Fini, M. Body Localization of ACE-2: On the Trail of the Keyhole of SARS-CoV-2. *Front Med (Lausanne)*. **7**, 594495 (2021). https://doi.org/10.3389/fmed.2020.594495.
3. Sridhar, S., & Nicholls, J. Pathophysiology of infection with SARS-CoV-2-What is known and what remains a mystery. *Respirology*. **26**(7), 652-665 (2021). https://doi.org/10.1111/resp.14091.
4. Al-Aly, Z., Xie, Y., & Bowe, B. High-dimensional characterization of post-acute sequelae of COVID-19. *Nature*. **594**(7862), 259-264 (2021). https://doi.org/10.1038/s41586-021-03553-9.
5. Crook, H., Raza, S., Nowell, J., Young, M., & Edison, P. Long covid-mechanisms, risk factors, and management. *BMJ*. **374**, n1648 (2021). https://doi.org/10.1136/bmj.n1648.
6. Puelles, V. G., *et al*. Multiorgan and Renal Tropism of SARS-CoV-2. *N Engl J Med*. **383**(6), 590-592 (2020). https://doi.org/10.1056/NEJMc2011400.
7. Martines, R. B., *et al*. Pathology and Pathogenesis of SARS-CoV-2 Associated with Fatal Coronavirus Disease, United States. *Emerg Infect Dis*. **26**(9), 2005-2015 (2020). https://doi.org/10.3201/eid2609.202095.
8. Bhatnagar, J., *et al*. Evidence of Severe Acute Respiratory Syndrome Coronavirus 2 Replication and Tropism in the Lungs, Airways, and Vascular Endothelium of Patients

With Fatal Coronavirus Disease 2019: An Autopsy Case Series. *J Infect Dis*. **223**(5), 752-764 (2021). https://doi.org/10.1093/infdis/jiab039.

9. Dorward, D. A., *et al*. Tissue-Specific Immunopathology in Fatal COVID-19. *Am J Respir Crit Care Med*. **203**(2),192-201 (2021). https://doi.org/10.1164/rccm.202008-3265OC.
10. Schurink, B., *et al*. Viral presence and immunopathology in patients with lethal COVID-19: a prospective autopsy cohort study. *Lancet Microbe*. **1**(7), e290-e299 (2020). https://doi.org/10.1016/S2666-5247(20)30144-0.
11. Yao, X.H., *et al*. A cohort autopsy study defines COVID-19 systemic pathogenesis. *Cell Res*. **31**(8), 836-846 (2021). https://doi.org/10.1038/s41422-021-00523-8.
12. Remmelink, M., et al. Unspecific post-mortem findings despite multiorgan viral spread in COVID-19 patients. *Crit Care*. **24**(10), 495 (2020). https://doi.org/10.1186/s13054-020-03218-5.
13. Mukerji, S. S., & Solomon, I. H. What can we learn from brain autopsies in COVID-19? *Neurosci Lett*. **742**, 135528 (2021). https://doi.org/10.1016/j.neulet.2020.135528.
14. Matschke, J., et al. Neuropathology of patients with COVID-19 in Germany: a post-mortem case series. *Lancet Neurol*. **19**(11), 919-929 (2020). https://doi.org/10.1016/S1474-4422(20)30308-2.
15. Speranza, E., et al. Single-cell RNA sequencing reveals SARS-CoV-2 infection dynamics in lungs of African green monkeys. *Sci Transl Med*. **13**(578), eabe8146 (2021). https://doi.org/10.1126/scitranslmed.abe8146
16. Vannella, K. M., et al. Evidence of SARS-CoV-2-specific T-cell-mediated myocarditis in a MIS-A case. *Front Imunol*. Accepted (manuscript ID: 779026).

17. Desai, N., et al. Temporal and spatial heterogeneity of host response to SARS-CoV-2 pulmonary infection. *Nat Commun*. **11**(1), 6319 (2020). https://doi.org/10.1038/s41467-020-20139-7.

18. Tonkin-Hill, G., et al. Patterns of within-host genetic diversity in SARS-CoV-2. *Elife*. **10**, e66857 (2021). https://doi.org/10.7554/eLife.66857.

19. Lythgoe, K. A., et al. SARS-CoV-2 within-host diversity and transmission. *Science*. **372**(6539), eabg0821 (2021). https://doi.org/10.1126/science.abg0821.

20. Valesano, A. L., et al. Temporal dynamics of SARS-CoV-2 mutation accumulation within and across infected hosts. *PLoS Pathog*. **17**(4), e1009499 (2021). https://doi.org/10.1371/journal.ppat.1009499.

21. Ko, S. H., et al. High-throughput, single-copy sequencing reveals SARS-CoV-2 spike variants coincident with mounting humoral immunity during acute COVID-19. *PLoS Pathog*. 17(4), e1009431 (2021). https://doi.org/10.1371/journal.ppat.1009431.

22. Jacobs, J. L., *et al*. SARS-CoV-2 Viremia is Associated with COVID-19 Severity and Predicts Clinical Outcomes. *Clin Infect Dis*. **10**, ciab686 (2021). https://doi.org/10.1093/cid/ciab686.

23. Alexandersen, S., Chamings, A., & Bhatta, T. R. SARS-CoV-2 genomic and subgenomic RNAs in diagnostic samples are not an indicator of active replication. *Nat Commun*. **11**(1), 6059 (2020). https://doi.org/10.1038/s41467-020-19883-7.

24. Binnicker, M. J. Can Testing Predict SARS-CoV-2 Infectivity? The Potential for Certain Methods To Be Surrogates for Replication-Competent Virus. *J Clin Microbiol*. **59**(11), e0046921 (2021). https://doi.org/10.1128/JCM.00469-21.

25. Sidhu, M. S., et al. Defective measles virus in human subacute sclerosing panencephalitis brain. *Virology*. **202**(20), 631-641 (1994). https://doi.org/10.1006/viro.1994.1384.

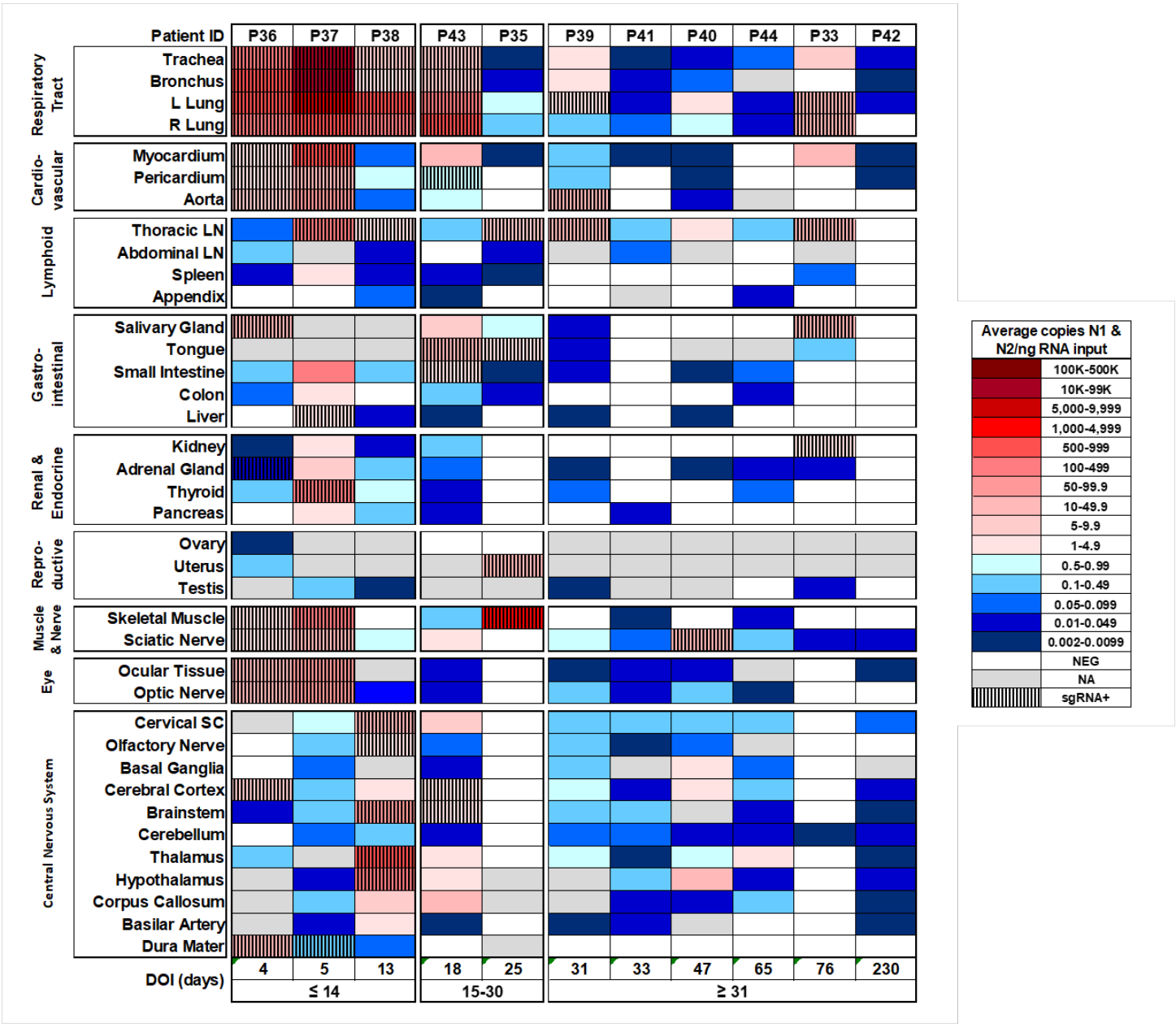

Fig. 1 **Distribution, quantification, and replication of SARS-Cov-2 across the human body and brain.** The heat map depicts the highest mean quantification of SARS-CoV-2 RNA (N) via ddPCR present within the tissues of eleven COVID-19 autopsy patients who underwent whole body and brain sampling. Patients are aligned from shortest to longest duration of illness (DOI) prior to death, listed at the bottom of the figure, and grouped into early (≤14 days), mid (15-30 days), and late (≥31 days) DOI. Tissues are grouped by tissue category beginning with the

444 respiratory tract at the top and central nervous system at the bottom. Viral RNA levels range
445 from 0.002 to 500,000 N gene copies per ng of RNA input, depicted as a gradient from dark blue
446 at the lowest level to dark red at the highest level. Tissues that were also positive for sgRNA via
447 real-time RT-PCR are shaded with black vertical bars. L/left, LN/lymph node, NA/not acquired,
448 R/right, SC/spinal cord.
449
450
451
452
453
454
455
456
457
458
459

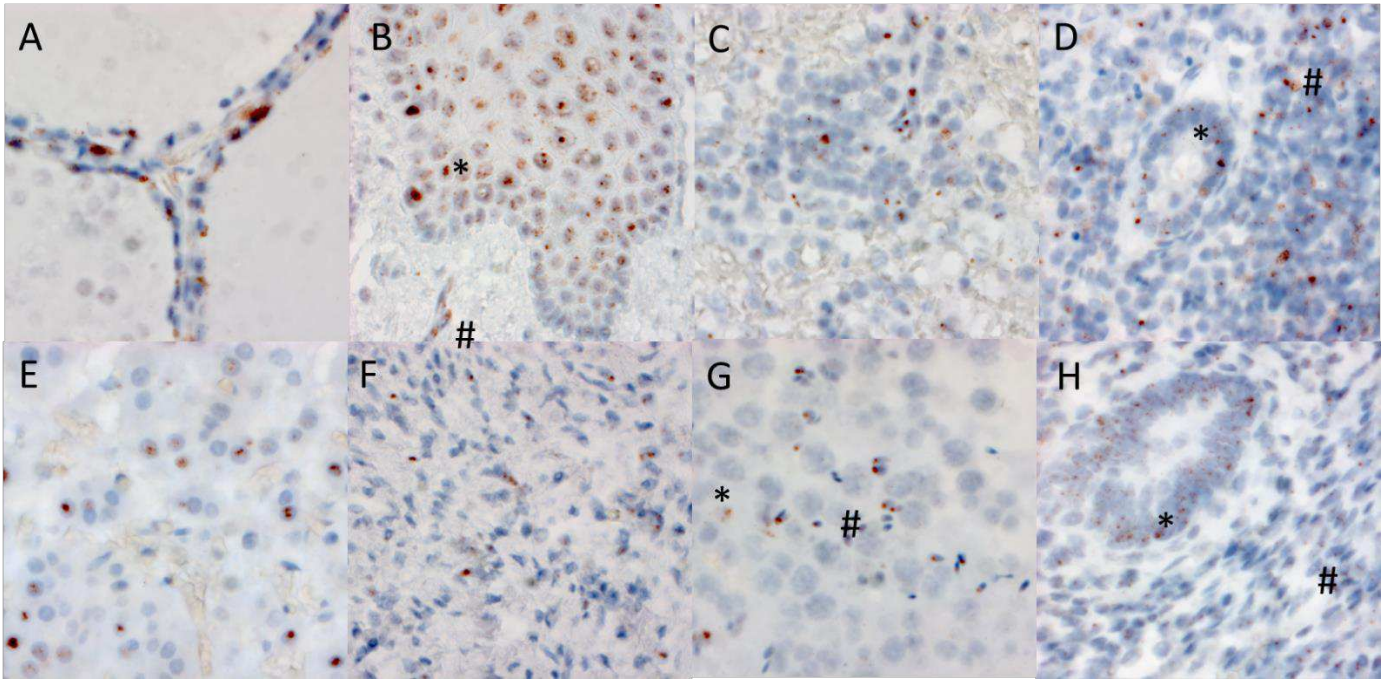

Fig. 2 **RNA *in situ* (RNAscope) detection of SARS-CoV-2 in extrapulmonary tissues**. SARS-CoV-2 virus is localized to the Golgi and endoplasmic, peri-nuclear in appearance, in the following organs and cell types (500 X magnifications): A) Thyroid, demonstrating presence of virus within follicular cells. B) Esophagus, demonstrating the presence of virus within the stratified squamous epithelium (*), as well as signal in capillaries within the stroma (#). C. Spleen, demonstrating the presence of mononuclear lymphoid cells within the white pulp. D) Appendix, demonstrating the presence of virus in both colonic epithelium (*) and mononuclear lymphoid cells in the stroma (#). E) Adrenal demonstrates virus within endocrine secretory cells of the adrenal gland. F) Ovary demonstrates the presence of virus in stromal cells of the ovary in a post-menopausal ovary. G) Testis demonstrates the presence of virus in both Sertoli cells (*) and maturing germ cells within the seminiferous tubules of the testis (#). H) Endometrium demonstrates the presence of virus within endometrial gland epithelium (*) and stromal cells (#), in a pre-menopausal endometrial sample.

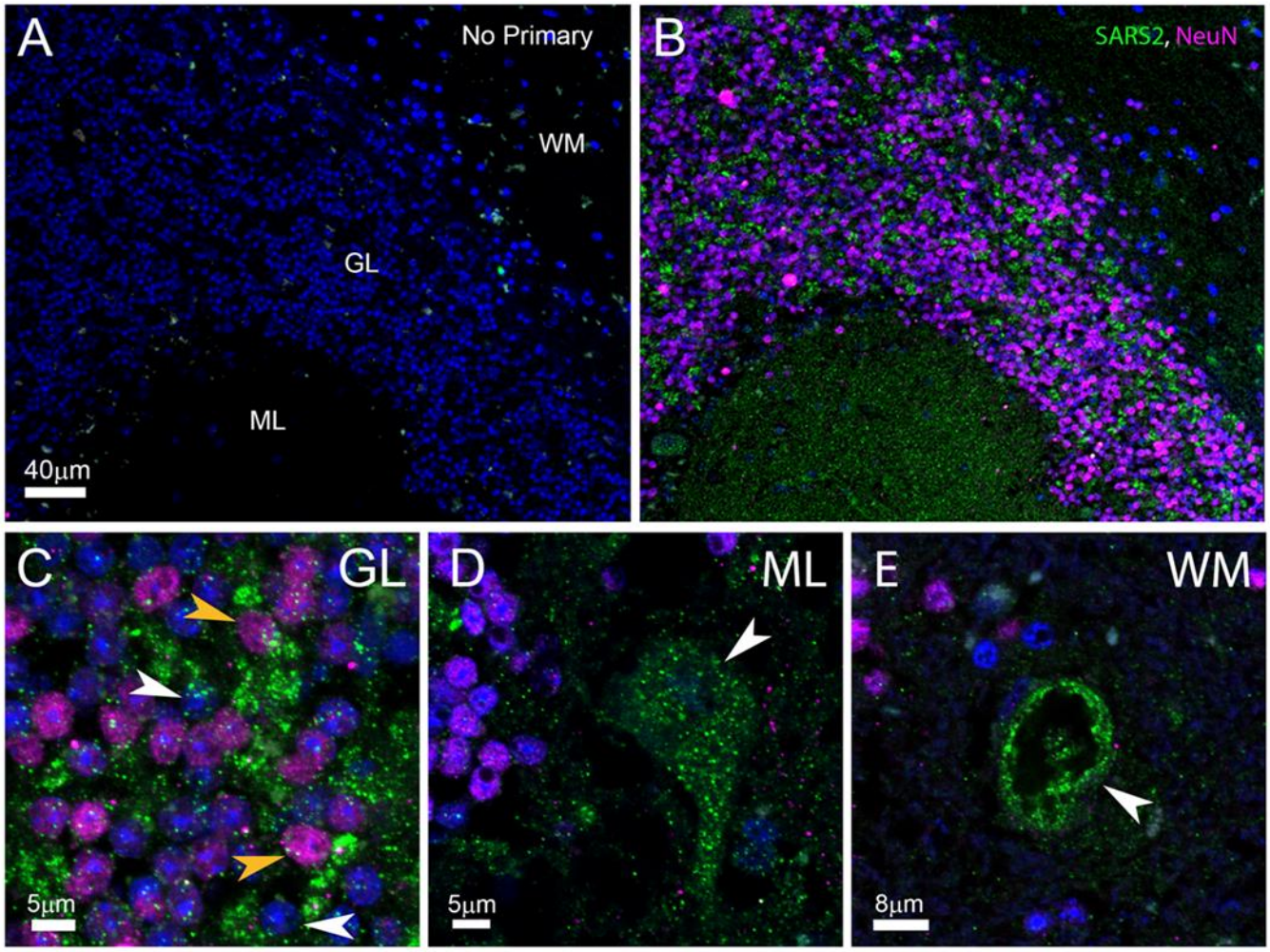

Fig. 3 **SARS-CoV-2 protein expression in human cerebellum**. Low magnification visualization of no-primary control (A) and primary-added adjacent (B) cerebellar sections labeled for SARS-CoV-2 (green) and NeuN (magenta) demonstrate viral-specific protein expression within the tissue. The locations of the molecular layer (ML), granular layer (GL), and white matter (WM) are indicated in (A) and also correspond to (B). Higher magnification images demonstrate cell type-specific infection (C-E). Both NeuN positive neurons (yellow arrows) and other unidentified cells (white arrows) are associated with viral protein in the GL (C). Purkinje cells adjacent to the ML are infected (D, white arrow). In rare instances, blood vessels adjacent

to the GL and WM were associated with viral protein (E, white arrow). The scale bars in A is also associated with B. All immunofluorescent images were obtained by confocal microscopy.

Methods:

Autopsies

Autopsies were performed and tissues were collected as previously described[26] in the National Cancer Institute's Laboratory of Pathology at the National Institutes of Health Clinical Center following consent of the legal next of kin.

Measurement of IgG and IgM antibodies against Nucleocapsid and Spike protein of SARS-CoV-2

Fluid-phase luciferase immunoprecipitation systems (LIPS) assays were used to study IgG and IgM antibody response to SARS-CoV-2. For IgG LIPS measurements, *Renilla* luciferase-nucleocapsid and *Gaussia* luciferase-spike protein extracts were employed with protein A/G beads (Protein A/G UltraLink Resin, Thermo Fisher Scientific) as the IgG capture reagent as previously described with microtiter filter plates[27]. For IgM measurements, anti-human IgM goat agarose beads (Sigma) were substituted as the capture reagent using both the microfilter plate and microtube format[28]. The IgM immunoprecipitation assays performed in 1.5 ml microfuge tube format containing 1 µl sera or plasma, *Renilla* luciferase-nucleocapsid (10 million light unit input per tube) or *Gaussia* luciferase-spike protein (40 million light input per tube) and buffer A (20 mM Tris, pH 7.5, 150 mM NaCl, 5 mM $MgCl_2$, 0.1% Triton X-100) to a total volume of 100 µl. After mixing, the tubes were incubated at room temp for 1 hour. Next 10 µl of the anti-human IgM agarose bead suspension was added to each tube for additional 60 minutes and tubes were placed on a rotating wheel at 4° C. The samples were then washed by brief centrifugation to collect the bead pellet at room temperature 3 times with 1.5 ml Buffer A and once with 1.5 ml of PBS. After the final wash, the beads were mixed with coelenterazine substrate (100 µl) and light

530 units measured in a tube luminometer. Known seronegative and seropositive samples for IgG and
531 IgM antibodies against nucleocapsid and spike proteins were used for assigning seropositive cut-
532 off values and for standardization.
533
534 **SARS-CoV-2 RNA quantification of tissues and body fluids**
535 Total RNA was extracted from RNAlater (Invitrogen)-preserved tissues and body fluids
536 collected at autopsy using the RNeasy Mini, RNeasy Fibrous Tissue Mini, RNeasy Lipid Tissue
537 Mini Kit, and QIAamp Viral RNA Mini Kits (Qiagen) according to the manufacturer's protocols.
538 Upstream tissue processing and subsequent RNA quantification have been previously
539 described[26]. The QX200 AutoDG Droplet Digital PCR System (Bio-Rad) was used to detect and
540 quantify SARS-CoV-2 RNA in technical replicates of 5.5 uL RNA for fluids and up to 550 ng
541 RNA for tissues as previously described[26]. Results were then normalized to copies of N1, N2,
542 and RP per mL of sample input for fluids and per ng of RNA concentration input for tissues. For
543 samples to be considered positive for SARS-CoV-2 N1 or N2 genes, they needed to mean the
544 manufacturer's limit of detection of ≥0.1 copies/µL and ≥2 positive droplets per well. Over 60
545 control autopsy tissues from uninfected patients, representing all organs collected for COVID-19
546 autopsy cases, were used to validate the manufacturer's EUA published LOD for nasopharyngeal
547 swabs for tissues (Extended Data Table 8). ddPCR data for P3[16] as well as a portion of tissues
548 from the oral cavity[26] have been previously reported.
549
550 **sgRNA analysis of ddPCR positive tissues**
551 Tissues that tested positive for one or both SARS-CoV-2 N gene targets via ddPCR had RNA
552 submitted for sgRNA analysis. Briefly, five µl RNA was used in a one-step real-time RT-PCR

assay to sgRNA (forward primer 5'- CGATCTCTTGTAGATCTGTTCTC-3'; reverse primer 5'-ATATTGCAGCAGTACGCACACA-3'; probe 5'-FAM-ACACTAGCCATCCTTACTGCGCTTCG-ZEN-IBHQ-3')[29] using the Rotor-Gene probe kit (Qiagen) according to instructions of the manufacturer. In each run, standard dilutions of counted RNA standards were run in parallel to calculate copy numbers in the samples. The limit of detection for this assay was determined to be <40 Cq (Supplemental Data 1) using 40 control autopsy tissues from uninfected patients, representing all organs collected for COVID-19 autopsy cases.

Viral isolation from select postmortem tissues

Select tissues with high viral RNA levels via ddPCR and sgRNA PCR measuring at or below a 30 Cq underwent virus isolation to prove the presence of infectious virus. Virus isolation was performed on tissues by homogenizing the tissue in 1ml DMEM and inoculating Vero E6 cells in a 24-well plate with 250 µl of cleared homogenate and a 1:10 dilution thereof. Plates were centrifuged for 30 minutes at 1000 rpm and incubated for 30 minutes at 37°C and 5% CO2. The inoculum was then removed and replaced with 500 µl DMEM containing 2% FBS, 50 U/ml penicillin and 50 µg/ml streptomycin. Six days after inoculation, cytopathic effect (CPE) was scored. A blind passage of samples where no CPE was present, was performed according to the same method. Supernatants from plates with CPE present were analyzed via PCR for SARS-CoV-2 to rule out other causes of CPE.

Virus Sequencing Methods

Patients with duration of illness ≤7 d (P27, P19) and 8-14 d (P18) with multiple body site tissues containing sgRNA levels ≤31 Cq value were selected for high throughput, single-genome amplification and sequencing (HT-SGS) as previously described[21]. Presence of variants of SARS-CoV-2 were analyzed within and between tissues.

SARS-CoV-2 RNA *in situ* hybridization

Chromogenic *in situ* detection was performed using the manual RNAScope 2.5 HD assay (Cat# 322310, Advanced Cell Diagnostics, Hayward, CA) with a modified pretreatment protocol. Briefly, formalin-fixed and paraffin-embedded (FFPE) tissue sections were cut at 7 μm, air dried overnight, and baked for 2 hrs at 60ºC. The FFPE tissue sections were deparaffinized, dehydrated, and then treated with pretreat 1 for 10 min at room temperature. The slides were boiled with pretreatment reagent for 15 min, digested with protease at 40ºC for 10 min, then hybridized for 2 hours at 40ºC with probe-*V-nCov2019-S* (Cat# 848561, Advanced Cell Diagnostics). In addition, probe-Hs-*PPIB* (Cat# 313901, Advanced Cell Diagnostics) and probe-*dapB* (Cat# 310043, Advanced Cell Diagnostics) were used as a positive and negative control, respectively. Subsequent amplification was done according to the original protocol. Detection of specific probe binding sites were visualized with RNAScope 2.5 HD Reagent kit-brown chromogenic labels (Advanced Cell Diagnostics). The slides were counterstained with hematoxylin and cover-slipped.

SARS-CoV-2 immunohistochemistry

FFPE cerebellar sections were deparaffinized, rehydrated and subject to 0.01M Citrate buffer antigen retrieval for 20min at 120°C. Slides were incubated in 0.1% TritonX100 in PBS for

30min, washed extensively with PBS and fresh True Black Plus® solution (1:40, Cat#23014, Biotium) applied for 7min. Following PBS wash, blocking serum (5% normal donkey serum/0.3M glycine) was applied for 30min. Primary antibodies against SARS-CoV-2 NP1 (1:250, custom made) and NeuN (1:200, Cat#MAB377, Chemicon) were diluted in blocking serum and applied to slides overnight at 4°C. Species-specific secondary conjugates (1:500, Cat#A32790 and #A32744, ThermoFisher) were applied for 1hr at RT. Hoescht 33342 applied for 10min (1:2000, Cat#H3570, ThermoFisher) labeled nuclei. Slides were cover-slipped with Prolong Gold (Cat#P36930, ThermoFisher).

Data Availability

The datasets that support the findings of this study are available in Supplementary Data 1, 2 and 3. Sequence data described in this manuscript have been deposited (database accession numbers XXXX). The bioinformatic pipeline for HT-SGS data analysis has been deposited (https://github.com/niaid/UMI-pacbio-pipeline). ISH images from our cohort as well as positive and negative controls are available in Supplementary Data 3, which is available at https://halo.cancer.gov, Authentication method: NIH, username: halocancernci@gmail.com, password: covid19N!H.

Methods References:

26. Huang, N., et al. SARS-CoV-2 infection of the oral cavity and saliva. *Nat Med*. **27**, 892–903 (2021). https://doi.org/10.1038/s41591-021-01296-8.
27. Burbelo, P. D., et al. Sensitivity in Detection of Antibodies to Nucleocapsid and Spike Proteins of Severe Acute Respiratory Syndrome Coronavirus 2 in Patients With

Coronavirus Disease 2019. *J Infect Dis*. **222**(2), 206-213 (2020). https://doi.org/10.1093/infdis/jiaa273.

28. Burbelo, P. D., Goldman, R., & Mattson, T. L. A simplified immunoprecipitation method for quantitatively measuring antibody responses in clinical sera samples by using mammalian-produced Renilla luciferase-antigen fusion proteins. *BMC Biotechnol*. **5**, 22 (2005). https://doi.org/10.1186/1472-6750-5-22.
29. Wölfel R., et al. Virological assessment of hospitalized patients with COVID-19. *Nature*. **581**(7809), 465-469 (2020). https://doi.org/10.1038/s41586-020-2196-x.

Acknowledgements:

This study was funded and supported by the Intramural Research Program of the National Institutes of Health, Clinical Center, National Institute of Dental and Craniofacial Research, and National Institute of Allergy and Infectious Diseases.

This research was made possible through the NIH Medical Research Scholars Program, a public-private partnership supported jointly by the NIH and contributions to the Foundation for the NIH from the Doris Duke Charitable Foundation, Genentech, the American Association for Dental Research, and the Colgate-Palmolive Company.

NIH COVID-19 Autopsy Consortium

Daniel S. Chertow[1,2], Kevin M. Vannella[1,2], Sydney R. Stein[1,2], Marcos J. Ramos-Benitez[1,2,4], Andrew P. Platt[1,2], James M. Dickey[1,2], Ashley L. Babyak[1,2], Luis J. Perez Valencia[1,2], Sabrina C. Ramelli[3], Shelly J. Curran[3], Mary E. Richert[3], David E. Kleiner[5], Stephen M. Hewitt[5], Martha Quezado[5], Willie J. Young[5], Sarah P. Young[5], Billel Gasmi[5], Michelly Sampaio De Melo[5],

Sabina Desar[5], Saber Tadros[5], Nadia Nasir[5], Xueting Jin[5], Sharika Rajan[5], Esra Dikoglu[5], Neval Ozkaya[5], Kris Ylaya[5], Joon-Yong Chung[5], Stefania Pittaluga[5], Grace Smith[5], Elizabeth R. Emanuel[6], Brian L. Kelsall[6], Justin A. Olivera[7], Megan Blawas[7], Robert A. Star[7], Alison Grazioli[8], Nicole Hays[9], Madeleine Purcell[9], Shreya Singireddy[9], Jocelyn Wu[9], Katherine Raja[9], Ryan Curto[9], Jean E. Chung[10], Amy J. Borth[10], Kimberly A. Bowers[10], Anne M. Weichold[10], Paula A. Minor[10], Mir Ahmad N. Moshref[10], Emily E. Kelly[10], Mohammad M. Sajadi[11,12], Kapil K. Saharia[11,12], Daniel L. Herr[13], Thomas M. Scalea[14], Douglas Tran[15], Ronson J. Madathil[15], Siamak Dahi[15], Kristopher B. Deatrick[15], Eric M. Krause[16], Joseph Rabin[17], Joseph A. Herrold[18], Ali Tabatabai[18], Eric S. Hochberg[18], Christopher R. Cornachione[18], Andrea R. Levine[18], Justin E. Richards[19], John Elder[20], Allen P. Burke[20], Michael A. Mazzeffi[21], Robert H. Christenson[22], Zackary A. Chancer[23], Mustafa Abdulmahdi[24], Sabrina Sopha[24], Tyler Goldberg[24], Shahabuddin Soherwardi[25], Yashvir Sangwan[26], Michael T. McCurdy[27,12], Kristen Sudano[27], Diane Blume[27], Bethany Radin[27], Madhat Arnouk[27], James W. Eagan Jr[28], Robert Palermo[29], Anthony D. Harris[30]

Affiliations:

1. Emerging Pathogens Section, Department of Critical Care Medicine, Clinical Center, National Institutes of Health, Bethesda, MD, USA
2. Laboratory of Immunoregulation, National Institute of Allergy and Infectious Diseases, Bethesda, MD, USA
3. Critical Care Medicine Department, Clinical Center, National Institutes of Health, Bethesda, MD, USA

4. Postdoctoral Research Associate Training Program, National Institute of General Medical Sciences, National Institutes of Health, Bethesda, MD, USA
5. Laboratory of Pathology, Center for Cancer Research, National Cancer Institute, National Institutes of Health, Bethesda, MD, USA
6. Mucosal Immunobiology Section, Laboratory of Molecular Immunology, National Institute of Allergy and Infectious Diseases, National Institutes of Health, Bethesda, MD, USA
7. Renal Diagnostics and Therapeutics Unit, Kidney Diseases Branch, National Institute of Diabetes and Digestive and Kidney Diseases, National Institutes of Health, Bethesda, MD, USA
8. Kidney Disease Section, Kidney Diseases Branch, National Institute of Diabetes and Digestive and Kidney Diseases, National Institutes of Health, Bethesda, MD, USA
9. University of Maryland School of Medicine, Baltimore, MD, USA
10. University of Maryland Medical Center, Baltimore, MD, USA
11. Institute of Human Virology, University of Maryland School of Medicine, Baltimore, MD, USA
12. Department of Medicine, Division of Pulmonary and Critical Care Medicine, University of Maryland School of Medicine, Baltimore, MD, USA
13. R Adams Cowley Shock Trauma Center, Department of Medicine and Program in Trauma, University of Maryland School of Medicine, Baltimore, MD, USA
14. Department of Shock Trauma Critical Care, University of Maryland School of Medicine, Baltimore, MD, USA

15. Department of Surgery, Division of Cardiac Surgery, University of Maryland School of Medicine, Baltimore, MD, USA
16. Department of Surgery, Division of Thoracic Surgery, University of Maryland School of Medicine, Baltimore, MD, USA
17. R Adams Cowley Shock Trauma Center, Department of Surgery and Program in Trauma, University of Maryland School of Medicine, Baltimore, MD, USA
18. Department of Medicine, Division of Infectious Disease, University of Maryland School of Medicine, Baltimore, MD, USA
19. Department of Anesthesiology, Division of Critical Care Medicine, University of Maryland School of Medicine, Baltimore, MD, USA
20. Department of Autopsy and Thoracic Pathology, University of Maryland School of Medicine, Baltimore, MD, USA
21. Department of Anesthesiology and Critical Care Medicine, George Washington School of Medicine and Health Sciences, Washington, DC USA
22. Department of Laboratory Science, University of Maryland School of Medicine, Baltimore, MD, USA
23. Department of Anesthesiology, University of Southern California Keck School of Medicine, Los Angeles, CA, USA
24. Critical Care Medicine, University of Maryland Baltimore Washington Medical Center, Glen Burnie, MD, USA
25. Hospitalist Department, TidalHealth Peninsula Regional, Salisbury, MD, USA
26. Department of Interventional Pulmonology, TidalHealth Peninsula Regional, Salisbury, MD, USA

27. Division of Critical Care Medicine, Department of Medicine, University of Maryland St. Joseph Medical Center, Towson, MD, USA
28. Department of Pathology, University of Maryland, St. Joseph Medical Center, Towson, MD, USA
29. Department of Pathology, Greater Baltimore Medical Center, Townson, MD, USA
30. Department of Epidemiology and Public Health, University of Maryland School of Medicine, Baltimore, MD, USA

Author Contributions

DSC, KMV, SRS, MJRB, ALB, LJPV, AG, DLH, SMH & DEK contributed to the study design and protocols for autopsy procurement. APP, JMD, MER, AG, NH, MP, SS, JW, KR, RC, JEC, AJB, KAB, AMW, PAM, MANM, EEK, MMS, KKS, DLH, TMS, DT, RJM, SD, KBD, EMK, JR, JAH, AT, ESH, CRC, ARL, JER, JE, APB, MAM, RHC, ZAC, MA, SS, TG, SS, YS, MTM, KS, DB, BR, MA, JWE Jr, RP, and ADH provided care for, recruited, collected samples from, and/or procured medical records for the patients in this study. DEK, SMH, MQ, WJY, SPY, BG, MSDM, SD, ST, NN, XJ, SR, ED, NO, KY, JYC, SP, and GS conducted the autopsies and/or histological and ISH analysis. SRS, MJRB, APP, JMD, ALB, LJPV, SCR, SJC, ERE, BLK, JAO, MB, and RAS assisted with procurement and preservation of autopsy specimens. SRS with assistance from SCR and JMD performed RNA extraction, ddPCR, and data analysis. MS, CKY, VJM, and EDW performed and analyzed data for sgRNA RT-PCR. CWW and KEP conducted IHC on cerebellum. PDB and JIC measured antibody responses to SARS-CoV-2 in perimortem plasma samples. SHK, FB, and EAB performed viral sequencing. SRS drafted the manuscript with critical input from DSC, KMV, SMH, DEK, SCR, APP, MJRB, EDW, VJM, AG, DLH,

KKS, MMS MTM, PDB, JIC, CWW, KEP, and SJC. All authors approved the submitted version of the manuscript.

Competing Interests:

The authors declare no competing or conflict of interest.

Additional Information:

Supplementary information is available for this paper.

Correspondence and requests for materials should be addressed to DSC.

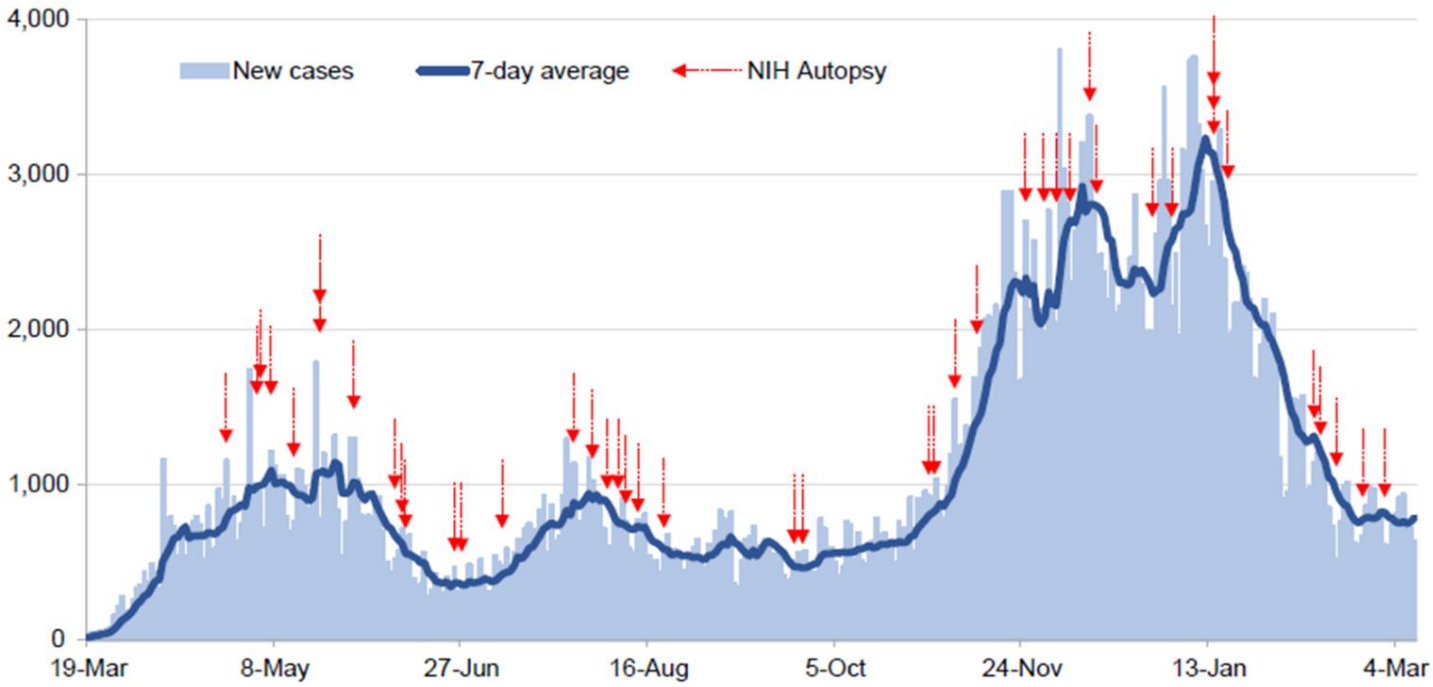

Extended Data Fig. 1 **Autopsy procurement relative to Maryland COVID-19 cases, March 19th, 2020 to March 9th, 2021**. Daily COVID-19 reported cases for Maryland (light blue bars) with 7-day average (dark blue line) with timing of autopsies (red arrows).

Patient ID
Sinus Turbinate
Nasal Placode
Proximal Trachea
Distal Trachea
L Bronchus
R Bronchus
L Superior Lobe
L Middle Lobe
L Inferior Lobe
R Superior Lobe
R Middle Lobe
R Inferior Lobe
Respiratory
R Ventricle
IV Septum
L Ventricle
Pericardium
Thoracic Aorta
Abdominal Aorta
Vena Cava
Carotid Body
Carotid Artery
Femoral Artery
Cardiovascular
Cervical LN
Tracheal LN
Bronchial LN
Vena Cava/Aorta LN
Mediastinal LN
Mesenteric LN
Inguinal/Appendix LN
Spleen
Thymus
Tonsils
Appendix
Lymphoid
Minor SG
Submandibular SG
Parotid SG
Tongue
Uvula
Buccal Mucosa
Esophagus
Duodenum
Jejunum
Ileum
Colon
Rectum
Liver
Gallbladder
Gastrointestinal
L Kidney
R Kidney
L Adrenal Gland
R Adrenal Gland
Thyroid
Parathyroid
Renal & Endocrine
Ovary
Uterus
Breast Tissue
Testis
Repro-ductive
Skeletal Muscle
Diaphragm
Intercostal Muscle
Skin
Subcutaneous Adipose
Central Adipose
Sciatic Nerve
Vagus Nerve
Other Nerve
Muscle, Skin, Adipose & Peripheral Nerves
Choroid/Sclera
Cornea
Lens
Retina
Optic Nerve
Lacrimal Gland
Ocular
Spinal Ganglia
Cervical Spinal Cord
Olfactory Nerve
Basal Ganglia
Frontal Lobe
Parietal Lobe
Temporal Lobe
Occipital Lobe
Medulla
Midbrain
Cerebellum
Dentate Nucleus
Thalamus
Hypothalamus
Corpus Callosum
CNS Vasculature
Dura Mater
Central Nervous System
DOI (days)
≤ 14
15-30
≥31
Average copies N1 & N2/ ng RNA input
100K-500K
10K-99K
5,000-9,999
1,000-4,999
500-999
100-499
50-99.9
10-49.9
5-9.9
1-4.9
0.5-0.99
0.1-0.49
0.05-0.099
0.01-0.049
0.0004-0.0099
NEG
NA
sgRNA +

Extended Data Fig. 2 **Distribution, quantification, and replication of SARS-CoV-2 across the body and brain over time.** The heat map depicts the highest average quantification of SARS-CoV-2 RNA (N) via ddPCR present within all sampled tissues of 44 autopsy cases. Patients are aligned from shortest to longest duration of illness (DOI) prior to death, listed at the bottom of the figure, and grouped into early (0-14 d), mid (15-30 d), and late (≥31 d) DOI. Tissues are grouped by body system beginning with the respiratory tract at the top and CNS at the bottom. Viral RNA levels range from 0.0004 to 500,000 copies per ng of RNA input, depicted as a gradient from dark blue at the lowest level to dark red at the highest level. Tissues that were also positive for sgRNA via real-time RT-PCR are shaded with black vertical bars.

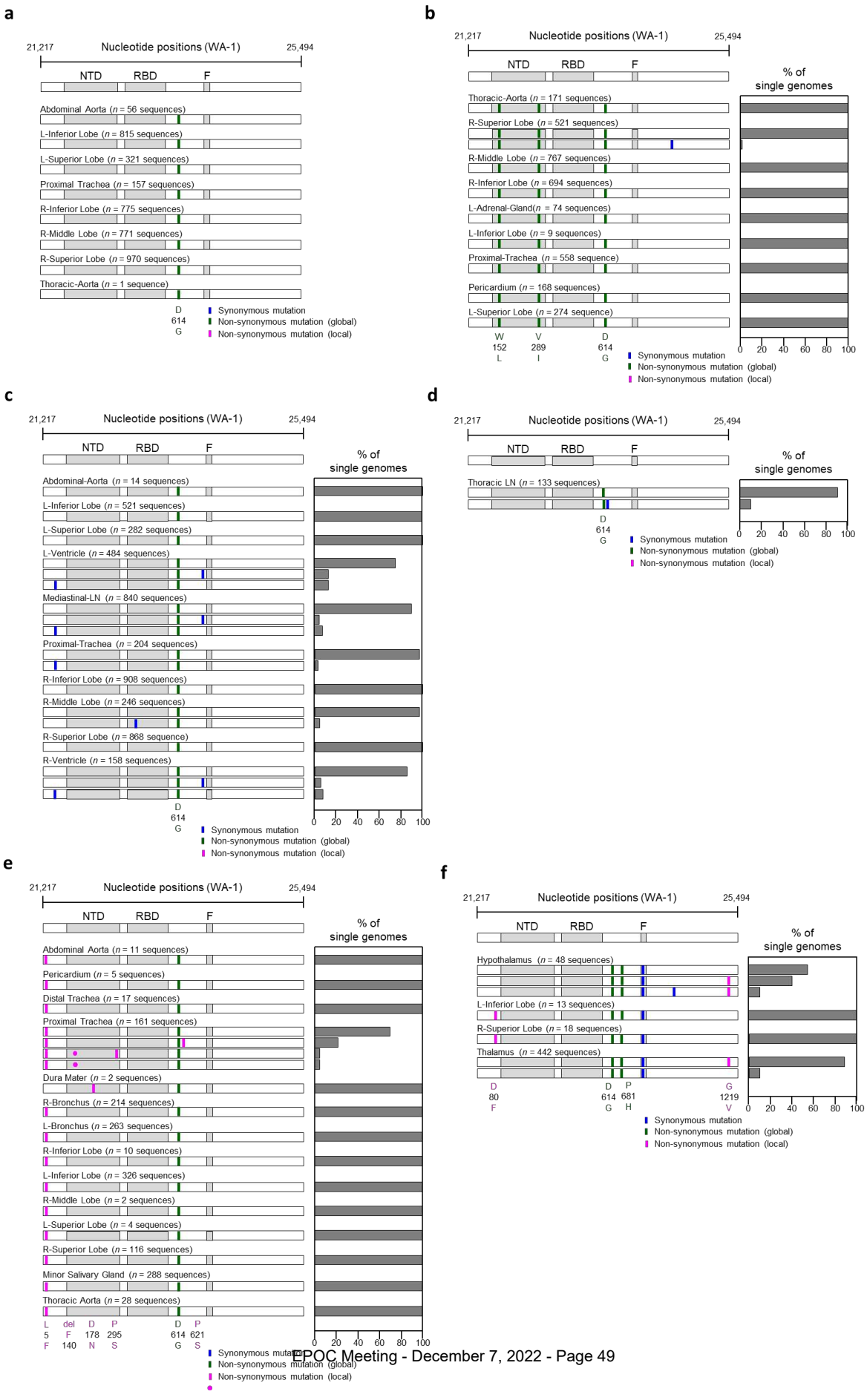
a
21,217
Nucleotide positions (WA-1)
25,494
NTD
RBD
F
Abdominal Aorta (n = 56 sequences)
L-Inferior Lobe (n = 815 sequences)
L-Superior Lobe (n = 321 sequences)
Proximal Trachea (n = 157 sequences)
R-Inferior Lobe (n = 775 sequences)
R-Middle Lobe (n = 771 sequences)
R-Superior Lobe (n = 970 sequences)
Thoracic-Aorta (n = 1 sequence)
D 614 G
Synonymous mutation
Non-synonymous mutation (global)
Non-synonymous mutation (local)
b
21,217
Nucleotide positions (WA-1)
25,494
NTD
RBD
F
% of single genomes
Thoracic-Aorta (n = 171 sequences)
R-Superior Lobe (n = 521 sequences)
R-Middle Lobe (n = 767 sequences)
R-Inferior Lobe (n = 694 sequences)
L-Adrenal-Gland(n = 74 sequences)
L-Inferior Lobe (n = 9 sequences)
Proximal-Trachea (n = 558 sequence)
Pericardium (n = 168 sequences)
L-Superior Lobe (n = 274 sequence)
W 152 L
V 289 I
D 614 G
0 20 40 60 80 100
Synonymous mutation
Non-synonymous mutation (global)
Non-synonymous mutation (local)
c
21,217
Nucleotide positions (WA-1)
25,494
NTD
RBD
F
% of single genomes
Abdominal-Aorta (n = 14 sequences)
L-Inferior Lobe (n = 521 sequences)
L-Superior Lobe (n = 282 sequences)
L-Ventricle (n = 484 sequences)
Mediastinal-LN (n = 840 sequences)
Proximal-Trachea (n = 204 sequences)
R-Inferior Lobe (n = 908 sequences)
R-Middle Lobe (n = 246 sequences)
R-Superior Lobe (n = 868 sequence)
R-Ventricle (n = 158 sequences)
D 614 G
0 20 40 60 80 100
Synonymous mutation
Non-synonymous mutation (global)
Non-synonymous mutation (local)
d
21,217
Nucleotide positions (WA-1)
25,494
NTD
RBD
F
% of single genomes
Thoracic LN (n = 133 sequences)
D 614 G
0 20 40 60 80 100
Synonymous mutation
Non-synonymous mutation (global)
Non-synonymous mutation (local)
e
21,217
Nucleotide positions (WA-1)
25,494
NTD
RBD
F
% of single genomes
Abdominal Aorta (n = 11 sequences)
Pericardium (n = 5 sequences)
Distal Trachea (n = 17 sequences)
Proximal Trachea (n = 161 sequences)
Dura Mater (n = 2 sequences)
R-Bronchus (n = 214 sequences)
L-Bronchus (n = 263 sequences)
R-Inferior Lobe (n = 10 sequences)
L-Inferior Lobe (n = 326 sequences)
R-Middle Lobe (n = 2 sequences)
L-Superior Lobe (n = 4 sequences)
R-Superior Lobe (n = 116 sequences)
Minor Salivary Gland (n = 288 sequences)
Thoracic Aorta (n = 28 sequences)
L 5 F
del F 140
D 178 N
P 295 S
D 614 G
P 621 S
0 20 40 60 80 100
Synonymous mutation
Non-synonymous mutation (global)
Non-synonymous mutation (local)
f
21,217
Nucleotide positions (WA-1)
25,494
NTD
RBD
F
% of single genomes
Hypothalamus (n = 48 sequences)
L-Inferior Lobe (n = 13 sequences)
R-Superior Lobe (n = 18 sequences)
Thalamus (n = 442 sequences)
D 80 F
D 614 G
P 681 H
G 1219 V
0 20 40 60 80 100
Synonymous mutation
Non-synonymous mutation (global)
Non-synonymous mutation (local)

Extended Data Figure 3: **Analysis of SARS-CoV-2 genetic diversity across body compartments in patients**. (a) P18, (b) P19, (c) P27, (d) P33, (e) P36, (f) P38. Haplotype diagrams (left) show SARS-CoV-2 spike single genome sequences detected in multiple organs. Spike NH2-terminal domain (NTD), receptor-binding domain (RBD), and furin cleavage site (F) regions are shaded grey, and remaining regions of the spike are shaded white. Ticks with different colors indicate mutations relative to the WA-1 reference sequence; green indicates non-synonymous differences from WA-1 detected in all sequences in the individual; blue indicates synonymous mutations detected variably within the individual, and pink indicates non-synonymous mutations detected variably within the individual. Bar graphs (right) show the percentage of all single genome sequences in the sample matching each haplotype.

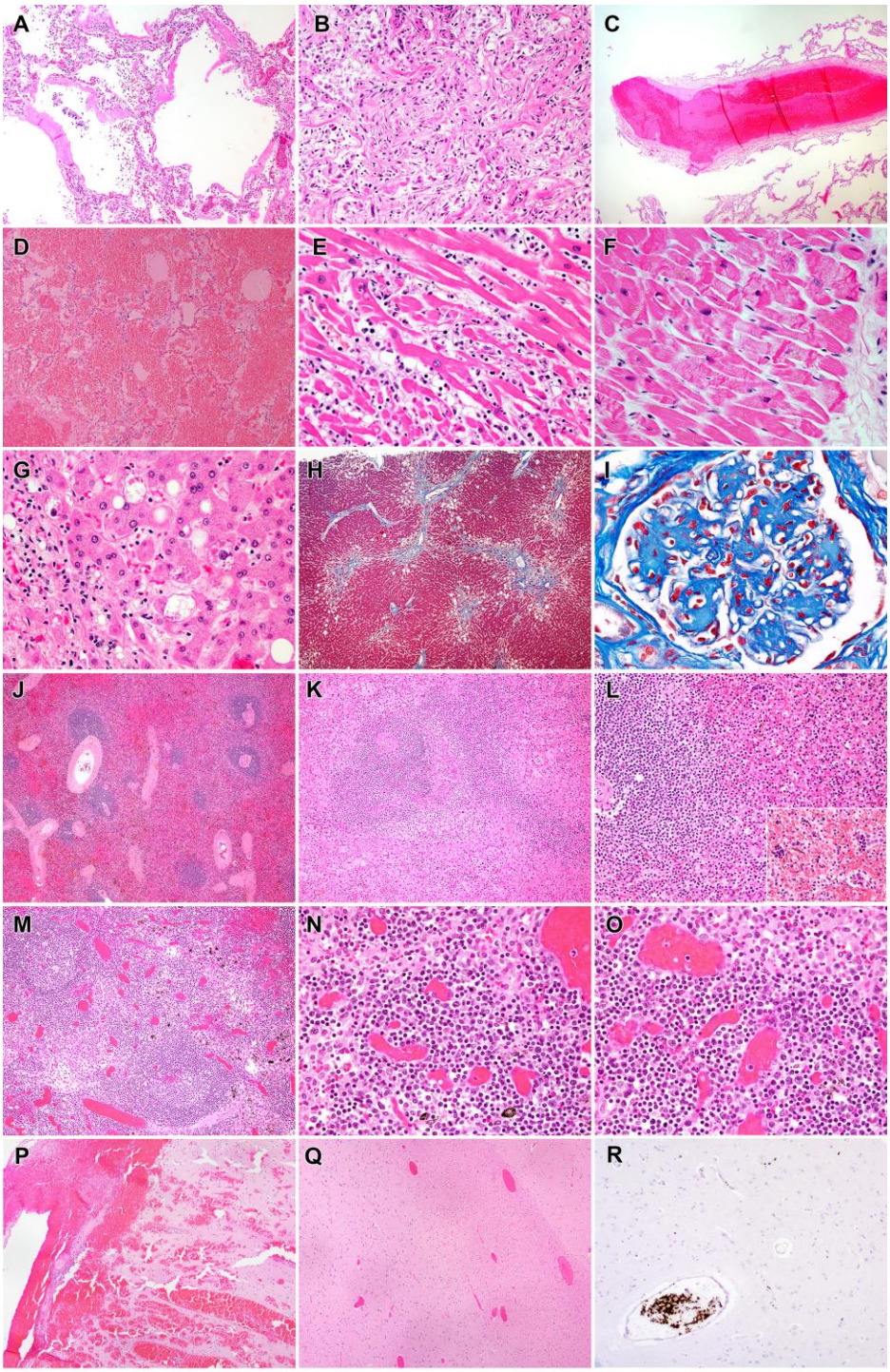

Extended Data Fig. 4 **Representative findings in patients in the COVID-19 cohort**. A. Lung, Subject P22. Exudative phase diffuse alveolar damage with hyaline membranes and mild interstitial inflammation (H&E, 100x). B. Lung, Subject P26. Proliferative phase diffuse alveolar

damage and sparse inflammation. (H&E, 200x). C. Lung, Subject P22. Organizing thrombus in medium sized pulmonary artery. (H&E, 40x). D. Lung, Subject P28. Diffuse pulmonary hemorrhage. (H&E, 100x). E. Heart, Subject P3. Active lymphocytic myocarditis with cardiomyocyte necrosis. (H&E, 400x). F. Heart, Subject P38. Microscopic focus of bland myocardial contraction band necrosis. (H&E, 400x). G. Liver, Subject P41. Steatohepatitis with mild steatosis and scattered ballooned hepatocytes. (H&E, 400x), H. Liver, Subject P41. Focal bridging fibrosis involving central hepatic veins. (Masson trichrome, 40x). I. Kidney, Subject P16. Nodular glomerulosclerosis. (Masson trichrome, 600x). J. Spleen, Subject P16. Preservation of white pulp and congestion (H&E, 40x) K. Spleen, Subject P14. Lymphoid depletion of white pulp with proteinaceous material and red pulp congestion. (H&E, 100x) L. Spleen, Subject P34. Relative preservation of white pulp with extramedullary hematopoiesis (inset) in red pulp (H&E, 200x) M. Lymph node, Subject P25. Follicular hyperplasia with well-defined follicles. (H&E,) N. Lymph node, Subject P25. Marked plasmacytosis in the medullary cord. (H&E, 400x) O. Lymph node, Subject P25. Marked plasmacytosis and sinus histiocytosis. (H&E, 400x) P. Brain, Subject P35, Focal subarachnoid and intraparenchymal hemorrhage. (H&E, 40x) Q. Brain, Subject P44, Vascular congestion. (H&E, 40x) R. Brain, Subject P43, Intravascular platelet aggregates. (anti-CD61 stain, 100x)

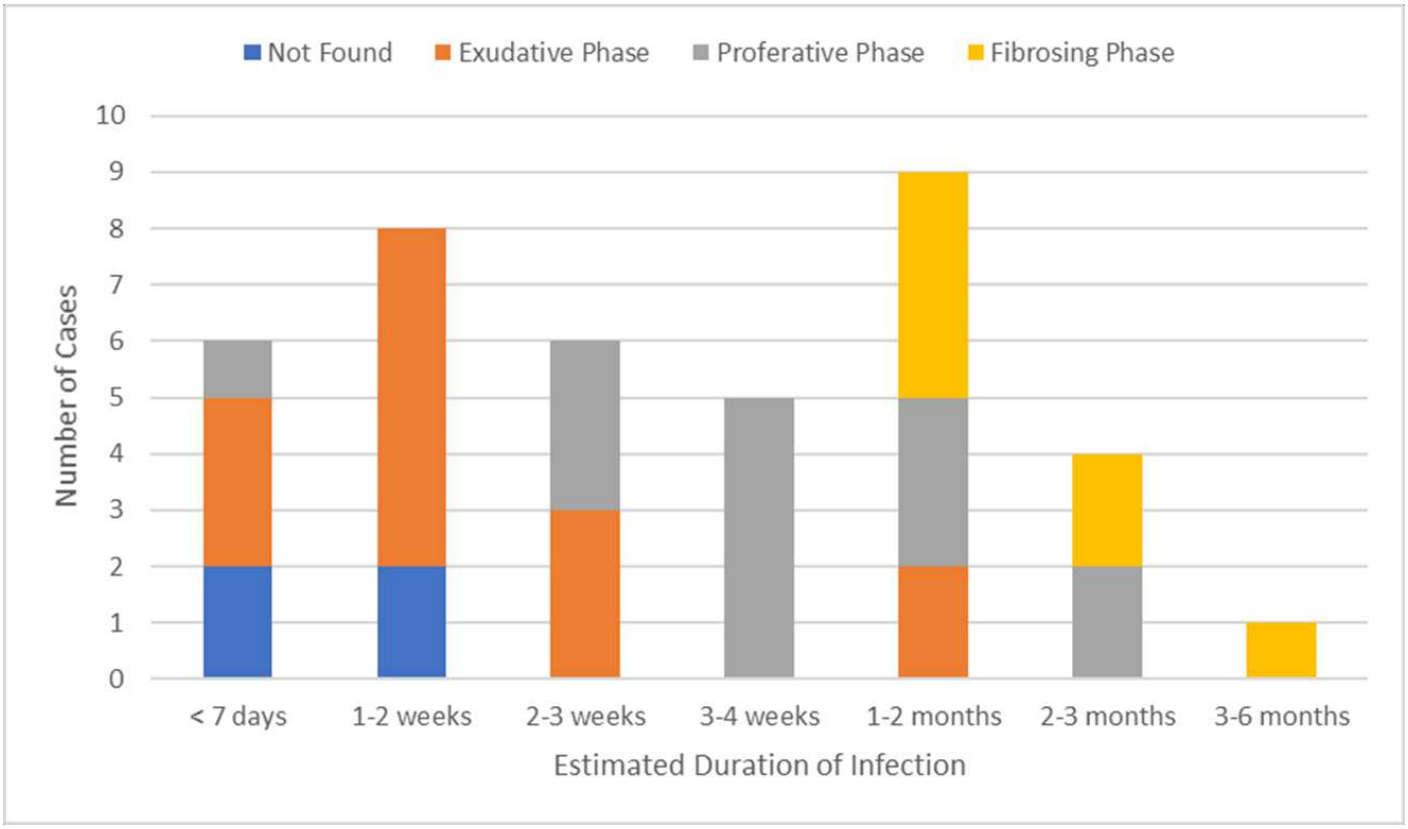

Extended Data Fig. 5 **Temporal association of diffuse alveolar damage in patients dying from COVID-19.** Number of autopsy cases with stages of diffuse alveolar damage via histopathologic analysis by duration of illness. Early time points mainly show the initial exudative phase of diffuse alveolar damage, while patients dying after prolonged illness are more likely to show organizing or fibrosing stages.

a

Age (years)	(n=44)
Mean (Min, Max)	59.2 (6, 91)
Age by group (years)	**n (%)**
0-17	1 (2.3)
18-24	1 (2.3)
25-34	2 (4.5)
35-44	6 (13.6)
45-54	4 (9.1)
55-64	11 (25.0)
65-74	11 (25.0)
75-84	5 (11.4)
≥85	3 (6.8)
Sex	
Male	30 (68.2)
Female	13 (29.5)
Intersex	1 (2.3)
Race/Ethnicity	
Non-Hispanic Asian	1 (2.3)
Non-Hispanic Black or African American	18 (40.9)
Non-Hispanic White	18 (40.9)
Hispanic or Latino	7 (15.9)
BMI	
<18.5	2 (4.5)
18.5-24.9	9 (20.5)
25-29.9	10 (22.7)
30-34.9	9 (20.5)
35.0-39.9	6 (13.6)
≥40	8 (18.1)
Comorbidities	
Autoimmune Disease	5 (11.4)
Cancer	7 (15.9)
Cardiovascular Disease	14 (31.8)
Cerebrovascular Disease	4 (9.1)
Chronic Immunosuppression	6 (13.6)
Chronic Respiratory Disease	15 (34.1)
Diabetes Mellitus	14 (31.8)
History of Thromboembolic Event(s)	3 (6.8)
Hypertension	24 (54.5)
Hyperlipidemia	14 (31.8)
Liver Disease	4 (9.1)
Obesity (body mass index ≥30)	23 (52.3)
Renal Disease	8 (18.2)
1+	42 (95.5)
2+	33 (75.0)
3+	29 (65.9)

b

Disease Course Intervals	Mean (Min, Max)
Symptom onset to hospital admission, days	9.4 (-4, 108)
Symptom onset to death, days	35.2 (1, 230)
Days hospitalized	26.4 (0, 188)
Postmortem Interval (hours)	26.2 (10, 67)
Pharmacologic Interventions	**n (%)**
Vasopressors	38 (86.4)
Antibiotics	41 (93.2)
Systemic Steroids	39 (88.6)
Systemic Anticoagulation	34 (77.3)
Paralytics	25 (56.8)
Inhaled Vasodilators	10 (22.7)
Remdesivir	16 (36.4)
Tocilizumab	4 (9.1)
Convalescent Plasma	6 (13.6)
Nonpharmacologic Interventions	
ECMO	10 (22.7)
Renal Replacement Therapy	18 (40.9)
Intubated	36 (81.8)
Tracheostomy	9 (20.5)
Chest Tube(s)	11 (25.0)

Extended Data Table 1 **Autopsy cohort demographics, comorbidities, and clinical intervention summary**. (a) Summary of demographics and known comorbidities for autopsy cases. (b) Summary of illness course and clinical care for autopsy cases. Data compiled from available patient medical records. ECMO/extracorporeal membrane oxygenation.

Patient ID	Sex	Age, years	Duration of illness, days	BMI	Comorbidities	Immediate Cause of death	Highest level of respiratory support	COVID-19 treatment(s)
Patient 1	M	61	25	31.80	DM, HTN, obesity	Bacterial sepsis and fungal pneumonia	Intubation	Systemic steroids, systemic anticoagulation
Patient 2	F	71	14	39.60	HTN, HLD, COPD, breast cancer, cerebrovascular event, Hx DVT/PE, CHF, AF, dementia, obesity, hypothyroidism, anemia, seizure disorder	Acute pyelonephritis with abscess and likely sepsis	Intubation	Systemic steroids
Patient 3	M	26	14	25.80	Asthma	Lymphocytic myocarditis	Intubation, ECMO	Systemic anticoagulation
Patient 4	M	68	18	31.40	HTN, HLD, obesity	DAD	Intubation	Systemic steroids, remdesivir, tocilizumab, convalescent plasma
Patient 5	M	41	42	50.60	Obesity	Fungal pneumonia	Intubation	Systemic steroids, Systemic anticoagulation
Patient 6	M	62	19	45.00	HTN, obesity	Acute bronchopnuemonia	Intubation	Systemic steroids, systemic anticoagulation, inhaled vasodilators
Patient 7	M	60	7	24.30	DM, CML, HTN, AF, CHF, CAD s/p bypass, PVD, CKD, Hx kidney transplant, chronic immunosuppression, HLD, hyperparathyroidism, hypothyroidism, anemia	Acute polymicrobial bronchopneumonia superimposed on DAD	Intubation	Systemic anticoagulation
Patient 8	F	68	24	58.10	HTN, asthma, COPD, cerebrovascular disease, obesity, anemia, chronic fatigue, fibromyalgia	Acute polymicrobial bronchopneumonia superimposed on DAD	Intubation	Systemic steroids, systemic anticoagulation
Patient 9	M	43	66	34.00	Obesity	Pneumonia and sepsis	Intubation, Tracheostomy, ECMO	Systemic steroids, systemic anticoagulation, paralytics, remdesivir, convalescent plasma
Patient 10	F	70	29	35.43	DM, HTN, HLD, CHF, COPD, obesity	Sepsis	Nasal Canula	Remdesivir
Patient 11	M	50	58	36.70	Obesity	Acute pneumonia	Intubation, Tracheostomy, ECMO	Systemic steroids, systemic anticoagulation, tocilizumab
Patient 12	M	61	48	41.80	DM, HTN, HLD, CHF, LV dysfunction, asthma, obesity	DAD, exudative phase	Intubation	Systemic anticoagulation
Patient 13	M	48	82	41.00	Obesity	DAD, organizing phase	Intubation, Tracheostomy, ECMO	Systemic steroids, systemic anticoagulation, tocilizumab, convalescent plasma
Patient 14	M	64	16	30.60	HTN, COPD, obesity	Acute bacterial bronchoneumonia	Intubation	Systemic steroids, systemic anticoagulation
Patient 15	M	65	27	19.70	HLD, sarcoidosis, chronic immunosuppression	Fungal pneumonia and sepsis	Intubation	Systemic steroids, systemic anticoagulation, remdesivir, convalescent plasma
Patient 16	M	87	8	26.90	DM, HTN, HLD, CAD, CHF, ESRD	DAD, exudative phase	AVAPS	Systemic steroids, systemic anticoagulation, convalescent plasma
Patient 17	M	36	14	27.17	Drug abuse	Bilateral bronchopneumonia	Intubation, ECMO	Systemic steroids, systemic anticoagulation
Patient 18	F	79	9	32.60	DM, HTN, COPD, Hx DVT, CAD, cirrhosis, CKD, obesity, anemia, seizure disorder	DAD, exudative phase	Intubation	Systemic steroids
Patient 19	M	43	7	21.90	DM	Sudden cardiac death	Intubation	Systemic steroids, systemic anticoagulation
Patient 20	M	42	99	23.50	DM, HLD	DAD, proliferative and fibrosing phase	Intubation, Tracheostomy, ECMO	Systemic steroids, systemic anticoagulation, convalescent plasma
Patient 21	M	77	12	25.20	DM, HTN, COPD, pulmonary fibrosis, CAD, CHF, CKD, Hx prostate cancer, cerebrovascular disease	DAD, exudative phase	High flow nasal canula, BiPAP	Systemic steroids, systemic anticoagulation
Patient 22	M	64	4	29.90	HTN, HLD	DAD/ARDS	Intubation	Systemic steroids, systemic anticoagulation
Patient 23	M	79	23	28.00		Pulmonary hemorrhage	Intubation	Systemic steroids, systemic anticoagulation
Patient 24	M	59	12	34.20	Hx recurrent aspiration pneumonia, MS, chronic immunosuppression, obesity	Acute pneumonia	BiPAP	Systemic steroids, systemic anticoagulation
Patient 25	F	91	9	16.50	Cardiomyopathy, arrhythmia, dementia, inflammatory polyneuropathy, anemia	DAD, acute phase	None	Systemic steroids, remdesivir
Patient 26	M	48	29	28.20		Cerebral hemorrhage	Intubation, ECMO	Systemic steroids, systemic anticoagulation, remdesivir
Patient 27	Inter-sex	76	1	20.90	Turner Syndrome, aortic stenosis, sick sinus syndrome s/p pacemaker, dementia, hypothyroidism	Bronchopneumonia and DAD, exudative phase	Intubation	Systemic steroids, systemic anticoagulation, remdesivir
Patient 28	F	44	7	30.9	HTN, obesity	Pulmonary thromboembolic disease in the setting of DAD, exudative phase of	None	
Patient 29	M	60	204	24.91	HTN, ILD, cerebrovascular disease, CAD, RA, Hx lung transplant, chronic immunosuppression	Herpetic tracheobronchitis and DAD, s/p bilateral lung transplantation	Intubation, Tracheostomy, ECMO	Systemic steroids, systemic anticoagulation
Patient 30	F	70	15	26.00	HTN, ILD, PH, CHF, CAD, PAD, CKD, ESRD, congenital heart malformation, calciphylaxis	Bacterial pneumonia, SARS-CoV-2 infection	Intubation	Systemic steroids, systemic anticoagulation, remdesivir
Patient 31	M	59	18	26.50	DM, HTN, HLD	Bacterial pneumonia	Intubation, Tracheostomy	Systemic steroids, systemic anticoagulation, remdesivir
Patient 32	F	71	6	31.50	Asthma, COPD, sarcoidosis, cirrhosis, ESRD, Hx endocarditis, obesity, hypothyroidism, seizure disorder, anemia	Right heart failure	BiPAP	Systemic steroids
Patient 33	M	71	76	29.1	HTN, CKD, Hx Lyme disease	Bacterial pneumonia	High flow nasal canula	Systemic steroids, systemic anticoagulation
Patient 34	M	87	36	22.20	HLD, MM, COPD, CKD, seizure disorder, chronic immunosuppression, hypothyroidism	DAD, organizing to fibrosing phase	Intubation	Systemic steroids, remdesivir
Patient 35	F	45	25	63.00	DM, HTN, HLD, COPD, obesity, chronic lower extremetity lymphedema	DAD, organizing phase	Intubation	Systemic steroids, systemic anticoagulation, remdesivir
Patient 36	F	6	4	17.40	Dravet syndrome, SCN1A gene mutation, seizure disorder	Acute cerebral ischemia with tonsillar herniation	Intubation	Systemic steroids, remdesivir
Patient 37	M	63	5	19.80	DM, HTN, Hx femoral artery thrombosis, CHF, CAD, PAD, AF, cardiomyopathy, Hx cardiac tamponade, hepatitis C, abnormal liver function, drug abuse	Bronchopneumonia	Intubation	Systemic steroids, systemic anticoagulation
Patient 38	M	71	13	40.20	HTN, HLD, COPD, prostate cancer, obesity	Bronchopneumonia	Intubation	Systemic steroids, systemic anticoagulation, remdesivir
Patient 39	M	27	31	39.20	Obesity	DAD, organizing to fibrotic phase and multiple pulmonary infarcts	Intubation, Tracheostomy, ECMO	Systemic steroids, systemic anticoagulation, remdesivir
Patient 40	F	68	47	35.11	HTN, uterine cancer, obesity	Sepsis with signs of cardiac dysfunction in the setting of DAD, proliferative and fibrotic phase	Intubation, Tracheostomy	Systemic steroids, systemic anticoagulation, remdesivir
Patient 41	F	75	33	24.94	DM, HTN, HLD, hypothyroidism	DAD, proliferative and fibrotic phase	Intubation	Systemic steroids
Patient 42	M	68	230	36.87	CAD, hepatitis A, liver failure, Hx liver transplant, chronic immunosuppression, obesity	Massive hepatic necrosis, status-post liver transplant	Intubation, Trachesostomy	Systemic steroids, systemic anticoagulation
Patient 43	F	61	18	32.22	DM, HTN, breast cancer, CAD, obesity	DAD, exudative and proliferative phase	Intubation	Systemic steroids, systemic anticoagulation
Patient 44	M	21	65	58.00	Obesity	Bacterial pneumonia superimposed on DAD, fibrosing stage	Intubation, ECMO	Systemic steroids, systemic anticoagulation, remdesivir, tocilizumab

Extended Data Table 2 **Individual case demographics and clinical summary.** Data obtained from available medical records. AF/atrial fibrillation, AVAPS/average volume-assured pressure support, BiPAP/bilevel positive airway pressure, CAD/coronary artery disease, CHF/congestive heart failure, CKD/chronic kidney disease, CML/chronic myeloid leukemia, COPD/chronic obstructive pulmonary disease, DAD/diffuse alveolar damage, DM/diabetes mellitus, DVT/deep vein thrombosis, ECMO/extracorporeal membrane oxygenation, ESRD/end-stage renal disease, HLD/hyperlipidemia, HTN/hypertension, Hx/historical, ILD/interstitial lung disease, LV/left ventricular, MS/multiple sclerosis, PE/pulmonary embolism, PVD/peripheral vascular disease, PH/pulmonary hypertension, s/p/status post.

a

Tissue Category	DOI (days)	Avg. N gene copies/ng RNA (SD)
Respiratory Tract	≤14	9,210.10 (43,179.20)
	15-30	19.67 (77.98)
	≥31	0.65 (2.61)
Cardiovascular	≤14	38.75 (106.08)
	15-30	0.59 (3.43)
	≥31	0.42 (2.51)
Lymphoid	≤14	30.01 (157.86)
	15-30	0.35 (1.28)
	≥31	0.73 (3.83)
Gastrointestinal	≤14	24.68 (99.37)
	15-30	0.87 (4.38)
	≥31	0.24 (2.17)
Renal & Endocrine	≤14	12.76 (59.01)
	15-30	0.03 (0.16)
	≥31	0.04 (0.33)
Reproductive	≤14	0.36 (0.58)
	15-30	1.87 (6.72)
	≥31	0.01 (0.02)
Muscle, Nerve, Adipose, & Skin	≤14	27.50 (101.13)
	15-30	50.65 (284.46)
	≥31	0.54 (3.03)
Ocular	≤14	57.40 (242.40)
	15-30	0.07 (0.24)
	≥31	0.03 (0.12)
Central Nervous System	≤14	32.93 (121.69)
	15-30	2.37 (7.34)
	≥31	0.39 (1.40)

b

Tissue	DOI (days)	ddPCR+ (n, %)	sgRNA+ (n,%)
All Respiratory		**43/44, 97.7**	**23/43, 53.5**
Trachea	≤14	15/17, 88.2	11/15, 73.3
	15-30	11/13, 84.6	1/11, 9.1
	≥31	12/14, 85.7	0/12, 0
	Total	*38/44, 86.4*	*12/38, 31.6*
Bronchus	≤14	15/17, 88.2	11/15, 73.3
	15-30	10/11, 90.9	1/10, 10.0
	≥31	11/13, 84.6	1/11, 9.1
	Total	*36/41, 87.8*	*13/36, 36.1*
Lung	≤14	16/17, 94.1	14/16, 87.5
	15-30	13/13, 100	5/13, 38.5
	≥31	14/14, 100	3/14, 21.4
	Total	*43/44, 97.7*	*22/43, 51.2*
All Cardiovascular		**35/44, 79.5**	**14/35, 40.0**
Myocardium	≤14	14/17, 82.4	8/14, 57.1
	15-30	8/13, 61.5	0/8, 0
	≥31	9/14, 64.3	0/9, 0
	Total	*31/44, 70.5*	*8/31, 25.8*
Pericardium	≤14	15/17, 88.2	7/15, 46.7
	15-30	5/13, 38.5	1/5, 20.0
	≥31	4/13, 30.8	0/4, 0
	Total	*24/43, 55.8*	*8/24, 33.3*
Aorta	≤14	13/14, 92.9	10/13, 76.9
	15-30	6/10, 60.0	1/5*, 20.0
	≥31	5/13, 38.5	1/5, 20.0
	Total	*24/37, 64.9*	*12/23, 52.2*
Vena Cava	≤14	5/5, 100	1/5, 20.0
	15-30	2/5, 40.0	0/2, 0
	≥31	0/2, 0.0	NA
	Total	*7/12, 58.3*	*1/7, 14.3*
All Lymphoid		**38/44, 86.4**	**16/38, 42.1**
LN from Thorax	≤14	15/17, 88.2	11/15, 73.3
	15-30	11/13, 84.6	2/11, 18.2
	≥31	12/13, 92.3	2/12, 16.7
	Total	*38/43, 88.4*	*15/38, 39.5*
LN from Abdomen	≤14	6/11, 54.5	2/6, 33.3
	15-30	4/8, 50	0/4, 0
	≥31	1/5, 20	0/1, 0
	Total	*11/24, 45.8*	*2/11, 18.2*
Spleen	≤14	12/17, 70.6	3/12, 25.0
	15-30	3/13, 23.1	0/3, 0
	≥31	2/14, 14.3	0/2, 0
	Total	*17/44, 38.6*	*3/17, 17.6*
Appendix	≤14	5/13, 38.5	1/5, 20.0
	15-30	2/9, 22.2	0/2, 0
	≥31	3/13, 23.1	1/3, 33.3
	Total	*10/35, 28.6*	*2/10, 20.0*
All Gastrointestinal		**32/44, 72.7**	**10/32, 31.3**
Salivary Glands	≤14	8/11, 72.7	4/8, 50.0
	15-30	5/11, 45.5	0/5, 0
	≥31	3/13, 23.1	1/3, 33.3
	Total	*16/35, 45.7*	*5/16, 31.3*
Tongue	≤14	2/2, 100	2/2, 100
	15-30	3/5, 60.0	2/3, 66.7
	≥31	3/5, 60.0	0/3, 0
	Total	*8/12, 66.7*	*4/8, 50.0*
Small Intestine	≤14	13/17, 76.5	2/13, 15.4
	15-30	7/13, 53.8	1/7, 14.3
	≥31	5/14, 35.7	0/5, 0
	Total	*25/44, 56.8*	*3/25, 12.0*
Colon	≤14	10/17, 58.8	2/10, 20.0
	15-30	4/11, 36.4	0/4, 0
	≥31	2/14, 14.3	0/2, 0
	Total	*16/42, 38.1*	*2/16, 12.5*
Liver	≤14	10/17, 58.8	4/10, 40.0
	15-30	5/13, 38.5	0/5, 0
	≥31	3/14, 21.4	0/2*, 0
	Total	*18/44, 40.9*	*4/17, 23.5*
All Renal & Endocrine		**28/44, 63.6**	**10/28, 35.7**
Kidney	≤14	12/17, 70.6	4/12, 33.3
	15-30	5/13, 38.5	0/5, 0
	≥31	3/14, 21.4	1/3, 33.3
	Total	*20/44, 45.5*	*5/20, 25.0*
Adrenal Gland	≤14	12/16, 75.0	5/12, 41.7
	15-30	4/13, 30.8	0/4, 0
	≥31	5/14, 35.7	0/5, 0
	Total	*21/43, 48.8*	*5/21, 23.8*
Thyroid	≤14	10/16, 62.5	7/10, 70.0
	15-30	4/12, 33.3	0/4, 0
	≥31	3/13, 23.1	0/3, 0
	Total	*17/41, 41.5*	*7/17, 41.2*
Pancreas	≤14	11/17, 64.7	3/11, 27.3
	15-30	3/12, 25.0	0/3, 0
	≥31	2/14, 14.3	0/2, 0
	Total	*16/43, 37.2*	*3/16, 18.8*

Tissue	DOI (days)	ddPCR+ (n, %)	sgRNA+ (n,%)
All Reproductive		**17/40, 42.5**	**2/17, 11.8**
Ovary	≤14	3/5, 60.0	0/3, 0
	15-30	0/3, 0	NA
	≥31	NA	NA
	Total	*3/8, 37.5*	*0/3, 0*
Uterus	≤14	1/1, 100	0/1, 0
	15-30	2/2, 100	1/2, 50.0
	≥31	NA	NA
	Total	*3/3, 100*	*1/3, 33.3*
Testis	≤14	7/10, 70.0	1/7, 14.3
	15-30	1/8, 12.5	0/1, 0
	≥31	3/12, 25.0	0/3, 0
	Total	*11/30, 36.7*	*1/11, 9.1*
Muscle, Skin, & Peripheral Nerves		**30/44, 68.2**	**9/30, 30.0**
Skeletal Muscle	≤14	12/17, 70.6	5/12, 41.7
	15-30	7/13, 53.8	1/7, 14.3
	≥31	3/14, 21.4	0/3, 0
	Total	*22/44, 50*	*6/22, 27.3*
Skin	≤14	3/3, 100	1/3, 33.3
	15-30	1/1, 100	0/1, 0
	≥31	1/7, 14.3	0/1, 0
	Total	*5/11, 45.5*	*1/5, 20.0*
Peripheral Nervous System	≤14	13/15, 86.7	5/13, 38.5
	15-30	6/11, 54.5	0/6, 0
	≥31	7/14, 50.0	2/7, 28.6
	Total	*26/40, 65.0*	*8/26, 30.8*
All Ocular		**22/38, 57.9**	**7/21*, 33.3**
Ocular Tissue	≤14	9/12, 75.0	6/9, 67.7
	15-30	4/9, 44.4	0/4, 0
	≥31	6/11, 54.5	1/5*, 20.0
	Total	*19/32, 59.4*	*7/18, 38.9*
Ocular Humor	≤14	6/13, 46.2	1/6, 16.7
	15-30	3/11, 27.3	0/3, 0
	≥31	2/10, 20.0	0/1*, 0
	Total	*11/34, 32.4*	*1/10, 10.0*
Optic Nerve	≤14	10/12, 83.3	3/10, 30.0
	15-30	2/6, 33.3	0/2, 0
	≥31	5/11, 45.5	0/5, 0
	Total	*17/29, 58.6*	*3/17, 17.6*
All Central Nervous System		**10/11, 90.9**	**4/10, 40.0**
Cervical Spinal Cord	≤14	2/2, 100	1/2, 50.0
	15-30	1/1, 100	0/1, 0
	≥31	5/6, 83.3	0/5, 0
	Total	*8/9, 88.9*	*1/8, 12.5*
Olfactory Nerve	≤14	2/3, 66.7	1/2, 50.0
	15-30	1/2, 50.0	0/1, 0
	≥31	3/5, 60.0	0/3, 0
	Total	*6/10, 60.0*	*1/6, 16.7*
Basal Ganglia	≤14	1/2, 50.0	0/1, 0
	15-30	1/2, 50.0	0/1, 0
	≥31	3/4, 75.0	0/3, 0
	Total	*5/8, 62.5*	*0/5, 0*
Cerebral Cortex	≤14	3/3, 100	1/3, 33.3
	15-30	1/2, 50.0	1/1, 100
	≥31	5/6, 83.3	0/5, 0
	Total	*9/11, 81.8*	*2/9, 22.2*
Brainstem	≤14	3/3, 100	1/3, 33.3
	15-30	1/2, 50.0	1/1, 100
	≥31	4/5, 80.0	0/4, 0
	Total	*8/10, 80.0*	*2/8, 25.0*
Cerebellum	≤14	2/3, 66.7	0/2, 0
	15-30	1/2, 50.0	0/1, 0
	≥31	6/6, 100	0/6, 0
	Total	*9/11, 81.8*	*0/9, 0*
Thalamus	≤14	2/2, 100	1/2, 50.0
	15-30	1/2, 50.0	0/1, 0
	≥31	5/6, 83.3	0/5, 0
	Total	*8/10, 80.0*	*1/8, 12.5*
Hypothalamus	≤14	2/2, 100	1/2, 50.0
	15-30	1/1, 100	0/1, 0
	≥31	4/4, 100	0/4, 0
	Total	*7/7, 100*	*1/7, 14.3*
Corpus Callosum	≤14	2/2, 100	0/2, 0
	15-30	1/1, 100	0/1, 0
	≥31	4/4, 100	0/4, 0
	Total	*7/7, 100*	*0/7, 0*
CNS Vasculature	≤14	2/2, 100	0/2, 0
	15-30	1/2, 50	0/1, 0
	≥31	3/5, 60	0/3, 0
	Total	*6/9, 66.7*	*0/6, 0*
Dura Mater	≤14	3/3, 100	2/3, 66.7
	15-30	0/1, 0	NA
	≥31	0/5, 0	NA
	Total	*3/9, 33.3*	*2/3, 66.7*

Extended Data Table 3 **Summary of SARS-CoV-2 RNA and sgRNA by tissue category over time**. (a) Summary of the average nucleocapsid gene copies/ng RNA across cases by tissue category and duration of illness (days). (b) Summary of the number and percentage of cases with SARS-CoV-2 RNA detected via droplet digital (dd)PCR by tissue category for all cases and by tissue and duration of illness (days). The number and percentage of tissues positive for ddPCR that were additionally positive for subgenomic (sg)RNA PCR is listed in the right most column. *A tissue positive via ddPCR was not tested via sgRNA PCR. CNS/central nervous system, LN/lymph node.

Cell Type	Locations
Bile duct epithelium	Liver
Chondrocytes	Bronchial cartilage rings
Collecting duct epithelium	Kidney
Distal tubule epithelium	Kidney
Endocrine cells of adrenal	Adrenal gland
Endocrine cells of thyroid	Thyroid
Endothelium	Vasculature, all
Ependyma	Brain
Exocrine cells of pancreas	Pancreas
Fibroblast-like cells	Pericardium, heart, trachea, bronchus
Germ cells	Testis
Glandular epithelum	Uterus
Glia	Brain, all locations
Hepatocytes	Liver
Hyaline Membrane	Lung
Interstitial cells of endometrium	Uterus
Intimal cells	Aorta
Kupffer cells	Liver
Leydig cells	Testis
Mononuclear leukocytes	Lung, spleen, lymph nodes, lymphoid aggregates of GI
Mucosal epithelium	Small intestine, colon
Mucus secreting epithelium, salivary type	Salivary glands, trachea, bronchus
Myocytes, Cardiac	Heart
Myocytes, Striated	Psoas muscle
Myocytes, Smooth	Uterus, GI
Neurons	Brain, all locations
Parietal cells	Kidney, Bowman's capsule
Pneumocytes, type I & II	Lung
Purkinje cell	Cerebellum
Schwann cells	Nerves, all
Sertoli cells	Testis
Stratified epithelium (& basal layer)	Trachea, esophagus
Stromal cells	Pericardium, uterus, ovary
Vascular smooth muscle	Arteries, all

Extended Data Table 4 **SARS-CoV-2 cellular tropism**. Summary of cell types that were identified as SARS-CoV-2 positive by ISH, and the corresponding anatomic sites in which this was observed.

Cause of Death	N = 44
Death with (but not from) COVID-19	5 (11%)
Death from COVID-19 or complications	39 (89%)
Pulmonary Findings[1]	**N (%) or Median (IQR)**
Left Lung Weight (g)[2]	795 (327)
Right Lung Weight (g)[2]	820 (365)
Combined Lung Weight (g)	1600 (528)
Diffuse Alveolar Damage	
Exudative	14 (32%)
Proliferate	15 (34%)
Fibrosing	7 (16%)
Not Found	8 (18%)
Acute Pneumonia	27 (61%)
Pulmonary Edema	30 (68%)
Pulmonary Hemorrhage (at least focal)	14 (32%)
Pulmonary Thromboembolism, Infarction	10 (23%)
Emphysematous changes (underlying COPD)	12 (27%)
Cardiac Findings	
Heart Weight (g)	500 (175)
Myocardial Infiltrate	4 (9%)
Focal infiltrate without myocyte necrosis	3 (7%)
Diffuse lymphocytic myocarditis	1 (2%)
Myocardial Ischemic Necrosis	
Remote, fibrotic	5 (11%)
Acute microscopic ischemia	4 (9%)
Coronary Artery Disease with ≥ 50% in at least 1 artery	16 (36%)
Renal Findings	
Left Kidney Weight (g)[4]	180 (107)
Right Kidney Weight (g)[4]	168 (79)
Changes consistent with Acute Kidney Injury	17 (39%)
Changes consistent with Diabetic glomerulopathy	10 (23%)
Splenic Findings	
Splenic Weight (g)	235 (215)
Follicular hyperplasia	15 (34%)
Lymphodepletion	
Present	8 (18%)
Some, Partial Preservation	34 (77%)
No Lymphodepletion	2 (5%)
Red Pulp Congestion	35 (80%)
Infarction	2 (5%)

Lymph Node Findings[5]	N (%) or Median (IQR)
Lymphodepletion	
Present	5 (12%)
Some, Partial Preservation	4 (10%)
No Lymphodepletion	31 (78%)
Follicular Hyperplasia	
Present	22 (55%)
Present, regressed	2 (5%)
Paracortical Hyperplasia	32 (80%)
Plasmacytosis	19 (48%)
Plasmablasts noted	4 (10%)
Hepatic Findings[3]	
Liver Weight (g)[4]	1670 (900)
Hepatic necrosis	
None	30 (70%)
Zonal	12 (28%)
% Zonal Necrosis	30% (40%)
Massive	1 (2%)
Steatosis	
None to Minimal	24 (56%)
Mild	14 (33%)
Moderate	5 (12%)
Steatohepatitis	5 (12%)
Portal Inflammation	
None to Minimal	16 (37%)
Mild	23 (53%)
Moderate	4 (9%)
Fibrosis	
None	27 (63%)
Periportal or perisinusoidal	6 (14%)
Periportal and perisinusoidal	1 (2%)
Bridging fibrosis	6 (14%)
Cirrhosis	3 (7%)
Central Nervous System Findings (N=11)	
Brain Weight (g)	1350 (230)
Hypoxic/Ischemic Injury (focal or diffuse)	5 (45%)
Vascular congestion	5 (45%)
Focal (microscopic) hemorrhage	2 (18%)
No pathological findings	3 (27%)

Extended Data Table 5 **Histopathologic findings of COVID-19 autopsy cases**. Summary of histopathologic findings across organ system across 44 autopsy cases. Central nervous system findings are reported for the 11 cases in which consent for sampling was obtained. [1]Includes one

883 case in which the COVID lungs were transplanted and data from explanted lungs used in table.

884 [2]Individual lung weights were missing in 4 cases. [3]Findings missing on 1 case due to extreme

885 autolysis. [4]Weight missing on one case. [5]Lymph node findings missing in 4 cases

Supplementary Files

This is a list of supplementary files associated with this preprint. Click to download.

- SupplementaryData1.xlsx
- SupplementaryData2.xlsx

Post–COVID-19 Symptoms and Conditions Among Children and Adolescents — United States, March 1, 2020–January 31, 2022

Lyudmyla Kompaniyets, PhD[1]; Lara Bull-Otterson, PhD[1]; Tegan K. Boehmer, PhD[1]; Sarah Baca[1,2]; Pablo Alvarez, MPH[1,2]; Kai Hong, PhD[1]; Joy Hsu, MD[1]; Aaron M. Harris, MD[1]; Adi V. Gundlapalli, MD, PhD[1]; Sharon Saydah, PhD[1]

Post–COVID-19 (post-COVID) symptoms and conditions* are new, recurring, or ongoing health problems that occur 4 or more weeks after infection with SARS-CoV-2 (the virus that causes COVID-19). Previous studies have characterized and estimated the incidence of post-COVID conditions among adults (*1*,*2*), but data among children and adolescents are limited (*3*–*8*). Using a large medical claims database, CDC assessed nine potential post-COVID signs and symptoms (symptoms) and 15 potential post-COVID conditions among 781,419 U.S. children and adolescents aged 0–17 years with laboratory-confirmed COVID-19 (patients with COVID-19) compared with 2,344,257 U.S. children and adolescents without recognized COVID-19 (patients without COVID-19) during March 1, 2020–January 31, 2022. The analysis identified several symptoms and conditions with elevated adjusted hazard ratios among patients with COVID-19 (compared with those without). The highest hazard ratios were recorded for acute pulmonary embolism (adjusted hazard ratio [aHR] = 2.01), myocarditis and cardiomyopathy (1.99), venous thromboembolic event (1.87), acute and unspecified renal failure (1.32), and type 1 diabetes (1.23), all of which were rare or uncommon in this study population. Conversely, symptoms and conditions that were most common in this study population had lower aHRs (near or below 1.0). Patients with COVID-19 were less likely than were patients without to experience respiratory signs and symptoms, symptoms of mental conditions, muscle disorders, neurological conditions, anxiety and fear-related disorders, mood disorders, and sleeping disorders. COVID-19 prevention strategies, including vaccination for all eligible children and adolescents, are critical to prevent SARS-CoV-2 infection and subsequent illness, including post-COVID symptoms and conditions (*9*).

CDC analyzed linked medical claims and commercial laboratory data for persons with a health care encounter possibly related to COVID-19.† Analyses were restricted to children and adolescents aged 0–17 years who were continuously enrolled in a health insurance plan during March 1, 2019–January 31, 2022. Children and adolescents aged 0–17 years with laboratory-confirmed COVID-19 and those without recognized COVID-19§ were matched 1:3 based on age at encounter, sex, and month of index date.¶ Patients were followed for a minimum of 60 days and a maximum of 365 days or until January 31, 2022, whichever occurred first. Scientific literature on symptoms and conditions associated with post-COVID illness among children or adults was reviewed (*1*–*5*). Symptoms and conditions were identified by the first occurrence and classified based on the *International Classification of Diseases, Tenth Revision, Clinical Modification* (ICD-10-CM)

* CDC defines post-COVID conditions as new, returning, or ongoing health problems occurring ≥4 weeks after being infected with SARS-CoV-2. https://www.cdc.gov/coronavirus/2019-ncov/long-term-effects/index.html

† This analysis used CDC-licensed HealthVerity, Inc. medical claims data linked to SARS-CoV-2 commercial laboratory data (May 2022 release). Patients were eligible for inclusion in CDC licensed data if they had a health care encounter (diagnosis, procedure, treatment, or laboratory test) possibly related to COVID-19 on or after December 1, 2019.

§ A retrospective cohort of children and adolescents aged 0–17 years with continuous enrollment in an insurance plan during March 1, 2019–January 31, 2022, was identified within a subset of CDC-licensed HealthVerity data that included persons with a health care encounter possibly related to COVID-19. Patients with COVID-19 were selected from among patients with a positive SARS-CoV-2 test result during March 2020–November 2021 or an ICD-10-CM code of B97.29 (other coronavirus as the cause of diseases classified elsewhere) during March–April 2020 or U07.1 code (COVID-19, virus-identified [laboratory-confirmed]) during April 2020–November 2021 (https://www.cdc.gov/nchs/data/icd/Announcement-New-ICD-code-for-coronavirus-3-18-2020.pdf). Patients without COVID-19 were selected after excluding patients who had any ICD-10-CM codes related to COVID-19 (A41.89, B34.2, B97.21, B94.8, J12.81, J12.82, J12.89, M30.3, M35.81, U07.1, or U07.2), a positive SARS-CoV-2 test result, or received treatment for COVID-19 (casirivimab/imdevimab, etesevimab/bamlanivimab, sotrovimab, bebtelovimab, nirmatrelvir, molnupiravir, or remdesivir) at any point during the study period. Vaccination status of patients was not included for this analysis.

¶ The index date for the group of patients with COVID-19 was the date of either the first claim with a COVID-19 diagnosis code or the first positive SARS-CoV-2 test result (whichever occurred first). The index date for patients without COVID-19 in the main analysis was the date of a randomly selected claim during the month in which the patient without COVID-19 was matched to a patient with COVID-19. The index date for patients without COVID-19 in the sensitivity analysis was the date of the first negative SARS-CoV-2 test result, first health care encounter possibly related to COVID-19 (associated with an ICD-10-CM code of B97.89, Z86.16, R05, R06.02, R50.9, R19.7, R53.8, R09.3, R04.2, R09.2, J00–J06, J09–J11, J12.9, J13–J18, or J80), or the first claim during the pandemic period if other dates were not available.

codes documented 31–365 days after the index date but not during the 7–365 days preceding the index date.**

The incidences (occurrence per 100,000 person-years) of nine potential post-COVID symptoms and 15 potential post-COVID conditions among children and adolescents aged 0–17 years were calculated. Separate Cox proportional hazards models were used to estimate aHRs for each symptom and condition, after excluding persons with that particular symptom or condition during the 7–365 days preceding the index date.†† All models were adjusted for age, sex, race, U.S. Census Bureau region, payor type, previous medical complexity (*10*), and previous hospitalization.§§ The same models were estimated separately for three age groups (2–4, 5–11, and 12–17 years).¶¶ A sensitivity analysis was performed to assess the incidences of potential post-COVID symptoms and conditions among children and adolescents aged 0–17 years who had not experienced any of the 24 assessed symptoms or conditions before the index date.*** Finally, incidence of each symptom and condition among patients with COVID-19 was plotted against aHRs from the main analysis. Analyses were conducted using R software (version 4.1.0; R Foundation); p-values <0.05 were considered statistically significant. This activity was reviewed by CDC and conducted consistent with applicable federal law and CDC policy.†††

During March 1, 2020–January 31, 2022, a total of 781,419 patients aged 0–17 years with COVID-19 and 2,344,257 patients aged 0–17 years without COVID-19 were identified (Table 1). The median age of both patients with and without COVID-19 was 12 years, and 50.0% in both groups were female; 72.2% of patients with COVID-19 were enrolled in Medicaid managed care, compared with 70.6% of patients without COVID-19. Patients without COVID-19 had a higher prevalence of previous hospitalization (4.5%) and complex chronic disease (15.6%), than did patients with COVID-19 (3.6% and 11.7%, respectively).

Patients with COVID-19 were significantly more likely than were those without to develop the following assessed post-COVID symptoms: smell and taste disturbances (aHR = 1.17), circulatory signs and symptoms (1.07), malaise and fatigue (1.05), and musculoskeletal pain (1.02) (Table 2). Patients with COVID-19 were also more likely than were those without to develop the following assessed post-COVID conditions: acute pulmonary embolism (2.01), myocarditis and cardiomyopathy (1.99), venous thromboembolic event (1.87), acute and unspecified renal failure (1.32), type 1 diabetes (1.23), coagulation and hemorrhagic disorders (1.18), type 2 diabetes (1.17), and cardiac dysrhythmias (1.16). Patients with COVID-19 were less likely than were those without to experience respiratory signs and symptoms (0.91), symptoms of mental conditions (0.91), sleeping disorders (0.91), neurological conditions (0.94), anxiety and fear-related

** Potential post-COVID conditions were selected from a range of body systems and were assessed by the first occurrence of at least one of the following ICD-10-CM codes documented 31–365 days after the index date but not during the 7–365 days preceding the index date: 1) circulatory system disorders: acute pulmonary embolism (I26), myocarditis and cardiomyopathy (A36.81, B33.20, B33.22, B33.24, B58.81, I25.5, I40, I41, I42.0–I42.5, I42.8, I42.9, I43, I51.4, J10.82, J11.82, and O90.3), cerebrovascular disease (G46 and I67–I68 [except I67.0 and I67.4]), venous thromboembolic event (I82.40, I82.49, I82.4Y, I82.4Z, I82.62, I82.50, I82.59, I82.5Y, I82.5Z, and I82.72), cardiac dysrhythmias (I47, I48.0, I48.19, I48.21, I48.3–I48.9, and I49.1–I49.9); 2) endocrine, nutritional, and metabolic disorders: type 1 diabetes (E10), type 2 diabetes (E11); 3) digestive system disorders: gastrointestinal and esophageal disorders (K20, K21, K22.0–K22.6, K22.89, K22.9, K23, K58, K59.0–K59.2, K59.89, K59.9, and K92.9); 4) musculoskeletal and connective tissue disorders: muscle disorders (M60.0, M60.1, M60.8, M60.9. M61, M62, and M63); 5) mental, behavioral, and neurodevelopmental disorders: anxiety and fear-related disorders (F06.4, F40.0, F40.1, F40.228, F40.230, F40.231, F40.232, F40.233, F40.240, F40.248, F40.8, F40.9, F41, and F93.0), mood disorders (F06.30, F34.8. F34.9, and F39); 6) nervous system disorders: neurological conditions (F05, R40.0, R41, R44, A85, A86, G04, G05, R29, R26, R27, G26, and G50–G65); 7) respiratory system disorders: asthma (J45); 8) genitourinary disorders: acute renal failure (N17 and N19), chronic kidney disease (N18 and R88.0); 9) blood system disorders: coagulation and hemorrhagic disorders (D47.3, D65, D68.3–D68.9, D69, D75.82, D75.83, and M36.2); 10) other symptoms, signs and abnormal clinical and laboratory findings: malaise and fatigue (G93.3, R53.1, and R53.8), respiratory signs and symptoms (R04–R09), smell and taste disturbances (R43.8 and R43.9), symptoms of mental conditions (F30.4, F31.70, F31.72, F31.74, F31.76, F31.78, F32.5, F33.40, F33.42, R45.0–R45.7, R45.8 [except R45.851 and R45.88], and R46), sleeping disorders (G47 and R06.3), circulatory signs and symptoms (R00, R01, R03.0, and R09.89), dizziness and syncope (I95.1, G90.9, R42, and R55), and musculoskeletal pain (M25.5, M25.6, M54.6, M54.8, M54.9, M79.1, M79.6, and M79.7).

†† Proportional hazards assumption was tested for every Cox proportional hazards model. In some models, proportionality assumption for certain variables was rejected, and the Schoenfeld residuals and survival curves were visually examined. Although slopes were not always parallel, the survival curves did not cross in any cases, indicating that the nonproportionality might not lead to severe bias in the results. The estimated aHRs from Cox models were compared against aHRs from Weibull models (estimated using "SurvRegCensCov" R package) and average aHRs from weighted Cox models (estimated using "coxphw" R package) and were found to be very close in magnitude and significance level.

§§ Previous hospitalization was defined by a presence of an inpatient claim during the 7–365 days before the index date. Previous medical complexity was defined using the validated pediatric medical complexity algorithm as presence of complex chronic disease (at least one claim with a progressive condition, at least one claim with malignant neoplasms, or at least one claim per body system for two different body systems), presence of noncomplex chronic disease (at least one claim for a single body system not flagged as progressive), or absence of chronic disease (reference category; none of the previously described encounters) during the 7–365 days before the index date.

¶¶ Age-stratified analyses were only performed when there were at least 10 patients with COVID-19 and at least 10 patients without COVID-19 in that age group with the specific symptom or condition. Each model was adjusted for age as a continuous covariate (to account for age differences within each age group), sex, race, U.S. Census Bureau region, payor type, previous medical complexity, and previous hospitalization.

*** The maximum possible matching ratio was used. For the main analysis, patients without COVID-19 were matched 3:1 to patients with COVID-19. For the analysis of a cohort of patients with no previous symptoms or conditions of interest, patients without COVID-19 were matched 2:1 to patients with COVID-19.

††† 45 C.F.R. part 46.102(l)(2), 21 C.F.R. part 56; 42 U.S.C. Sect. 241(d); 5 U.S.C. Sect. 552a; 44 U.S.C. Sect. 3501 et seq.

TABLE 1. Characteristics of children and adolescents aged 0–17 years with and without COVID-19 — HealthVerity medical claims database, United States, March 1, 2020–January 31, 2022

Characteristic*	No. (%)			
	All patients†		Patients without previous symptoms or conditions†	
	Patients without COVID-19§	Patients with COVID-19§	Patients without COVID-19§	Patients with COVID-19§
Total	**2,344,257**	**781,419**	**792,672**	**396,336**
Sex				
Female	1,172,481 (50.0)	390,827 (50.0)	394,536 (49.8)	197,268 (49.8)
Male	1,171,776 (50.0)	390,592 (50.0)	398,136 (50.2)	199,068 (50.2)
Age group, yrs				
Median (IQR)	12 (8–15)	12 (8–15)	12 (8–15)	12 (8–15)
<2	2,952 (0.1)	984 (0.1)	564 (0.1)	282 (0.1)
2–4	155,190 (6.6)	51,730 (6.6)	48,550 (6.1)	24,275 (6.1)
5–11	904,284 (38.6)	301,428 (38.6)	316,010 (39.9)	158,005 (39.9)
12–17	1,281,831 (54.7)	427,277 (54.7)	427,548 (53.9)	213,774 (53.9)
Race¶				
Asian	74,943 (3.2)	23,241 (3.0)	26,039 (3.3)	12,213 (3.1)
Black or African American	566,891 (24.2)	196,887 (25.2)	198,705 (25.1)	101,839 (25.7)
White	1,178,288 (50.3)	382,371 (48.9)	381,841 (48.2)	189,895 (47.9)
Other	73,401 (3.1)	24,648 (3.2)	26,044 (3.3)	12,889 (3.3)
Unknown or unavailable	450,734 (19.2)	154,272 (19.7)	160,043 (20.2)	79,500 (20.1)
Payor type				
Commercial	666,068 (28.4)	214,371 (27.4)	244,047 (30.7)	118,300 (29.8)
Medicaid	1,655,886 (70.6)	563,860 (72.2)	541,415 (68.3)	276,422 (69.7)
Medicare Advantage	13,466 (0.6)	1,277 (0.2)	4,415 (0.6)	676 (0.2)
Unknown or unavailable	8,837 (0.4)	1,911 (0.2)	2,795 (0.4)	938 (0.2)
U.S. Census Bureau region**				
Northeast	283,916 (12.1)	86,436 (11.1)	79,015 (10.0)	44,770 (11.3)
Midwest	527,527 (22.5)	132,879 (17.0)	167,233 (21.1)	68,471 (17.3)
South	1,160,472 (49.5)	448,844 (57.4)	397,624 (50.2)	217,886 (55.0)
West	372,342 (15.9)	113,260 (14.5)	148,800 (18.8)	65,209 (16.5)
Hospitalization during 7–365 days preceding index date				
Yes	104,768 (4.5)	28,294 (3.6)	8,030 (1.0)	4,007 (1.0)
No	2,239,489 (95.5)	753,125 (96.4)	784,642 (99.0)	392,329 (99.0)
Medical complexity during 7–365 days preceding index date				
No chronic disease	1,328,582 (56.7)	506,026 (64.8)	672,355 (84.8)	333,882 (84.2)
Non-complex chronic disease	649,710 (27.7)	184,188 (23.6)	95,337 (12.0)	50,980 (12.9)
Complex chronic disease	365,965 (15.6)	91,205 (11.7)	24,980 (3.2)	11,474 (2.9)

Abbreviation: ICD-10-CM = *International Classification of Diseases, Tenth Revision, Clinical Modification*.

* Categories might not sum to 100% because of rounding or missing values.

† Columns 2 and 3 describe the main cohort: patients with COVID-19 and patients without COVID-19 who were matched 1:3 based on age, sex, and month of the index date (for patients with COVID-19, the date of either the first claim with a COVID-19 diagnosis code or the first positive SARS-CoV-2 test result, whichever occurred first; for patients without COVID-19, the date of a randomly selected claim during the month in which the patient without COVID-19 was matched to a patient with COVID-19). Columns 4 and 5 describe a cohort of patients with none of the 24 assessed symptoms or conditions during 7–365 days before the index date; patients with COVID-19 and patients without COVID-19 were matched 1:2 based on age, sex, and month of the index date (for patients with COVID-19, the date of either the first claim with a COVID-19 diagnosis code or the first positive SARS-CoV-2 test result, whichever occurred first; for patients without COVID-19, the date of the first negative SARS-CoV-2 test result, first health care encounter possibly related to COVID-19, or the first claim during the pandemic period if other dates were not available).

§ The cohort consisted of children and adolescents aged 0–17 years with continuous enrollment in an insurance plan during March 1, 2019–January 31, 2022, identified within a subset of CDC-licensed HealthVerity data that included persons with a health care encounter possibly related to COVID-19. Patients with COVID-19 were selected from patients who received a positive SARS-CoV-2 test result during March 2020–November 2021 or an ICD-10-CM code of B97.29 during March–April 2020 or U07.1 code during April 2020–November 2021. Patients without COVID-19 were selected after excluding patients who had an ICD-10-CM code related to COVID-19 (A41.89, B34.2, B97.21, B97.29, B94.8, J12.81, J12.82, J12.89, M30.3, M35.81, U07.1, or U07.2), a positive SARS-CoV-2 test result, or received treatment for COVID-19 (casirivimab/imdevimab, etesevimab/bamlanivimab, sotrovimab, bebtelovimab, nirmatrelvir, molnupiravir, or remdesivir) at any point during the study period. Vaccination status of patients was not included for this analysis.

¶ Analysis did not include ethnicity.

** U.S. Census Bureau regions: *Northeast*: Connecticut, Maine, Massachusetts, New Hampshire, New Jersey, New York, Pennsylvania, Rhode Island, and Vermont; *Midwest*: Illinois, Indiana, Iowa, Kansas, Michigan, Minnesota, Missouri, Nebraska, North Dakota, Ohio, South Dakota, and Wisconsin; *South*: Alabama, Arkansas, Delaware, District of Columbia, Florida, Georgia, Kentucky, Louisiana, Maryland, Mississippi, North Carolina, Oklahoma, South Carolina, Tennessee, Texas, Virginia, and West Virginia; *West*: Alaska, Arizona, California, Colorado, Hawaii, Idaho, Montana, Nevada, New Mexico, Oregon, Utah, Washington, and Wyoming.

disorders (0.85), mood disorders (0.78), and muscle disorders (0.94); no significant associations were found for the remaining five symptoms and conditions.

In age-stratified analysis of three age groups (2–4, 5–11, and 12–17 years), the unadjusted incidences of symptoms and conditions differed by age group (Supplementary Table, https://stacks.cdc.gov/view/cdc/118760). Among children aged 2–4 years, the highest aHRs for patients with COVID-19 compared with patients without COVID-19 were for myocarditis and cardiomyopathy (aHR = 2.39), acute and unspecified renal failure (1.52), and coagulation and hemorrhagic disorders (1.47) (Table 3). Unlike other age groups, children aged 2–4 years had higher rates of asthma diagnosis (1.12) and respiratory signs and symptoms (1.07) after COVID-19. Among children aged 5–11 years, the highest aHRs for patients with COVID-19 compared with those without were for myocarditis and cardiomyopathy (2.84), venous thromboembolic event (2.69), and acute and unspecified renal failure (1.38). Among patients aged 12–17 years, the highest aHRs for those with COVID-19 compared with those without were for acute pulmonary embolism (2.03), myocarditis and cardiomyopathy (1.66), and venous thromboembolic event (1.52).

TABLE 2. Incidence* and adjusted hazard ratios of selected potential post–COVID-19 symptoms and conditions among children and adolescents aged 0–17 years with and without COVID-19 — HealthVerity medical claims database, United States, March 1, 2020–January 31, 2022

	All patients†			Patients without previous symptoms or conditions†		
	No. (incidence)*			No. (incidence)*		
Outcome	Patients without COVID-19	Patients with COVID-19	aHR (95% CI)§	Patients without COVID-19	Patients with COVID-19	aHR (95% CI)§
Symptom						
Smell and taste disturbances	5,028 (296)	1,924 (340)	1.17 (1.11–1.24)¶	1,173 (205)	715 (250)	1.21 (1.11–1.33)¶
Circulatory signs and symptoms	80,900 (5,092)	27,207 (5,126)	1.07 (1.05–1.08)¶	18,729 (3,334)	10,518 (3,727)	1.12 (1.09–1.14)¶
Malaise and fatigue	74,908 (4,659)	24,970 (4,648)	1.05 (1.03–1.06)¶	15,712 (2,784)	8,964 (3,168)	1.13 (1.10–1.16)¶
Musculoskeletal pain	201,899 (14,819)	67,744 (14,800)	1.02 (1.02–1.03)¶	62,417 (11,647)	34,460 (12,662)	1.09 (1.07–1.10)¶
Dizziness and syncope	48,976 (2,993)	15,731 (2,876)	1.01 (0.99–1.03)	10,890 (1,923)	5,630 (1,980)	1.03 (0.99–1.06)
Gastrointestinal and esophageal disorders	94,395 (6,195)	30,266 (5,898)	1.01 (0.99–1.02)	22,411 (4,021)	11,686 (4,151)	1.03 (1.00–1.05)
Sleeping disorders	51,227 (3,203)	14,011 (2,588)	0.91 (0.90–0.93)¶	9,138 (1,616)	4,238 (1,488)	0.92 (0.89–0.95)¶
Respiratory signs and symptoms	283,139 (23,456)	85,279 (20,948)	0.91 (0.91–0.92)¶	80,364 (15,200)	47,690 (17,796)	1.16 (1.14–1.17)¶
Symptoms of mental conditions	47,138 (2,906)	12,944 (2,364)	0.91 (0.89–0.93)¶	9,268 (1,637)	4,529 (1,591)	0.97 (0.94–1.00)
Condition						
Acute pulmonary embolism	224 (13)	131 (23)	2.01 (1.62–2.50)¶	43 (8)	36 (13)	1.74 (1.12–2.72)¶
Myocarditis and cardiomyopathy	1,172 (69)	692 (122)	1.99 (1.81–2.19)¶	224 (39)	264 (92)	2.34 (1.96–2.79)¶
Venous thromboembolic event	315 (18)	164 (29)	1.87 (1.54–2.26)¶	51 (9)	37 (13)	1.48 (0.97–2.26)
Acute and unspecified renal failure	2,116 (124)	788 (139)	1.32 (1.22–1.43)¶	347 (61)	223 (78)	1.30 (1.10–1.54)¶
Type 1 diabetes	2,080 (123)	792 (140)	1.23 (1.13–1.33)¶	641 (112)	349 (122)	1.10 (0.96–1.25)
Coagulation and hemorrhagic disorders	4,454 (263)	1,582 (280)	1.18 (1.12–1.25)¶	849 (148)	537 (188)	1.26 (1.14–1.41)¶
Type 2 diabetes	6,197 (366)	2,170 (384)	1.17 (1.11–1.23)¶	1,210 (212)	729 (255)	1.19 (1.09–1.31)¶
Cardiac dysrhythmias	13,031 (774)	4,595 (817)	1.16 (1.12–1.20)¶	2,391 (419)	1,442 (504)	1.20 (1.13–1.28)¶
Cerebrovascular disease	441 (26)	149 (26)	1.20 (1.00–1.45)	67 (12)	28 (10)	0.84 (0.54–1.30)
Chronic kidney disease	1,105 (65)	321 (57)	1.07 (0.95–1.22)	171 (30)	81 (28)	0.99 (0.76–1.29)
Asthma	82,105 (5,625)	27,327 (5,557)	1.00 (0.99–1.01)	26,470 (4,785)	12,751 (4,533)	0.93 (0.91–0.95)¶
Muscle disorders	23,655 (1,424)	6,807 (1,222)	0.94 (0.91–0.96)¶	4,075 (715)	2,109 (738)	1.03 (0.98–1.09)
Neurological conditions	64,436 (4,077)	18,681 (3,485)	0.94 (0.92–0.95)¶	12,954 (2,298)	6,513 (2,295)	0.99 (0.96–1.02)
Anxiety and fear-related disorders	112,234 (7,686)	31,274 (6,107)	0.85 (0.84–0.86)¶	28,624 (5,166)	13,016 (4,634)	0.90 (0.88–0.91)¶
Mood disorders	23,108 (1,406)	5,248 (944)	0.78 (0.75–0.80)¶	3,656 (642)	1,531 (535)	0.83 (0.78–0.88)¶

Abbreviation: aHR = adjusted hazard ratio.

* Occurrences per 100,000 person-years.

† Columns 2, 3, and 4 represent analyses of incidences and aHRs obtained after 1:3 matching of patients with COVID-19 and patients without COVID-19. Incidences and aHRs for each symptom or condition were calculated after excluding patients who had that particular symptom or condition during 7–365 days before the index date (for patients with COVID-19, the date of either the first claim with a COVID-19 diagnosis code or the first positive SARS-CoV-2 test result, whichever occurred first; for patients without COVID-19, the date of a randomly selected claim during the month in which the patient without COVID-19 was matched to a patient with COVID-19). Columns 5, 6, and 7 represent incidences and aHRs obtained after 1:2 matching of patients with COVID-19 and those without who had not experienced any of the 24 assessed symptoms or conditions during 7–365 days before the index date (for patients with COVID-19, the date of either the first claim with a COVID-19 diagnosis code or the first positive SARS-CoV-2 test result, whichever occurred first; for patients without COVID-19, the date of the first negative SARS-CoV-2 test result, first health care encounter possibly related to COVID-19, or the first claim during the pandemic period if other dates were not available).

§ Each aHR was obtained from a single Cox proportional hazards model, with the specific symptom or condition as the outcome and the following covariates: presence of COVID-19, age group, sex, race, U.S. Census Bureau region, payor type, previous medical complexity, and previous hospitalization.

¶ P-value <0.05.

The sensitivity analysis of 396,336 patients with COVID-19 and 792,672 matched patients without COVID-19 (without previous symptoms or conditions of interest) found that patients in both groups were healthier at baseline than their counterparts in the main cohort; 84.2% of persons with COVID-19 and 84.8% patients without COVID-19 had no previous documentation of chronic disease, compared with 64.8% and 56.7%, respectively in the main cohort (Table 1). Higher rates of five symptoms and six conditions among patients with COVID-19 compared with those without were found in the sensitivity analysis, whereas the main analysis found higher rates of four symptoms and eight conditions. In the sensitivity analysis, aHRs for type 1 diabetes and venous thromboembolic event were not statistically significant, and the aHR for respiratory signs and symptoms was elevated (1.16) (Table 2).

Analysis of the relationship between incidence rates among patients with COVID-19 and aHRs found that five post-COVID conditions with the highest aHRs had low incidence rates, ranging from 23 (acute pulmonary embolism) to 140 (type 1 diabetes) per 100,000 person-years (Supplementary Figure, https://stacks.cdc.gov/view/cdc/118761). Conversely, this analysis found that five symptoms and conditions with the highest incidence rates among patients with COVID-19 had lower aHRs (near or below 1.0): respiratory signs and symptoms (0.91), musculoskeletal pain (1.02), anxiety and fear-related disorders (0.85), gastrointestinal and esophageal disorders (1.01), and asthma (1.00).

Discussion

This analysis found increased incidence rates of several symptoms and conditions during the 31–365 days after a diagnosis of COVID-19 among children and adolescents aged 0–17 years. The highest aHRs were associated with potentially serious conditions, such as acute pulmonary embolism, myocarditis and cardiomyopathy, venous thromboembolic event, acute and unspecified renal failure, and type 1 diabetes. These conditions with the highest aHRs were rare or uncommon among children and adolescents in this analysis. Some of the study's findings are consistent with previous evidence of elevated risk for new onset of diabetes (*5*), myocarditis (*6*), and certain symptoms (*4*), whereas other conditions (acute

TABLE 3. Adjusted hazard ratios of selected potential post–COVID-19 symptoms and conditions among children and adolescents aged 2–17 years with and without COVID-19, by age group — HealthVerity medical claims database, United States, March 1, 2020–January 31, 2022

Outcome	Adjusted hazard ratio (95% CI)*		
	Aged 2–4 yrs	Aged 5–11 yrs	Aged 12–17 yrs
Symptom			
Smell and taste disturbances	1.22 (0.70–2.15)	0.94 (0.83–1.07)	1.23 (1.16–1.31)†
Circulatory signs and symptoms	1.17 (1.12–1.23)†	1.11 (1.08–1.13)†	1.04 (1.02–1.06)†
Malaise and fatigue	1.13 (1.05–1.22)†	1.08 (1.05–1.12)†	1.03 (1.01–1.04)†
Musculoskeletal pain	1.16 (1.10–1.21)†	1.06 (1.04–1.07)†	1.00 (0.99–1.01)
Dizziness and syncope	1.08 (0.90–1.29)	1.03 (0.99–1.08)	1.00 (0.98–1.02)
Gastrointestinal and esophageal disorders	1.15 (1.10–1.20)†	1.02 (1.00–1.04)†	0.97 (0.95–0.99)†
Sleeping disorders	0.99 (0.93–1.06)	0.89 (0.86–0.92)†	0.91 (0.89–0.94)†
Respiratory signs and symptoms	1.07 (1.04–1.10)†	0.93 (0.92–0.94)†	0.88 (0.87–0.89)†
Symptoms of mental conditions	1.03 (0.97–1.10)	0.92 (0.90–0.95)†	0.89 (0.86–0.91)†
Condition			
Acute pulmonary embolism	—§	—§	2.03 (1.61–2.56)†
Myocarditis and cardiomyopathy	2.39 (1.57–3.65)†	2.84 (2.39–3.37)†	1.66 (1.48–1.88)†
Venous thromboembolic event	—§	2.69 (1.73–4.19)†	1.52 (1.22–1.91)†
Acute and unspecified renal failure	1.52 (1.07–2.14)†	1.38 (1.16–1.63)†	1.27 (1.15–1.40)†
Type 1 diabetes	1.01 (0.57–1.78)	1.31 (1.13–1.53)†	1.20 (1.09–1.33)†
Coagulation and hemorrhagic disorders	1.47 (1.20–1.80)†	1.28 (1.15–1.43)†	1.10 (1.03–1.19)†
Type 2 diabetes	1.24 (0.85–1.81)	1.14 (1.02–1.28)†	1.18 (1.11–1.24)†
Cardiac dysrhythmias	1.44 (1.22–1.70)†	1.23 (1.14–1.32)†	1.12 (1.08–1.17)†
Cerebrovascular disease	1.66 (0.85–3.23)	1.14 (0.79–1.64)	1.18 (0.93–1.48)
Chronic kidney disease	0.86 (0.54–1.36)	1.04 (0.83–1.31)	1.12 (0.96–1.31)
Asthma	1.12 (1.07–1.18)†	1.02 (1.00–1.05)†	0.96 (0.94–0.98)†
Muscle disorders	0.87 (0.77–0.98)†	0.86 (0.82–0.91)†	0.96 (0.93–0.99)†
Neurological conditions	0.98 (0.93–1.04)	0.96 (0.93–0.98)†	0.91 (0.89–0.93)†
Anxiety and fear-related disorders	0.91 (0.83–1.00)	0.86 (0.83–0.88)†	0.84 (0.82–0.85)†
Mood disorders	0.82 (0.62–1.08)	0.73 (0.69–0.77)†	0.80 (0.77–0.83)†

* Each adjusted hazard ratio was obtained from a single Cox proportional hazards model stratified by age group, with the specific symptom or condition as the outcome and the following covariates: presence of COVID-19, age (continuous variable), sex, race, U.S. Census Bureau region, payor type, previous medical complexity, and previous hospitalization.

† P-value <0.05.

§ Age-stratified analyses were only performed when there were at least 10 patients with COVID-19 and at least 10 patients without COVID-19 in that age group with the specific symptom or condition.

pulmonary embolism, venous thromboembolic event, acute renal failure, coagulation and hemorrhagic disorders, and cardiac dysrhythmias) have not been previously reported as post-COVID conditions among children and adolescents.

Several symptoms and conditions (respiratory signs and symptoms, mental health symptoms and conditions, neurological conditions, muscle disorders, and sleeping disorders) were less likely to occur among patients with COVID-19 than among patients without COVID-19. Reasons for these observed associations are likely multifactorial, and might be, in part, because patients without COVID-19 were selected from a cohort of patients with a health care encounter possibly related to COVID-19 and were less healthy than were patients with COVID-19 at baseline. Although most of the symptoms and conditions selected for the analysis were based on those observed in previous post-COVID studies, they are not unique to patients with a history of COVID-19, and many are common among children and adolescents. A United Kingdom study found a high prevalence of poor mental health and well-being among all children and adolescents aged 11–17 years during the pandemic, but no difference among those with positive and negative SARS-CoV-2 test results (*7*). Respiratory signs and symptoms were less likely to occur among patients with COVID-19 than among those without in the main cohort. The opposite result was found in a subset of children aged 2–4 years and in a cohort of children and adolescents with no previous symptoms or conditions of interest; new respiratory signs and symptoms were more likely to occur among children and adolescents who had COVID-19, compared with those without a history of COVID-19.

The findings in this report are subject to at least seven limitations. First, the definitions of potential post-COVID symptoms and conditions are subject to misclassification bias because the symptoms and conditions were defined by a single ICD-10-CM code and no information on laboratory assessments or degree of severity was available. Second, because the incidence date of a symptom or a condition was based on the first occurrence of the ICD-10-CM code, the actual incidence date of that symptom or condition might have occurred prior to COVID-19. Third, patients infected with SARS-CoV-2 without a documented COVID-19 diagnosis or positive test result might have been misclassified as not having had COVID-19, potentially reducing the magnitude of observed associations. Fourth, the aHR estimates might be reduced because patients without COVID-19 were patients with a health care encounter possibly related to COVID-19. Fifth, because patients' vaccination status was likely underreported in this dataset, this analysis was not adjusted for previous receipt of COVID-19 vaccines. Sixth, although this study relied on statistical significance for interpreting the increased rates of symptoms and conditions, further understanding of the clinical significance of the observed associations, including whether these symptoms and conditions are transient or chronic, is necessary. Finally, generalizability might be limited because the analysis was restricted to children and adolescents aged 0–17 years included in a medical claims database, approximately 70% of whom were enrolled in Medicaid managed care; therefore, findings are not necessarily representative of all children and adolescents with COVID-19 or of those who do not seek health care.

These findings can be used to apprise health care professionals and caregivers about new symptoms and conditions that occur among children and adolescents in the months after SARS-CoV-2 infection. COVID-19 prevention strategies, including vaccination for all eligible persons aged ≥6 months, are critical for preventing SARS-CoV-2 infection and subsequent illness and for reducing the public health impact of post-COVID symptoms and conditions.

Summary

What is already known about this topic?

Children and adolescents might be at risk for certain post-COVID symptoms and conditions.

What is added by this report?

Compared with patients aged 0–17 years without previous COVID-19, those with previous COVID-19 had higher rates of acute pulmonary embolism (adjusted hazard ratio = 2.01), myocarditis and cardiomyopathy (1.99), venous thromboembolic event (1.87), acute and unspecified renal failure (1.32), and type 1 diabetes (1.23), all of which were rare or uncommon in this study population.

What are the implications for public health practice?

COVID-19 prevention strategies, including vaccination for all eligible persons aged ≥6 months, are critical to preventing SARS-CoV-2 infection and subsequent illness, and reducing the public health impact of post-COVID symptoms and conditions among persons aged 0–17 years.

Acknowledgments

Members of the Data, Analytics, and Visualization Task Force, CDC COVID-19 Emergency Response Team; Matthew Oster, Center on Birth Defects and Developmental Disabilities, CDC; John R. Pleis, Division of Research and Methodology, National Center for Health Statistics, CDC.

Corresponding author: Lyudmyla Kompaniyets, opt4@cdc.gov.

[1]CDC COVID-19 Emergency Response Team; [2]GAP Solutions Inc, Herndon, Virginia.

All authors have completed and submitted the International Committee of Medical Journal Editors form for disclosure of potential conflicts of interest. No potential conflicts of interest were disclosed.

References

1. Al-Aly Z, Xie Y, Bowe B. High-dimensional characterization of post-acute sequelae of COVID-19. Nature 2021;594:259–64. PMID:33887749 https://doi.org/10.1038/s41586-021-03553-9
2. Chevinsky JR, Tao G, Lavery AM, et al. Late conditions diagnosed 1–4 months following an initial coronavirus disease 2019 (COVID-19) encounter: a matched-cohort study using inpatient and outpatient administrative data—United States, 1 March–30 June 2020. Clin Infect Dis 2021;73(Suppl 1):S5–16. PMID:33909072 https://doi.org/10.1093/cid/ciab338
3. Kikkenborg Berg S, Dam Nielsen S, Nygaard U, et al. Long COVID symptoms in SARS-CoV-2-positive adolescents and matched controls (LongCOVIDKidsDK): a national, cross-sectional study. Lancet Child Adolesc Health 2022;6:240–8. PMID:35143771 https://doi.org/10.1016/S2352-4642(22)00004-9
4. Hernandez-Romieu AC, Carton TW, Saydah S, et al. Prevalence of select new symptoms and conditions among persons aged younger than 20 years and 20 years or older at 31 to 150 days after testing positive or negative for SARS-CoV-2. JAMA Netw Open 2022;5:e2147053. PMID:35119459 https://doi.org/10.1001/jamanetworkopen.2021.47053
5. Barrett CE, Koyama AK, Alvarez P, et al. Risk for newly diagnosed diabetes >30 days after SARS-CoV-2 infection among persons aged <18 years—United States, March 1, 2020–June 28, 2021. MMWR Morb Mortal Wkly Rep 2022;71:59–65. PMID:35025851 https://doi.org/10.15585/mmwr.mm7102e2
6. Boehmer TK, Kompaniyets L, Lavery AM, et al. Association between COVID-19 and myocarditis using hospital-based administrative data—United States, March 2020–January 2021. MMWR Morb Mortal Wkly Rep 2021;70:1228–32. PMID:34473684 https://doi.org/10.15585/mmwr.mm7035e5
7. Stephenson T, Pinto Pereira SM, Shafran R, et al; CLoCk Consortium. Physical and mental health 3 months after SARS-CoV-2 infection (long COVID) among adolescents in England (CLoCk): a national matched cohort study. Lancet Child Adolesc Health 2022;6:230–9. PMID:35143770 https://doi.org/10.1016/S2352-4642(22)00022-0
8. Magnusson K, Skyrud KD, Suren P, et al. Healthcare use in 700 000 children and adolescents for six months after covid-19: before and after register based cohort study. BMJ 2022;376:e066809. PMID:35039315 https://doi.org/10.1136/bmj-2021-066809
9. Taquet M, Dercon Q, Harrison PJ. Six-month sequelae of post-vaccination SARS-CoV-2 infection: a retrospective cohort study of 10,024 breakthrough infections. Brain Behav Immun 2022;103:154-162. PMID:35447302 https://doi.org/10.1016/j.bbi.2022.04.013
10. Simon TD, Haaland W, Hawley K, Lambka K, Mangione-Smith R. Development and validation of the pediatric medical complexity algorithm (PMCA) version 3.0. Acad Pediatr 2018;18:577–80. PMID:29496546 https://doi.org/10.1016/j.acap.2018.02.010

Med (N Y). 2021 Jun 11; 2(6): 720–735.e4.
doi: 10.1016/j.medj.2021.03.013: 10.1016/j.medj.2021.03.013
PMCID: PMC8011689
PMID: 33821250

Alterations in T and B cell function persist in convalescent COVID-19 patients

Halima A. Shuwa,[1,11] Tovah N. Shaw,[1,2,11] Sean B. Knight,[1,3] Kelly Wemyss,[1] Flora A. McClure,[1] Laurence Pearmain,[4,5] Ian Prise,[1] Christopher Jagger,[1] David J. Morgan,[1] Saba Khan,[1] Oliver Brand,[1] Elizabeth R. Mann,[1,6] Andrew Ustianowski,[7] Nawar Diar Bakerly,[3] Paul Dark,[5,10] Christopher E. Brightling,[8] Seema Brij,[9] CIRCO, Timothy Felton,[5] Angela Simpson,[5] John R. Grainger,[1,12] Tracy Hussell,[1,12] Joanne E. Konkel,[1,12,13,*] and Madhvi Menon[1,12,**]

[1]Lydia Becker Institute of Immunology and Inflammation, Division of Infection, Immunity, and Respiratory Medicine, School of Biological Sciences, Faculty of Biology, Medicine, and Health, University of Manchester, Manchester Academic Health Science Centre, Room 2.16, Core Technology Facility, 46 Grafton Street, Manchester, M13 9PL, UK
[2]Institute of Immunology and Infection Research, School of Biological Sciences, University of Edinburgh, Ashworth Laboratories, Edinburgh EH9 3FL, UK
[3]Department of Respiratory Medicine, Salford Royal NHS Foundation Trust, Stott Lane, Salford M6 8HD, UK
[4]Wellcome Trust Centre for Cell Matrix Research, The University of Manchester, Manchester M13 9PT, UK
[5]Division of Infection, Immunity, and Respiratory Medicine, Manchester NIHR BRC, Education and Research Centre, Wythenshawe Hospital, Manchester, UK
[6]Maternal and Fetal Health Centre, Division of Developmental Biology, School of Medical Sciences, Faculty of Biology, Medicine, and Health, The University of Manchester, 5th Floor, St. Mary's Hospital, Oxford Road, Manchester M13 9WL, UK
[7]Regional Infectious Diseases Unit, North Manchester General Hospital, Manchester, UK
[8]Department of Respiratory Sciences, University of Leicester, Leicester LE3 9QP, UK
[9]Department of Respiratory Medicine, Manchester Royal Infirmary, Manchester University NHS Foundation Trust, Manchester, UK
[10]Intensive Care Department, Salford Royal NHS Foundation Trust, Stott Lane, Salford M6 8HD, UK
Joanne E. Konkel: joanne.konkel@manchester.ac.uk; Madhvi Menon: madhvi.menon@manchester.ac.uk
*Corresponding author joanne.konkel@manchester.ac.uk
**Corresponding author madhvi.menon@manchester.ac.uk
[11]These authors contributed equally
[12]Senior author
[13]Lead contact

Received 2020 Oct 15; Revised 2021 Mar 1; Accepted 2021 Mar 19.

Summary

Background

Emerging studies indicate that some coronavirus disease 2019 (COVID-19) patients suffer from persistent symptoms, including breathlessness and chronic fatigue; however, the long-term immune response in these patients presently remains ill-defined.

Methods

Here, we describe the phenotypic and functional characteristics of B and T cells in hospitalized COVID-19 patients during acute disease and at 3–6 months of convalescence.

Findings

We report that the alterations in B cell subsets observed in acute COVID-19 patients were largely recovered in convalescent patients. In contrast, T cells from convalescent patients displayed continued alterations with persistence of a cytotoxic program evident in $CD8^+$ T cells as well as elevated production of type 1 cytokines and interleukin-17 (IL-17). Interestingly, B cells from patients with acute COVID-19 displayed an IL-6/IL-10 cytokine imbalance in response to Toll-like receptor activation, skewed toward a pro-inflammatory phenotype. Whereas the frequency of $IL\text{-}6^+$ B cells was restored in convalescent patients irrespective of clinical outcome, the recovery of $IL\text{-}10^+$ B cells was associated with the resolution of lung pathology.

Conclusions

Our data detail lymphocyte alterations in previously hospitalized COVID-19 patients up to 6 months following hospital discharge and identify 3 subgroups of convalescent patients based on distinct lymphocyte phenotypes, with 1 subgroup associated with poorer clinical outcome. We propose that alterations in B and T cell function following hospitalization with COVID-19 could affect longer-term immunity and contribute to some persistent symptoms observed in convalescent COVID-19 patients.

Funding

Provided by UKRI, Lister Institute of Preventative Medicine, the Wellcome Trust, The Kennedy Trust for Rheumatology Research, and 3M Global Giving.

Keywords: COVID-19, T cells, B cells, long COVID, viral Infection, convalescent patients

Graphical abstract

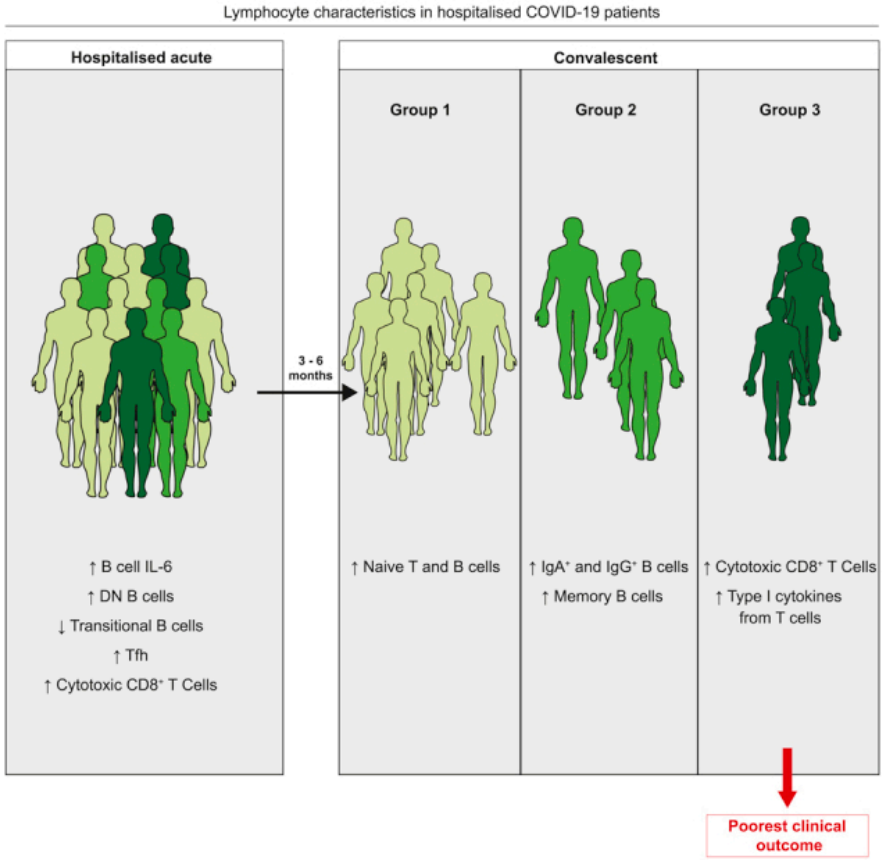

Introduction

The coronavirus disease 2019 (COVID-19) pandemic, caused by the emergence of a novel coronavirus strain, has resulted at this time in >106 million infections and 2.3 million deaths worldwide. Infection with severe acute respiratory syndrome-coronavirus-2 (SARS-CoV-2) has a plethora of consequences, ranging from mild influenza-like symptoms to life-threatening and fatal acute respiratory distress syndrome.[1,2] In all cases, the pathology is underpinned by not merely the virus itself but also an aberrant inflammatory host immune response. Research efforts detailing immune parameters in patients with acute COVID-19 have significantly improved our understanding of the disease, highlighting

profound alterations in the innate and adaptive immune compartments.[3, 4, 5, 6, 7] Lymphopenia and altered lymphocyte function have been reported to correlate with disease severity,[1,8] indicating key roles for T and B cells in COVID-19 pathology.

Emerging evidence suggests that COVID-19 patients can develop a spectrum of long-lasting symptoms, including chronic fatigue, myalgia, brain fog, fibrotic lung disease, and pulmonary vascular disease.[9, 10, 11] Although the immune response in acute COVID-19 patients has been well characterized, the long-term consequences of SARS-CoV-2 infection remain poorly understood. Since SARS-CoV-2-specific lymphocytes are likely critical for long-term protection against SARS-CoV-2 following disease resolution, it is pivotal to understand their contribution to acute disease, recovery, and long-lasting post-COVID-19 symptoms. Groundbreaking studies are demonstrating that antigen-specific responses to this virus can persist for several months post-infection.[12, 13, 14, 15] However, given the vast numbers of previously infected individuals across the globe, it is also vital to understand the impact of COVID-19 on the phenotype and functional potential of all lymphocytes, not just those reactive to SARS-CoV2. This will allow for a better understanding of the long-term effects of being hospitalized with COVID-19 on effective immunity. Long-term follow-up of Ebola patients has outlined immune dysfunction persisting for up to 2 years of convalescence.[16] Following much shorter periods of convalescence, individuals hospitalized with influenza infection have been shown to exhibit continued elevation in $CD8^+$ T cell activation and proliferation.[17] Given the prolonged and profound immune dysregulation seen during acute SARS-CoV2 infection, there is a compelling need to determine whether these alterations translate into longer-term immune alterations and subsequent dysfunction in convalescent individuals.

Here, we examined lymphocytes in COVID-19 patients during hospitalization and in convalescent patients over 6 months following hospital discharge. Specifically, we examined lymphocyte characteristics in peripheral blood mononuclear cells (PBMCs) from blood samples taken from COVID-19 patients within 7 days of hospitalization, at hospital discharge, and at up to 6 months post-hospital discharge. Samples were collected as part of the Coronavirus Immune Response and Clinical Outcomes (CIRCO) study based at 4 hospitals in greater Manchester, UK.[5] Examination of these samples allowed us to ascertain changes to lymphocytes during acute disease and upon convalescence in COVID-19 patients. We identify key alterations in B cell populations in acute COVID-19 patients with severe disease, which indicate that imbalances within the B cell compartment could contribute to COVID-19 disease severity. Specifically, we demonstrate that in severe COVID-19 patients, there was a loss of transitional B cells and an expansion of double-negative memory B cells. Moreover, B cells exhibited altered functionality with increased production of interleukin-6 (IL-6) during acute disease, which was restored in convalescent patients. Intriguingly, B cell production of IL-10 was higher in convalescent patients with good clinical outcomes compared to patients with poor outcomes. In line with this, we also report changes within the $CD4^+$ T cell compartment of acute COVID-19 patients, specifically increases in T follicular helper cells (Tfh) that were recovered in convalescent patients. In contrast, we outline persistent alterations in the functional potential of $CD8^+$ T cells, with T cells from

convalescent patients exhibiting elevated expression of a cytotoxic program and production of type 1 cytokines. These data describe alterations to lymphocytes, detailing previously undescribed imbalances within the B cell compartment associated with the severity of acute disease and alterations in lymphocyte potential that persist for at least 6 months of convalescence. Furthermore, compiling B and T cell immune parameters from convalescent patients identified 3 patient subgroups, defined by (1) increased cytotoxic T cells and T cell type 1 cytokine production, (2) high proportions of memory, IgA^+, and IgG^+ B cells, and (3) the highest expression of trafficking molecules and increased proportions of naive B and T cells. It is noteworthy that the convalescent group defined by the highest proportions of cytotoxic $CD8^+$ T cells and type 1 cytokine production was enriched in patients with a poorer outcome at follow-up, defined by abnormal chest X-ray. Our study provides a deeper understanding of lymphocyte responses over the course of COVID-19 and into recovery, highlighting persistent alterations in lymphocyte functionality in convalescent COVID-19 patients up to 6 months following hospital discharge.

Results and discussion

Clinical characteristics

Between March 29 and July 15, 2020, we recruited patients during their in-patient stay for COVID-19, who had clinical and lymphocyte data available and who were recruited within 7 days of admission. “Convalescent” patients were recruited between July 14 and October 2020 from outpatient clinical follow-up for COVID-19. Convalescent patients are therefore classified as previously hospitalized COVID-19 patients who are clinically stable and have been discharged from any further inpatient care. Convalescent patients were sampled between 53 and 180 days of convalescence. For convalescent patients sampled twice during their convalescence, they were initially sampled between 67 and 180 days of convalescence and then sampled between 20 and 113 days later (with the latest second sample being taken at day 201 following discharge). For convalescent disease samples, one patient was excluded due to a significant coexisting pathology during inpatient admission for COVID-19; all others were included in the analysis. The median age and overall gender proportions were similar between acute and convalescent groups. There was a larger proportion of severe patients within the convalescent group, reflecting that patients with more severe disease were prioritized for limited face to face appointments in participating trusts. The clinical characteristics of all of the patients recruited to the study are summarized in Tables S1 and S2.

Altered B cell phenotypes in severe COVID-19 patients are restored upon convalescence

In agreement with previously published studies,[5,6] we report significantly reduced circulating B cell frequencies in severe COVID-19 patients that were normalized in convalescent patients (Figure 1A). Furthermore, increased Ki-67 expression (indicative of proliferation) in hospitalized patients was not

observed in convalescent patients (Figures 1B and S1A). When characterizing B cell subsets based on the expression of CD27 and immunoglobulin D (IgD), we saw an expansion of $CD27^{-}IgD^{-}$ double-negative (DN) memory B cells in severe COVID-19 patients that was still present in convalescent patients (Figures 1C and 1D). No differences in unswitched memory (USM), switched memory (SM), or naive B cells were observed between the patient groups and controls. Further classification of B cell subsets into transitional ($CD24^{hi}CD38^{hi}$) and mature ($CD24^{int}CD38^{int}$) B cells revealed a significant reduction in transitional B cells in patients with severe COVID-19 that was restored in convalescent patients (Figures 1E and 1F). A t-distributed stochastic neighbor embedding (tSNE) representation of the data highlights proportions of subsets in acute and convalescent COVID-19 patients (Figure 1G). Importantly, $CD27^{hi}CD38^{hi}$ plasmablasts were the only B cell subset expanded in all COVID-19 patients irrespective of severity, yet proportions were restored in convalescent patients (Figures 1H and S1B). We found that the frequency of plasmablasts positively correlated with the expression of IgG and IgA, but not with IgM expression by B cells in acute COVID-19 patients (Figures 1I, S1C, and S1D), providing further evidence supporting an expansion of class-switched IgA and IgG antibodies in COVID-19 patients.[18, 19, 20]

Examining B cell phenotypes in individual COVID-19 patients, and tracking them longitudinally from acute hospitalization into convalescence, showed similar alterations in B cell populations. Specifically, we observed a reduction in Ki-67^{+} B cells and plasmablasts at convalescent time points compared to acute disease and a trend toward an increase in transitional B cells (Figure S1E). Interestingly, tracking individual patients from acute disease into convalescence revealed a decrease in DN B cells, despite the global expansion of this subset observed in both severe acute and convalescent patients (Figure S1F). These data highlight alterations in B cell subsets during severe acute COVID-19 that are largely restored upon convalescence.

Convalescent COVID-19 patients retain phenotypically altered $CD8^{+}$ T cells

Previous studies have detailed $CD8^{+}$ and $CD4^{+}$ T cell activation in COVID-19 patients.[6,21, 22, 23] Here, we show that convalescent patients exhibited elevated proportions of T effector memory cells positive for CD45RA (TEMRA; $CD45RA^{+}CCR7^{-}$) (Figures 2A–2C). Despite this, T cells from convalescent patients did not display elevated expression of the proliferation marker Ki-67 (Figure 2D; see Figures S1G–S1K for representative fluorescence-activated cell sorting (FACS) staining).[6] $CD8^{+}$ T cells from acute COVID-19 patients exhibit robust expression of a cytotoxic program, with increases in perforin, granzyme, and CD107a expression in unstimulated cells (Figures 2E–2G). Induction of this program was still evident in convalescent patients, whose $CD8^{+}$ T cells exhibited increased expression of both perforin and granzyme (Figures 2E and 2F). However, the proportions of $CD107a^{+}$ and Ki-$67^{+}GranzymeB^{+}CD8^{+}$ T cells in convalescent patients were reduced compared to those with acute COVID-19, suggesting that cytotoxic $CD8^{+}$ T cells in convalescent patients were no longer actively proliferating or degranulating (Figure 2G). Showing the same pattern, longitudinal tracking of individual patients from their acute time point into convalescence showed unchanged perforin and

granzyme B expression in $CD8^+$ T cells (Figure 2H), but reduced Ki-67^+, $CD107a^+$, and Ki-67^+GranzymeB^+CD8^+ T cells at convalescent compared to acute time points (Figure 2I). We also noted a persistence of this cytotoxic profile in $CD8^+$ T cells in a small subset of convalescent patients examined beyond 6 months after hospital discharge. Obtaining a second convalescent sample from the same patient at a later time point of convalescence demonstrated persistence of this cytotoxic program beyond 6 months (Figure S1L).

In contrast to these phenotypic changes persisting in the $CD8^+$ T cell compartment up to, and potentially beyond, 6 months of convalescence, alterations noted in acute disease in $CD4^+$ T cells were normalized in convalescent patients. There were no significant changes in regulatory T cells (Tregs) across the disease trajectory (Figure 2J), but during acute disease, there was an expansion in Tfh, defined as $CD4^+CXCR5^+$PD-1^+ICOS^+ (Figure 2K). While an increase in Tfh has been reported previously in acute COVID-19 patients,[6,24,25,26] we show it was reduced in convalescent patients (Figure 2K). This decrease in Tfh in convalescent patients occurred following hospital discharge (Figure 2L) and could be identified when following the same patient from acute disease into convalescence (Figure 2M). These data demonstrate changes in the functional potential of $CD8^+$ T cells up to 6 months following hospital discharge, outlining the continued expression of a cytotoxic program.

Lymphocytes from acute COVID-19 patients exhibit altered trafficking molecule expression that is restored upon convalescence

Lymphopenia is a well-established hallmark of COVID-19 patients[1,8]; although the drivers of peripheral blood lymphocyte loss remain unknown, altered trafficking could contribute. Given the importance of appropriate coordination between immune cells during an effective antiviral response and the implications of altered trafficking molecule expression, we examined the expression of chemokine receptors on lymphocytes during acute and convalescent COVID-19. B cells from acute COVID-19 patients displayed a significantly reduced expression of chemokine receptors CXCR3, CXCR5, and the gut homing molecule integrin β7, particularly in patients with more severe disease (Figures S2A–S2D). The expression of CXCR5 and CXCR3 was largely normalized in convalescent patients regardless of acute disease severity (Figure S2E).

Similar to B cells, CXCR5 and CXCR3 expression was substantially reduced in both $CD4^+$ and $CD8^+$ T cells in acute COVID-19 patients (Figures S2F–S2K), but with β7 exhibiting no alterations in acute disease. This reduction in CXCR3 and CXCR5 occurred irrespective of acute disease severity (Figures S2L and S2M). The loss of CXCR3 and CXCR5 expression was recovered on T cells from convalescent patients (Figures S2F, S2G, S2I, and S2J). In agreement with previous reports examining the expression of CXCR5,[6] our data outline reduced the expression of multiple trafficking molecules on lymphocytes during acute COVID-19 that are mostly restored upon convalescence. Reduced CXCR3 and CXCR5 expression could reflect reduced homing of lymphocytes into lymph nodes and follicles, which have

been reported to contribute to immune dysfunction in other infections, such as advanced HIV.[27, 28, 29] Here, we identify changes in chemokine receptor expression during acute disease that are recovered upon convalescence.

Alterations in lymphocyte cytokine potential in convalescent COVID-19 patients

To understand the impact of COVID-19 on the potential of lymphocytes to make distinct cytokines, we stimulated PBMCs with phorbol myristrate acetate (PMA) and ionomycin and examined cytokine production by T cells (see Figure S3A for example staining). Unlike previously published studies probing antigen specificity of T cells in COVID-19 patients,[14,30] we more broadly assessed the potential of all T cells in COVID-19 patients to secrete cytokines. This approach allowed us to assess the impact of COVID-19 hospitalization on any subsequent immune response, as opposed to the development of SARS-CoV2-specific memory. IL-10$^+$ CD4$^+$ T cells were expanded in acute COVID-19 patients, but this was not observed in convalescent patients (Figure 3A). Normalization of IL-10 production from CD4$^+$ T cells did not occur during hospitalization, as a decrease in IL-10$^+$CD4$^+$ T cells was not evident upon discharge (Figure S3B). As previously reported to occur in response to anti-CD3 and anti-CD28 stimulation,[31] PMA and ionomycin stimulation resulted in increased IL-17$^+$CD4$^+$ T cells in COVID-19 patients (Figure 3B). Remarkably, enhanced IL-17$^+$CD4$^+$ T cells persisted into convalescence. We next queried whether the elevated production of IL-17 during convalescence was associated with any specific clinical phenotypes. Increased IL-17$^+$CD4$^+$ T cells in convalescent patients were seen irrespective of whether patients were stratified by the presentation of normal or abnormal chest X-rays (Figure 3B), reporting versus not reporting increased fatigue, or based upon initial disease severity (Figure S3C).

Despite increased IL-10$^+$ and IL-17$^+$CD4$^+$ T cells, neither CD4$^+$ or CD8$^+$ T cells from acute COVID-19 patients exhibited altered proportions of cells staining positive for the canonical Th1 cytokines interferon γ (IFNγ) or tumor necrosis factor α (TNF-α) (Figures 3C and 3D). Although a previous study has reported that high proportions of antigen-specific IFNγ T cells are associated with reduced disease severity,[26] our observation is in line with other studies demonstrating that total peripheral T cell populations exhibit no enhanced production of these cytokines despite ongoing disease[6,32] and irrespective of acute disease severity (Figures S3D and S3E). In stark contrast, both CD4$^+$ and CD8$^+$ T cells from convalescent COVID-19 patients exhibited enhanced production of type 1 cytokines (Figures 3C and 3D). This increase in cytokine production was not evident at hospital discharge (Figures S3F and S3G). Increased type 1 cytokines occurred when stratifying convalescent patients by the presentation of normal or abnormal chest X-rays (Figures 3C and 3D) and those reporting increased fatigue (Figure S3H). Of note, no significant increase in IFNγ$^+$CD4$^+$ T cells was seen when stratifying patients for fatigue. Increased production of type 1 cytokines in convalescent patients was associated with COVID-19 disease severity, apart from for IFNγ$^+$CD4$^+$ T cells, as patients who had moderate and severe disease showed significant increases in cytokine-positive cells relative to controls (Figures 3E and 3F). As such, the increases seen in total convalescent patients could be due to increased proportions

of patients who exhibited severe disease. However, comparing proportions of cytokine-positive cells in severe patients at acute and convalescent time points still showed an elevation in cytokine-producing T cells, apart from for TNF-α^+CD8$^+$ T cells (Figures S3I and S3J). More important, longitudinal data tracking the same patient across their acute and convalescent disease time points also showed increased production of these type 1 cytokines (except for IFNγ^+TNF-α^+CD4$^+$ T cells) (Figures 3G and 3H). In a small subset of patients, we also obtained a second convalescent sample after 6 months from hospital discharge. In this small group, we noted unchanged proportions of cytokine-positive T cells, suggesting the persistence of elevated cytokine production beyond 6 months (Figures S3K and S3L). These data fit with previous studies showing IFNγ^+ and TNF-α^+ SARS-CoV-2-specific T cells in convalescent patients,[14,30,33] but further outline that altered cytokine potential is a general feature of all T cells during COVID-19 convalescence.

Next, to assess cytokine production by B cells, we stimulated PBMCs from COVID-19 patients with CpGB (a TLR9 agonist) for 48 h and measured cytokine expression by flow cytometry. We observed a significant expansion of IL-6$^+$ B cells in acute COVID-19 patients and a trend toward a decrease in IL-10$^+$ B cells, suggesting an imbalance in B cells toward a more pro-inflammatory phenotype (Figures 3I and S4A–S4D). The frequency of IL-6$^+$ B cells was restored in convalescent patients and was not affected by the presentation of normal or abnormal chest X-rays (Figure 3I) or fatigue (Figure S4D). Interestingly, B cell production of IL-10 was higher in convalescent patients with a good clinical outcome compared to those with a poor outcome. Increased proportions of IL-10$^+$ B cells in convalescent patients with normal chest X-rays compared to those with abnormal chest X-rays (Figure 3I) suggests a positive outcome may be associated with the expansion of regulatory B cells. No significant differences in the frequency of TNF-α^+ B cells were observed in acute and convalescent COVID-19 patients (Figures 3I and S4D). Frequencies of cytokine-positive B cells in both acute and convalescent patients were not affected by disease severity (Figures S4E and S4F). Longitudinal analysis of individual patients from acute disease into convalescence showed no change in either IL-6$^+$ or TNF-α^+ B cells, but it did demonstrate a recovery of IL-10$^+$ B cells upon convalescence (Figure 3J). Of note, only 1 of 13 patients whose B cells were followed longitudinally exhibited an abnormal chest X-ray at follow-up. These data demonstrate an expansion of IL-6$^+$ B cells during acute disease and reduced proportions of IL-10$^+$ B cells in convalescent patients with poor clinical outcomes.

Identification of COVID-19 convalescent immunotypes based on lymphocyte parameters

Our data establish alterations in the lymphocyte compartment that persist up to 6 months post-hospital discharge in convalescent patients. To further probe lymphocyte changes within convalescent COVID-19 patients, we clustered patients based on T and B cell features. Unsupervised clustering revealed 3 groups of convalescent patients with distinct compositions of lymphocyte signatures (Figure 4A). Group 1 was associated with a high expression of trafficking molecules and increased proportions of naive B and T cells; group 2 was characterized by high proportions of IgA$^+$ and IgG$^+$ B cells and memory B cells (both switched and unswitched); group 3 displayed increased cytotoxic T cells, CD8$^+$

TEMRA, and type 1 cytokines by both $CD8^+$ and $CD4^+$ T cells. These data suggest the existence of subgroups of convalescent COVID-19 patients based on lymphocyte phenotypes. We next queried whether these groups could identify convalescent patients based on clinical outcome. Higher proportions of patients in group 3 presented with an abnormal chest X-ray and reported breathlessness at their convalescent follow-up (group 1: abnormal chest X-ray, 23.7%, and dyspnea, 43.2%; group 2: abnormal chest X-ray, 26.3%, and dyspnea, 44.4%; group 3: abnormal chest X-ray, 62.5%, and dyspnea, 62.5%). Examining characteristics of the patients within each group (Figures 4B–4G), we noted that group 1 contained most patients who had had mild disease, younger patients, and a greater proportion of female patients, indicating that these parameters could be affecting this convalescent phenotype. In contrast, we noted very little difference in the demographics or acute disease information between patients in groups 2 and 3. For example, both had a similar proportion of patients who had exhibited severe COVID-19 (group 2, 66.6%; group 3, 50%) and similar proportions of males (group 2, 70.5%; group 3, 75%). Despite similar patient characteristics, these 2 patient groups present with distinct lymphocyte profiles and different outcomes, with group 3 exhibiting the poorest clinical outcome (abnormal chest X-ray, group 2, 26.3%; group 3, 62.5%). Our data provide an important foundation for future work supporting the identification of hospitalized COVID-19 patients at risk of developing long COVID symptoms. Our study can now be expanded to explore additional clinical implications of COVID-19, ascertaining whether specific clinical outcomes are associated with distinct convalescent patient subgroups. These consequences can be ascertained as platforms such as the post-hospitalization COVID-19 study (PHOSP-COVID) in the United Kingdom exist to support such future studies. Moreover, any future studies should also explore whether the lymphocyte alterations defined here are specific to COVID-19 convalescence or occur following hospitalization with any respiratory virus.

In summary, here, we report lymphocyte changes across the COVID-19 disease trajectory into convalescence. Our data demonstrate a high degree of activation of a cytotoxic program within $CD8^+$ T cells during acute disease, as previously reported.[3,5,34] We extend these data by showing the persistence of this program within circulating $CD8^+$ T cells up to at least 6 months of convalescence. Whereas previous studies have shown a persistence of low frequencies of SARS-CoV2-specific $CD8^+$ T cells with a cytotoxic profile,[33] importantly, here, we show the elevation of cytotoxic markers within total circulating $CD8^+$ T cells. Although the specificity of T cells in our study remains to be determined, increases in $CD8^+$ T cells with a cytotoxic potential would result in an altered T cell landscape that could affect tissue integrity, depending on their trafficking capabilities and cytokine responsiveness. Moreover, our data raise questions about the impact that this increase in cytotoxic cells would have on subsequent infection, be that bacterial, viral, or fungal. The importance of this question is further underscored by the elevated potential of total $CD8^+$ and $CD4^+$ T cells to produce IFNγ and TNF-α in convalescent patients, outlining a persistent alteration in cytokine potential that could be either beneficial or detrimental to subsequent immune responses.

In contrast, altered B cell subsets in acute disease are recovered upon convalescence. Several recent studies have reported the detection of virus-specific antibodies for several months post-recovery from SARS-CoV-2 infection.[35, 36, 37] Here, we show that circulating plasmablast frequencies correlate positively with IgA/IgG and negatively with IgM, further supporting an expansion of class-switched antibodies in COVID-19 patients. In addition to secreting antibodies, B cells produce cytokines and are classified into effector (Beff; IL-6^+ and TNF-α^+) and regulatory B cell (Breg; IL-10^+) subsets based on the cytokines that they produce.[38] Significant decreases in transitional B cells, the precursors of human Bregs,[39] along with IL-10^+ B cells, suggest a loss of immunosuppressive Bregs and an expansion of Beff cells in severe COVID-19 patients, as also observed in chronic inflammatory disorders such as systemic lupus erythematosus (SLE) and rheumatoid arthritis (RA).[39, 40, 41] Interestingly, the resolution of lung pathology in COVID-19 patients was found to be associated with higher proportions of IL-10^+ B cells, suggesting that these cells could be important in suppressing excess inflammation, and are associated with positive long-term outcomes.

In summary, we report phenotypic and functional alterations to B and T cells across the trajectory of SARS-CoV-2 responses from acute disease requiring hospitalization into convalescence, identifying immune alterations that persist in convalescent COVID-19 patients for up to 6 months. Our study therefore identifies lymphocyte changes in convalescent COVID-19 patients, which could have longer-term effects on subsequent anti-pathogen or auto-inflammatory responses.

Limitations of study

Our study has limitations, including the reduced number of samples from patients at acute disease (n = 58) relative to those during convalescence (n = 83); in fact, for some parameters, only 30 acute samples were examined. Furthermore, disease severity in the acute group did not match that in the convalescent group; the latter contained more severe patients (acute = 22.4%; convalescence = 49.4%). In addition, only 14 patients were followed longitudinally from acute disease into convalescence. Our study would have been significantly enhanced if we could have followed more individual patients. Our study would have been further enhanced were it possible to examine convalescent patients at later time points—for example, 9 months and 1 year.

Consortia

The members of CIRCO are Rohan Ahmed, Miriam Avery, Katharine Birchall, Evelyn Charsley, Alistair Chenery, Christine Chew, Richard Clark, Emma Connolly, Karen Connolly, Simon Dawson, Laura Durrans, Hannah Durrington, Jasmine Egan, Kara Filbey, Claire Fox, Helen Francis, Miriam Franklin, Susannah Glasgow, Nicola Godfrey, Kathryn J. Gray, Seamus Grundy, Jacinta Guerin, Pamela Hackney, Chantelle Hayes, Emma Hardy, Jade Harris, Anu John, Bethany Jolly, Verena Kästele, Gina Kerry, Sylvia Lui, Lijing Lin, Alex G. Mathioudakis, Joanne Mitchell, Clare Moizer,

Katrina Moore, Stuart Moss, Syed Murtuza Baker, Rob Oliver, Grace Padden, Christina Parkinson, Michael Phuycharoen, Ananya Saha, Barbora Salcman, Nicholas A. Scott, Seema Sharma, Jane Shaw, Joanne Shaw, Elizabeth Shepley, Lara Smith, Simon Stephan, Ruth Stephens, Gael Tavernier, Rhys Tudge, Louis Wareing, Roanna Warren, Thomas Williams, Lisa Willmore, and Mehwish Younas.

STAR★Methods

Key resources table

Resource availability

Lead contact Further information and requests for resources and information should be directed to the Lead Contact, Joanne E. Konkel (Joanne.konkel@manchester.ac.uk).

Materials availability This study did not generate new unique reagents.

Data and code availability All relevant data outputs are within the paper and supplemental information.

Experimental models and subject details

Study design and participants Two cohorts of patients were recruited from Manchester University Foundation Trust (MFT), Salford Royal NHS Foundation Trust (SRFT) and Pennine Acute NHS Trust (PAT) under the framework of the Manchester Allergy, Respiratory and Thoracic Surgery (ManARTS) Biobank (study no M2020-88) for MFT or the Northern Care Alliance Research Collection (NCARC) tissue biobank (study no NCA-009) for SRFT and PAT. Ethical approval obtained from the National Research Ethics Service (REC reference 15/NW/0409 for ManARTS and 18/WA/0368 for NCARC). Informed consent was obtained from each patient, clinical information was extracted from written/electronic medical records including demographic data, presenting symptoms, comorbidities, radiographic findings, vital signs, and laboratory data. Patients were included if they tested positive for SARS-CoV-2 by reverse-transcriptase–polymerase-chain-reaction (RT-PCR) on nasopharyngeal/oropharyngeal swabs or sputum during their in-patient admission for COVID-19. Patients with negative nasopharyngeal RTPCR results were also included if there was a high clinical suspicion of COVID-19, the radiological findings supported the diagnosis, and there was no other explanation for symptoms. Patients were excluded if an alternative diagnosis was reached, where indeterminate imaging findings were combined with negative SARS-CoV-2 nasopharyngeal (NP) test, or there was another confounding acute illness not directly related to COVID-19. The severity of disease was scored each day, based on criteria for escalation of care (Table S3). Where severity of

disease changed during admission, the highest disease severity score was selected for classification. Peripheral blood samples were collected within 7 days of hospital admission, at discharge and then at 3-9 months post hospital discharge when patients returned to out-patient clinics.

Demographics and clinical information for acute and convalescent patients can be found in Tables S1 and S2.

Healthy controls Recruiting healthy individuals from the community for blood sampling during the SARS-CoV-2 outbreak was not possible, and therefore we sampled frontline workers from NHS Trusts and University of Manchester staff with an age range that was similar to our COVID-19 patients (age range 35-71; median age = 50.9; 52% males). All healthy controls tested negative for anti-Spike1 receptor binding domain antibodies.

Method details

PBMC isolation Fresh blood samples from COVID-19 patients and healthy individuals were collected in EDTA tubes. Blood was diluted 1:1 with PBS and layered gently on Ficoll-Paque in SepMATE tubes (StemCell Technologies) followed by density gradient centrifugation. Cells were thoroughly washed and were either freshly stained for flow cytometry or are stored in 10% dimethyl sulfoxide (DMSO) in fetal bovine serum (FBS) at −150°C.

Cell culture Frozen PBMC were thawed, washed and resuspended in RPMI containing 10% FBS, L-Glutamine, non-essential amino acids, HEPES, and penicillin plus streptomycin. 2.5×10^5 cells were stimulated with; (i) 2μL/ml of stimulation cocktail (eBioScience) in the presence of 10 μg/ml Brefeldin A for three hours (T cells), (ii) 1 μM CpG for 48 hours followed by 2μL/ml of stimulation cocktail (eBioScience) in the presence of 10 μg/ml Brefeldin A in the last four hours (B cells). Following stimulation cells were washed and stained for flow cytometric analysis.

Flow cytometry PBMCs (fresh/thawed/stimulated) were stained with fluorophore conjugated antibodies (see Key resources table) and viability dyes. Samples were acquired on an LSRFortessa cell analyzer (Becon Dickinson) and analyzed using FlowJo (TreeStar).

Quantification and statistical analysis

Clustering of T and B cell phenotypes T cell and B cell data were scaled using unit variance scaling, clustered and graphed using correlation distance and average linkage on the heatmap tool on ClustVis.[42]

Statistics Results are presented as individual data points with medians. Normality tests were performed on all datasets. Groups were compared using an unpaired Mann-Whitney test for healthy individuals versus COVID-19 patients, one-way ANOVA with Holm-Sidak post hoc testing (normal distribution) or Kruskal-Wallis test with Dunn's post hoc testing (failing normality testing) for multiple comparisons, or Spearman's rank correlation coefficient test for correlation of separate parameters within the COVID-19 patient group, using Prism 8 software (GraphPad). In all cases, a p value of ≤ 0.05 was considered significant. Where no statistical difference is shown there was no significant difference. Details of statistical tests and definitions of n can be found in each figure legend.

Acknowledgments

This study was funded by the BBSRC (BB/M025977/1, to J.E.K. and BB/S01103X/1, to T.N.S.), by the Lister Institute (Prize Fellowship to J.E.K.), by PTDF (SHS/1327/18, to H.A.S.), the Wellcome Trust (202865/Z/16/Z, to T.H.), The Kennedy Trust for Rheumatology Research (Rapid Response Award to J.R.G.), Versus Arthritis (F.A.M. and J.E.K. studentship), and philanthropy awards from 3M Global Giving (J.R.G. and T.H.) and the University of Manchester COVID-19 fund (J.E.K. and M.M.). J.R.G. is the recipient of a Senior Fellowship funded by The Kennedy Trust for Rheumatology Research. This work also was partly funded by UKRI/NIHR through the UK Coronavirus Immunology Consortium (UK-CIC). This report is independent research supported by the North West Lung Centre Charity and the NIHR Manchester Clinical Research Facility at Wythenshawe Hospital. We acknowledge the Manchester Allergy, Respiratory, and Thoracic Surgery Biobank and thank the study participants for their contribution. The views expressed in this publication are those of the authors and not necessarily those of the NHS, the National Institute for Health Research, or the Department of Health. Angela Simpson, Tim Felton, Paul Dark, and Tracy Hussell are supported by the NIHR Manchester Biomedical Research Centre. In addition, we would like to thank the following for technical and scientific discussions: the Lydia Becker Institute of Immunology and Inflammation, the University of Manchester Flow Cytometry Facility, The NIHR Respiratory TRC, the UK Coronavirus Immunology Consortium, and PHOSP-COVID.

Author contributions

Conceptualization, J.E.K. and M.M.; methodology, J.E.K., M.M., J.R.G., and T.H.; investigation, H.A.S., T.N.S., K.W., F.A.M., S.B.K., I.P., C.J., D.J.M., S.K., O.B., E.R.M., and the CIRCO investigators; formal analysis, I.P. and S.B.K.; resources, S.B.K., L.P., A.U., N.D.B., P.D., C.E.B., S.B., T.F., and A.S.; data curation, S.B.K.; writing – original draft, J.E.K. and M.M.; writing – review & editing, H.A.S., T.N.S., J.E.K., M.M., J.R.G., and T.H.; visualization, K.W.; supervision, J.E.K. and M.M.; funding acquisition, J.E.K., M.M., J.R.G., and T.H.

Declaration of interests

The authors declare no competing interests.

Notes

Published: March 31, 2021

Footnotes

Supplemental information can be found online at https://doi.org/10.1016/j.medj.2021.03.013.

Contributor Information

CIRCO:

Rohan Ahmed, Miriam Avery, Katharine Birchall, Evelyn Charsley, Alistair Chenery, Christine Chew, Richard Clark, Emma Connolly, Karen Connolly, Simon Dawson, Laura Durrans, Hannah Durrington, Jasmine Egan, Kara Filbey, Claire Fox, Helen Francis, Miriam Franklin, Susannah Glasgow, Nicola Godfrey, Kathryn J. Gray, Seamus Grundy, Jacinta Guerin, Pamela Hackney, Chantelle Hayes, Emma Hardy, Jade Harris, Anu John, Bethany Jolly, Verena Kästele, Gina Kerry, Sylvia Lui, Lijing Lin, Alex G. Mathioudakis, Joanne Mitchell, Clare Moizer, Katrina Moore, Stuart Moss, Syed Murtuza Baker, Rob Oliver, Grace Padden, Christina Parkinson, Michael Phuycharoen, Ananya Saha, Barbora Salcman, Nicholas A. Scott, Seema Sharma, Jane Shaw, Joanne Shaw, Elizabeth Shepley, Lara Smith, Simon Stephan, Ruth Stephens, Gael Tavernier, Rhys Tudge, Louis Wareing, Roanna Warren, Thomas Williams, Lisa Willmore, and Mehwish Younas

Supplemental information

Document S1. Tables S1–S3 and Figures S1–S4:

Document S2. Article plus supplemental information:

References

1. Huang C., Wang Y., Li X., Ren L., Zhao J., Hu Y., Zhang L., Fan G., Xu J., Gu X. Clinical features of patients infected with 2019 novel coronavirus in Wuhan, China. *Lancet.* 2020;**395**:497–506. [PMCID: PMC7159299] [PubMed: 31986264]

2. Guan W.-J., Ni Z.-Y., Hu Y., Liang W.H., Ou C.Q., He J.X., Liu L., Shan H., Lei C.L., Hui D.S.C., China Medical Treatment Expert Group for Covid-19 Clinical Characteristics of Coronavirus Disease 2019 in China. *N. Engl. J. Med.* 2020;**382**:1708–1720. [PMCID: PMC7092819] [PubMed: 32109013]

3. Kuri-Cervantes L., Pampena M.B., Meng W., Rosenfeld A.M., Ittner C.A.G., Weisman A.R., Agyekum R.S., Mathew D., Baxter A.E., Vella L.A. Comprehensive mapping of immune perturbations associated with severe COVID-19. *Sci. Immunol.* 2020;**5**:eabd7114. [PMCID: PMC7402634] [PubMed: 32669287]

4. Lucas C., Wong P., Klein J., Castro T.B.R., Silva J., Sundaram M., Ellingson M.K., Mao T., Oh J.E., Israelow B., Yale IMPACT Team Longitudinal analyses reveal immunological misfiring in severe COVID-19. *Nature.* 2020;**584**:463–469. [PMCID: PMC7477538] [PubMed: 32717743]

5. Mann E.R., Menon M., Knight S.B., Konkel J.E., Jagger C., Shaw T.N., Krishnan S., Rattray M., Ustianowski A., Bakerly N.D., NIHR Respiratory TRC. CIRCO Longitudinal immune profiling reveals key myeloid signatures associated with COVID-19. *Sci. Immunol.* 2020;**5**:eabd6197. [PMCID: PMC7857390] [PubMed: 32943497]

6. Mathew D., Giles J.R., Baxter A.E., Oldridge D.A., Greenplate A.R., Wu J.E., Alanio C., Kuri-Cervantes L., Pampena M.B., D'Andrea K., UPenn COVID Processing Unit Deep immune profiling of COVID-19 patients reveals distinct immunotypes with therapeutic implications. *Science.* 2020;**369**:eabc8511. [PMCID: PMC7402624] [PubMed: 32669297]

7. Wilk A.J., Rustagi A., Zhao N.Q., Roque J., Martínez-Colón G.J., McKechnie J.L., Ivison G.T., Ranganath T., Vergara R., Hollis T. A single-cell atlas of the peripheral immune response in patients with severe COVID-19. *Nat. Med.* 2020;**26**:1070–1076. [PMCID: PMC7382903] [PubMed: 32514174]

8. Chen G., Wu D., Guo W., Cao Y., Huang D., Wang H., Wang T., Zhang X., Chen H., Yu H. Clinical and immunological features of severe and moderate coronavirus disease 2019. *J. Clin. Invest.* 2020;**130**:2620–2629. [PMCID: PMC7190990] [PubMed: 32217835]

9. Fraser E. Long term respiratory complications of covid-19. *BMJ.* 2020;**370**:m3001. [PubMed: 32747332]

10. Williams F.M.K., Muirhead N., Pariante C. Covid-19 and chronic fatigue. *BMJ.* 2020;**370**:m2922. [PubMed: 32732337]

11. Greenhalgh T., Knight M., A'Court C., Buxton M., Husain L. Management of post-acute covid-19 in primary care. *BMJ.* 2020;**370**:m3026. [PubMed: 32784198]

12. Rodda L.B., Netland J., Shehata L., Pruner K.B., Morawski P.A., Thouvenel C.D., Takehara K.K., Eggenberger J., Hemann E.A., Waterman H.R. Functional SARS-CoV-2-Specific Immune Memory Persists after Mild COVID-19. *Cell.* 2021;**184**:169–183.e17. [PMCID: PMC7682481] [PubMed: 33296701]

13. Dan J.M., Mateus J., Kato Y., Hastie K.M., Yu E.D., Faliti C.E., Grifoni A., Ramirez S.I., Haupt S., Frazier A. Immunological memory to SARS-CoV-2 assessed for up to 8 months after infection. *Science.* 2021;**371**:eabf4063. [PMCID: PMC7919858] [PubMed: 33408181]

14. Peng Y., Mentzer A.J., Liu G., Yao X., Yin Z., Dong D., Dejnirattisai W., Rostron T., Supasa P., Liu C., Oxford Immunology Network Covid-19 Response T cell Consortium. ISARIC4C Investigators Broad and strong memory $CD4^+$ and $CD8^+$ T cells induced by SARS-CoV-2 in UK convalescent individuals following COVID-19. *Nat. Immunol.* 2020;**21**:1336–

1345. [PMCID: PMC7611020] [PubMed: 32887977]

15. Pradenas E., Trinité B., Urrea V., Marfil S., Ávila-Nieto C., Rodríguez de la Concepción M.L., Tarrés-Freixas F., Pérez-Yanes S., Rovirosa C., Ainsua-Enrich E. Stable neutralizing antibody levels 6 months after mild and severe COVID-19 episode. *Med (N Y)* 2021;**2**:313–320.e4. [PMCID: PMC7847406] [PubMed: 33554155]

16. Wiedemann A., Foucat E., Hocini H., Lefebvre C., Hejblum B.P., Durand M., Krüger M., Keita A.K., Ayouba A., Mély S., PostEboGui Study Group Long-lasting severe immune dysfunction in Ebola virus disease survivors. *Nat. Commun.* 2020;**11**:3730. [PMCID: PMC7381622] [PubMed: 32709840]

17. Wong S.-S., Oshansky C.M., Guo X.J., Ralston J., Wood T., Seeds R., Newbern C., Waite B., Reynolds G., Widdowson M.A., SHIVERS Investigation Team Severe Influenza Is Characterized by Prolonged Immune Activation: Results From the SHIVERS Cohort Study. *J. Infect. Dis.* 2018;**217**:245–256. [PMCID: PMC7335675] [PubMed: 29112724]

18. Ma H., Zeng W., He H., Zhao D., Jiang D., Zhou P., Cheng L., Li Y., Ma X., Jin T. Serum IgA, IgM, and IgG responses in COVID-19. *Cell. Mol. Immunol.* 2020;**17**:773–775. [PMCID: PMC7331804] [PubMed: 32467617]

19. Long Q.-X., Liu B.-Z., Deng H.-J., Wu G.C., Deng K., Chen Y.K., Liao P., Qiu J.F., Lin Y., Cai X.F. Antibody responses to SARS-CoV-2 in patients with COVID-19. *Nat. Med.* 2020;**26**:845–848. [PubMed: 32350462]

20. Yu H.Q., Sun B.Q., Fang Z.F., Zhao J.C., Liu X.Y., Li Y.M., Sun X.Z., Liang H.F., Zhong B., Huang Z.F. Distinct features of SARS-CoV-2-specific IgA response in COVID-19 patients. *Eur. Respir. J.* 2020;**56**:2001526. [PMCID: PMC7236821] [PubMed: 32398307]

21. Laing A.G., Lorenc A., Del Molino Del Barrio I., Das A., Fish M., Monin L., Muñoz-Ruiz M., McKenzie D.R., Hayday T.S., Francos-Quijorna I. A dynamic COVID-19 immune signature includes associations with poor prognosis. *Nat. Med.* 2020;**26**:1623–1635. [PubMed: 32807934]

22. Hadjadj J., Yatim N., Barnabei L., Corneau A., Boussier J., Smith N., Péré H., Charbit B., Bondet V., Chenevier-Gobeaux C. Impaired type I interferon activity and inflammatory responses in severe COVID-19 patients. *Science.* 2020;**369**:718–724. [PMCID: PMC7402632] [PubMed: 32661059]

23. Chen Z., John Wherry E. T cell responses in patients with COVID-19. *Nat. Rev. Immunol.* 2020;**20**:529–536. [PMCID: PMC7389156] [PubMed: 32728222]

24. Thevarajan I., Nguyen T.H.O., Koutsakos M., Druce J., Caly L., van de Sandt C.E., Jia X., Nicholson S., Catton M., Cowie B. Breadth of concomitant immune responses prior to patient recovery: a case report of non-severe COVID-19. *Nat. Med.* 2020;**26**:453–455. [PMCID: PMC7095036] [PubMed: 32284614]

25. Yang X., Dai T., Zhou X., Qian H., Guo R., Lei L., Zhang X., Zhang D., Shi L., Cheng Y. Analysis of adaptive immune cell populations and phenotypes in the patients infected by SARS-CoV-2. *medRxiv.* 2020 doi: 10.1101/2020.03.23.20040675. [CrossRef: 10.1101/2020.03.23.20040675]

26. Moderbacher C.R., Ramirez S.I., Dan J.M., Grifoni A., Hastie K.M., Weiskopf D., Belanger S., Abbott R.K., Kim C., Choi J. Antigen-specific adaptive immunity to SARS-CoV-2 in acute COVID-19 and associations with age and disease severity. *Cell.* 2020;**183**:996–1012.e19. [PMCID: PMC7494270] [PubMed: 33010815]

27. Brainard D.M., Tager A.M., Misdraji J., Frahm N., Lichterfeld M., Draenert R., Brander C., Walker B.D., Luster A.D. Decreased CXCR3+ CD8 T cells in advanced human immunodeficiency virus infection suggest that a homing defect contributes to cytotoxic T-lymphocyte dysfunction. *J. Virol.* 2007;**81**:8439–8450. [PMCID: PMC1951383] [PubMed: 17553894]

28. Henneken M., Dörner T., Burmester G.-R., Berek C. Differential expression of chemokine receptors on peripheral blood B cells from patients with rheumatoid arthritis and systemic lupus erythematosus. *Arthritis Res. Ther.* 2005;**7**:R1001–R1013. [PMCID: PMC1257429] [PubMed: 16207316]

29. Moser B. CXCR5, the Defining Marker for Follicular B Helper T (TFH) Cells. *Front. Immunol.* 2015;**6**:296. [PMCID: PMC4459225] [PubMed: 26106395]

30. Sekine T., Perez-Potti A., Rivera-Ballesteros O., Strålin K., Gorin J.-B., Olsson A., Llewellyn-Lacey S., Kamal H., Bogdanovic G., Muschiol S. Robust T cell immunity in convalescent individuals with asymptomatic or mild COVID-19. *Cell.* 2020;**183**:158–168.e14. [PMCID: PMC7427556] [PubMed: 32979941]

31. De Biasi S., Meschiari M., Gibellini L., Bellinazzi C., Borella R., Fidanza L., Gozzi L., Iannone A., Lo Tartaro D., Mattioli M. Marked T cell activation, senescence, exhaustion and skewing towards TH17 in patients with COVID-19 pneumonia. *Nat. Commun.* 2020;**11**:3434. [PMCID: PMC7338513] [PubMed: 32632085]

32. Qin C., Zhou L., Hu Z., Zhang S., Yang S., Tao Y., Xie C., Ma K., Shang K., Wang W., Tian D.S. Dysregulation of Immune Response in Patients With Coronavirus 2019 (COVID-19) in Wuhan, China. *Clin. Infect. Dis.* 2020;**71**:762–768. [PMCID: PMC7108125] [PubMed: 32161940]

33. Neidleman J., Luo X., Frouard J., Xie G., Gill G., Stein E.S., McGregor M., Ma T., George A.F., Kosters A. SARS-CoV-2-Specific T Cells Exhibit Phenotypic Features of Helper Function, Lack of Terminal Differentiation, and High Proliferation Potential. *Cell Rep. Med.* 2020;**1**:100081. [PMCID: PMC7437502] [PubMed: 32839763]

34. Zheng H.-Y., Zhang M., Yang C.-X., Zhang N., Wang X.C., Yang X.P., Dong X.Q., Zheng Y.T. Elevated exhaustion levels and reduced functional diversity of T cells in peripheral blood may predict severe progression in COVID-19 patients. *Cell. Mol. Immunol.* 2020;**17**:541–543. [PMCID: PMC7091621] [PubMed: 32203186]

35. Compeer E.B., Uhl L.F.K. Antibody response to SARS-CoV-2 — sustained after all? *Nat. Rev. Immunol.* 2020;**20**:590. [PMCID: PMC7418089] [PubMed: 32782353]

36. Ni L., Ye F., Cheng M.-L., Feng Y., Deng Y.Q., Zhao H., Wei P., Ge J., Gou M., Li X. Detection of SARS-CoV-2-Specific Humoral and Cellular Immunity in COVID-19 Convalescent Individuals. *Immunity.* 2020;**52**:971–977.e3. [PMCID: PMC7196424] [PubMed: 32413330]

37. Tonn T., Corman V.M., Johnsen M., Richter A., Rodionov R.N., Drosten C., Bornstein S.R. Stability and neutralising capacity of SARS-CoV-2-specific antibodies in convalescent plasma. *Lancet Microbe.* 2020;**1**:e63. [PMCID: PMC7279746] [PubMed: 32835332]

38. Matsushita T. Regulatory and effector B cells: friends or foes? *J. Dermatol. Sci.* 2019;**93**:2–7. [PubMed: 30514664]

39. Blair P.A., Noreña L.Y., Flores-Borja F., Rawlings D.J., Isenberg D.A., Ehrenstein M.R., Mauri C. CD19(+)CD24(hi)CD38(hi) B cells exhibit regulatory capacity in healthy individuals but are functionally impaired in systemic Lupus Erythematosus patients. *Immunity.* 2010;**32**:129–140. [PubMed: 20079667]

40. Flores-Borja F., Bosma A., Ng D., Reddy V., Ehrenstein M.R., Isenberg D.A., Mauri C. CD19+CD24hiCD38hi B cells maintain regulatory T cells while limiting TH1 and TH17 differentiation. *Sci. Transl. Med.* 2013;**5**:173ra23. [PubMed: 23427243]

41. Mauri C., Menon M. Human regulatory B cells in health and disease: therapeutic potential. *J. Clin. Invest.* 2017;**127**:772–779. [PMCID: PMC5330739] [PubMed: 28248202]

42. Metsalu T., Vilo J. ClustVis: a web tool for visualizing clustering of multivariate data using Principal Component Analysis and heatmap. *Nucleic Acids Res.* 2015;**43**(W1):W566–W570. [PMCID: PMC4489295] [PubMed: 25969447]

Figures and Tables

Figure 1

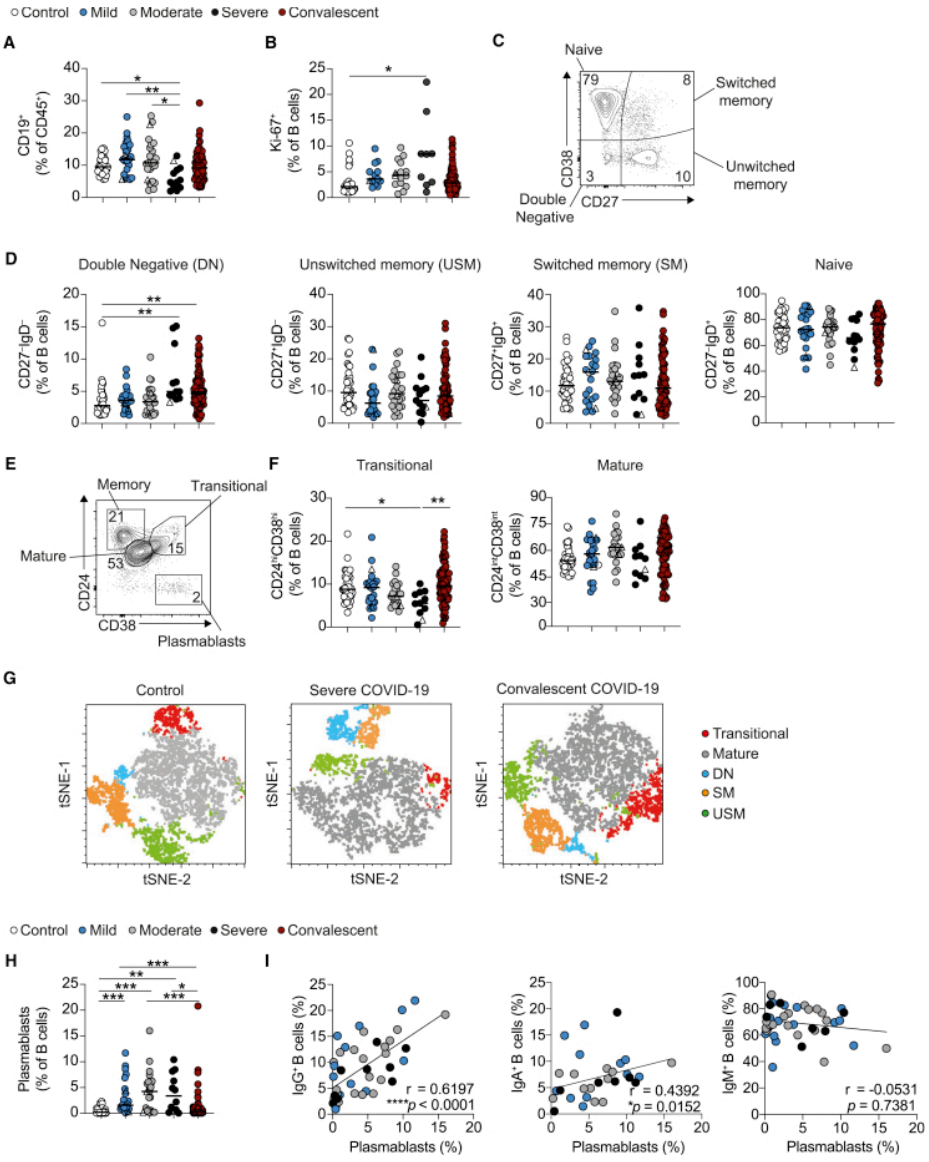

Alterations in B cell subsets during acute COVID-19 are recovered upon convalescence

(A) Cumulative data show *ex vivo* frequency of $CD19^+$ B cells in healthy individuals (n = 38) and COVID-19 patients with mild (n = 24), moderate (n = 26), and severe (n = 12) disease and at convalescence (n = 83).

(B) Cumulative data show Ki-67 expression by B cells in healthy individuals (n = 28) and COVID-19 patients with mild (n = 13), moderate (n = 15), and severe (n = 9) disease and at convalescence (n = 75).

(C and D) Representative flow cytometry plots and cumulative data show frequencies of naive ($CD27^{-}IgD^{+}$), unswitched memory ($CD27^{+}IgD^{+}$), switched memory ($CD27^{+}IgD^{-}$), and double-negative ($CD27^{-}IgD^{-}$) B cells in healthy individuals (n = 38–40) and COVID-19 with mild (n = 22–24), moderate (n = 25–26), and severe (n = 12–13) disease and at convalescence (n = 78–80).

(E and F) Representative flow cytometry plots and cumulative data show *ex vivo* frequency of $CD24^{hi}CD38^{hi}$ transitional B cells and $CD24^{int}CD38^{int}$ mature B cells in healthy individuals (n = 37) and COVID-19 patients with mild (n = 24), moderate (n = 23), and severe (n = 11) disease and at convalescence (n = 80).

(G) tSNE projection of flow cytometry panel visualizing B cell subsets in PBMCs. Representative images for healthy individuals, severe COVID-19 patients, and convalescent patients. Key indicates cell subsets identified on the image.

(H) Cumulative data show frequency of $CD27^{hi}CD38^{hi}$ plasmablasts in healthy controls (n = 38) and COVID-19 patients with mild (n = 23), moderate (n = 23), and severe (n = 12) disease and at convalescence (n = 81).

(I) Graph showing correlation between plasmablasts and IgG^{+} (left), IgA^{+} (center), or IgM^{+} (right) B cell frequencies in acute COVID-19 patients. Graphs show individual patient data, with the bar representing median values.

In all graphs, open triangles represent SARS-CoV-2 PCR^{-} patients. $*p < 0.05$, $**p < 0.01$, $***p < 0.001$, 1-way ANOVA with Kruskal-Wallis test with Dunn's post hoc testing for multiple comparisons or Spearman ranked coefficient correlation test.

See also Figures S1 and S2.

Figure 2

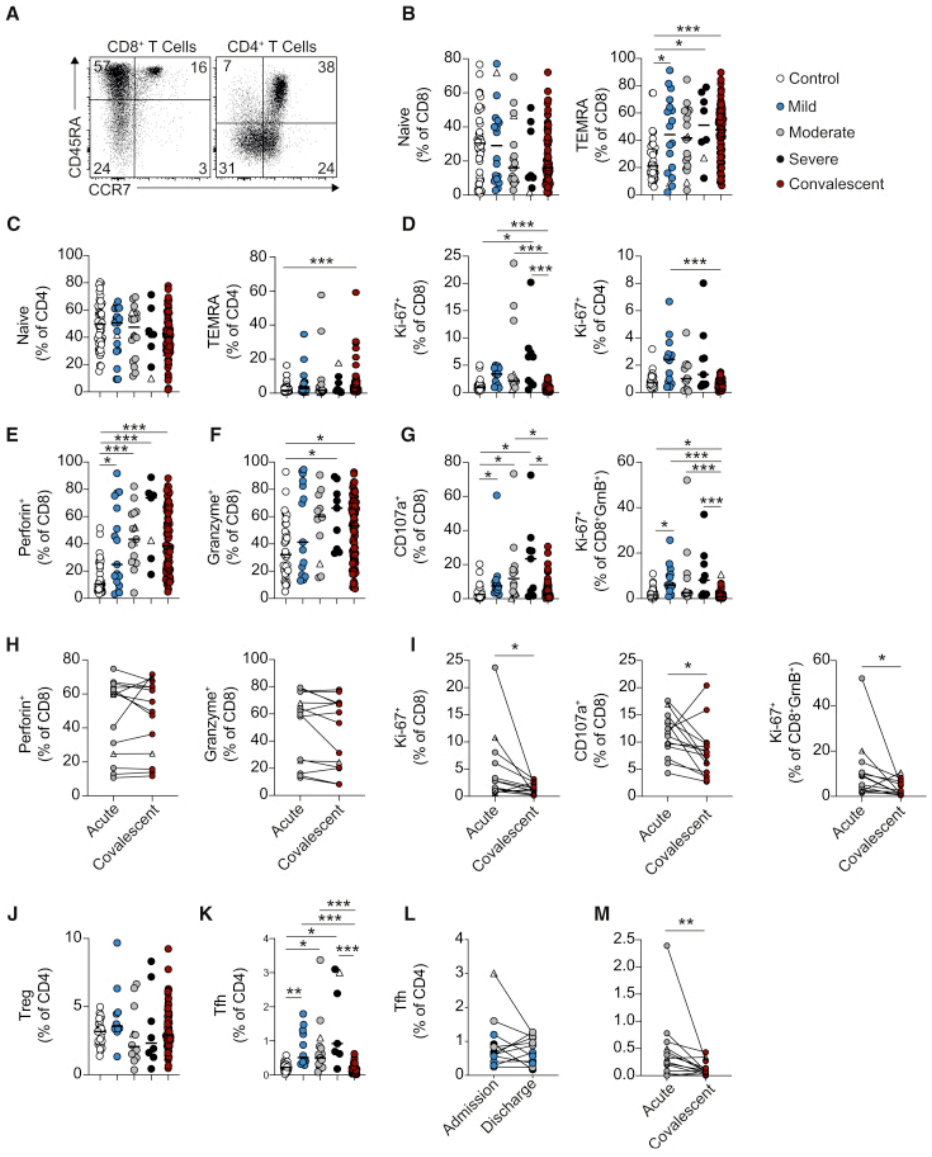

Acute alterations in CD4$^+$ T cells and persistent alterations in CD8$^+$ T cells during COVID-19

(A) Representative FACS plots showing CD45RA and CCR7 staining on CD4$^+$ (gated CD3$^+$CD8$^-$) and CD8$^+$ (gated CD3$^+$CD4$^-$) T cells.

(B and C) Graphs showing frequencies of (B) CD8$^+$ and (C) CD4$^+$ T cells that have a naive (CD45RA$^+$CCR7$^+$) and TEMRA (CD45RA$^+$CCR7$^-$) phenotype in healthy individuals (n = 44) and COVID-19 patients with mild (n = 18–19), moderate (n = 18), and severe (n = 8) disease and at up to 6 months of convalescence (n = 83).

(D) Graphs showing frequencies of CD8$^+$ and CD4$^+$ T cells that stain positive for Ki-67 in healthy individuals (n = 28–30), and COVID-19 patients with mild (n = 14), moderate (n = 11–13), and severe (n = 9) disease and at convalescence (n = 81).

(E–G) Graphs showing frequencies of (E) CD8$^+$Perforin$^+$ cells, (F) CD8$^+$GranzymeB$^+$ cells, and (G) CD8$^+$CD107a$^+$ cells and CD8$^+$GranzymeB$^+$ Ki-67$^+$ cells in healthy individuals (n = 29–37), and COVID-19 patients with mild (n = 12–17), moderate (n = 12–15), and severe (n = 7–9) disease and at convalescence (n = 81–83).

(H and I) Graphs track frequencies of (H) Perforin$^+$ and GranzymeB$^+$ and (I) Ki-67$^+$, CD107a$^+$, and GranzymeB$^+$Ki-67$^+$CD8$^+$ T cells in the same COVID-19 patient at acute (gray circles) and convalescent (maroon circles) time points (n = 14).

(J) Graph shows frequencies of Tregs within CD4$^+$ T cells of healthy individuals (n = 20) and COVID-19 patients with mild (n = 10), moderate (n = 12), and severe (n = 8) disease and at convalescence (n = 82).

(K) Graph shows frequencies of Tfh within CD4$^+$ T cells of healthy individuals (n = 34) and COVID-19 patients with mild (n = 12), moderate (n = 15), and severe (n = 7) disease and at convalescence (n = 83).

(L) Graph shows frequencies of Tfh in individual acute COVID-19 patients with mild (n = 4), moderate (n = 5), and severe (n = 3) disease at their first and last time points of hospitalization.

(M) Graph tracks frequency of Tfh CD4$^+$ T cells in the same COVID-19 patient at acute (gray circles) and convalescent (maroon circles) time points (n = 14). Graphs show individual patient data, with the bar representing median values.

In all graphs, open triangles represent SARS-CoV-2 PCR$^-$ patients. $*p < 0.05$, $**p < 0.01$, $***p < 0.001$, 1-way ANOVA with Kruskal-Wallis test with Dunn's post hoc testing for multiple comparisons (for B–G and K) or Wilcoxon matched-pairs signed rank test (I and M).

See also Figures S1 and S2.

Figure 3

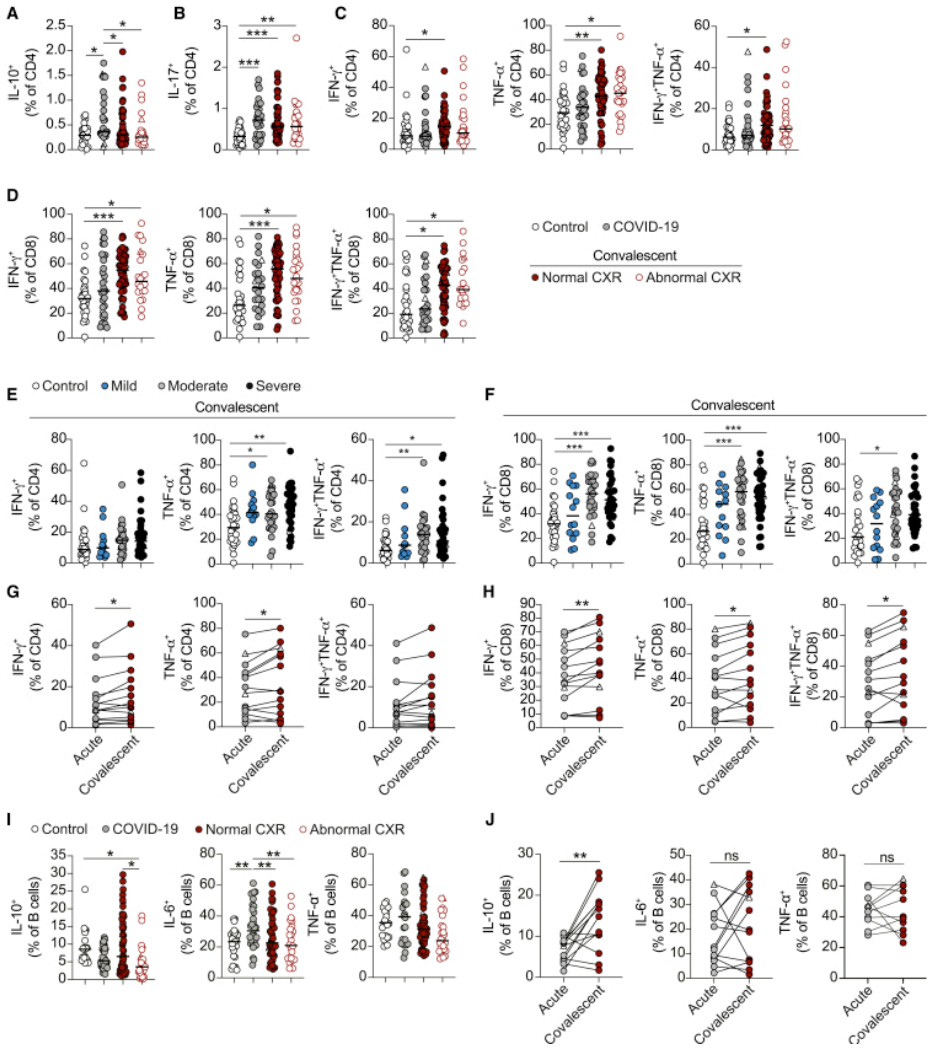

Changes in cytokine production by lymphocytes during acute and convalescent COVID-19

(A–C) Graphs showing frequencies of $CD4^+$ T cells that stain positive for (A) IL-10, (B) IL-17, and (C) IFNγ and TNF-α following 3-h stimulation with PMA and ionomycin in healthy individuals (n = 25–30), acute COVID-19 patients (n = 29–33), and convalescent COVID-19 patients with normal (n = 55–57) or abnormal chest X-ray findings (n = 25–26).

(D) Graphs showing frequencies of $CD8^+$ T cells that stain positive for IFNγ and TNF-α following 3-h stimulation with PMA and ionomycin in healthy individuals (n = 28), acute COVID-19 patients (n = 24–31), and convalescent COVID-19 patients with normal (n = 54–57) or abnormal chest X-ray findings (n = 21–24).

(E and F) Graphs show frequencies of (E) $CD4^+$ and (F) $CD8^+$ T cells that stain positive for IFNγ and TNF-α following 3-h stimulation with PMA and ionomycin in convalescent COVID-19 patients who initially presented with mild (n = 13–14), moderate (n = 25–28), and severe (n = 34–41) disease.

(G and H) Graphs track frequencies of (G) $CD4^+$ and (H) $CD8^+$ T cells that stain positive for IFNγ and TNF-α in the same COVID-19 patient at acute (gray circles) and convalescent (maroon circles) time points (n = 14).

(I) Graphs showing frequencies of $CD19^+$ B cells positive for IL-10, IL-6, and TNF-α following 48-h stimulation with CpGB in healthy individuals (n = 22–27), acute COVID-19 patients (n = 22–32), and convalescent COVID-19 patients with normal (n = 52–54) or abnormal chest X-ray findings (n = 24–27).

(J) Graphs track frequencies of $CD19^+$ B cells that stain positive for IL-10, IL-6, and TNF-α in the same COVID-19 patient at acute (gray circles) and convalescent (maroon circles) time points (n = 11–14). Graphs show individual patient data, with the bar representing median values.

In all graphs, open triangles represent SARS-CoV-2 PCR^- patients. $*p < 0.05$, $**p < 0.01$, $***p < 0.001$, 1-way ANOVA with Kruskal-Wallis test with Dunn's post hoc testing for multiple comparisons, except for graphs showing $CD4^+TNF\text{-}\alpha^+$ and $CD8^+IFN\gamma^+$ T cells in (E) and (F), where 1-way ANOVA with Holm-Sidak post hoc test was used, or Wilcoxon matched-pairs signed rank test (G, H, and J).

See also Figures S3 and S4.

Figure 4

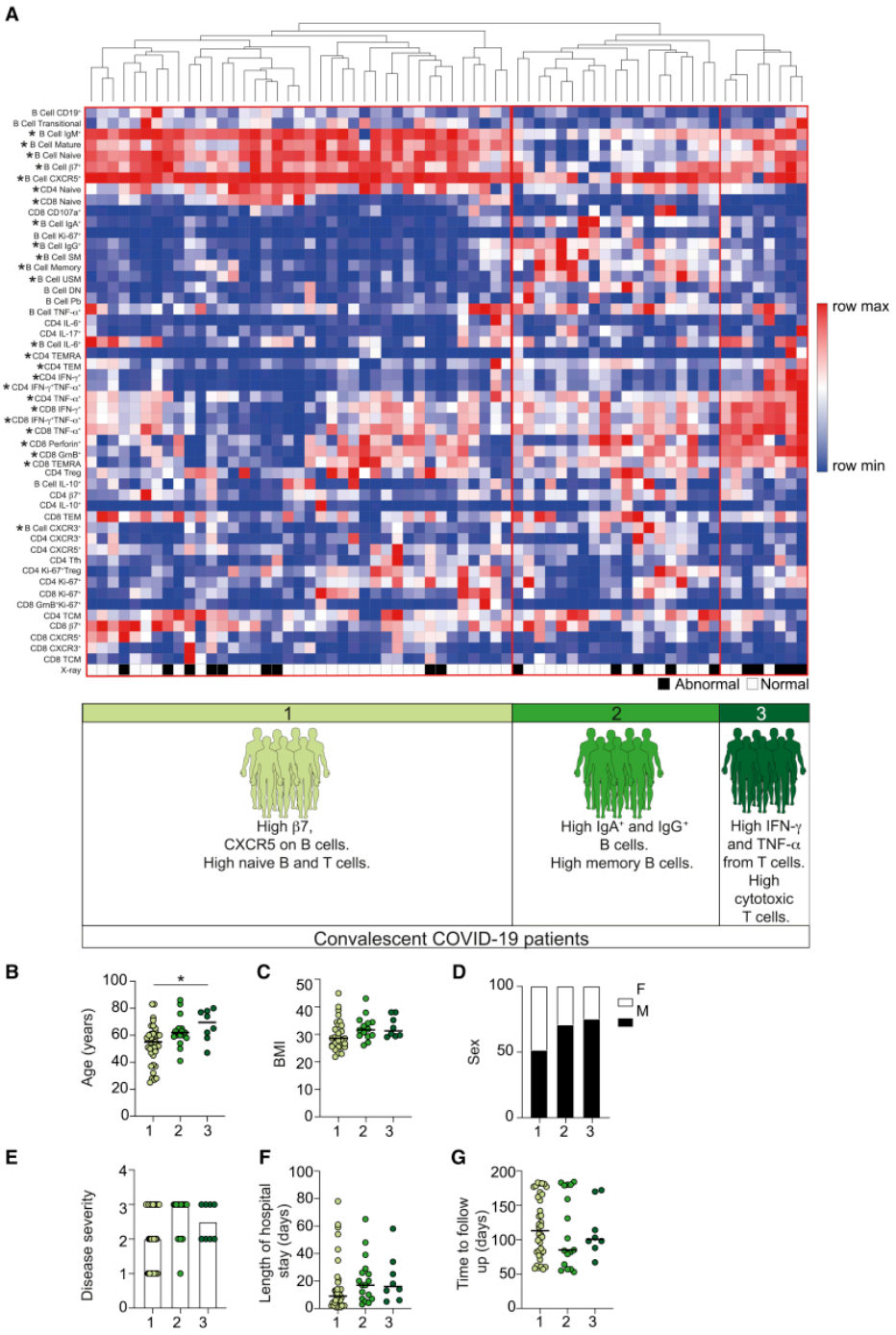

Distinct immune profiles emerge in previously hospitalized convalescent COVID-19 patients

(A) Heatmap of indicated immune parameters by row. Each column represents an individual convalescent COVID-19 patient. The patients were clustered using one minus Pearson correlation hierarchical clustering. Significance was determined by 2-way ANOVA, followed by a Tukey's multiple comparison test. Asterisk next to lymphocyte characteristic indicates a significant difference between patient groups. Dominant immune characteristics of each group are indicated at the bottom of the heatmap. Black and white squares indicate patients displaying a normal (white) or abnormal (black) chest X-ray at follow-up.

(B–G) Graphs show patient characteristics and clinical details of convalescent COVID-19 patients in each of the 3 immune groups identified, specifically: (B) age; (C) BMI; (D) sex; (E) severity of acute COVID-19 (with 1 being mild, 2 moderate and 3 severe); (F) length, in days, of hospitalization for acute COVID-19; and (G) time, in days, from hospital discharge to follow-up of convalescent patients.

Graphs show individual patient data, with the bar representing median values. $*p < 0.05$, 1-way ANOVA with Kruskal-Wallis test with Dunn's post hoc testing for multiple comparisons.

REAGENT or RESOURCE	SOURCE	IDENTIFIER
Antibodies		
Human TruStain FcX (Fc Receptor Blocking solution) (5ul/stain)	Biolegend	Cat# 422302; RRID: AB_2818986
PE-Cyanine7 anti-human CD19 (clone: HIB19, 1 in 50)	Biolegend	Cat# 302216; RRID: AB_314246
PE-Dazzle 594 anti-human CD27 (clone: M-T271, 1 in 50)	Biolegend	Cat# 356422; RRID: AB_2564101
PerCP-Cyanine 5.5 anti-human CD38 (clone: HIT2, 1 in 50)	Biolegend	Cat# 303522; RRID: AB_893314
Brilliant Violet 605 anti-human IgD (clone: IA6-2, 1 in 50)	Biolegend	Cat# 348232; RRID: AB_2563337
Brilliant Violet 421 anti-human IgG (clone: M1310G05, 1 in 50)	Biolegend	Cat# 410704; RRID: AB_2565626
Brilliant Violet 510 anti-human IgM (clone: MHM-88, 1 in 50)	Biolegend	Cat# 314522; RRID: AB_2562916
APC anti-human IgA (clone: REA1014, 1 in 100)	Miltenyi Biotech	Cat# 130-116-879; RRID: AB_2727739
Brilliant Violet 785 anti-human CD11c (clone: 3.9, 1 in 50)	Biolegend	Cat# 301644; RRID: AB_2565779
PE anti-human CD86 (clone: BU63, 1 in 50)	Biolegend	Cat# 374206; RRID: AB_2721633
PE anti-human IL-6 (clone: MQ2-13A5, 1 in 100)	Biolegend	Cat# 501107; RRID: AB_315155
APC anti-human IL-10 (clone: JES3-19F1, 1 in 25)	Biolegend	Cat# 506807; RRID: AB_315457
Brilliant Ultra Violet 395 anti-human TNFa (clone: Mab11, 1 in 50)	BD Biosciences	Cat# 563996; RRID: AB_2738533
Alexa Fluor 700 anti-human IL-17 (clone: BL168, 1 in 50)	Biolegend	Cat# 512318; RRID: AB_2124868
PE-Cyanine7 anti-human IFNg (clone: 4S.B3, 1 in 50)	Biolegend	Cat# 502528; RRID: AB_2123323
Alexa Fluor 700 anti-human Ki-67 (clone: Ki-67, 1 in 50)	Biolegend	Cat# 350530; RRID: AB_2564040
Brilliant Violet 510 anti-human CXCR3 (clone: G025H7, 1 in 50)	Biolegend	Cat# 353726; RRID: AB_2563642
APC anti-human CXCR5 (clone: J252D4, 1 in 50)	Biolegend	Cat# 356907; RRID: AB_2561816
Brilliant Violet 605 anti-human b7 (clone: FIB504, 1 in 50)	BD Biosciences	Cat# 564284; RRID: AB_2738729
Brilliant Violet 650 anti-human b7 (clone: FIB504, 1 in 50)	BD Biosciences	Cat# 564285; RRID: AB_2738730

Alexa Fluor 488 anti-human Blimp1 (clone: 646702, 1 in 25)	R&D Systems	Cat# IC36081G; RRID: AB_11129439
APC-eFluor 780 anti-human CD24 (clone: eBioSN3, 1 in 50)	eBioscience	Cat# 47-0247-42; RRID: AB_10735091
FITC anti-human CD56 (clone: 5.1H11, 1 in 50)	Biolegend	Cat# 362546; RRID: AB_2565964
Brilliant Violet 650 anti-human CD3 (clone: OKT3, 1 in 50)	Biolegend	Cat# 317324; RRID: AB_2563352
Brilliant Violet 605 anti-human CD3 (clone: OKT3, 1 in 50)	Biolegend	Cat# 317322; RRID: AB_2561911
Brilliant Ultra Violet 395 anti-human CD3 (clone: SK7, 1 in 50)	BD Biosciences	Cat# 564001; RRID: AB_2744382
PerCP-Cyanine 5.5 anti-human CD4 (clone: SK3, 1 in 50)	Biolegend	Cat# 344608; RRID: AB_1953235
Alexa Fluor 700 anti-human CD4 (clone: SK3, 1 in 50)	Biolegend	Cat# 344622; RRID: AB_2563150

nature medicine

Article

https://doi.org/10.1038/s41591-022-02051-3

Acute and postacute sequelae associated with SARS-CoV-2 reinfection

Received: 12 June 2022

Accepted: 23 September 2022

Published online: 10 November 2022

Check for updates

Benjamin Bowe[1,2], Yan Xie[1,2] & Ziyad Al-Aly[1,2,3,4,5]

First infection with severe acute respiratory syndrome coronavirus 2 (SARS-CoV-2) is associated with increased risk of acute and postacute death and sequelae in various organ systems. Whether reinfection adds to risks incurred after first infection is unclear. Here we used the US Department of Veterans Affairs' national healthcare database to build a cohort of individuals with one SARS-CoV-2 infection (n = 443,588), reinfection (two or more infections, n = 40,947) and a noninfected control (n = 5,334,729). We used inverse probability-weighted survival models to estimate risks and 6-month burdens of death, hospitalization and incident sequelae. Compared to no reinfection, reinfection contributed additional risks of death (hazard ratio (HR) = 2.17, 95% confidence intervals (CI) 1.93–2.45), hospitalization (HR = 3.32, 95% CI 3.13–3.51) and sequelae including pulmonary, cardiovascular, hematological, diabetes, gastrointestinal, kidney, mental health, musculoskeletal and neurological disorders. The risks were evident regardless of vaccination status. The risks were most pronounced in the acute phase but persisted in the postacute phase at 6 months. Compared to noninfected controls, cumulative risks and burdens of repeat infection increased according to the number of infections. Limitations included a cohort of mostly white males. The evidence shows that reinfection further increases risks of death, hospitalization and sequelae in multiple organ systems in the acute and postacute phase. Reducing overall burden of death and disease due to SARS-CoV-2 will require strategies for reinfection prevention.

A large body of evidence suggests that first infection with SARS-CoV-2 is associated with increased risk of acute and postacute death and sequelae in the pulmonary and broad array of extrapulmonary organ systems[1–8]. However, many people around the globe are experiencing repeat SARS-CoV-2 infections (reinfections). Previous epidemiological studies of SARS-CoV-2 reinfection have been limited to investigations of the risk of getting reinfection and the comparative evaluation of risk differences of hospitalization or death between first and second SARS-CoV-2 infections during their acute phase[9,10]. Whether and to what extent reinfection adds to the risk incurred after the first infection is not clear (that is, evaluation of the risk of reinfection versus no reinfection). Whether reinfection contributes to the increased risk of acute and postacute sequelae is also not known. Addressing these questions has broad public health implications since it will inform whether strategies to prevent or reduce the risk of reinfection should be implemented.

In this study, we used the electronic healthcare database of the US Department of Veterans Affairs to address the question of whether SARS-CoV-2 reinfection adds to the health risks associated with a first

[1]Clinical Epidemiology Center, Research and Development Service, Veteran Affairs Saint Louis Health Care System, St. Louis, MO, USA. [2]Veterans Research and Education Foundation of St. Louis, St. Louis, MO, USA. [3]Department of Medicine, Washington University School of Medicine, St. Louis, MO, USA. [4]Nephrology Section, Medicine Service, Veteran Affairs St. Louis Health Care System, St. Louis, MO, USA. [5]Institute for Public Health, Washington University in St. Louis, St. Louis, MO, USA. e-mail: zalaly@gmail.com

SARS-CoV-2 infection. We characterized the risks and 6-month burdens of a range of prespecified outcomes in a cohort of people who experienced a SARS-CoV-2 reinfection compared to those with no reinfection, characterized the risks of acute and postacute outcomes in people who had reinfection and finally estimated the cumulative risks and one-year burdens associated with one, two, three or more infections compared to a noninfected control cohort.

Results

There were 443,588 cohort participants with no SARS-CoV-2 reinfection (only a single SARS-CoV-2 infection) and 40,947 participants who had SARS-CoV-2 reinfection (two or more infections) (Extended Data Fig. 1); 5,334,729 participants with no record of positive SARS-CoV-2 infection were in the noninfected control group. Among those who had reinfection, 37,997 (92.8%) people had two infections, 2,572 (6.3%) people had three infections and 378 (0.9%) people had four or more infections. The median distribution of time between the first and second infection was 191 d (interquartile range (IQR) = 127–330) and between the second and third was 158 d (IQR = 115–228). The demographic and health characteristics of those with no reinfection, reinfection and the noninfected control group are presented in Supplementary Table 1.

Sequelae of SARS-CoV-2 reinfection

To gain a better understanding of whether reinfection adds risk, we first conducted analyses to examine the risks of all-cause mortality, hospitalization and a set of prespecified outcomes in people who had reinfection compared to those with no reinfection.

We provide two measures of risk: (1) we estimated the adjusted HRs of a set of incident prespecified outcomes comparing people who had reinfection versus no reinfection and (2) estimated the adjusted excess burden of each outcome per 1,000 persons 6 months after SARS-CoV-2 reinfection on the basis of the difference between the estimated incidence rate in individuals who had reinfection and no reinfection. Follow-up began at the time of reinfection, where reinfection was defined as a SARS-CoV-2 positive test at least 90 d after the initial positive test; this time frame of 90 d was specified to reduce the probability that a positive test was related to the first infection. Assessment of standardized mean differences of participant characteristics (from data domains including diagnoses, medications and laboratory test results) after application of weighting showed they were well balanced in each analysis of incident outcomes (Supplementary Table 2 and Supplementary Fig. 1).

Compared to those with no reinfection, those who had reinfection exhibited an increased risk of all-cause mortality (HR = 2.17, 95% CI = 1.93–2.45) and excess burden of all-cause mortality estimated at 19.33 (95% CI = 15.34–23.82) per 1,000 persons at 6 months; all burden estimates represent excess burden and are given per 1,000 persons at 6 months (Fig. 1 and Supplementary Table 3). People with a reinfection also had an increased risk of hospitalization (HR = 3.32, 95% CI = 3.13–3.51; a burden of 100.19 (92.53–108.25)) and having at least one sequela of SARS-CoV-2 infection (HR = 2.10, 95% CI = 2.04–2.16; a burden of 235.91 (225.54–246.34)) (Fig. 1 and Supplementary Table 3).

Compared to those with no reinfection, those who had reinfection exhibited increased risk of sequelae in the pulmonary (HR = 3.54, 95% CI = 3.29–3.82; burden = 75.74, 95% CI = 68.47–83.50) and several extrapulmonary organ systems including cardiovascular disorders (HR = 3.02, 95% CI = 2.80–3.26; burden = 62.80, 95% CI = 56.17–69.91), coagulation and hematological disorders (HR = 3.10, 95% CI = 2.77–3.47; burden = 33.85, 95% CI = 28.55–39.74), fatigue (HR = 2.33, 95% CI = 2.14–2.53; burden = 46.92, 95% CI = 40.46–53.89), gastrointestinal disorders (HR = 2.48, 95% CI = 2.35–2.62; burden = 100.30, 95% CI = 91.88–109.09), kidney disorders (HR = 3.55, 95% CI = 3.18–3.97; burden = 38.31, 95% CI = 32.86–44.37), mental health disorders (HR = 2.14, 95% CI = 2.04–2.24; burden = 116.13, 95% CI = 106.71–125.87), diabetes (HR = 1.70, 95% CI = 1.41–2.05; burden = 6.46, 95% CI = 3.77–9.69), musculoskeletal disorders (HR = 1.64, 95% CI = 1.49–1.80; burden = 25.55, 95% CI = 19.73–31.91) and neurological disorders (HR = 1.60, 95% CI = 1.51–1.69; burden = 52.91, 95% CI = 45.48–60.70). Risks and excess burdens of reinfection are provided in Fig. 1 and Supplementary Table 3. Analyses examining whether the length of time from first infection to reinfection might modify the association between reinfection and the risks of all-cause mortality, hospitalization and at least one sequela suggested no effect modification on the multiplicative scale (*P* values for effect modification of 0.224, 0.156 and 0.356, respectively).

Analyses of prespecified subgroups based on vaccination status before reinfection (no vaccination, one vaccination or two or more vaccinations) showed that reinfection (compared to no reinfection) was associated with a higher risk of all-cause mortality, hospitalization, at least one sequela and sequelae in the different organ systems (Fig. 2 and Supplementary Table 4) regardless of vaccination status.

Acute and postacute sequelae of SARS-CoV-2 reinfection

We examined whether the risk of sequelae of SARS-CoV-2 reinfection was present in the acute and postacute phases of reinfection. We conducted analyses examining risk and burden starting from the time of reinfection up to 180 d later in 30-day increments. Compared to those with no reinfection, those who had reinfection exhibited increased risk and excess burden of all-cause mortality, hospitalization and at least one sequela in the acute and postacute phases of reinfection. The risks and excess burdens of all-cause mortality, hospitalization and at least one sequela during the postacute phase gradually attenuated over time but remained evident even 6 months after reinfection (Fig. 3 and Supplementary Table 5). Examination of sequelae by organ system suggested an increased risk and excess burden in all organ systems during the acute phase (Fig. 4 and Supplementary Table 5). The risks and burdens persisted in the postacute phase of reinfection and were still evident at 6 months after reinfection.

Cumulative risk and burden of one, two and three or more SARS-CoV-2 infections

To better understand the cumulative risks incurred by people with multiple infections, we estimated the cumulative risk and burden of a set of prespecified outcomes in those who did not have a reinfection (had only one infection), and those who had two or three or more infections during the 1-year period after the acute phase of the first infection, compared to a noninfected control group. Cohort characteristics are provided in Supplementary Table 6. There was a graded association in that the risks of adverse health outcomes increased as the number of infections increased. Compared to the noninfected control group, those who only had one infection had an increased risk of at least one sequela (HR = 1.37, 95% CI = 1.36–1.38; burden per 1,000 persons at one-year = 108.88, 95% CI = 105.89–111.87); the risk was higher in those who had two infections (HR = 2.07, 95% CI = 2.03–2.11; burden = 260.41, 95% CI = 253.70–267.09) and highest in those with three or more infections (HR = 2.35, 95% CI = 2.12–2.62; burden = 305.44, 95% CI = 268.07–341.11). In a pairwise comparison of those with two infections versus one infection, those with two infections had an increased risk of at least one sequela (HR = 1.51, 95% CI = 1.48–1.54; burden = 151.53, 95% CI = 144.83–158.21); in pairwise comparison of those with three or more infections versus those with only two infections, those with three or more infections had a higher risk of at least one sequela (HR = 1.14, 95% CI = 1.02–1.27; burden = 45.02, 95% CI = 7.66–80.70). Results were consistent when hospitalization and sequelae by organ system were examined (Fig. 5 and Supplementary Tables 7–12).

Positive and negative outcome controls

We conducted a positive outcome control analysis to examine whether our approach reproduced previous established knowledge, testing

https://doi.org/10.1038/s41591-022-02051-3

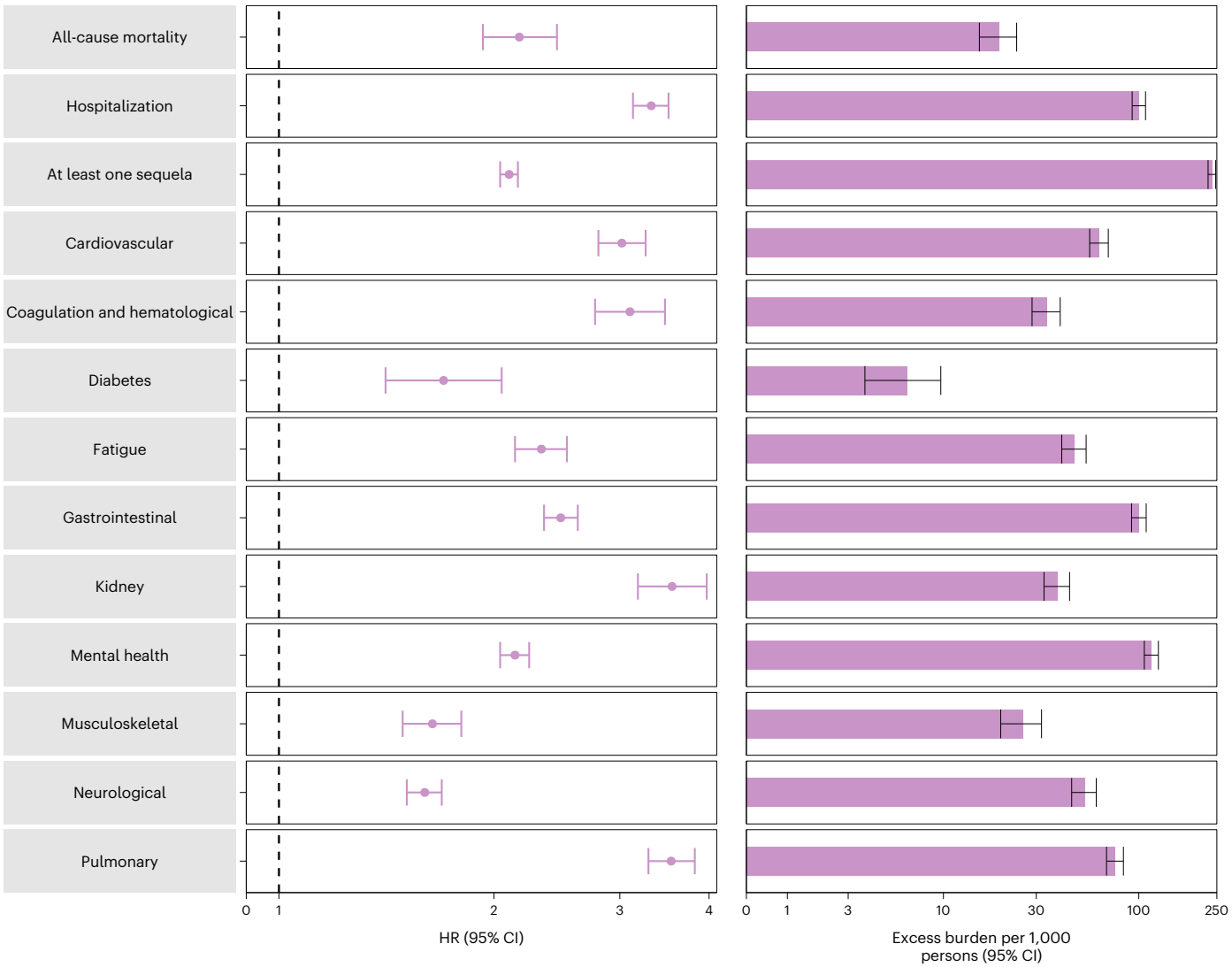

Fig. 1 | Risk and burden of sequelae in people with SARS-CoV-2 reinfection versus no reinfection. Risk and 6-month excess burden of all-cause mortality, hospitalization, at least one sequela and sequelae by organ system are plotted. Incident outcomes were assessed from reinfection to the end of the follow-up. Results from SARS-CoV-2 reinfection (n = 40,947) and no SARS-CoV-2 reinfection (n = 443,588) are compared. Adjusted HRs (dots) and 95% CIs (error bars) are presented, as are the estimated excess burden (bars) and 95% CIs (error bars). Burdens are presented per 1,000 persons at 6 months of follow-up from the time of reinfection.

whether the association of a SARS-CoV-2 infection (irrespective of reinfection) was associated with risk of fatigue (a well-characterized, cardinal postacute sequela of COVID-19, where a positive association would be expected based on previous evidence). Results showed that, compared to a noninfected control group, those with a SARS-CoV-2 infection exhibited an increased risk of fatigue (HR = 1.72, 95% CI = 1.70–1.74).

We then conducted a set of negative outcome control analyses to test for the potential presence of spurious associations using the same data sources, cohort construction processes, covariate selections and definitions (including predefined and algorithmically selected high-dimensional covariates), covariate balance methods and result interpretations as those of our primary analysis. Results examining the risk of atopic dermatitis and neoplasms (negative outcome controls), where there was no previous biological or epidemiological evidence to suggest an association should be expected, did not show a significant association in those who had reinfection compared to those with no reinfection (HR = 1.06, 95% CI = 0.91–1.24 and HR = 1.03, 95% CI = 0.97–1.10, respectively).

Discussion

In this study of 5,819,264 people, including 443,588 people with a first infection, 40,947 people who had reinfection and 5,334,729 noninfected controls, we showed that compared to people with no reinfection, people who had reinfection exhibited increased risks of all-cause mortality, hospitalization and several prespecified outcomes. The risks were evident in those who were unvaccinated and had one vaccination or two or more vaccinations before reinfection. The risks were most pronounced in the acute phase but persisted in the postacute phase of reinfection, and risks for all sequelae were still evident at 6 months. Compared to noninfected controls, assessment of the cumulative risks of repeat infection showed that the risk and burden of all-cause mortality and the prespecified health outcomes increased in a graded fashion according to the number of infections (that is, risks were lowest in people with one infection, increased in people with two infections and were highest in people with three or more infections). Altogether, the findings show that reinfection further increases risks of all-cause mortality and adverse health outcomes in both the acute and postacute phases of reinfection. The findings highlight the clinical consequences

https://doi.org/10.1038/s41591-022-02051-3

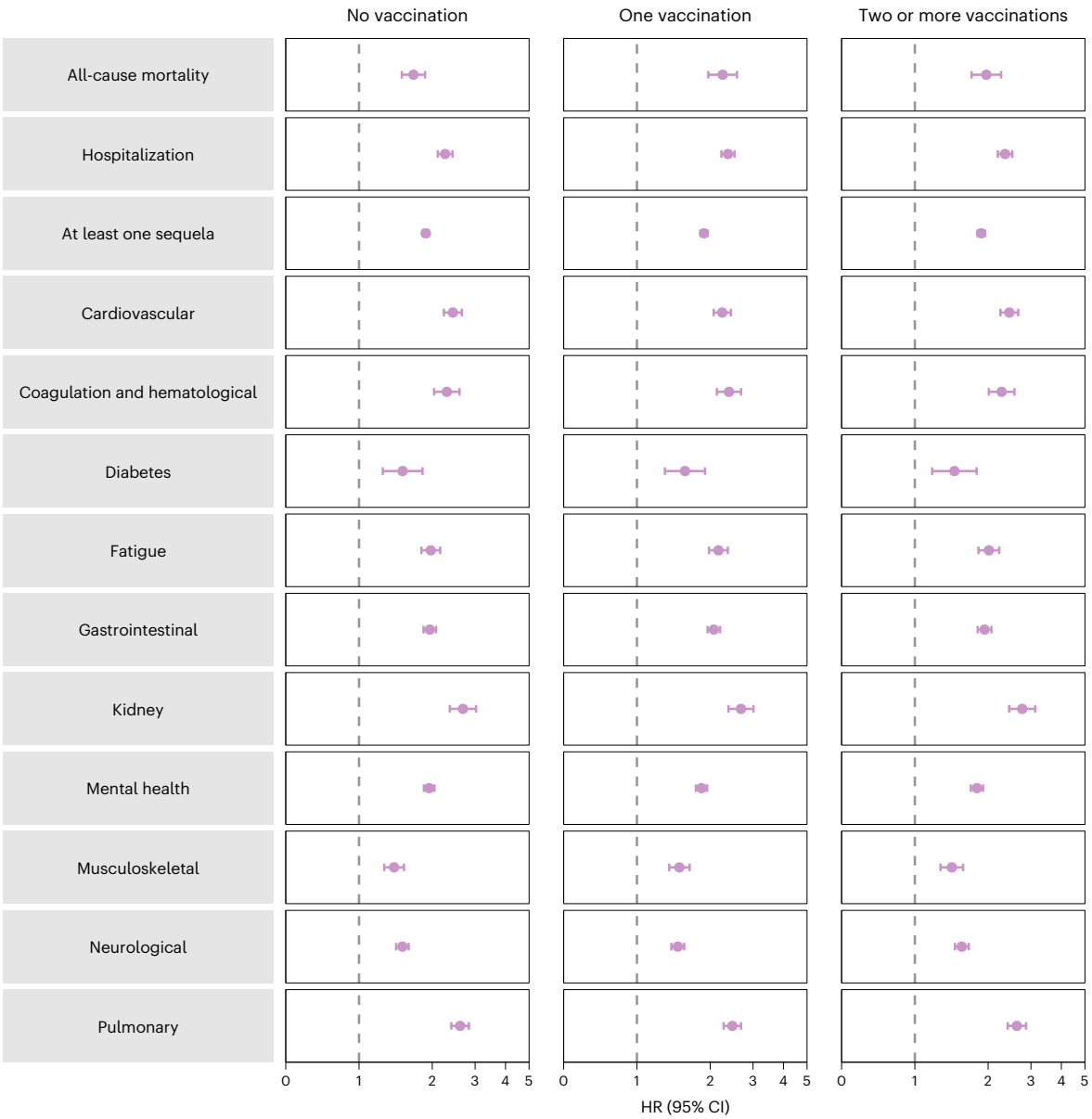

Fig. 2 | Risk and burden of sequelae in people with SARS-CoV-2 reinfection versus no reinfection by vaccination status before reinfection. Risk of all-cause mortality, hospitalization, at least one sequela and sequelae by organ system are plotted. Incident outcomes were assessed from reinfection to the end of the follow-up. Results from SARS-CoV-2 reinfection (n = 40,947) versus no SARS-CoV-2 reinfection (n = 443,588) are compared. At the time of comparison, there were 51.3%, 12.6% and 36.2% with no, one and two or more vaccinations, respectively, among those who had reinfection. At the time of comparison, there were 41.1%, 11.7% and 47.2% with no, one and two or more vaccinations, respectively, among the no reinfection group. Adjusted HRs (dots) and 95% CIs (error bars) are presented.

of reinfection and emphasize the importance of preventing reinfection by SARS-CoV-2.

Estimates suggest that more than half a billion people around the globe have been infected with SARS-CoV-2 at least once[11]. For the large and growing number of people who encountered a first infection, the question of whether a second infection carries additional risks is important. In this work, we showed that reinfection further increases risks of all-cause mortality and adverse health outcomes in both the acute and postacute phases of reinfection, suggesting that for people who have already been infected once, continued vigilance to reduce the risk of reinfection may be important to lessen the overall risk to one's health.

Given the likelihood that SARS-CoV-2 will continue to mutate and might remain a threat for years if not decades, leading to the emergence of variants or subvariants that might be more immune-evasive, and given that reinfections are occurring and might continue to occur due to these emerging SARS-CoV-2 variants at scale in many countries across the globe, and given that reinfection contributes nontrivial health risk both in the acute and postacute phases, a strategy that would result in vaccines that are more durable, cover a broad array of variants (variant-proof vaccine strategy), reduce transmission (and subsequently reduce the risk of infection and reinfection) and reduce both acute and long-term consequences in people who get infected or reinfected is urgently needed[12]. Other pharmaceutical and nonpharmaceutical interventions to lessen both the risk of reinfection and its adverse health consequences are also urgently needed.

Questions have been raised with regard to whether reinfection increases the risk of long COVID—the umbrella term encompassing the postacute sequelae of SARS-CoV-2 infection. Our results show

https://doi.org/10.1038/s41591-022-02051-3

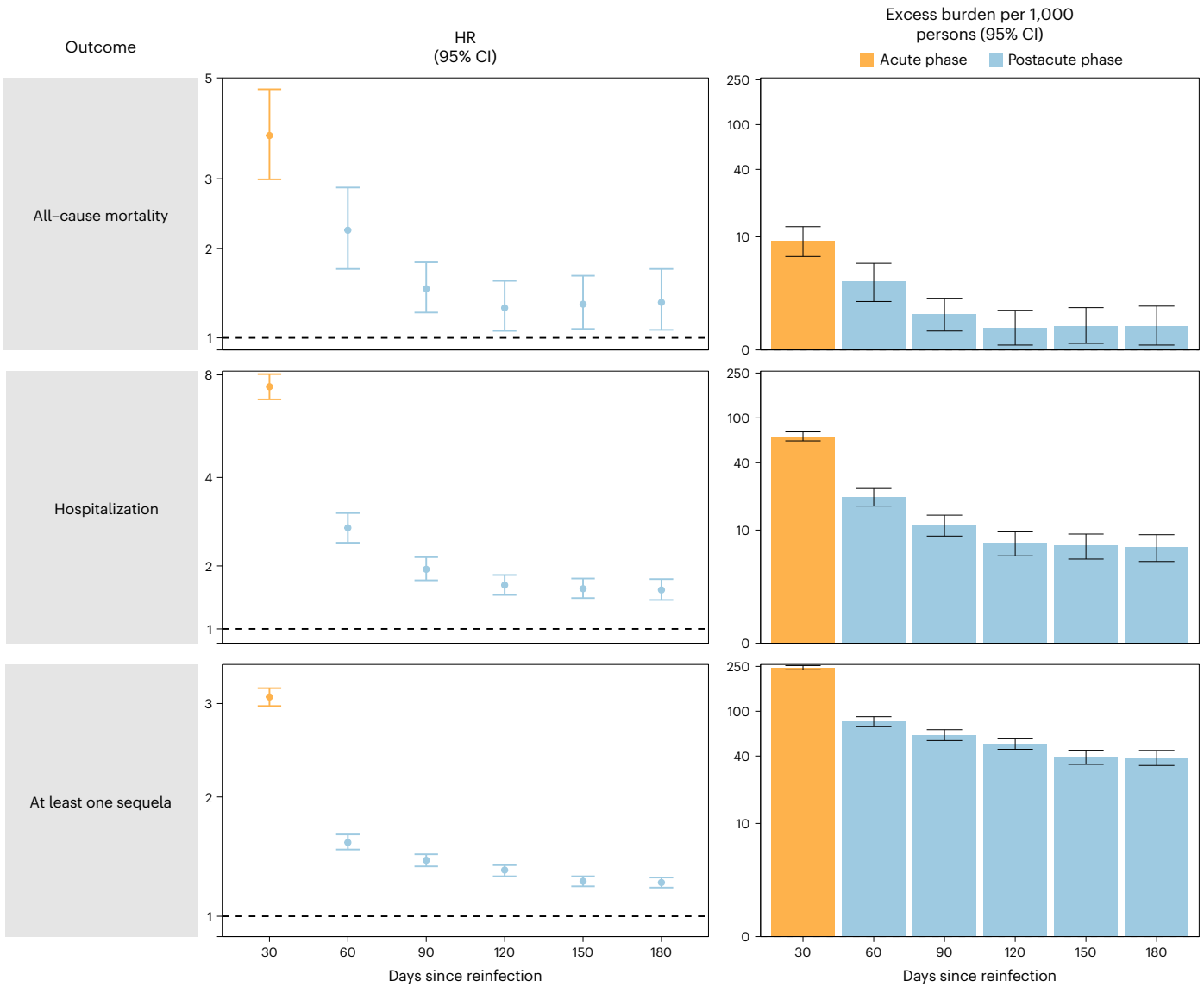

Fig. 3 | Risk and burden of all-cause mortality, hospitalization and at least one sequela in the acute and postacute phases of SARS-CoV-2 reinfection versus no reinfection. Risk and 6-month burden of all-cause mortality, hospitalization and at least one sequela of SARS-CoV-2 reinfection versus no reinfection in 30-d intervals covering the acute and postacute phases of reinfection. Incident outcomes were assessed from reinfection to the end of the follow-up. Results from SARS-CoV-2 reinfection (n = 40,947) versus first SARS-CoV-2 infection (n = 443,588) by time since reinfection were compared. Adjusted HRs (dots) and 95% CIs (error bars) are presented for each 30-d period since the time of reinfection, as are the estimated excess burden (bars) and 95% CIs (error bars). Burdens are presented per 1,000 persons at every 30-d period of the follow-up from the time of reinfection.

that beyond the acute phase, reinfection with SARS-CoV-2 contributes substantial additional risks of all-cause mortality, hospitalization and postacute sequelae in the pulmonary and broad array of extra pulmonary organ systems.

The mechanisms underpinning the increased risks of death and adverse health outcomes in reinfection are not completely clear. Previous exposure to the virus may be expected to hypothetically reduce risk of reinfection and its severity[9,13]; however, SARS-CoV-2 is mutating rapidly and new variants and subvariants are replacing older ones every few months. Evidence suggests that the reinfection risk is especially higher with the Omicron variant, which was shown to have a marked ability to evade immunity from previous infection[10,14]. Any protection from previous infection (against reinfection and its severity) also wanes over time[10]; evidence suggests that protection from reinfection declined as time increased since the last immunity-conferring event in people who had previously been infected with SARS-CoV-2, regardless of vaccination status[15]. Furthermore, impaired health as a consequence of the first infection might result in increased risk of adverse health consequences upon reinfection. Our results expand this evidence base and show that in people who get reinfected, reinfection (compared to no reinfection) further increases risk in both the acute and postacute phases and that this was evident even among fully vaccinated people, suggesting that even combined (a hybrid of) natural immunity (from previous infection) and vaccine-induced immunity does not abrogate the risk of adverse health effects after reinfection. The totality of evidence suggests that strategies to prevent reinfection might benefit people regardless of previous history of infection and vaccination status.

This study has several strengths. To our knowledge, this is the first study to characterize both the short- and long-term health risks of reinfection. We used the US Department of Veterans Affairs national healthcare database (the largest nationally integrated healthcare

https://doi.org/10.1038/s41591-022-02051-3

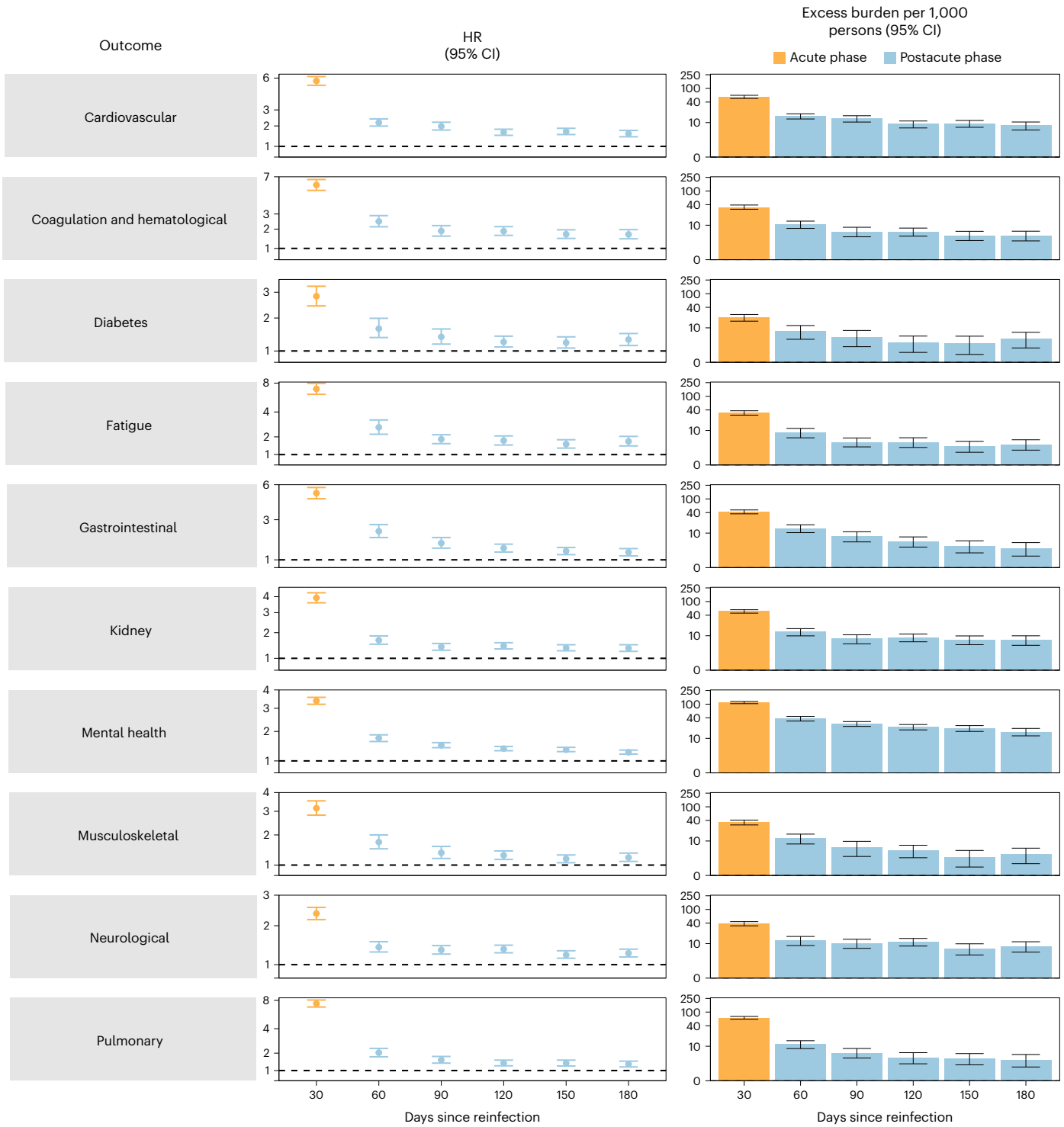

Fig. 4 | Risk and burden of sequelae by organ system in the acute and postacute phases of SARS-CoV-2 reinfection versus no reinfection. Risk and 6-month excess burden of sequelae by organ system of SARS-CoV-2 reinfection versus no reinfection in 30-d intervals covering the acute and postacute phases of reinfection. Incident outcomes were assessed from reinfection to the end of the follow-up. Results from SARS-CoV-2 reinfection (n = 40,947) versus first SARS-CoV-2 infection (n = 443,588) by time since reinfection are compared. Adjusted HRs (dots) and 95% CIs (error bars) are presented for each 30-d period since the time of reinfection, as are the estimated excess burden (bars) and 95% CIs (error bars). Burdens are presented per 1,000 persons at every 30-d period of the follow-up from the time of reinfection.

delivery system in the US) to undertake the analyses. We used advanced statistical methodologies and adjusted through weighting for a set of predefined covariates selected based on previous knowledge and algorithmically selected covariates from high-dimensional data domains including diagnoses, prescription records and laboratory test results. Because the virus is mutating over time and the proportion of different variants may vary geographically, and because different variants may have different effects on outcomes, we further adjusted our analyses for measures of the time and geographical region where participants first tested positive for SARS-Cov-2 and additionally for the proportions

https://doi.org/10.1038/s41591-022-02051-3

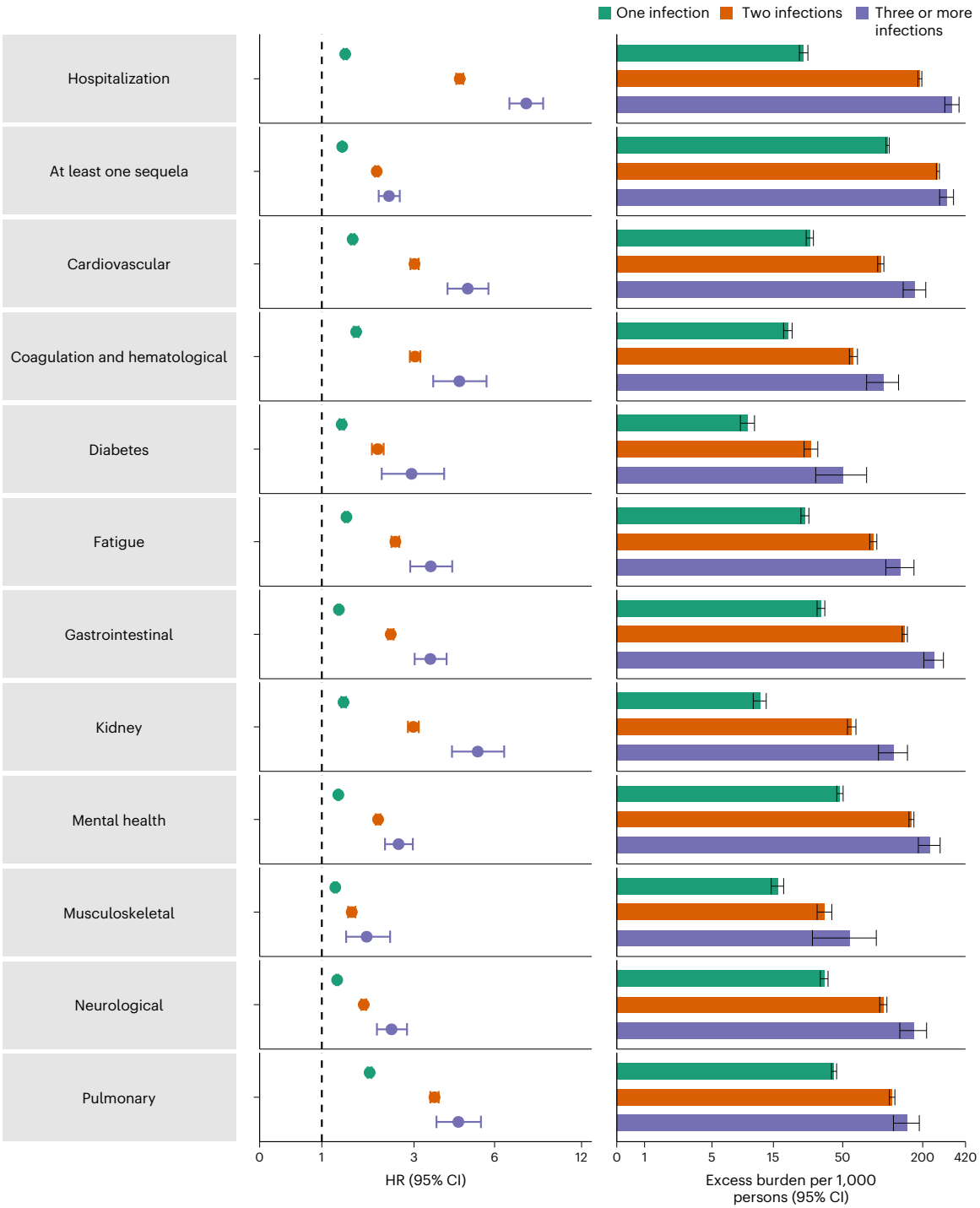

Fig. 5 | Cumulative risk and burden of sequelae in people with one, two and three or more SARS-CoV-2 infections compared to noninfected controls. Risk and 1-year excess burden of hospitalization, at least one sequela and sequelae by organ system are plotted. Incident outcomes were assessed from 30 d after the first positive SARS-CoV-2 test to the end of the follow-up. Results from one SARS-CoV-2 infection (n = 234,990), two SARS-CoV-2 infections (n = 28,509) and three or more SARS-CoV-2 infections (n = 1,023) versus noninfected controls (n = 5,334,729), in those with a first infection before the Omicron wave, are compared. Adjusted HRs (dots) and 95% CIs (error bars) are presented, as are the estimated excess burden (bars) and 95% CIs (error bars). Burdens are presented per 1,000 persons at 1 year of follow-up.

of each variant at the time and region of their first infection. We evaluated both acute and postacute outcomes of reinfection and examined risks according to vaccination status before reinfection. We evaluated the rigor of our approach by testing positive and negative outcome controls to determine whether our approach would produce results consistent with pretest expectations.

The study has several limitations. The cohorts of people with one, two, three or more infections included those that had a positive test for SARS-CoV-2 and did not include those who may have had an infection with SARS-CoV-2 but were not tested; this may have resulted in misclassification of exposure since these people would have been enrolled in the control groups. If present in large numbers and if their

true risk of adverse health outcomes is substantially higher than the noninfected controls, then this may have resulted in underestimation of the risks of reinfection. Although we leveraged several Veterans Affairs and non-Veterans Affairs data sources, our datasets may not have comprehensively captured care received outside the Veterans Affairs (including exposure (positive SARS-CoV-2), covariates (for example, vaccination) and outcomes), which may contribute to potential misclassification. Although the Veterans Affairs population which consists of those who are mostly older and male may not be representative of the general population, our cohorts included 10.3% women, which amounted to 589,573 participants, and 12% were under 38.8 years of age (the median age of the US population in 2021), which amounted to 680,358 participants. Subgroup analyses were not conducted by age, sex and race. Although we balanced characteristics of the exposure groups through weighting using a set of predefined and algorithmically selected covariates, which included demographic, behavioral, contextual and clinical characteristics, we cannot completely rule out residual confounding from unmeasured or otherwise unknown confounders. The COVID-19 pandemic is a highly dynamic global event that is still unfolding in real time; as various epidemiological drivers of this pandemic change over time (including emergence of new variants, increase in vaccine uptake and waning vaccine immunity), it is likely that the epidemiology of reinfection and its health consequences may also change over time. The aim of our analyses was to examine the health risks associated with those individuals who had reinfection (compared to no reinfection). Our analyses should not be interpreted as an assessment of severity of a second infection versus that of a first infection, nor should they be interpreted as an examination of the risks of adverse health outcomes after a second infection compared to risks incurred after a first infection. Our analyses do not provide a comparative assessment of the risks of reinfection with different variants or subvariants.

In sum, in this study of 5,819,264 individuals, we provide evidence that reinfection contributes to additional health risks beyond those incurred in the first infection including all-cause mortality, hospitalization and sequelae in a broad array of organ systems. The risks were evident in the acute and postacute phases of reinfection. The evidence suggests that for people who already had a first infection, prevention of a second infection may protect from additional health risks. Prevention of infection and reinfection with SARS-CoV-2 should continue to be the goal of public health policy.

Online content

Any methods, additional references, Nature Research reporting summaries, source data, extended data, supplementary information, acknowledgements, peer review information; details of author contributions and competing interests; and statements of data and code availability are available at https://doi.org/10.1038/s41591-022-02051-3.

References

1. Al-Aly, Z., Xie, Y. & Bowe, B. High-dimensional characterization of post-acute sequelae of COVID-19. *Nature* **594**, 259–264 (2021).
2. Cohen, K. et al. Risk of persistent and new clinical sequelae among adults aged 65 years and older during the post-acute phase of SARS-CoV-2 infection: retrospective cohort study. *BMJ* **376**, e068414 (2022).
3. Bull-Otterson L, B. S. et al. Post–COVID conditions among adult COVID-19 survivors aged 18–64 and ≥65 years—United States, March 2020–November 2021. *MMWR Morb. Mortal. Wkly Rep.* **71**, 713–717 (2022).
4. Daugherty, S. E. et al. Risk of clinical sequelae after the acute phase of SARS-CoV-2 infection: retrospective cohort study. *BMJ* **373**, n1098 (2021).
5. Ayoubkhani, D. et al. Post-covid syndrome in individuals admitted to hospital with covid-19: retrospective cohort study. *BMJ* **372**, n693 (2021).
6. Carfi, A., Bernabei, R. & Landi, F. Persistent symptoms in patients after acute COVID-19. *JAMA* **324**, 603–605 (2020).
7. Xie, Y., Bowe, B. & Al-Aly, Z. Burdens of post-acute sequelae of COVID-19 by severity of acute infection, demographics and health status. *Nat. Commun.* **12**, 6571 (2021).
8. Al-Aly, Z., Bowe, B. & Xie, Y. Long COVID after breakthrough SARS-CoV-2 infection. *Nat. Med.* **28**, 1461–1467 (2022).
9. Abu-Raddad, L. J., Chemaitelly, H. & Bertollini, R. Severity of SARS-CoV-2 reinfections as compared with primary infections. *N. Engl. J. Med.* **385**, 2487–2489 (2021).
10. Pulliam, J. R. C. et al. Increased risk of SARS-CoV-2 reinfection associated with emergence of Omicron in South Africa. *Science* **376**, eabn4947 (2022).
11. Coronavirus Resource Center. COVID-19 map (Johns Hopkins Univ., 2020); https://coronavirus.jhu.edu/map.html
12. Topol, E. J. & Iwasaki, A. Operation nasal vaccine-lightning speed to counter COVID-19. *Sci. Immunol.* **7**, eadd9947 (2022).
13. Chemaitelly, H., Bertollini, R. & Abu-Raddad, L. J. Efficacy of natural immunity against SARS-CoV-2 reinfection with the beta variant. *N. Engl. J. Med.* **385**, 2585–2586 (2021).
14. Altarawneh, H. N. et al. Protection against the Omicron variant from previous SARS-CoV-2 infection. *N. Engl. J. Med.* **386**, 1288–1290 (2022).
15. Goldberg, Y. et al. Protection and waning of natural and hybrid immunity to SARS-CoV-2. *N. Engl. J. Med.* **386**, 2201–2212 (2022).

Methods

Ethics statement

This study was approved by the institutional review board of the Veterans Affairs St. Louis Health Care System, which granted a waiver of informed consent (protocol no. 1606333). All participants who were eligible for this study were enrolled; no a priori sample size analyses were conducted to guide enrollment. All analyses were observational, and investigators were aware of participant exposure and outcome status.

Setting

Participants were selected from the US Veterans Health Administration (VHA) electronic health database. The VHA delivers healthcare to discharged Veterans of the US armed forces in a network of nationally integrated healthcare systems including more than 1,415 healthcare facilities. Veterans enrolled for care in the VHA have access to extensive medical benefits, such as inpatient and outpatient services, preventative, primary and specialty care, mental health services, geriatric care, long-term and home healthcare, medications and medical equation and prosthetics. The VHA electronic health database is updated daily.

Cohorts

A flowchart of cohort construction is provided in Extended Data Fig. 1. We first identified users of the VHA with at least one positive SARS-CoV-2 test between 1 March 2020 and 6 April 2022 (n = 519,767), enrolling these participants at the date of first positive test (set as T_0). Use of the VHA was defined as having record of use of outpatient or inpatient service, receipt of medication or use of laboratory service with the VHA healthcare system in the 2 years before enrollment. We selected those still alive 90 d after their first positive SARS-CoV-2 test (n = 489,779). We then further selected participants who experienced reinfection, defined as a positive SARS-CoV-2 test 90 d or more after the first infection, where reinfection could occur between 1 June 2020 and 25 June 2022, which spans the time frame in the US in which pre-Delta, Delta and Omicron variants predominated[16–19]. The 90-d minimum time frame to define reinfection was specified to minimize inclusion of repeat positive tests that may be related to the first infection[16–19]. There were 40,947 participants who had a reinfection, where the time of reinfection was set as T_1. To ensure a similar distribution of follow-up time in the no reinfection and reinfection groups, participants in the no reinfection group were randomly assigned a T_1 based on the distribution of T_1 of those in the reinfection group who shared the same calendar month as the date of first infection, resulting in a group of 443,588 participants with no reinfection that were alive at their assigned T_1.

We then constructed a noninfected control group. We first identified 5,760,792 VHA users between 1 March 2020 and 6 April 2022 with no record of a positive SARS-CoV-2 test. We then randomly assigned a T_0 to each participant in the group on the basis of the distribution of the T_0 dates in those with at least one positive SARS-CoV-2 test, selecting the 5,458,815 who were alive at their assigned T_0. We selected those who were alive 90 d after their T_0 (n = 5,408,880). After randomly assigning a T_1, there were 5,334,729 in the noninfected control cohort. All cohort participants were followed until 25 June 2022.

Data sources

Participant data were obtained from the VHA Corporate Data Warehouse. The patient and vital status domains provided data on demographic characteristics. VHA mortality information contains both inhospital and nonhospital deaths collected from the Veterans Affairs and non-Veterans Affairs sources including the VHA's Beneficiary Identification Record Locator System and medical inpatient datasets, as well as Medicare Vital Status File, Social Security Administration's Master File and information from death certificates and the National Cemetery Administration[20]. The outpatient and inpatient encounter domains provided information on health characteristics including details on date and place of encounter with the healthcare system and diagnostic and procedural information. The Pharmacy and Bar Code Medication Administration domains provided medication records, while the laboratory results domain provided laboratory test results for tests conducted in both inpatient and outpatient settings[7,21]. Information about SARS-CoV-2 tests and vaccinations were obtained from the COVID-19 Shared Data Resource. Positive SARS-CoV-2 tests consisted of results from PCR or antigen tests conducted in the Veterans Affairs or reported to the Veterans Affairs. The 2019 Area Deprivation Index at the residential address of each cohort participant was used as a contextual measure of socioeconomic disadvantage[22]. Information from the US Center for Disease Control and Prevention provided the proportion of SARS-CoV-2 variant by week in each Health and Human Services (HHS) region.

Outcomes

Outcomes were prespecified on the basis of previous evidence[1–8,21,23–29]. Outcomes included all-cause mortality, hospitalization, having at least one sequela and organ system disorders including cardiovascular disorders, coagulation and hematological disorders, diabetes, fatigue, gastrointestinal disorders, kidney disorders, mental health disorders, musculoskeletal disorders, neurological disorders and pulmonary disorders. Organ system disorders were defined as a composite outcome of a set of prespecified individual sequelae in that system at the date of first incident sequela in that system during follow-up. Organ system disorders were defined on the basis of inpatient or outpatient diagnostic codes, medication prescriptions or laboratory values. A list of the individual sequelae by organ system are provided in Supplementary Table 13. The outcome of 'at least one sequela' was defined at the time of occurrence of first incident sequela among all individual sequelae. For a participant, for a given outcome, each individual sequela was included in the assessed outcome only when there was no record of that health condition in the 2 years before T_0. Participants were excluded from the analysis of an outcome if they had previous history of all the individual sequelae that contributed to the outcome being examined. Hospitalization was defined as first inpatient admittance during follow-up. In analyses of kidney disorders, participants with a previous history of end-stage kidney disease were excluded and follow-up was censored at the time of end-stage kidney disease (Supplementary Table 13).

Covariates

Covariates included a set of variables that were predefined based on previous knowledge[4–7,21,23,25–27,30–33] and a set of variables that were selected algorithmically. Predefined covariates included demographic information (age, race and sex), contextual information (Area Deprivation Index) and measures of healthcare use in the 2 years before T_0, which included the number of outpatient visits, inpatient visits, unique medication prescriptions, routine laboratory blood panels and use of Medicare services, as well as a previous history of receiving an influenza vaccination. Smoking status was also included as a covariate. Characteristics of the participants' health history included record of anxiety, cancer, cardiovascular disease, cerebrovascular disease, chronic kidney disease, chronic obstructive pulmonary disease, dementia, depression, type 2 diabetes mellitus, estimated glomerular filtration rate, immunocompromised status, peripheral artery disease, systolic and diastolic blood pressure and body mass index on the basis of inpatient or outpatient diagnostic codes, medication prescriptions, laboratory values and vital signs. Immunocompromised status was defined according to the US Center for Disease Control and Prevention definitions by a history of organ transplantation, advanced kidney disease (an estimated glomerular filtration rate <15 ml min $^{-1}$1.73 m^{-2} or end-stage renal disease), cancer, HIV or conditions with prescriptions of more than 30-d use of corticosteroids or immunosuppressants including systemic lupus erythematosus and rheumatoid arthritis.

We also included a set of covariates related to the acute phase of the first infection: severity of the acute phase of the disease, defined in

mutually exclusive groups of nonhospitalized, hospitalized and admitted to the intensive care unit during the acute phase and whether the participant received SARS-CoV-2 treatment of antivirals, antibodies and immunomodulators including corticosteroids, interleukin-6 inhibitors and kinase inhibitors. We also included—as measures of spatiotemporal differences—the calendar week of enrollment and geographical region of receipt of care defined by the Veterans Integrated Services Networks. We also adjusted for vaccination status, which was defined as receiving no, one, two and three or more Janssen (Ad26.COV2.S; Johnson & Johnson), Pfizer-BioNTech (BNT162b2) or Moderna (mRNA-1273) vaccination shots. In consideration of the dynamicity of the pandemic, additional covariates included hospital system capacity (the total number of inpatient hospital beds), inpatient bed occupancy rates (the percentage of hospital beds that were occupied) and a measure of the proportions of SARS-CoV-2 variants by HHS region[33]. These measures were ascertained for each participant in the week of cohort enrollment at the location of the healthcare system they received care at.

In addition to the predefined covariates, we leveraged the high dimensionality of Veterans Affairs electronic health records by employing a high-dimensional variable selection algorithm to identify additional covariates that may potentially confound the examined associations[34]. We used the diagnostic classifications system from the Clinical Classifications Software Refined v.2021.1, available from the Healthcare Cost and Utilization Project sponsored by the Agency for Healthcare Research and Quality, to classify more than 70,000 International Classification of Diseases, 10th revision diagnosis codes in the 2 years before T_0 for each participant into 540 diagnostic categories[35–37]. Using the Veterans Affairs national drug classification system, we also classified 3,425 different medications into 543 medication classes[38,39]. Finally, on the basis of Logical Observation Identifiers Names and Codes, we classified laboratory results from 38 different laboratory measurements into 62 laboratory test abnormalities, defined by being above or below the corresponding reference ranges. Of the high-dimensional variables that occurred at least 100 times in participants in each group, we selected the top 100 variables with the highest relative risk for differences in group membership in first infection or reinfection.

Statistical analysis

Mean (s.d.) and frequency (percentage) of characteristics are reported for those with no SARS-CoV-2 reinfection, SARS-CoV-2 reinfection and the noninfected control group, where appropriate. We provide information on the distribution of frequency of reinfections, time between infections and variant of reinfection (defined by predominant variant given the calendar week and HHS region of the residential location of cohort participants when reinfection occurred).

All associations were estimated based on weighting approaches combined with survival analyses. We conducted a primary analysis to evaluate the risk and burden of reinfection compared to no reinfection (Supplementary Fig. 2). Logistic regressions were constructed to estimate the propensity score of group membership; regressions included predefined covariates, high-dimensional covariates and time from T_0 to T_1 as a means to adjust for residual differences in duration of follow-up. A reference cohort of the overall infected cohort at T_0 was used as the target population. Inverse probability weighting was then used to balance the covariates. A weighted Cox survival model was then used to estimate the average risk and event rate difference between those with a reinfection and those with no reinfection. Standard errors were estimated by applying the robust sandwich variance estimator method. Covariate balance among all predefined and high-dimensional variables were assessed through the standardized mean difference, where a difference <0.1 was taken as evidence of balance. We estimated the incidence rate difference (referred to as excess burden) between groups per 1,000 participants at 6 months after the start of the follow-up based on the difference in survival probability between the groups. These analyses were repeated by subgroup on the basis of the number of vaccination shots received (0, 1 or 2+) before reinfection using an overlap weighting approach. To test whether the risk on the multiplicative scale differed between participants with different duration between T_0 and T_1, a model with a linear interaction term between reinfection status and duration was constructed and the corresponding *P* value is reported for the outcomes of all-cause mortality, hospitalization and having at least one sequela.

To examine whether risks associated with a reinfection were present in the acute and postacute phases of reinfection, we conducted analyses to examine risks in 30-d time intervals starting at the time of reinfection up to 180 d after reinfection. HRs and 30-d burdens were estimated independently for each 30-d time interval. During each 30-d interval, outcomes were defined at the time of first occurrence within this interval in those who did not have that outcome in the 2 years before the first infection.

We then used a doubly robust approach to examine the risk and cumulative burden per 1,000 persons at one-year after first infection of sequelae associated with one, two and three or more infections versus a noninfected control (Supplementary Fig. 3). A third or more infection was defined as a positive test at least 90 d after the second infection. The number of infections and outcomes were assessed in the 360 d after T_0 + 30 d. Since those with three or more infections predominantly had their first infection before the Omicron variant was present, to enhance comparison across groups, we restricted this analysis to those with a T_0 period before Omicron became the predominant variant in at least one HHS region (11 December 2022). Because participants with three or more infections must have not died during the follow-up period to have that third (or more) infection, we did not examine the outcome of all-cause mortality due to immortal time bias.

Positive and negative controls

We examined, as positive outcome controls, the risk of fatigue in those with a SARS-CoV-2 infection compared to the noninfected control group as a means of testing whether our approach would reproduce established knowledge[4,5,25–27].

The application of a negative outcome control may help detect both suspected and unsuspected sources of spurious biases. Therefore, we examined the difference in risks of atopic dermatitis and neoplasms between those who had reinfection and the first infection, where no previous knowledge suggested that an association should be expected. The testing of positive and negative outcome controls may lessen, although not eliminate, concerns about biases related to study design, covariate selection, analytical approach, outcome ascertainment, unmeasured confounding and other potential sources of latent biases[40,41].

All analyses were two-sided. In all analyses, a 95% CI that excluded unity was considered evidence of statistical significance. All analyses were conducted in SAS Enterprise Guide v.8.2, and all figures were generated in R v.4.0.4.

Reporting summary

Further information on research design is available in the Nature Research Reporting Summary linked to this article.

Data availability

The data that support the findings of this study are available from the US Department of Veterans Affairs. Veterans Affairs data are made freely available to researchers behind the Veterans Affairs firewall with an approved Veterans Affairs study protocol. For more information, please visit https://www.virec.research.va.gov or contact the Veterans Affairs Information Resource Center at VIReC@va.gov.

Code availability

The code used for the analysis is available at https://github.com/BcBowe3.

References

16. Yahav, D. et al. Definitions for coronavirus disease 2019 reinfection, relapse and PCR re-positivity. *Clin. Microbiol. Infect.* **27**, 315–318 (2021).
17. Centers for Disease Control and Prevention. Reinfection: clinical considerations for care of children and adults with confirmed COVID-19 https://www.cdc.gov/coronavirus/2019-ncov/hcp/clinical-care/clinical-considerations-reinfection.html (2022).
18. Wang, J., Kaperak, C., Sato, T. & Sakuraba, A. COVID-19 reinfection: a rapid systematic review of case reports and case series. *J. Investig. Med.* **69**, 1253–1255 (2021).
19. Tillett, R. L. et al. Genomic evidence for reinfection with SARS-CoV-2: a case study. *Lancet Infect. Dis.* **21**, 52–58 (2021).
20. Arnold, N., Sohn, M., Maynard, C. & Hynes, D. M. *VIReC Technical Report 2: VA-NDI Mortality Data Merge Project* (Edward Hines Jr. VA Hospital VA Information Resource Center, 2006).
21. Bowe, B., Xie, Y., Xu, E. & Al-Aly, Z. Kidney outcomes in long COVID. *J. Am. Soc. Nephrol.* **32**, 2851–2862 (2021).
22. Kind, A. J. H. & Buckingham, W. R. Making neighborhood-disadvantage metrics accessible—the Neighborhood Atlas. *N. Engl. J. Med.* **378**, 2456–2458 (2018).
23. Xie, Y., Xu, E., Bowe, B. & Al-Aly, Z. Long-term cardiovascular outcomes of COVID-19. *Nat. Med.* **28**, 583–590 (2022).
24. Xie, Y., Xu, E. & Al-Aly, Z. Risks of mental health outcomes in people with Covid-19: cohort study. *BMJ* **376**, e068993 (2022).
25. Taquet, M. et al. Incidence, co-occurrence, and evolution of long-COVID features: a 6-month retrospective cohort study of 273,618 survivors of COVID-19. *PLoS Med.* **18**, e1003773 (2021).
26. Davis, H. E. et al. Characterizing long COVID in an international cohort: 7 months of symptoms and their impact. *EClinicalMedicine* **38**, 101019 (2021).
27. Taquet, M., Geddes, J. R., Husain, M., Luciano, S. & Harrison, P. J. 6-month neurological and psychiatric outcomes in 236 379 survivors of COVID-19: a retrospective cohort study using electronic health records. *Lancet Psychiatry* **8**, 416–427 (2021).
28. Xie, Y. & Al-Aly, Z. Risks and burdens of incident diabetes in long COVID: a cohort study. *Lancet Diabetes Endocrinol.* **10**, 311–321 (2022).
29. Xu, E., Xie, Y. & Al-Aly, Z. Long-term neurologic outcomes of COVID-19. *Nat Med* https://doi.org/10.1038/s41591-022-02001-z (2022).
30. Spudich, S. & Nath, A. Nervous system consequences of COVID-19. *Science* **375**, 267–269 (2022).
31. Cai, M., Bowe, B., Xie, Y. & Al-Aly, Z. Temporal trends of COVID-19 mortality and hospitalisation rates: an observational cohort study from the US Department of Veterans Affairs. *BMJ Open* **11**, e047369 (2021).
32. Nalbandian, A. et al. Post-acute COVID-19 syndrome. *Nat. Med.* **27**, 601–615 (2021).
33. Sharma, A., Oda, G. & Holodniy, M. COVID-19 vaccine breakthrough infections in Veterans Health Administration. Preprint at *medRxiv* https://doi.org/10.1101/2021.09.23.21263864 (2021).
34. Schneeweiss, S. et al. High-dimensional propensity score adjustment in studies of treatment effects using health care claims data. *Epidemiology* **20**, 512–522 (2009).
35. Wei, Y. et al. Short term exposure to fine particulate matter and hospital admission risks and costs in the Medicare population: time stratified, case crossover study. *BMJ* **367**, l6258 (2019).
36. Aubert, C. E. et al. Best definitions of multimorbidity to identify patients with high health care resource utilization. *Mayo Clin. Proc. Innov. Qual. Outcomes* **4**, 40–49 (2020).
37. Agency for Healthcare Research and Quality. Healthcare cost and utilization project (HCUP) (AHRQ, 2021).
38. Olvey, E. L., Clauschee, S. & Malone, D. C. Comparison of critical drug–drug interaction listings: the Department of Veterans Affairs medical system and standard reference compendia. *Clin. Pharmacol. Ther.* **87**, 48–51 (2010).
39. Greene, M., Steinman, M. A., McNicholl, I. R. & Valcour, V. Polypharmacy, drug–drug interactions, and potentially inappropriate medications in older adults with human immunodeficiency virus infection. *J. Am. Geriatr. Soc.* **62**, 447–453 (2014).
40. Lipsitch, M., Tchetgen, E. & Cohen, T. Negative controls: a tool for detecting confounding and bias in observational studies. *Epidemiology* **21**, 383–388 (2010).
41. Shi, X., Miao, W. & Tchetgen, E. T. A selective review of negative control methods in epidemiology. *Curr. Epidemiol. Rep.* **7**, 190–202 (2020).

Acknowledgements

This study used data from the VA COVID-19 Shared Data Resource. This research was funded by the US Department of Veterans Affairs (Z.A.-A.) and two American Society of Nephrology and KidneyCure fellowship awards (B.B. and Y.X.). The funders had no role in study design, data collection and analysis, decision to publish or preparation of the manuscript. The contents do not represent the views of the US Department of Veterans Affairs or the US Government.

Author contributions

Z.A.-A., B.B. and Y.X. contributed to the development of the study concept and design and data analysis and interpretation. Z.A.-A. and B.B. drafted the manuscript. Critical revision of the manuscript was contributed to by Z.A.-A., B.B. and Y.X. Z.A.-A. provided administrative, technical and material support, as well as supervision and mentorship. Z.A.-A. is the guarantor of the work. Each author contributed important intellectual content during manuscript drafting or revision and accepts accountability for the overall work by ensuring that questions pertaining to the accuracy or integrity of any portion of the work are appropriately investigated and resolved. All authors approved the final version of the manuscript. The corresponding author attests that all the listed authors meet the authorship criteria and that no others meeting the criteria have been omitted.

Competing interests

The authors declare no competing interests.

Additional information

Extended data is available for this paper at https://doi.org/10.1038/s41591-022-02051-3.

Supplementary information The online version contains supplementary material available at https://doi.org/10.1038/s41591-022-02051-3.

Correspondence and requests for materials should be addressed to Ziyad Al-Aly.

Peer review information *Nature Medicine* thanks Zachary Strasser and the other, anonymous, reviewer(s) for their contribution to the peer review of this work. The primary handling editor was Ming Yang, in collaboration with the *Nature Medicine* team.

https://doi.org/10.1038/s41591-022-02051-3

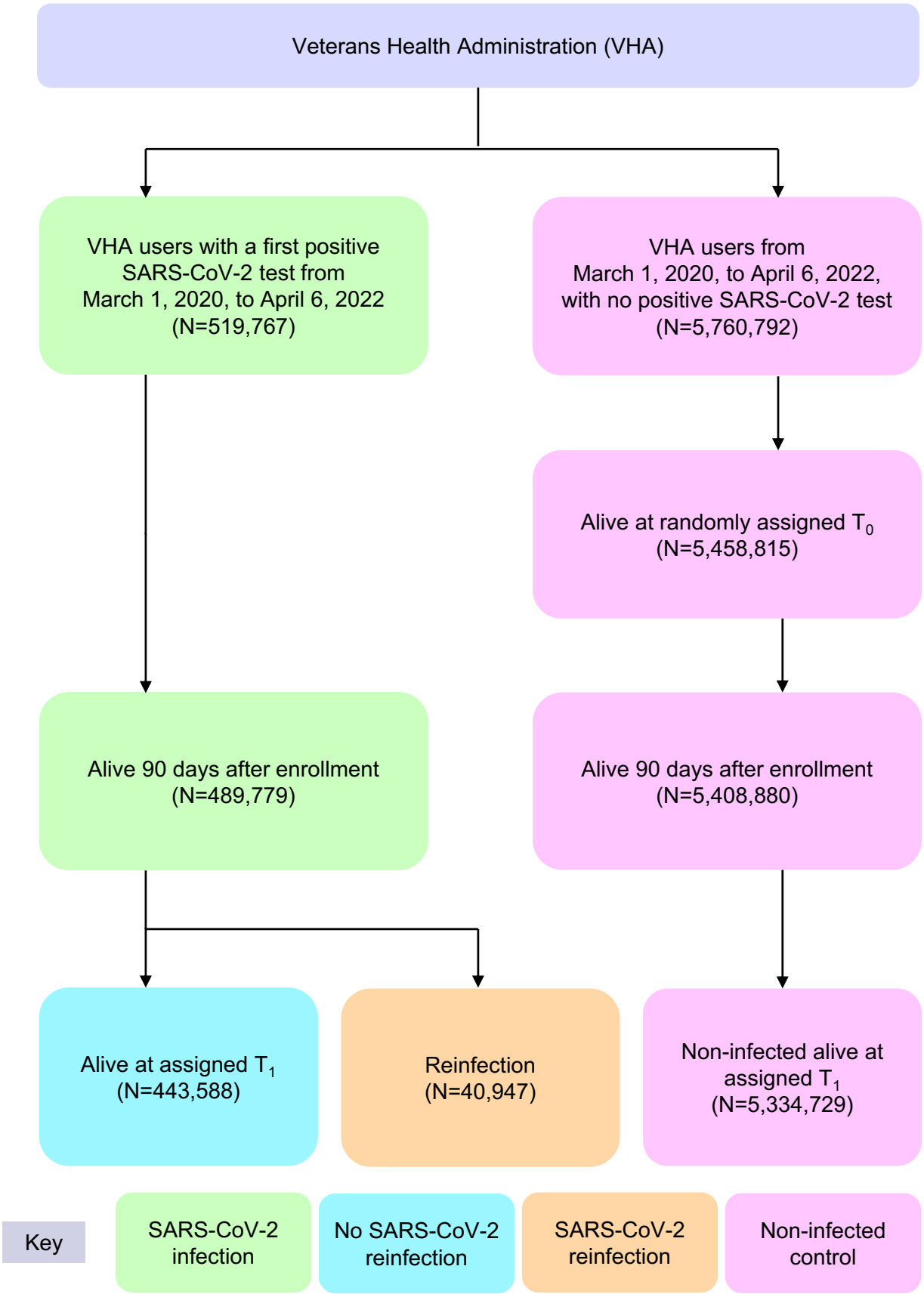

Extended Data Fig. 1 | Cohort flowchart.

nature research

Corresponding author(s): Ziyad Al-Aly

Last updated by author(s): Aug 2, 2022

Reporting Summary

Nature Research wishes to improve the reproducibility of the work that we publish. This form provides structure for consistency and transparency in reporting. For further information on Nature Research policies, see our Editorial Policies and the Editorial Policy Checklist.

Statistics

For all statistical analyses, confirm that the following items are present in the figure legend, table legend, main text, or Methods section.

n/a	Confirmed
☐	☒ The exact sample size (*n*) for each experimental group/condition, given as a discrete number and unit of measurement
☐	☒ A statement on whether measurements were taken from distinct samples or whether the same sample was measured repeatedly
☐	☒ The statistical test(s) used AND whether they are one- or two-sided *Only common tests should be described solely by name; describe more complex techniques in the Methods section.*
☐	☒ A description of all covariates tested
☐	☒ A description of any assumptions or corrections, such as tests of normality and adjustment for multiple comparisons
☐	☒ A full description of the statistical parameters including central tendency (e.g. means) or other basic estimates (e.g. regression coefficient) AND variation (e.g. standard deviation) or associated estimates of uncertainty (e.g. confidence intervals)
☐	☒ For null hypothesis testing, the test statistic (e.g. *F*, *t*, *r*) with confidence intervals, effect sizes, degrees of freedom and *P* value noted *Give P values as exact values whenever suitable.*
☒	☐ For Bayesian analysis, information on the choice of priors and Markov chain Monte Carlo settings
☒	☐ For hierarchical and complex designs, identification of the appropriate level for tests and full reporting of outcomes
☒	☐ Estimates of effect sizes (e.g. Cohen's *d*, Pearson's *r*), indicating how they were calculated

Our web collection on statistics for biologists contains articles on many of the points above.

Software and code

Policy information about availability of computer code

Data collection	SAS Enterprise Guide version 8.2 was used to collect data for the study.
Data analysis	All analyses were done using SAS Enterprise Guide version 8.2 (SAS Institute, Cary, NC). Data visualizations were performed in R 4.0.4 (R Foundation for Statistical Computing, Vienna, Austria). Analytic codes are available at https://github.com/BcBowe3

For manuscripts utilizing custom algorithms or software that are central to the research but not yet described in published literature, software must be made available to editors and reviewers. We strongly encourage code deposition in a community repository (e.g. GitHub). See the Nature Research guidelines for submitting code & software for further information.

Data

Policy information about availability of data

All manuscripts must include a data availability statement. This statement should provide the following information, where applicable:

- Accession codes, unique identifiers, or web links for publicly available datasets
- A list of figures that have associated raw data
- A description of any restrictions on data availability

The data that support the findings of this study are available from the US Department of Veterans Affairs. VA data are made freely available to researchers behind the VA firewall with an approved VA study protocol. For more information, please visit https://www.virec.research.va.gov or contact the VA Information Resource Center (VIReC) at VIReC@va.gov

Field-specific reporting

Please select the one below that is the best fit for your research. If you are not sure, read the appropriate sections before making your selection.

☒ Life sciences ☐ Behavioural & social sciences ☐ Ecological, evolutionary & environmental sciences

For a reference copy of the document with all sections, see nature.com/documents/nr-reporting-summary-flat.pdf

Life sciences study design

All studies must disclose on these points even when the disclosure is negative.

Sample size	To achieve better precision of the study results, we enrolled all users of the US Veterans Health Administration. This included people with a first SARS-CoV-2 infection (n=443,588), reinfection (2 or more infections, n=40,947), and a non-infected control group (n=533,4729). Among those with a reinfection, 2,572 had three infections, and 378 had four or more infections. Participants were followed until 180 days after reinfection, up to June 25, 2022, or death. Across all groups there were 589,573 were female.
Data exclusions	To examine the risk of sequelae associated with reinfection, we predefined our exclusion criteria and excluded participants who did not survive the first 30 days of the first SARS-CoV-2 infection.
Replication	The finding was not replicated because no external dataset with similar features is available to us.
Randomization	We conducted an observational study. Exposure allocation was not random. To balance the exposure groups, both predefined and algorithmically selected covariates were adjusted for through the inverse probability weighting methods.
Blinding	We conducted an observational study. Blinding was not possible.

Reporting for specific materials, systems and methods

We require information from authors about some types of materials, experimental systems and methods used in many studies. Here, indicate whether each material, system or method listed is relevant to your study. If you are not sure if a list item applies to your research, read the appropriate section before selecting a response.

Materials & experimental systems

n/a	Involved in the study
☒	☐ Antibodies
☒	☐ Eukaryotic cell lines
☒	☐ Palaeontology and archaeology
☒	☐ Animals and other organisms
☐	☒ Human research participants
☒	☐ Clinical data
☒	☐ Dual use research of concern

Methods

n/a	Involved in the study
☒	☐ ChIP-seq
☒	☐ Flow cytometry
☒	☐ MRI-based neuroimaging

Human research participants

Policy information about studies involving human research participants

Population characteristics	Study participants are users of the US Veteran Health Administration.This included people with a first SARS-CoV-2 infection (n=443,588), reinfection (2 or more infections, n=40,947), and a non-infected control group (n=5,334,729). Among those with a reinfection, 2,263 had three infections, and 246 had four or more infections. Average age 63.17 years, 72.11% White, 18.12% Black, 89.70% males, 10.30% females. Average systolic blood pressure was 131.84 mmhg. Average area deprivation index was 53.27. Sex is presented as a binary variable and is based off birth-certificates; it is not self report.
Recruitment	Participants were recruited if they had at least 1 encounter with the US Veteran Health Administration in the two years prior to cohort enrollment. Non users of the VA health care system were not included. The characteristics of the study population may be different from the general population (US or global population). Other biases due to recruitment including self-selection bias are unlikely to bias the results of this study.
Ethics oversight	This study was approved the VA St. Louis Health Care System Institutional Review Board (protocol number 1606333) which granted waiver of informed consent.

Note that full information on the approval of the study protocol must also be provided in the manuscript.

International Journal of
Environmental Research and Public Health

MDPI

Article

The Role of Portable Air Purifiers and Effective Ventilation in Improving Indoor Air Quality in University Classrooms

Mohammad Aldekheel [1,2], Abdulmalik Altuwayjiri [3], Ramin Tohidi [1], Vahid Jalali Farahani [1] and Constantinos Sioutas [1,*]

[1] Department of Civil and Environmental Engineering, University of Southern California, Los Angeles, CA 90089, USA
[2] Department of Civil Engineering, Kuwait University, P.O. Box 5969, Kuwait City 13060, Kuwait
[3] Department of Civil and Environmental Engineering, College of Engineering, Majmaah University, Al-Majmaah 11952, Saudi Arabia
* Correspondence: sioutas@usc.edu; Tel.: +1-213-740-6134; Fax: +1-213-744-1426

Abstract: In this study we investigated the effectiveness of air purifiers and in-line filters in ventilation systems working simultaneously inside various classrooms at the University of Southern California (USC) main campus. We conducted real-time measurements of particle mass (PM), particle number (PN), and carbon dioxide (CO_2) concentrations in nine classrooms from September 2021 to January 2022. The measurement campaign was carried out with different configurations of the purifier (i.e., different flow rates) while the ventilation system was continuously working. Our results showed that the ventilation systems in the classrooms were adequate in providing sufficient outdoor air to dilute indoor CO_2 concentrations due to the high air exchange rates (2.63–8.63 h^{-1}). The particle penetration coefficients (P) of the investigated classrooms were very low for PM (<0.2) and PN (<0.1), with the exception of one classroom, corroborating the effectiveness of in-line filters in the ventilation systems. Additionally, the results showed that the efficiency of the air purifier exceeded 95% in capturing ultrafine and coarse particles and ranged between 82–88% for particles in the accumulation range (0.3–2 μm). The findings of this study underline the effectiveness of air purifiers and ventilation systems equipped with efficient in-line filters in substantially reducing indoor air pollution.

Keywords: air pollution; indoor air quality; particulate matter (PM); ventilation; ultrafine particles; portable air purifier

Citation: Aldekheel, M.; Altuwayjiri, A.; Tohidi, R.; Jalali Farahani, V.; Sioutas, C. The Role of Portable Air Purifiers and Effective Ventilation in Improving Indoor Air Quality in University Classrooms. *Int. J. Environ. Res. Public Health* **2022**, *19*, 14558. https://doi.org/10.3390/ijerph192114558

Academic Editors: Nuno Canha, Marta Almeida, Evangelia Diapouli and Paul B. Tchounwou

Received: 5 September 2022
Accepted: 3 November 2022
Published: 6 November 2022

1. Introduction

Improving indoor air quality using air filtration technologies is essential since people spend most of their time in closed environments [1–4]. Indoor air pollution leads to adverse health outcomes and almost 3.8 million premature deaths annually [5]. Occupants' exposure to indoor particle pollutants can cause a number of adverse health effects, including respiratory illnesses, lung cancer, strokes, heart failure, asthma, and eye problems [6–10]. In addition to the health drawbacks, indoor pollution in working environments can lead to fatigue and a decline in focus and productivity [11].

In addition to ambient particles infiltrating indoors and particles emitted by indoor sources, human-generated particles (i.e., airborne aerosol particles released by the exhaled breath of humans) are major routes of airborne transmission of bacteria and viruses, including SARS-CoV-2, especially in confined environments with high population density, such as classrooms [12–15]. The exhaled particles generally have an aerodynamic diameter of less than 1 μm, mostly in the range of 0.1 to 0.5 μm [16–18]. The larger exhaled droplets settle on the ground within seconds due to the gravitational force and/or evaporate to smaller particles in a few seconds [19]. The smaller particles remain suspended in the indoor environment for several hours and can be carried by air currents as far as several

meters from their source [15,20]. These smaller particles have a greater capacity to increase the infection potential than large particles since they can travel longer distances [21].

Given the health impacts caused by indoor airborne pollutants, employing air purification means in indoor spaces is essential for decreasing pollutant concentrations [15,18]. There are two main methods used to enhance indoor air quality and remove indoor particle pollutants, including in-line filters in ventilation systems and portable air purifiers [22]. Portable air purification units have been widely used in recent years due to their efficient removal of indoor pollutants [23–25]. They have been placed in approximately 30% of private residential buildings in developed countries, and a steady growth in the use of these cleaning devices is expected in the upcoming years [1,24]. The existence of in-line filtration in mechanical ventilation systems reduces the infiltration of outdoor particles to indoor spaces to a certain level depending on the filter's characteristics, filter efficiency, and particle size [26–28]. The effectiveness of these in-line filters in capturing ambient particles is assessed by the penetration coefficient (P), which describes the fraction of outdoor particles that successfully penetrate the building into the indoor environment [26,29,30]. Moreover, the adequacy of the ventilation systems in bringing sufficient outdoor air to the indoor environment is assessed by the air exchange rate value [31,32]. Air exchange rate (*AER*) is the rate at which indoor air is entirely replaced by outdoor air in a specific closed environment (e.g., classrooms). The replacement of indoor air with outdoor air occurs by various means, such as natural ventilation (e.g., doors and windows) and forced ventilation (e.g., mechanical ventilation systems). Indoor air quality can be improved by increasing the air exchange rate, since allowing more air to enter the space will dilute indoor pollution, except in cases where outdoor pollution is substantially high [31,33] in which the outdoor air needs to be purified by some sort of in-line filter.

The main objective of this study was to explore the effectiveness of air purifiers and mechanical ventilation systems equipped with in-line filters in removing indoor airborne particles originating from outdoor and indoor sources in university classrooms. Several studies supported the effective work of the air purifier inside classrooms in improving indoor air quality and mitigating the transmission of bacteria and viruses [34–37]. However, this study provided additional insights by examining the performance of both air purifiers and in-line filters in the ventilation systems working simultaneously inside various university classrooms with different characteristics. In addition, we investigated the adequacy of the ventilation systems in bringing sufficient outdoor air to the indoor environment. The findings of this work provide significant insights for public health officials, especially in educational institutions, to implement air pollution control systems and enhance the quality of air in indoor environments.

2. Methods

2.1. Measurement Sites and Protocol

The measurements were conducted inside classrooms in the University of Southern California (USC) main campus area over a 5-month period from September 2021 to January 2022. Table 1 shows the details of the selected classrooms, including volume, floor area, and the total number of students. These classrooms were solely dependent on forced ventilation (i.e., mechanical ventilation systems) as the means of air exchange between outdoor and indoor environments. Natural ventilation was minimized in all classrooms by closing all doors and windows. The indoor monitoring was performed in two separate campaigns; the first campaign was held in all selected classrooms with students attending classes, while the second campaign was conducted in an empty classroom (i.e., classroom 3). In the first measurement campaign, indoor air quality measurements were conducted in three phases in 9 classrooms located in 7 different buildings; each phase had a different setting of an air purifier (Model Trio Plus^{TM}, Field Controls, Kinston, NC, USA) equipped with H13 HEPA filters. The first phase was carried out without the presence of the portable air purifier to evaluate the effectiveness of ventilation systems equipped with in-line filters in reducing indoor pollutant levels without the interference of additional air-cleaning

devices. In the second phase, we conducted the measurements while both the classroom's ventilation system and the air purifier (with flow rate of 267 m^3/h) were active. In the third phase, the air purifier was set at the highest possible flow rate (i.e., 748 m^3/h) while the ventilation system was operating simultaneously. We performed real-time measurements for indoor and outdoor $PM_{2.5}$ mass concentrations (PM), particle number concentrations (PN), and CO_2 levels during active 2-hour lectures in the presence of students. It should be noted that strong indoor particle generation sources (e.g., chalkboard dust and cleaning activities) were not present in the classrooms during the lectures. Pollutants' monitoring in each classroom started 15 min before the beginning of the lecture and continued until 15 min after the end of the lecture. On the same day, we also monitored the outdoor pollutant concentrations for 15 min before and after the lecture to ensure that the outdoor concentration had not changed considerably while the lecture was ongoing. For each classroom, we repeated the previous procedure on three different days by changing the configuration of the purifier according to the three phases discussed earlier. Moreover, the location of the monitoring devices in the classrooms could affect the readings of the indoor pollutant concentrations. Therefore, we investigated the spatial variance in the pollutant concentrations by placing the monitoring devices in the middle and corners of the classrooms, the results of which are shown in Figure 1 for two different classrooms as an example (the rest of the classrooms yielded similar results). The results indicate overall spatial homogeneity for PM, PN, and CO_2 concentrations inside the classrooms. This observation shows that the particle and gas pollutants are well mixed due to the overall high air exchange rates in the classrooms; thus, the location of the measuring devices in different spots within the classroom should not result in notable differences between the readings. According to the findings of Küpper et al. (2019) [22] regarding the possible spatial variance in the purifier's removal efficacy, changing the location of the purifier will provide almost identical removal efficiencies and lead to the same distribution of clean air in the space. Therefore, we positioned the purifier in a fixed location (i.e., the center of the classroom) during the entire campaign.

Table 1. Characteristics of the investigated classrooms.

No.	Classroom	Building Name	Number of Students	Room Height (m)	Floor Area (m^2)	Volume (m^3)
1	OHE136	Olin Hall (OHE)	21	3.05	86.12	262.50
2	RTH 105	Tutor Hall (RTH)	7	3.05	97.73	297.89
3	SGM 226	Seeley G. Mudd Building (SGM)	8	3.05	63.64	193.97
4	GFS 221	Grace Ford Salvatori Hall (GFS)	20	3.05	36.42	111.00
5	GFS 205	Grace Ford Salvatori Hall (GFS)	12	3.05	36.51	111.29
6	KAP159	Kaprielian Hall (KAP)	20	3.05	37.63	114.68
7	OHE 120	Olin Hall (OHE)	6	3.05	56.49	172.17
8	KDC 236	Glorya Kaufman International Dance Center (KDC)	26	3.05	89.00	271.28
9	THH 118	Taper Hall (THH)	22	3.05	76.83	234.18

The second measurement campaign was carried out in classroom 3 in the presence of an indoor pollution source (i.e., sodium chloride aerosols) to simulate exhaled particles of humans. Particles can be generated by humans through various activities, including breathing, speaking, coughing, and sneezing. The particle size that is generally produced by breathing ranges between 0.1 and 1.0 µm [17,38–40]. On the other hand, coughing, sneezing, and speaking generate larger particles compared to breathing; these particles are typically larger than 5 µm and will either settle gravitationally or evaporate to smaller particles (<1 µm) [19,34,41,42]. To corroborate the use of sodium chloride (NaCl) as a representative for human exhaled particles, we measured the size distribution of NaCl particles by means of an optical particle sizer (OPS) (Model 3330, TSI, Shoreview, MN, USA) and a scanning mobility particle sizer (SMPS) (Model 3936, TSI, Shoreview, MN, USA). At first, we prepared

a suspension by dissolving 50 mg of sodium chloride in 100 mL of ultrapure Milli-Q water to reach a concentration of 500 µg/mL. The suspension was sonicated in an ultrasonic bath for 30 min to achieve a homogenous solution. NaCl suspension was subsequently aerosolized using a commercially available nebulizer (Model 11310 HOPE^{TM} nebulizer, B&B Medical Technologies, Carlsbad, CA, USA) that was connected to a compressor pump (Model VP0625-V1014-P2-0511, Medo Inc., Roselle, IL, USA) equipped with a HEPA capsule (Model 12144, Pall Corporation, USA) to supply compressed filtered air to the nebulizer. The nebulizer was connected to both the SMPS and OPS by a clear vinyl tube to obtain the number-based particle size distribution. The particle size distribution is shown in Figure S1 and indicates that NaCl particles mostly fall in the range of 0.071 to 1.13 µm with a peak at 0.51 µm, which supports the use of NaCl as a representative of the particles generated by humans. A number of previously published studies used NaCl as the aerosol test agent to assess the effectiveness of air filtration means [18,43–46]. In addition, the National Institute for Occupational Safety and Health (NIOSH) considered NaCl as a standard test aerosol for measuring the effectiveness of respiratory protective equipment (e.g., N95 masks) [47]. Following the same setup and sample preparation discussed earlier, NaCl suspension was aerosolized in classroom 3 to act as an indoor source of aerosols.

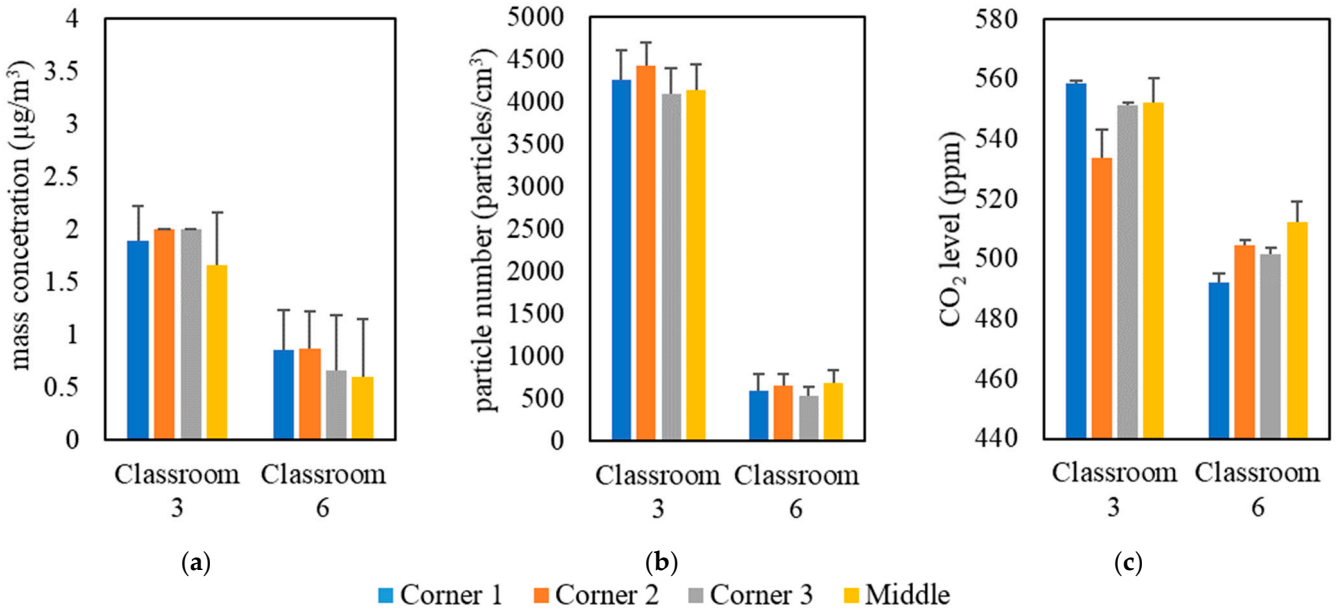

Figure 1. Spatial variability in classrooms 3 and 6 based on (**a**) PM, (**b**) PN, and (**c**) CO_2. The error bars indicate standard deviations of values measured in a single day.

2.2. Instrumentation

Various air quality monitors were used in this study to measure different pollutant concentrations. We employed the DiSCmini nanoparticle counter (Model Testo DiSCmini, Testo, West Chester, PA, USA) in our experiments to measure particle number concentrations. The TSI DustTrak monitor (Model 8520, TSI, Shoreview, MN, USA) was used to obtain real-time $PM_{2.5}$ particle mass concentrations. In addition, we employed a Q-track device (Model 8551, TSI, Shoreview, MN, USA) to measure indoor and outdoor CO_2 levels. One of the objectives of the second measurement campaign in the empty classroom was to estimate the purifier's efficiency for each particle size. This was done using the optical particle sizer (OPS) (Model 3330, TSI, Shoreview, MN, USA) to obtain particle concentrations and size distributions. The OPS measures particle sizes from 0.3 to 10 µm, which are particles in the coarse and accumulation size ranges. Further details about the calibration of the monitoring instruments are available in the supplementary material.

2.3. Additional Calculations

2.3.1. Indoor Particle Penetration (P) in the Set of Classrooms

The indoor particle penetration (P) was calculated based on the steady-state approach, which is similar to that of Chao et al. (2003) [48]. Treating the classroom as a closed system allows for the application of the mass balance equation. Equation (1) illustrates the mass balance applied in the tested classrooms:

$$\frac{dC_{in}}{dt} = \frac{S}{V} + C_{out} AER\ (P) - C_{in} AER - C_{in} k \quad (1)$$

where dC_{in}/dt is the change of indoor particle concentration with time, S represents the indoor particle production rate, V is the volume of the classroom (m^3), k is the deposition rate of particles (h^{-1}), and C_{in} and C_{out} are the indoor and outdoor particle concentrations, respectively. The indoor particle production rate in Equation (1) was neglected (i.e., $S = 0$) since there was no indoor source for particles in the studied classrooms during the active lectures. The presence of students inside the classrooms did not result in noticeable increases in the indoor particle concentrations since the particle emission rate by humans is negligible compared to the particles infiltrating from outdoor sources [49–51]. The indoor particle concentration in the classrooms reached a steady-state condition after 5–8 min from the beginning of the lecture (i.e., $dC_{in}/dt = 0$), which means Equation (1) can be rearranged to the following equation:

$$P = \frac{C_{in}(AER + k)}{C_{out} AER} \quad (2)$$

The above expression has been widely used for the calculation of effective penetration or the steady-state indoor concentration (C_{in}) in numerous previous studies [52–54]. The calculation of particle penetration indoors was carried out in the first phase of measurements when the air purifier was switched off. The particle penetration should not be affected by using the air purifier in the second and third phases of measurements. However, to show the agreement of penetration coefficients in the three phases, the following equation was used when the air purifier was active:

$$P = \frac{C_{in}\left(AER + k + \frac{CADR}{V}\right)}{C_{out}\ AER} \quad (3)$$

where $CADR$ is the clean air delivery rate of the purifier (m^3/h), and V is the volume of the classroom (m^3). Although the operation of an air purifier does not affect the penetration coefficient, it significantly affects the indoor-to-outdoor ratio. Equation (3) demonstrates that the addition of the $(CADR/V)$ term will decrease the (C_{in}/C_{out}) ratio. Moreover, increasing the purifier's flow rate leads to a further reduction in the indoor-to-outdoor ratio.

The penetration coefficient in the studied classrooms was used as a metric for assessing the effectiveness of the in-line filters of the ventilation systems in capturing particles penetrating the building from the outdoor space. The air handling units in all tested classrooms, except classroom 3, were equipped with a dual direction 12-inch MERV 14 filter with a fiberglass media (Model Aerostar FP Mini-Pleat, Filtration Group, Santa Rosa, CA, USA). MERV 14 efficiently filters the outside air and the air returning from the indoor space. The air handling unit of classroom 3 had a 2-inch MERV 13 filter with a synthetic air media (Model Aerostar Green Pleat, Filtration Group, Santa Rosa, CA, USA). According to the manual of Aerostar filters, MERV 13 filters have lower particle removal efficiency than MERV 14 filters.

2.3.2. Air Purifier's Efficiency in Classroom 3

The second measurement campaign consisted of three stages leading to the determination of the purifier's efficiency. In the first stage, the background indoor pollutant concentrations were measured without operating the pollution source and the purifier. The

second stage started when the indoor pollutant generator was switched on until a stabilized particle concentration was reached. In the third and last stage, the indoor pollutant source was switched off, and the air purifier was switched on. The purpose of the third stage was to investigate the particle decay rate ($K_{purifier}$) in the presence of the air purifier. The experiment was repeated three times by changing the third-stage scenario. In the first scenario, the purifier was switched off in order to measure the natural decay rate of particles ($K_{natural}$) when the ventilation system was only switched on. In the second scenario, the purifier was operated at a flow rate of 267 m^3/h to obtain the particle decay rate ($K_{purifier\ (low)}$). The last scenario was conducted while operating the purifier at a flow rate of 748 m^3/h to measure the decay rate at the purifier's maximum fan speed ($K_{purifier\ (high)}$). In order to calculate the particle decay rate after switching off the NaCl source, we treated the classroom as a closed system and applied the mass balance equation below:

$$\frac{dC_{in}}{dt} = C_{out} AER\ (P) - C_{in}(K) \tag{4}$$

where dC_{in}/dt is the change of the indoor particle concentration with time, K is the particle decay rate (h^{-1}), AER is the air exchange rate (h^{-1}), P is the particle penetration coefficient, and C_{in} and C_{out} are the indoor and outdoor particle concentrations, respectively. Based on the integration of Equation (4), the general equation for the indoor concentration is expressed as follows:

$$C_{in(t)} = \frac{C_{out} AER\ (P)}{K}(1 - e^{-(K)t}) + C_{in(o)} e^{-(K)t} \tag{5}$$

where $C_{in(t)}$ is the concentration of the particles at time t and $C_{in(o)}$ represents the concentration of the particles at time 0. In order to analyze the decay of the particles (i.e., reduction in particle concentration) with time, we subtracted the concentration of the particles continuously infiltrating indoors (i.e., the first term of Equation (5)) from the measured concentrations during the decay period. This allowed us to use the exponential equation below to obtain the decay rate of the particles:

$$C_{in(t)} = C_{in(o)} e^{-(K)\ t} \tag{6}$$

The particle decay rate is a function of the air exchange rate, particle deposition rate, and particle removal rate by the purifier. Thus, Equations (7) and (8) were used to express the decay rate in the natural condition (i.e., without the purifier) and in the presence of the purifier, respectively:

$$K_{Natural} = AER + k \tag{7}$$

$$K_{Purifier} = AER + k + \eta \frac{Q}{V} \tag{8}$$

where AER is the air exchange rate (h^{-1}), k is the particle deposition rate (h^{-1}), η represents the purifier efficiency, Q is the air volumetric flow rate of the purifier (m^3/h), and V represents the volume of the classroom (m^3). By combining Equations (7) and (8), we can calculate the purifier's efficiency, as shown in Equation (9):

$$\eta = \frac{(K_{Purifier} - K_{Natural})_V}{Q} \tag{9}$$

The decay in the particle mass and number concentrations was plotted as a function of time after switching off the aerosol source. Decay curves were obtained for a range of particle sizes (0.3–10 μm) to estimate the purifier's efficiency in removing different particle sizes. In addition, the purifier removal efficiency for ultrafine particles was estimated using PN data obtained from the DiSCmini since it mainly detected particles with diameters below 0.3 μm.

of time after switching off the aerosol source. Decay curves were obtained for a range of particle sizes (0.3–10 μm) to estimate the purifier's efficiency in removing different particle sizes. In addition, the purifier removal efficiency for ultrafine particles was estimated using PN data obtained from the DiSCmini since it mainly detected particles with diameters below 0.3 μm.

3. Results and Discussion

3.1. Indoor Monitoring of PM, PN, and CO_2 Concentrations in the Set of Classrooms

3.1.1. Indoor CO_2 Levels

Figure 2 demonstrates the actual air exchange rates (*AER*) in the selected classrooms, which were measured and showed a very good agreement with the *AER* received from the USC facilities and the management department as shown in Figure S2. The detailed methodology of calculating the *AER* inside the classrooms is described in the supplementary material. *AER* is the metric for assessing the adequacy of the applied ventilation (i.e., mechanical ventilation system) in bringing in sufficient outdoor air and diluting indoor CO_2 concentrations. However, high air exchange rates will also increase the infiltration of outdoor particulate pollutants, especially if the ventilation system operates without an in-line filtration system that removes a fraction of outdoor particle pollutants [26,31]. As shown in Figure 2, the classrooms' *AER* values ranged from 2.63 h^{-1} (Classroom 7) to 8.63 h^{-1} (Classroom 4). The American Society of Heating, Refrigerating and Air-Conditioning Engineers (ASHRAE) standard 62.1 (2016) recommended a minimum ventilation rate of 7.5 L/sec (27 m^3/h) per person in closed environments [55]. Figure 2 shows the alignment of the *AER* values with the ASHRAE's recommendation in all investigated classrooms. Therefore, these *AER* values indicate sufficient outdoor-to-indoor air circulation and adequate ventilation.

Figure 2 demonstrates the actual air exchange rates (*AER*) in the selected classrooms, which were measured and showed a very good agreement with the *AER* received from the USC facilities and the management department as shown in Figure S2. The detailed methodology of calculating the *AER* inside the classrooms is described in the supplementary material. *AER* is the metric for assessing the adequacy of the applied ventilation (i.e., mechanical ventilation system) in bringing in sufficient outdoor air and diluting indoor CO_2 concentrations. However, high air exchange rates will also increase the infiltration of outdoor particulate pollutants, especially if the ventilation system operates without an in-line filtration system that removes a fraction of outdoor particle pollutants [26,31]. As shown in Figure 2, the classrooms' *AER* values ranged from 2.63 h^{-1} (Classroom 7) to 8.63 h^{-1} (Classroom 4). The American Society of Heating, Refrigerating and Air-Conditioning Engineers (ASHRAE) standard 62.1 (2016) recommended a minimum ventilation rate of 7.5 L/sec (27 m^3/h) per person in closed environments [55]. Figure 2 shows the alignment of the *AER* values with the ASHRAE's recommendation in all investigated classrooms. Therefore, these *AER* values indicate sufficient outdoor-to-indoor air circulation and adequate ventilation.

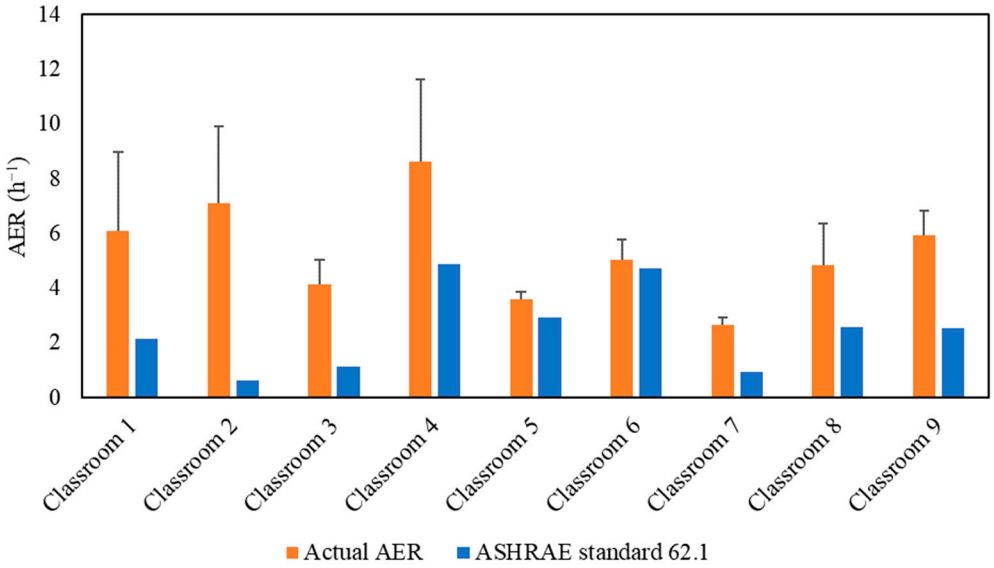

Figure 2. Air exchange rate (*AER*) values for the tested classrooms. The error bars indicate standard deviations of the values measured on three different days.

After approximately 10 min from the beginning of each lecture, the indoor CO_2 concentration reached a well-mixed steady-state condition when the production of CO_2 by the students was equal to the losses of CO_2 due to air circulation in the ventilation system. The ASHRAE standard 62.1 (2016) recommended that the indoor steady-state CO_2 concentration should not exceed the outdoor CO_2 level by more than 700 ppm [55]. Figure 3 presents the average outdoor and indoor CO_2 concentrations during the three phases of measurements in the studied classrooms. The comparable indoor CO_2 levels in the three phases confirm that the indoor CO_2 concentrations are not affected by the use of air purifiers since the latter remove particulate and not gaseous air pollutants. Elevated concentrations of CO_2 can impact productivity [56–58] and lead to headaches, tiredness [59,60], and sick building syndrome (SBS) symptoms (e.g., difficulty in concentration, dizziness) [61–64]. According to the recommended indoor CO_2 level by ASHRAE (not exceeding the outdoor level by 700 ppm) and the measured outdoor CO_2 level (400–500 ppm), the indoor CO_2 levels in the tested classrooms should not exceed 1100–1200 ppm. This is consistent with our measurements inside the classrooms which showed values ranging between

3 presents the average outdoor and indoor CO_2 concentrations during the three phases of measurements in the studied classrooms. The comparable indoor CO_2 levels in the three phases confirm that the indoor CO_2 concentrations are not affected by the use of air purifiers since the latter remove particulate and not gaseous air pollutants. Elevated concentrations of CO_2 can impact productivity [56–58] and lead to headaches, tiredness [59,60], and sick building syndrome (SBS) symptoms (e.g., difficulty in concentration, dizziness) [61–64]. According to the recommended indoor CO_2 level by ASHRAE (not exceeding the outdoor level by 700 ppm) and the measured outdoor CO_2 level (400–500 ppm), the indoor CO_2 levels in the tested classrooms should not exceed 1100–1200 ppm. This is consistent with our observation in the classrooms, which showed indoor levels ranging between 500 ppm and 900 ppm. This observation corroborates that the ventilation systems in all the tested classrooms are adequate and provide sufficient outdoor air to dilute indoor CO_2 concentrations as a result of the generally high air exchange rates (2.63–8.63 h^{-1}) in each classroom [32,65,66].

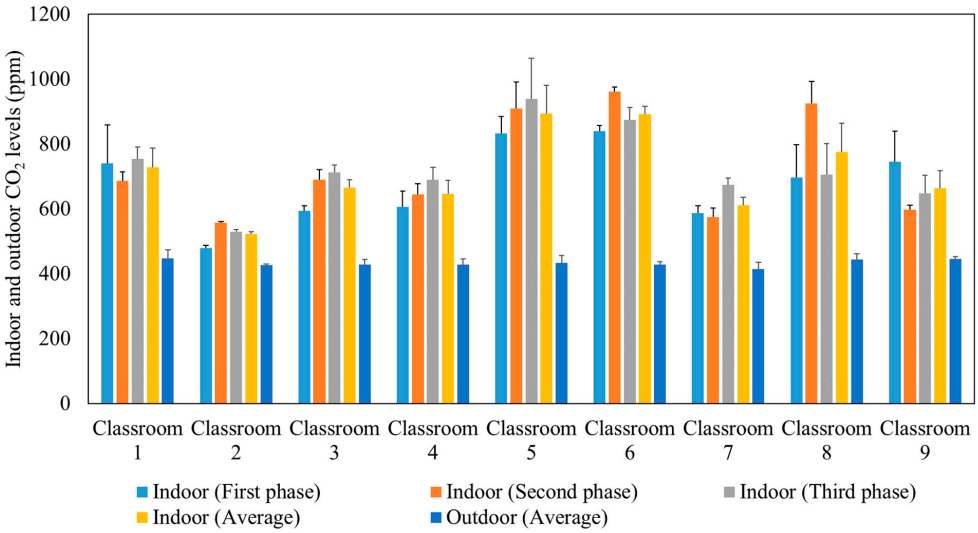

Figure 3. Average outdoor and indoor CO_2 levels during the three phases in the studied classrooms. The error bars indicate standard deviations of values measured in a single day.

3.1.2. Particle Mass and Number Concentrations and Indoor-to-Outdoor Ratios inside the Classrooms

Table 2 summarizes the ambient, indoor, and indoor-to-outdoor (I/O) ratios of $PM_{2.5}$ mass concentrations and particle number concentrations in the occupied classrooms for the first, second, and third measurement phases. During the first phase, classroom 3 exhibited the highest indoor $PM_{2.5}$ mass concentration (8.62 $\mu g/m^3$), followed by classroom 9 with an indoor mass concentration of 2.43 $\mu g/m^3$. The indoor mass concentration during the three phases does not accurately reflect the effectiveness of the air purification unit in reducing indoor pollution because the ambient pollution has a significant influence on the indoor concentration. For example, classroom 9 showed a higher PM indoor concentration (2.43 $\mu g/m^3$) compared to classroom 8 (0.95 $\mu g/m^3$) in the first phase, while the corresponding outdoor levels were 21.67 and 5.69 $\mu g/m^3$, respectively. Therefore, we used the indoor-to-outdoor ratio as a metric for measuring the effectiveness of ventilation and air purifiers in reducing indoor pollutant levels. Excluding classroom 3, all classrooms had PM and PN I/O ratios below 0.2 in the first phase without using the purification unit. This observation indicates that the ambient PM and PN were initially reduced by 80% or more in most classrooms by just the in-line filters of the ventilation system. In classroom 3, the ambient PM and PN concentrations in the first phase were reduced by 56 % and 65%, respectively. The low I/O values in the first phase did not allow for a proper investigation of the purifier's efficiency in removing particles in the subsequent phases. For example, the PN I/O ratio in classroom 4 decreased from 0.05 in the first phase to 0.04 in the third phase when the purifier was operated at the maximum volumetric flow rate (748 m^3/h). Starting with a low I/O value did not allow the purifier to reduce the I/O ratio substantially and, more importantly, the indoor PM levels approached the limit of detection of the DustTrak, such as classrooms 2 and 7.

Table 2. Indoor, ambient, and indoor-to-outdoor (I/O) ratios of PM and PN in the three measurement phases. LOD refers to the limit of detection of the employed instrument.

	$PM_{2.5}$ Mass Concentration (PM) ($\mu g/m^3$)								
	First Phase			Second Phase			Third Phase		
	Indoor	Outdoor	I/O	Indoor	Outdoor	I/O	Indoor	Outdoor	I/O
Classroom 1	1.19	7.90	0.15	0.07	2.04	0.03	0.21	9.00	0.02
Classroom 2	0.31	8.2	0.04	0.48	46.01	0.01	<LOD	24.33	NA
Classroom 3	8.62	19.55	0.44	1.25	3.04	0.41	10.97	42.39	0.26
Classroom 4	1.29	10.60	0.12	0.61	9.56	0.06	2.03	28.22	0.07
Classroom 5	1.24	13.44	0.09	1.04	10.31	0.10	0.73	6.60	0.11
Classroom 6	1.00	5.63	0.18	0.15	2.75	0.05	0.77	22.93	0.03
Classroom 7	0.27	7.83	0.03	<LOD	4.08	NA	<LOD	11.67	NA
Classroom 8	0.95	5.69	0.17	2.99	33.91	0.09	2.20	60.25	0.04
Classroom 9	2.43	21.67	0.11	1.92	18.71	0.10	0.87	11.85	0.07
	Particle Number Concentration (PN) (particles/cm^3)								
	First Phase			Second Phase			Third Phase		
	Indoor	Outdoor	I/O	Indoor	Outdoor	I/O	Indoor	Outdoor	I/O
Classroom 1	207.4	8523.5	0.02	90.6	4798.5	0.02	84.0	2972.8	0.03
Classroom 2	113.73	2290.07	0.05	165.87	5285.31	0.03	42.76	3672.92	0.01
Classroom 3	2328.7	6693.6	0.35	1800.0	5557.3	0.32	1917.8	7050.2	0.27
Classroom 4	258.6	5537.9	0.05	306.2	6704.9	0.05	253.8	6944.3	0.04
Classroom 5	345.6	8453.6	0.04	151.0	8414.1	0.02	363.1	17704.5	0.02
Classroom 6	1389.0	14338.6	0.10	299.1	12158.4	0.02	89.4	10312.7	0.01
Classroom 7	76.36	6215.27	0.01	52.33	4425.42	0.01	53.41	5573.16	0.01
Classroom 8	388.0	13783.6	0.03	220.0	7050.2	0.03	90.4	5807.8	0.02
Classroom 9	1100.2	17763.5	0.06	673.5	14862.2	0.05	543.5	15294.1	0.04

The effective indoor penetration was measured for each classroom to assess the effectiveness of the in-line filtration in the air handling units. Figure 4 shows the penetration coefficients for PM and PN during each phase, as well as the average values throughout all three phases. Unlike the I/O ratio, the penetration coefficient values are independent of the purifier as corroborated by the comparable values in the three phases. The penetration coefficients for PM were higher than PN as the latter primarily consists of ultrafine particles (i.e., size < 0.3 μm), which are easier to remove by filters due to their diffusivity. The P values in the majority of classrooms were low for both PM (<0.2) and PN (<0.1), which can be attributed to the presence of efficient in-line filters (i.e., MERV 14) in the ventilation systems of almost all classrooms. Higher penetration coefficient values for PM (0.51) and PN (0.45) were observed in classroom 3 due to the less efficient in-line filter (i.e., MERV 13) used in its mechanical ventilation system. Based on the penetration values in classroom 3, the in-line filtration system could only reduce ambient PM and PN by approximately 49% and 55%, respectively. Therefore, we selected classroom 3 to conduct our experiments for the second measurement campaign.

3.2. Indoor Monitoring of PM, PN, and CO_2 Concentrations in Classroom 3 in the Presence of Indoor Particle Pollution Source

Real-time monitoring of PM, PN, and CO_2 was conducted in the presence of an aerosol-generating source emitting sodium chloride in classroom 3. As discussed earlier, classroom 3 was selected for the second measurement campaign due to its higher penetration coefficient compared to the other classrooms. The measured indoor CO_2 level in classroom 3 was constant during the three stages due to the absence of indoor CO_2 sources (e.g., students). Indoor CO_2 levels were not affected by the generation of aerosols or the change of the purifier setting, as we would expect; however, PN and PM concentrations were heavily affected.

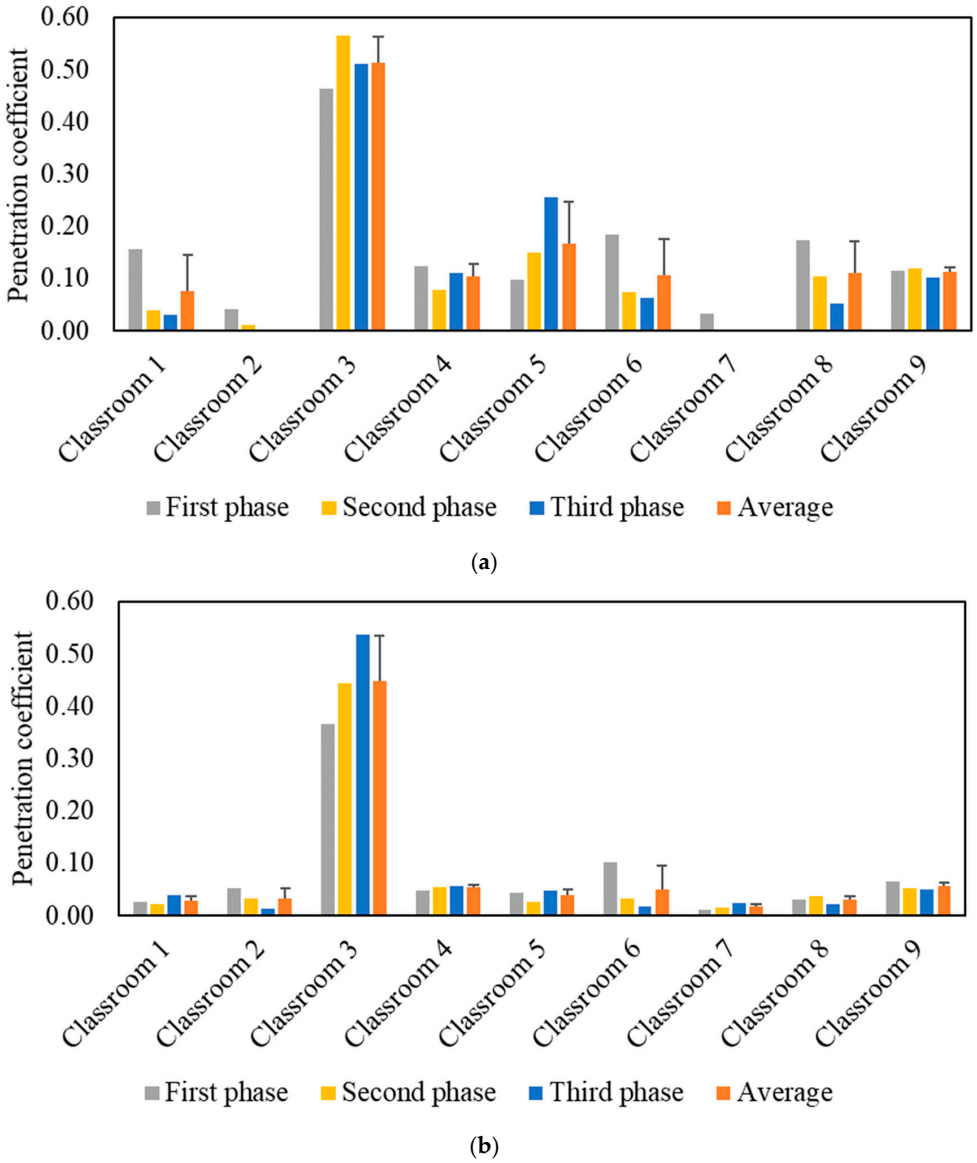

Figure 4. Particle indoor penetration based on: (**a**) $PM_{2.5}$ mass concentration and (**b**) particle number concentration. The error bars indicate standard deviations of the values measured on three different days.

3.2.1. PM and PN Decay Rates with and without the Use of Air Purifier at Different Volumetric Flow Rates

Figure S3 presents the real-time measurements of PM and PN concentrations during the three stages: (i) background condition, (ii) NaCl indoor source is switched on, (iii) purifier is switched on and the source is switched off. It also shows the PM and PN measurements for different configurations of the third stage (i.e., without the purifier, the purifier at a low flow rate of 267 m^3/hr, and the purifier at a high flow rate of 748 m^3/h). Figure 5 shows the PM and PN particle decay curves in classroom 3, which were obtained and analyzed based on the third-stage data. The natural decay rates of the particles without the application of the air purifier were in the range of 3.9 to 4.8 h^{-1}, where the K values were 4.74 h^{-1} and 3.95 h^{-1} for PM and PN, respectively. When the purifier was switched on at a low flow rate (267 m^3/h), the decay rates increased to 5.0–5.3 h^{-1}, with K values of 5.09 h^{-1} for PM and 5.26 h^{-1} for PN. Operating the purifier at the maximum air flow rate (748 m^3/h) resulted in a significant increase in the particle decay rates (6.5–6.7 h^{-1}), with decay values of 6.70 h^{-1} and 6.58 h^{-1} for PM and PN, respectively. The theoretical

values of the decay rates were calculated using Equations (7) and (8). According to Long et al. (2001) [54], the deposition rate is dependent on the particle size and ranges between 0.10–0.25 h^{-1} for $PM_{2.5}$ particles. Table 3 shows a good agreement between the theoretical and experimental decay rates for PM.

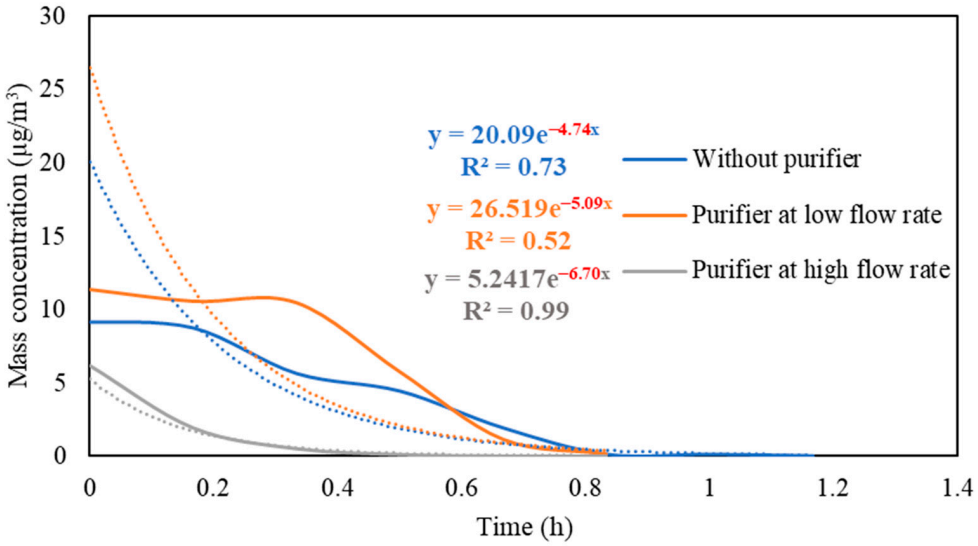

(**a**)

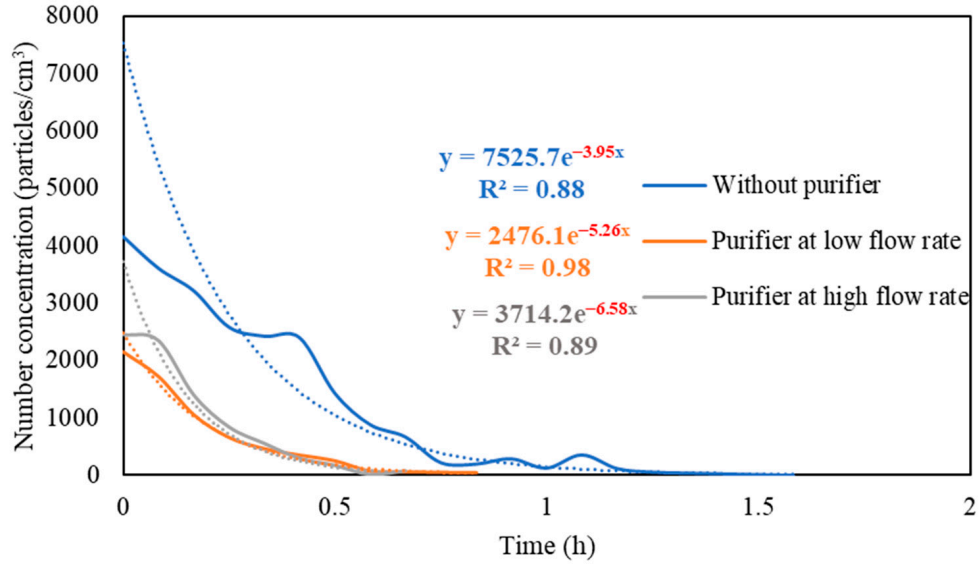

(**b**)

Figure 5. Decay rate curves with and without the use of purifier at different flow rates based on (**a**) PM and (**b**) PN in classroom 3. The dotted curves represent exponential trendlines.

Table 3. Theoretical versus experimental decay rates for particle mass (PM) with and without the use of purifier at different settings in classroom 3.

	Theoretical K (h^{-1})	Experimental K (h^{-1})
Without purifier ($K_{natural}$)	4.32	4.74 ± 0.15
Purifier at low setting ($K_{purifier\ (low)}$)	5.22	5.09 ± 0.13
Purifier at high setting ($K_{purifier\ (high)}$)	6.90	6.70 ± 0.33

The quick reduction in particle concentrations clearly demonstrates the effectiveness of the air purifier. In the first stage, the initial PM and PN concentrations at the beginning of the decay period reached a 50% reduction after 35–40 min when only mechanical ventilation was on. Using the purifier at a low flow rate of 267 m^3/h and a high flow rate of 748 m^3/h reduced the particle number concentrations by 50% after 25–30 min and 10–15 min, respectively. According to Szabadi et al. (2022) [18], operating the purifier at the maximum flow rate caused a 50% reduction in the particle number concentration after 20 min of switching off the aerosol source, which is consistent with our study. Lower decay rates will result in longer particle residence times indoors and, if these aerosols contain viruses (e.g., SARS-CoV-2), the probability of transmission and infection will increase [35,36,44,67]. Zuraimi et al. (2011) [44] reported that using an air purifier at its maximum fan setting reduced the residence time of coughing and sneezing particles from 4–6 h to 30–40 min. All the aforementioned studies support the use of an air purifier at the maximum flow rate to increase the particle decay, which will decrease the risk of viruses' transmission in case an infectious person is present in the classroom.

3.2.2. Removal Efficiency as a Function of Particle Size

The measurements of the particle number concentration at the purifier's flow rate of 267 m^3/h were used to determine the purifier's removal efficiency as a function of particle size in classroom 3. Figure 6 presents different particle decay rates based on various particle size ranges. As shown in the figure, the increase in particle size is associated with a higher value of particle decay rate. The efficiencies for each particle size range were calculated and shown in Figure 7. The particle removal efficiencies of the purifier for the size ranges (0.3–0.5 µm), (0.5–1 µm), (1–2 µm), (2–5 µm), and (5–10 µm) were 82.8%, 85.3%, 87.7%, 95.0%, and 99.4%, respectively. Higher efficiencies were achieved for coarse particles, which indicates the efficient performance of HEPA filters in capturing coarse particles. HEPA filters are less efficient in removing particles in the accumulation mode (0.3–2 µm), with removal efficiencies between 82% and 88%.

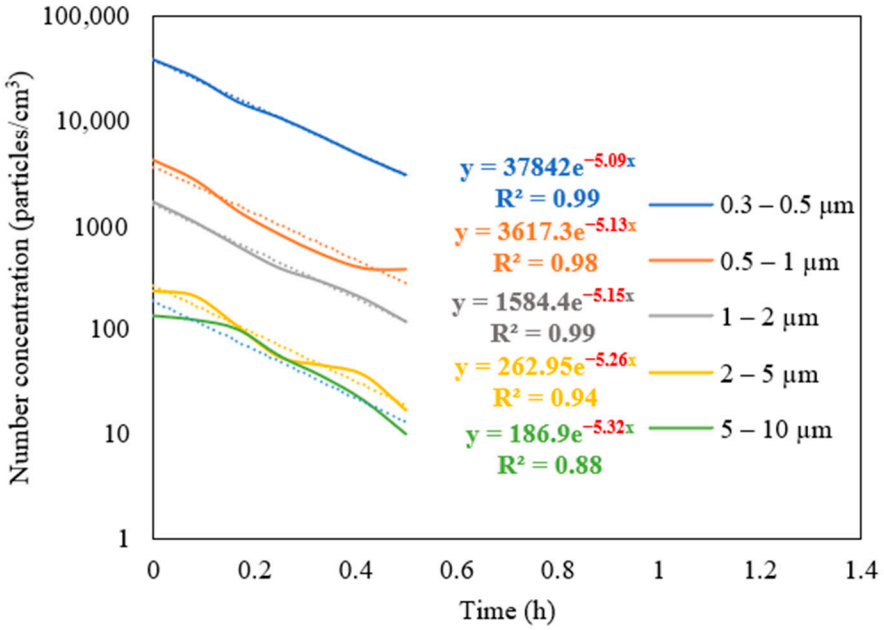

Figure 6. Decay rate curves as a function of particle size in classroom 3 after switching off the NaCl source and operating the purifier at a flow rate of 267 m^3/h. The dotted curves represent exponential trendlines.

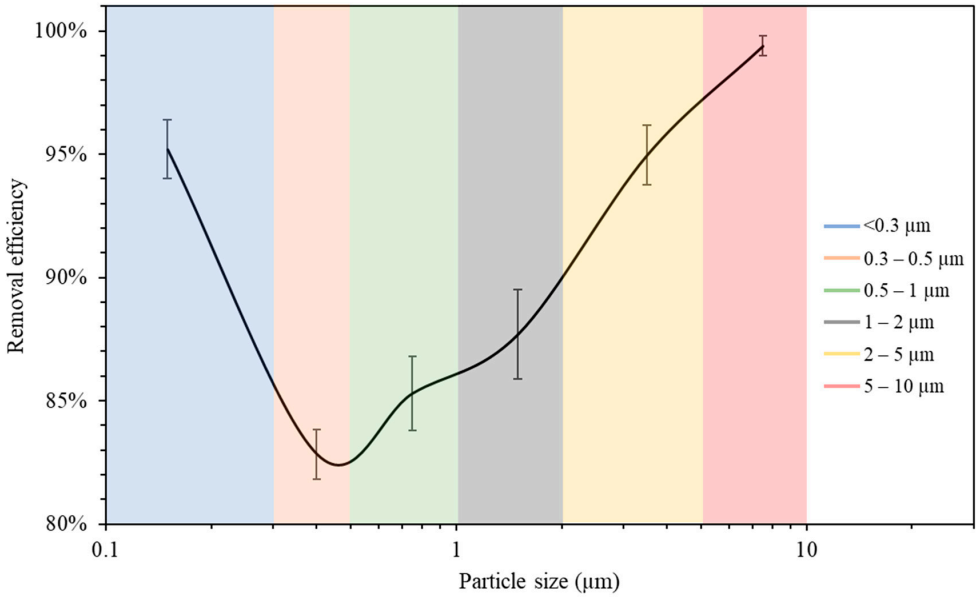

Figure 7. Air purifier removal efficiency as a function of particle size. The error bars indicate standard deviations of values measured in a single day. Values in x-axis are the mid-point diameters of each particle size range.

The measurements of the particle number concentration in Figure 5b were used to assess the removal efficiency of ultrafine particles since PN data were dominated by particles with a size range of less than 0.3 μm. The decay rate at the purifier's flow rate of 267 m^3/h was calculated as 5.26 h^{-1}, corresponding to a removal efficiency value of 95.2%. These results lead to the conclusion that the air purifier equipped with HEPA filters is more efficient in removing both ultrafine particles (<0.3 μm) and coarse particles (2–10 μm). However, particles in the intermediate size range (0.3–2 μm) were somewhat less efficiently removed compared to those in the coarse and ultrafine ranges, although the removal efficiency even in that particle range was between 82 and 88%. These results are consistent with various previously published studies and are a result of the fact that smaller particles are easily removed by filters due to their high diffusivity, and larger particles are primarily removed because of their high interception and inertia impaction [68,69].

4. Summary and Conclusions

This work investigated the effectiveness of air purifiers working in conjunction with in-line filters of mechanical ventilation systems inside different classrooms and their role in improving air quality and capturing pollutants originating from both indoor and outdoor sources. The mechanical ventilation systems in all classrooms, except one, were equipped with 12-inch MERV 14 filters that significantly reduced ambient PM and PN concentrations by more than 80%. The less efficient in-line filter (MERV 13) in the ventilation system of classroom 3 reduced ambient PM and PN by 49% and 55%, respectively. The indoor CO_2 levels in the analyzed classrooms (500–900 ppm) were below the ASHRAE 62.1 standard, indicating adequate ventilation and sufficient outdoor-to-indoor air circulation due to the high air exchange rates (2.63–8.63 h^{-1}). Moreover, operating the purifier at the maximum flow rate (748 m^3/h) in classroom 3 resulted in increasing the particle decay rate from 3.9–4.8 h^{-1} (without the purifier) to 6.5–6.7 h^{-1}, corresponding to a 50% reduction in indoor PM and PN after 10–15 min of switching off the aerosol source. The efficiency of the HEPA air purifier exceeded 95% in capturing ultrafine and coarse particles and ranged between 82–88% for particles in the accumulation range. This study highlighted the significance of mitigating indoor pollution in closed environments, especially in densely seated classrooms where the infection risk of viruses' transmission is high. The findings

of this study recommend the use of HEPA air purifiers in closed environments, especially when the ventilation system is not equipped with an efficient in-line filter.

Supplementary Materials: The following supporting information can be downloaded at: https://www.mdpi.com/article/10.3390/ijerph192114558/s1. Figure S1: Number-based size distribution curve of NaCl particles; Figure S2: Actual *AER* measured in the selected classrooms in comparison with the *AER* received from USC facilities and management (FM) department; Figure S3: PM and PN measurements in classroom 3 (a) without using purifier, (b) with purifier at low flow rate (267 m^3/h), and (c) with purifier at maximum flow rate (748 m^3/h). References [70,71] are cited in Supplementary Materials.

Author Contributions: Conceptualization, M.A. and C.S.; Data curation, M.A., A.A., R.T. and V.J.F.; Methodology, M.A., A.A., R.T. and V.J.F.; Project administration, C.S.; Supervision, C.S.; Validation, V.J.F.; Visualization, R.T.; Writing—original draft, M.A.; Writing—review & editing, A.A., R.T., V.J.F. and C.S. All authors have read and agreed to the published version of the manuscript.

Funding: This research was funded by the dean's office at USC Viterbi School of Engineering (Internal grant).

Institutional Review Board Statement: Not applicable.

Informed Consent Statement: Informed consent was obtained from all subjects involved in the study.

Data Availability Statement: The data that support the findings of this study are available on request from the corresponding author.

Acknowledgments: The authors would like to acknowledge the Ph.D. fellowship awards from the University of Southern California (USC) and Kuwait University. They would also wish to thank the dean's office at USC Viterbi School of Engineering for the internal grant to support this study.

Conflicts of Interest: The authors declare no conflict of interest.

References

1. Ma, H.; Shen, H.; Shui, T.; Li, Q.; Zhou, L. Experimental Study on Ultrafine Particle Removal Performance of Portable Air Cleaners with Different Filters in an Office Room. *Int. J. Environ. Res. Public Health* **2016**, *13*, 102. [CrossRef] [PubMed]
2. Cheek, E.; Guercio, V.; Shrubsole, C.; Dimitroulopoulou, S. Portable Air Purification: Review of Impacts on Indoor Air Quality and Health. *Sci. Total Environ.* **2021**, *766*, 142585. [CrossRef] [PubMed]
3. Cooper, E.; Wang, Y.; Stamp, S.; Burman, E.; Mumovic, D. Use of Portable Air Purifiers in Homes: Operating Behavior, Effect on Indoor PM2.5 and Perceived Indoor Air Quality. *Build. Environ.* **2021**, *191*, 107621. [CrossRef]
4. Pacitto, A.; Amato, F.; Moreno, T.; Pandolfi, M.; Fonseca, A.; Mazaheri, M.; Stabile, L.; Buonanno, G.; Querol, X. Effect of Ventilation Strategies and Air Purifiers on the Children's Exposure to Airborne Particles and Gaseous Pollutants in School Gyms. *Sci. Total Environ.* **2020**, *712*, 135673. [CrossRef] [PubMed]
5. World Health Organization (WHO). Household Air Pollution and Health. Available online: https://www.who.int/health-topics/air-pollution (accessed on 19 March 2022).
6. Polichetti, G.; Cocco, S.; Spinali, A.; Trimarco, V.; Nunziata, A. Effects of Particulate Matter (PM10, PM2.5 and PM1) on the Cardiovascular System. *Toxicology* **2009**, *261*, 1–8. [CrossRef] [PubMed]
7. Anderson, J.O.; Thundiyil, J.G.; Stolbach, A. Clearing the Air: A Review of the Effects of Particulate Matter Air Pollution on Human Health. *J. Med. Toxicol.* **2012**, *8*, 166–175. [CrossRef]
8. Oberdörster, G. Toxicology of Ultrafine Particles: In Vivo Studies. *Philos. Trans. R. Soc. A Math. Phys. Eng. Sci.* **2000**, *358*, 2719–2740. [CrossRef]
9. Hoskins, J.A. Health Effects Due to Indoor Air Pollution. *Indoor Built Environ.* **2003**, *12*, 427–433. [CrossRef]
10. Perez-Padilla, R.; Schilmann, A.; Riojas-Rodriguez, H.; Murray, J.F. Respiratory Health Effects of Indoor Air Pollution. *Int. J. Tuberc. Lung Dis.* **2010**, *14*, 1079–1086.
11. Chang, T.Y.; Zivin, J.G.; Gross, T.; Neidell, M. The Effect of Pollution on Worker Productivity: Evidence from Call Center Workers in China. *Am. Econ. J. Appl. Econ.* **2019**, *11*, 151–172. [CrossRef]
12. Jayaweera, M.; Perera, H.; Gunawardana, B.; Manatunge, J. Transmission of COVID-19 Virus by Droplets and Aerosols: A Critical Review on the Unresolved Dichotomy. *Environ. Res.* **2020**, *188*, 109819. [CrossRef] [PubMed]
13. Morawska, L.; Cao, J. Airborne Transmission of SARS-CoV-2: The World Should Face the Reality. *Environ. Int.* **2020**, *139*, 105730. [CrossRef] [PubMed]
14. Kähler, C.J.; Fuchs, T.; Hain, R. Can Mobile Indoor Air Cleaners Effectively Reduce an Indirect Risk of SARS-CoV-2 Infection by Aerosols? *MMWR* **2020**, *70*, 972–976.

15. Piscitelli, P.; Miani, A.; Setti, L.; de Gennaro, G.; Rodo, X.; Artinano, B.; Vara, E.; Rancan, L.; Arias, J.; Passarini, F.; et al. The Role of Outdoor and Indoor Air Quality in the Spread of SARS-CoV-2: Overview and Recommendations by the Research Group on COVID-19 and Particulate Matter (RESCOP Commission). *Environ. Res.* **2022**, *211*, 113038. [CrossRef]
16. Schwarz, K.; Biller, H.; Windt, H.; Koch, W.; Hohlfeld, J.M. Characterization of Exhaled Particles from the Human Lungs in Airway Obstruction. *J. Aerosol Med. Pulm. Drug Deliv.* **2015**, *28*, 52–58. [CrossRef]
17. Scheuch, G. Breathing Is Enough: For the Spread of Influenza Virus and SARS-CoV-2 by Breathing Only. *J. Aerosol Med. Pulm. Drug Deliv.* **2020**, *33*, 230–234. [CrossRef]
18. Szabadi, J.; Meyer, J.; Lehmann, M.; Dittler, A. Simultaneous Temporal, Spatial and Size-Resolved Measurements of Aerosol Particles in Closed Indoor Environments Applying Mobile Filters in Various Use-Cases. *J. Aerosol Sci.* **2022**, *160*, 105906. [CrossRef]
19. Lindsley, W.G.; Noti, J.D.; Blachere, F.M.; Szalajda, J.V.; Beezhold, D.H. Efficacy of Face Shields against Cough Aerosol Droplets from a Cough Simulator. *J. Occup. Environ. Hyg.* **2014**, *11*, 509–518. [CrossRef]
20. Xie, X.; Li, Y.; Chwang, A.T.Y.; Ho, P.L.; Seto, W.H. How Far Droplets Can Move in Indoor Environments-Revisiting the Wells Evaporation-Falling Curve. *Indoor Air* **2007**, *17*, 211–225. [CrossRef]
21. Fennelly, K.P. Particle Sizes of Infectious Aerosols: Implications for Infection Control. *Lancet Respir. Med.* **2020**, *8*, 914–924. [CrossRef]
22. Küpper, M.; Asbach, C.; Schneiderwind, U.; Finger, H.; Spiegelhoff, D.; Schumacher, S. Testing of an Indoor Air Cleaner for Particulate Pollutants under Realistic Conditions in an Office Room. *Aerosol Air Qual. Res.* **2019**, *19*, 1655. [CrossRef]
23. Sultan, Z.M.; Nilsson, G.J.; Magee, R.J. Removal of Ultrafine Particles in Indoor Air: Performance of Various Portable Air Cleaner Technologies. *HVAC R Res.* **2011**, *17*, 513–525. [CrossRef]
24. Shaughnessy, R.J.; Sextro, R.G. What Is an Effective Portable Air Cleaning Device? A Review. *J. Occup. Environ. Hyg.* **2006**, *3*, 169–181. [CrossRef]
25. Kim, H.J.; Han, B.; Kim, Y.J.; Jeong, C.S.; Lee, S.H. A Simple and Efficient Method for Evaluating Air-Cleaning Performance against Airborne Allergen Particles. *Build. Environ.* **2013**, *60*, 272–279. [CrossRef]
26. van der Zee, S.C.; Strak, M.; Dijkema, M.B.A.; Brunekreef, B.; Janssen, N.A.H. The Impact of Particle Filtration on Indoor Air Quality in a Classroom near a Highway. *Indoor Air* **2017**, *27*, 291–302. [CrossRef] [PubMed]
27. Sublett, J.L. Effectiveness of Air Filters and Air Cleaners in Allergic Respiratory Diseases: A Review of the Recent Literature. *Curr. Allergy Asthma Rep.* **2011**, *11*, 395–402. [CrossRef]
28. Batterman, S.; Godwin, C.; Jia, C. Long Duration Tests of Room Air Filters in Cigarette Smokers' Homes. *Environ. Sci. Technol.* **2005**, *39*, 7260–7268. [CrossRef]
29. Barn, P.; Larson, T.; Noullett, M.; Kennedy, S.; Copes, R.; Brauer, M. Infiltration of Forest Fire and Residential Wood Smoke: An Evaluation of Air Cleaner Effectiveness. *J. Expo. Sci. Environ. Epidemiol.* **2008**, *18*, 503–511. [CrossRef]
30. Lin, C.C.; Peng, C.K. Characterization of Indoor PM10, PM2.5, and Ultrafine Particles in Elementary School Classrooms: A Review. *Environ. Eng. Sci.* **2010**, *27*, 915–922. [CrossRef]
31. Guo, H.; Morawska, L.; He, C.; Gilbert, D. Impact of Ventilation Scenario on Air Exchange Rates and on Indoor Particle Number Concentrations in an Air-Conditioned Classroom. *Atmos. Environ.* **2008**, *42*, 757–768. [CrossRef]
32. You, Y.; Niu, C.; Zhou, J.; Liu, Y.; Bai, Z.; Zhang, J.; He, F.; Zhang, N. Measurement of Air Exchange Rates in Different Indoor Environments Using Continuous CO_2 Sensors. *J. Environ. Sci.* **2012**, *24*, 657–664. [CrossRef]
33. Li, Y.; Chen, Z. A Balance-Point Method for Assessing the Effect of Natural Ventilation on Indoor Particle Concentrations. *Atmos. Environ.* **2003**, *37*, 4277–4285. [CrossRef]
34. Zhao, B.; Liu, Y.; Chen, C. Air Purifiers: A Supplementary Measure to Remove Airborne SARS-CoV-2. *Build. Environ.* **2020**, *177*, 106918. [CrossRef] [PubMed]
35. Curtius, J.; Granzin, M.; Schrod, J. Testing Mobile Air Purifiers in a School Classroom: Reducing the Airborne Transmission Risk for SARS-CoV-2. *Aerosol Sci. Technol.* **2021**, *55*, 586–599. [CrossRef]
36. Burgmann, S.; Janoske, U. Transmission and Reduction of Aerosols in Classrooms Using Air Purifier Systems. *Phys. Fluids* **2021**, *33*, 033321. [CrossRef]
37. Liu, D.T.; Phillips, K.M.; Speth, M.M.; Besser, G.; Mueller, C.A.; Sedaghat, A.R. Portable HEPA Purifiers to Eliminate Airborne SARS-CoV-2: A Systematic Review. *Otolaryngol.-Head Neck Surg.* **2022**, *166*, 615–622. [CrossRef]
38. Holmgren, H.; Ljungström, E.; Almstrand, A.-C.; Bake, B.; Olin, A.-C. Size Distribution of Exhaled Particles in the Range from 0.01 to 2.0 μm. *J. Aerosol Sci.* **2010**, *41*, 439–446. [CrossRef]
39. Johnson, G.R.; Morawska, L. The Mechanism of Breath Aerosol Formation. *J. Aerosol Med. Pulm. Drug Deliv.* **2009**, *22*, 229–237. [CrossRef]
40. Fabian, P.; McDevitt, J.J.; DeHaan, W.H.; Fung, R.O.P.; Cowling, B.J.; Chan, K.H.; Leung, G.M.; Milton, D.K. Influenza Virus in Human Exhaled Breath: An Observational Study. *PLoS ONE* **2008**, *3*, e2691. [CrossRef]
41. Han, Z.Y.; Weng, W.G.; Huang, Q.Y. Characterizations of Particle Size Distribution of the Droplets Exhaled by Sneeze. *J. R. Soc. Interface* **2013**, *10*, 20130560. [CrossRef]
42. Chao, C.Y.H.; Wan, M.P.; Morawska, L.; Johnson, G.R.; Ristovski, Z.D.; Hargreaves, M.; Mengersen, K.; Corbett, S.; Li, Y.; Xie, X.; et al. Characterization of Expiration Air Jets and Droplet Size Distributions Immediately at the Mouth Opening. *J. Aerosol Sci.* **2009**, *40*, 122–133. [CrossRef] [PubMed]

43. Elsaid, A.M.; Ahmed, M.S. Indoor Air Quality Strategies for Air-Conditioning and Ventilation Systems with the Spread of the Global Coronavirus (COVID-19) Epidemic: Improvements and Recommendations. *Environ. Res.* **2021**, *199*, 111314. [CrossRef] [PubMed]
44. Zuraimi, M.S.; Nilsson, G.J.; Magee, R.J. Removing Indoor Particles Using Portable Air Cleaners: Implications for Residential Infection Transmission. *Build. Environ.* **2011**, *46*, 2512–2519. [CrossRef]
45. Heim, M.; Mullins, B.J.; Wild, M.; Meyer, J.; Kasper, G. Filtration Efficiency of Aerosol Particles below 20 Nanometers. *Aerosol Sci. Technol.* **2005**, *39*, 782–789. [CrossRef]
46. Edwards, N.J.; Colder, B.; Sullivan, J.; Naramore, L. A Practical Approach to Indoor Air Quality for Municipal Public Health and Safety. *Open J. Polit. Sci.* **2021**, *11*, 176–191. [CrossRef]
47. National Institute for Occupational Safety and Health (NIOSH). *Determination of Particulate Filter Efficiency Level for N95 Series Filters against Solid Particulates for Non-Powered, Air-Purifying Respirators Standard Testing Procedure (STP)*; National Personal Protective Technology Laboratory: Washington, DC, USA, 2019.
48. Chao, C.Y.H.; Wan, M.P.; Cheng, E.C.K. Penetration Coefficient and Deposition Rate as a Function of Particle Size in Non-Smoking Naturally Ventilated Residences. *Atmos. Environ.* **2003**, *37*, 4233–4241. [CrossRef]
49. Morawska, L.; Johnson, G.R.; Ristovski, Z.D.; Hargreaves, M.; Mengersen, K.; Corbett, S.; Chao, C.Y.H.; Li, Y.; Katoshevski, D. Size Distribution and Sites of Origin of Droplets Expelled from the Human Respiratory Tract during Expiratory Activities. *J. Aerosol Sci.* **2009**, *40*, 256–269. [CrossRef]
50. Alsved, M.; Matamis, A.; Bohlin, R.; Richter, M.; Bengtsson, P.-E.; Fraenkel, C.-J.; Medstrand, P.; Löndahl, J. Exhaled Respiratory Particles during Singing and Talking. *Aerosol Sci. Technol.* **2020**, *54*, 1245–1248. [CrossRef]
51. Asadi, S.; Wexler, A.S.; Cappa, C.D.; Barreda, S.; Bouvier, N.M.; Ristenpart, W.D. Effect of Voicing and Articulation Manner on Aerosol Particle Emission during Human Speech. *PLoS ONE* **2020**, *15*, e0227699. [CrossRef]
52. Koutrakis, P.; Briggs, S.; Leaderer, B. Source Apportionment of Indoor Aerosols in Suffolk and Onondaga Counties, New York. *Environ. Sci. Technol.* **1992**, *26*, 521–527. [CrossRef]
53. Wallace, L. Indoor Particles: A Review. *J. Air Waste Manag. Assoc.* **1996**, *46*, 98–126. [CrossRef] [PubMed]
54. Long, C.M.; Suh, H.H.; Catalano, P.J.; Koutrakis, P. Using Time- and Size-Resolved Particulate Data to Quantify Indoor Penetration and Deposition Behavior. *Environ. Sci. Technol.* **2001**, *35*, 2089–2099. [CrossRef] [PubMed]
55. American Society of Heating Refrigerating and Air Conditioning (ASHRAE). Engineers Standard 62.1: Ventilation for Acceptable Indoor Air Quality. Available online: https://www.ashrae.org/technical-resources/standards-and-guidelines/read-only-versions-of-ashrae-standards (accessed on 23 April 2022).
56. MacNaughton, P.; Spengler, J.; Vallarino, J.; Santanam, S.; Satish, U.; Allen, J. Environmental Perceptions and Health before and after Relocation to a Green Building. *Build. Environ.* **2016**, *104*, 138–144. [CrossRef] [PubMed]
57. Allen, J.G.; MacNaughton, P.; Satish, U.; Santanam, S.; Vallarino, J.; Spengler, J.D. Associations of Cognitive Function Scores with Carbon Dioxide, Ventilation, and Volatile Organic Compound Exposures in Office Workers: A Controlled Exposure Study of Green and Conventional Office Environments. *Environ. Health Perspect.* **2016**, *124*, 805–812. [CrossRef]
58. Simoni, M.; Annesi-Maesano, I.; Sigsgaard, T.; Norback, D.; Wieslander, G.; Nystad, W.; Cancianie, M.; Sestini, P.; Viegi, G. School Air Quality Related to Dry Cough, Rhinitis and Nasal Patency in Children. *Eur. Respir. J.* **2010**, *35*, 742–749. [CrossRef]
59. Myhvold, A.; Olsen, E.; Lauridsen, O. Indoor Environment in Schools: Pupils Health & Performance in Regard to CO_2 Concentrations. *Indoor Air* **1996**, *96*, 369–374.
60. Norbäck, D.; Nordström, K.; Zhao, Z. Carbon Dioxide (CO_2) Demand-Controlled Ventilation in University Computer Classrooms and Possible Effects on Headache, Fatigue and Perceived Indoor Environment: An Intervention Study. *Int. Arch. Occup. Environ. Health* **2013**, *86*, 199–209. [CrossRef]
61. Vehviläinen, T.; Lindholm, H.; Rintamäki, H.; Pääkkönen, R.; Hirvonen, A.; Niemi, O.; Vinha, J. High Indoor CO_2 Concentrations in an Office Environment Increases the Transcutaneous CO_2 Level and Sleepiness during Cognitive Work. *J. Occup. Environ. Hyg.* **2016**, *13*, 19–29. [CrossRef]
62. Shriram, S.; Ramamurthy, K.; Ramakrishnan, S. Effect of Occupant-Induced Indoor CO_2 Concentration and Bioeffluents on Human Physiology Using a Spirometric Test. *Build. Environ.* **2019**, *149*, 58–67. [CrossRef]
63. Kim, J.; Hong, T.; Kong, M.; Jeong, K. Building Occupants' Psycho-Physiological Response to Indoor Climate and CO_2 Concentration Changes in Office Buildings. *Build. Environ.* **2020**, *169*, 106596. [CrossRef]
64. Azuma, K.; Kagi, N.; Yanagi, U.; Osawa, H. Effects of Low-Level Inhalation Exposure to Carbon Dioxide in Indoor Environments: A Short Review on Human Health and Psychomotor Performance. *Environ. Int.* **2018**, *121*, 51–56. [CrossRef] [PubMed]
65. Hou, Y.; Liu, J.; Li, J. Investigation of Indoor Air Quality in Primary School Classrooms. *Procedia Eng.* **2015**, *121*, 830–837. [CrossRef]
66. di Gilio, A.; Palmisani, J.; Pulimeno, M.; Cerino, F.; Cacace, M.; Miani, A.; de Gennaro, G. CO_2 Concentration Monitoring inside Educational Buildings as a Strategic Tool to Reduce the Risk of Sars-CoV-2 Airborne Transmission. *Environ. Res.* **2021**, *202*, 111560. [CrossRef]
67. Zhai, Z.; Li, H.; Bahl, R.; Trace, K. Application of Portable Air Purifiers for Mitigating COVID-19 in Large Public Spaces. *Buildings* **2021**, *11*, 329. [CrossRef]
68. Lowther, S.D.; Deng, W.; Fang, Z.; Booker, D.; Whyatt, D.J.; Wild, O.; Wang, X.; Jones, K.C. How Efficiently Can HEPA Purifiers Remove Priority Fine and Ultrafine Particles from Indoor Air? *Environ. Int.* **2020**, *144*, 106001. [CrossRef] [PubMed]

69. Christopherson, D.A.; Yao, W.C.; Lu, M.; Vijayakumar, R.; Sedaghat, A.R. High-Efficiency Particulate Air Filters in the Era of COVID-19: Function and Efficacy. *Otolaryngol.-Head Neck Surg.* **2020**, *163*, 1153–1155. [CrossRef]
70. Fruin, S.A.; Hudda, N.; Sioutas, C.; Delfino, R.J. Predictive Model for Vehicle Air Exchange Rates Based on a Large, Representative Sample. *Environ. Sci. Technol.* **2011**, *45*, 3569–3575. [CrossRef]
71. Hudda, N.; Kostenidou, E.; Sioutas, C.; Delfino, R.J.; Fruin, S.A. Vehicle and Driving Characteristics That Influence In-Cabin Particle Number Concentrations. *Environ. Sci. Technol.* **2011**, *45*, 8691–8697. [CrossRef]

People who reported always wearing a mask in indoor public settings were less likely to test positive for COVID-19 than people who didn't*

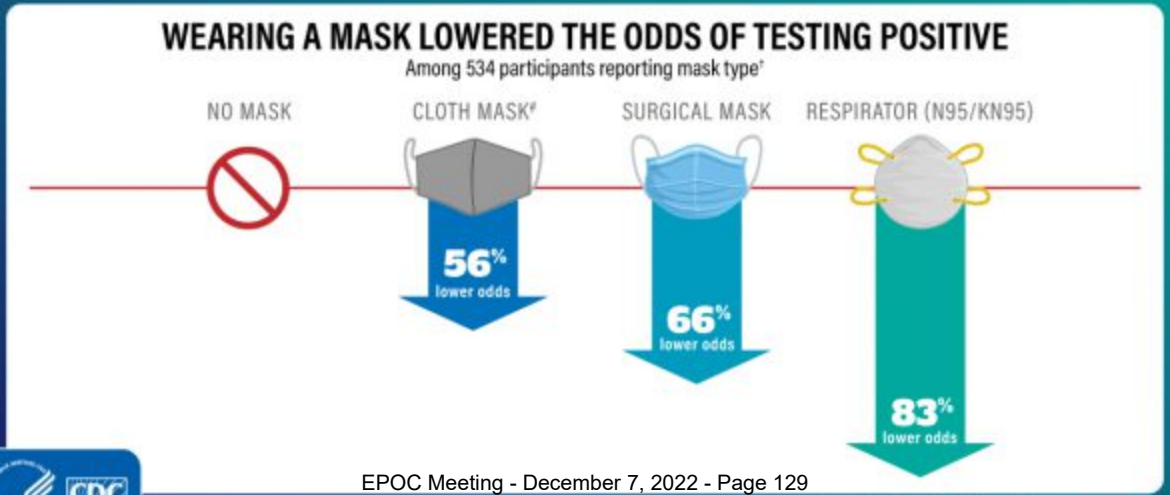

bit.ly/MMWR7106

* Matched case-control study, 1,828 people, Feb 10–Dec 1, 2021
† Compared people with similar characteristics (e.g., vaccination)
‡ Not statistically significant

MMWR

Centers for Disease Control and Prevention
MMWR
Morbidity and Mortality Weekly Report
Early Release / Vol. 71
February 4, 2022

Effectiveness of Face Mask or Respirator Use in Indoor Public Settings for Prevention of SARS-CoV-2 Infection — California, February–December 2021

Kristin L. Andrejko[1,2,*]; Jake M. Pry, PhD[2,*]; Jennifer F. Myers, MPH[2]; Nozomi Fukui[2]; Jennifer L. DeGuzman, MPH[2]; John Openshaw, MD[2]; James P. Watt, MD[2]; Joseph A. Lewnard, PhD[1,3,4]; Seema Jain, MD[2]; California COVID-19 Case-Control Study Team

The use of face masks or respirators (N95/KN95) is recommended to reduce transmission of SARS-CoV-2, the virus that causes COVID-19 (*1*). Well-fitting face masks and respirators effectively filter virus-sized particles in laboratory conditions (*2*,*3*), though few studies have assessed their real-world effectiveness in preventing acquisition of SARS-CoV-2 infection (*4*). A test-negative design case-control study enrolled randomly selected California residents who had received a test result for SARS-CoV-2 during February 18–December 1, 2021. Face mask or respirator use was assessed among 652 case-participants (residents who had received positive test results for SARS-CoV-2) and 1,176 matched control-participants (residents who had received negative test results for SARS-CoV-2) who self-reported being in indoor public settings during the 2 weeks preceding testing and who reported no known contact with anyone with confirmed or suspected SARS-CoV-2 infection during this time. Always using a face mask or respirator in indoor public settings was associated with lower adjusted odds of a positive test result compared with never wearing a face mask or respirator in these settings (adjusted odds ratio [aOR] = 0.44; 95% CI = 0.24–0.82). Among 534 participants who specified the type of face covering they typically used, wearing N95/KN95 respirators (aOR = 0.17; 95% CI = 0.05–0.64) or surgical masks (aOR = 0.34; 95% CI = 0.13–0.90) was associated with significantly lower adjusted odds of a positive test result compared with not wearing any face mask or respirator. These findings reinforce that in addition to being up to date with recommended COVID-19 vaccinations, consistently wearing a face mask or respirator in indoor public settings reduces the risk of acquiring SARS-CoV-2 infection. Using a respirator offers the highest level of personal protection against acquiring infection, although it is most important to wear a mask or respirator that is comfortable and can be used consistently.

This study used a test-negative case-control design, enrolling persons who received a positive (case-participants) or negative (control-participants) SARS-CoV-2 test result, from among all California residents, without age restriction, who received a molecular test result for SARS-CoV-2 during February 18–December 1, 2021 (*5*). Potential case-participants were randomly selected from among all persons who received a positive test result during the previous 48 hours and were invited to participate by telephone. For each enrolled case-participant, interviewers enrolled one control-participant matched by age group, sex, and state region; thus, interviewers were not blinded to participants' SARS-CoV-2 infection status. Participants who self-reported having received a previous positive test result (molecular, antigen, or serologic) or clinical diagnosis of COVID-19 were not eligible to participate. During February 18–December 1, 2021, a total of 1,528 case-participants and 1,511 control-participants were enrolled in the study among attempted calls placed to 11,387 case- and 17,051 control-participants (response rates were 13.4% and 8.9%, respectively).

After obtaining informed consent from participants, interviewers administered a telephone questionnaire in English or Spanish. All participants were asked to indicate whether they had been in indoor public settings (e.g., retail stores, restaurants or bars, recreational facilities, public transit, salons, movie theaters, worship services, schools, or museums) in the 14 days preceding testing and whether they wore a face mask or respirator all, most, some, or none of the time in those settings. Interviewers recorded participants' responses regarding COVID-19 vaccination status, sociodemographic characteristics, and history of exposure to anyone known or suspected to have been infected with SARS-CoV-2 in the 14 days before participants were tested. Participants enrolled during September 9–December 1, 2021, (534) were also

* These authors contributed equally to this report.

U.S. Department of Health and Human Services
Centers for Disease Control and Prevention

asked to indicate the type of face covering typically worn (N95/KN95 respirator, surgical mask, or cloth mask) in indoor public settings.

The primary analysis compared self-reported face mask or respirator use in indoor public settings 14 days before SARS-CoV-2 testing between case- (652) and control- (1,176) participants. Secondary analyses accounted for consistency of face mask or respirator use all, most, some, or none of the time. To understand the effects of masking on community transmission, the analysis included the subset of participants who, during the 14 days before they were tested, reported visiting indoor public settings and who reported no known exposure to persons known or suspected to have been infected with SARS-CoV-2. An additional analysis assessed differences in protection against SARS-CoV-2 infection by the type of face covering worn, and was limited to a subset of participants enrolled after September 9, 2021, who were asked to indicate the type of face covering they typically wore; participants who indicated typically wearing multiple different mask types were categorized as wearing either a cloth mask (if they reported cloth mask use) or a surgical mask (if they did not report cloth mask use). Adjusted odds ratios comparing history of mask-wearing among case- and control-participants were calculated using conditional logistic regression. Match strata were defined by participants' week of SARS-CoV-2 testing and by county-level SARS-CoV-2 risk tiers as defined under California's Blueprint for a Safer Economy reopening scheme.[†] Adjusted models accounted for self-reported COVID-19 vaccination status (fully vaccinated with ≥2 doses of BNT162b2 [Pfizer-BioNTech] or mRNA-1273 [Moderna] or 1 dose of Ad.26.COV2.S [Janssen (Johnson & Johnson)] vaccine >14 days before testing versus zero doses), household income, race/ethnicity, age, sex, state region, and county population density. Statistical significance was defined by two-sided Wald tests with p-values <0.05. All analyses were conducted using R software (version 3.6.1; R Foundation). This activity was approved as public health surveillance by the State of California Health and Human Services Agency Committee for the Protection of Human Subjects.

A total of 652 case- and 1,176 control-participants were enrolled in the study equally across nine multi-county regions in California (Table 1). The majority of participants (43.2%) identified as non-Hispanic White; 28.2% of participants identified as Hispanic (any race). A higher proportion of case-participants (78.4%) was unvaccinated compared with control-participants (57.5%). Overall, 44 (6.7%) case-participants and 42 (3.6%) control-participants reported never wearing a face mask or respirator in indoor public settings (Table 2), and 393 (60.3%) case-participants and 819 (69.6%) control-participants reported always wearing a face mask or respirator in indoor public settings. Any face mask or respirator use in indoor public settings was associated with significantly lower odds of a positive test result compared with never using a face mask or respirator (aOR = 0.51; 95% CI = 0.29–0.93). Always using a face mask or respirator in indoor public settings was associated with lower adjusted odds of a positive test result compared with never wearing a face mask or respirator (aOR = 0.44; 95% CI = 0.24–0.82); however, adjusted odds of a positive test result suggested stepwise reductions in protection among participants who reported wearing a face mask or respirator most of the time (aOR = 0.55; 95% CI = 0.29–1.05) or some of the time (aOR = 0.71; 95% CI = 0.35–1.46) compared with participants who reported never wearing a face mask or respirator.

Wearing an N95/KN95 respirator (aOR = 0.17; 95% CI = 0.05–0.64) or wearing a surgical mask (aOR = 0.34; 95% CI = 0.13–0.90) was associated with lower adjusted odds of a positive test result compared with not wearing a mask (Table 3). Wearing a cloth mask (aOR = 0.44; 95% CI = 0.17–1.17) was associated with lower adjusted odds of a positive test compared with never wearing a face covering but was not statistically significant.

Discussion

During February–December 2021, using a face mask or respirator in indoor public settings was associated with lower odds of acquiring SARS-CoV-2 infection, with protection being highest among those who reported wearing a face mask or respirator all of the time. Although consistent use of any face mask or respirator indoors was protective, the adjusted odds of infection were lowest among persons who reported typically wearing an N95/KN95 respirator, followed by wearing a surgical mask. These data from real-world settings reinforce the importance of consistently wearing face masks or respirators to reduce the risk of acquisition of SARS-CoV-2 infection among the general public in indoor community settings.

These findings are consistent with existing research demonstrating that face masks or respirators effectively filter viruses in laboratory settings and with ecological studies showing reductions in SARS-CoV-2 incidence associated with community-level masking requirements (*6*,*7*). While this study evaluated the protective effects of mask or respirator use in reducing the risk the wearer acquires SARS-CoV-2 infection, a previous evaluation estimated the additional benefits of masking for source control, and found that wearing face masks or respirators in the context of exposure to a person with confirmed SARS-CoV-2 infection was associated with similar reductions in risk for infection (*8*). Strengths of the current study include

[†] https://www.cdph.ca.gov/Programs/CID/DCDC/Pages/COVID-19/COVID19CountyMonitoringOverview.aspx

TABLE 1. Characteristics of case- and control-participants included in analysis of the effectiveness of mask use in indoor public settings, by SARS-CoV-2 test result — California,* February–December 2021

Characteristic	No. (%) Case-participants (SARS-CoV-2–positive) N = 652	Control-participants (SARS-CoV-2–negative) N = 1,176
Age group, yrs		
0–6	8 (1.2)	43 (3.7)
7–12	15 (2.3)	49 (4.2)
13–17	25 (3.8)	57 (4.8)
18–29	210 (32.2)	359 (30.5)
30–49	237 (36.3)	409 (34.8)
50–64	109 (16.7)	180 (15.3)
≥65	48 (7.4)	79 (6.7)
Sex		
Male	321 (49.2)	581 (49.4)
Female	331 (50.8)	595 (50.6)
Annual household income		
<$50,000	191 (29.3)	258 (21.9)
$50,000–$99,999	147 (22.5)	254 (21.6)
$100,000–$150,000	60 (9.2)	171 (14.5)
>$150,000	77 (11.8)	197 (16.8)
Refused	106 (16.3)	184 (15.6)
Not sure	71 (10.9)	112 (9.5)
State region†		
San Francisco Bay Area	79 (12.1)	147 (12.5)
Greater Los Angeles Area	77 (11.8)	130 (11.1)
Greater Sacramento Area	53 (8.1)	131 (11.1)
San Diego and southern border	73 (11.2)	142 (12.1)
Central Coast	87 (13.3)	132 (11.2)
Northern Sacramento Valley	69 (10.6)	134 (11.4)
San Joaquin Valley	79 (12.1)	130 (11.1)
Northwestern California	78 (12.0)	113 (9.6)
Sierras	57 (8.7)	117 (9.9)
Race/Ethnicity		
White, non-Hispanic	292 (44.8)	506 (43.0)
Black, non-Hispanic	39 (6.0)	42 (3.6)
Hispanic (any race)	201 (30.8)	315 (26.8)
Asian, non-Hispanic	56 (8.6)	134 (11.4)
American Indian or Alaska Native, non-Hispanic	9 (1.4)	10 (0.9)
Native Hawaiian or Other Pacific Islander, non-Hispanic	2 (0.3)	12 (1.0)
More than one race	40 (6.1)	131 (11.1)
Refused	13 (2.0)	26 (2.2)
COVID-19 vaccination status§		
Unvaccinated or incompletely vaccinated	511 (78.4)	676 (57.5)
Fully vaccinated	115 (17.6)	377 (32.1)
Unknown	26 (4.0)	123 (10.5)
Reopening tier in California¶		
Tier 1 (most restrictive)	125 (19.2)	237 (20.2)
Tier 2	152 (23.3)	255 (21.7)
Tier 3	119 (18.3)	272 (23.1)
Tier 4 (least restrictive)	18 (2.8)	32 (2.7)
After June 15, 2021	238 (36.5)	380 (32.3)

TABLE 1. (*Continued*) Characteristics of case- and control-participants included in analysis of the effectiveness of mask use in indoor public settings, by SARS-CoV-2 test result — California,* February–December 2021

Characteristic	No. (%) Case-participants (SARS-CoV-2–positive) N = 652	Control-participants (SARS-CoV-2–negative) N = 1,176
Reasons for SARS-CoV-2 testing**		
Experiencing symptoms	508 (77.9)	196 (16.7)
Testing required for medical procedure	40 (6.1)	199 (16.9)
Routine screening through work or school	71 (10.9)	507 (43.1)
Pre-travel test	33 (5.1)	120 (10.2)
Just wanted to see if I was infected	65 (10.0)	172 (14.6)
Test required for admission to an event or gathering	3 (0.5)	21 (1.8)

* A random sample of California residents with a molecular SARS-CoV-2 test result was invited to participate in a telephone-based survey to document frequency of face mask or respirator use and type of face mask or respirator typically worn in indoor public settings 2 weeks before testing. For each enrolled case-participant (person with a positive SARS-CoV-2 test result), interviewers attempted to enroll one control-participant (person with a negative SARS-CoV-2 test result) whose test result was posted to the reportable disease registry during the 48 hours preceding the call and matched the case-participant by age group, sex, and state region. Among 1,947 case- and control-participants who visited indoor public settings and did not report a known or suspected exposure to SARS-CoV-2 in the 14 days before getting a SARS-CoV-2 test, 119 (6.1%) participants were unable to report face mask use and were excluded from analysis. Parents or guardians served as proxy respondents and answered questions throughout the telephone survey on behalf of children aged <13 years.

† California counties were divided into nine geographic regions. Counties included in each geographic region are listed online in Table S1. https://academic.oup.com/cid/advance-article/doi/10.1093/cid/ciab640/6324500#supplementary-data

§ Vaccination status was defined using self-reported dates and manufacturers of doses received. Participants were asked to reference their COVID-19 vaccination card while providing vaccination history. Participants who could not provide a complete vaccination history (dates of doses received and manufacturers) were coded as unknown. Full vaccination was defined as receipt of 2 doses of BNT162b2 [Pfizer-BioNTech] or mRNA-1273 [Moderna], or receipt of 1 dose of Ad.26.COV2.S (Janssen [Johnson & Johnson]) >14 days before SARS-CoV-2 testing. Of the 492 fully vaccinated participants, 22 (4.5%) had received a booster dose at the time of enrollment. All other participants were considered unvaccinated or incompletely vaccinated.

¶ Reopening tiers in California were determined by the Blueprint for a Safer Economy the State of California implemented during February 24 to June 15, 2021. This was a tiered system of public health restrictions tied to county-level positive test results and incidence. On June 15, 2021, California retired the tiered reopening system and removed most restrictions on public gatherings, while some counties maintained guidelines for guests and workers to show proof of vaccination or a negative test result to gather in certain types of venues and workplaces. The tier of a given participant was determined by using the date that occurred 14 days before the SARS-CoV-2 specimen collection date recorded for each participant in the California Reportable Disease Registry.

** Case- and control-participants were asked to indicate their reasons for seeking a SARS-CoV-2 test as a free-text response. Trained interviewers (N = 29) recategorized the free-text response into the categories listed in the table. Interviewers were trained to ask probing questions if the free-text response could not be categorized into the reasons listed above. Probing questions and coding decisions may slightly vary by interviewer. Reasons for testing might sum to numbers larger than the total number of case-participants or control-participants because participants could indicate more than one reason for seeking a SARS-CoV-2 test.

TABLE 2. Face mask or respirator use in indoor public settings among persons with positive and negative SARS-CoV-2 test results — California, February–December 2021

	SARS-CoV-2 infection status, no. (%)		Odds ratio (95% CI)	
Mask type and use*	Positive (case-participant) N = 652	Negative (control-participant) N = 1,176	Unadjusted† [p-value]	Adjusted§ [p-value]
None (Ref)	44 (6.7)	42 (3.6)	—	—
Any use†	608 (93.3)	1,134 (96.4)	0.57 (0.37–0.90) [0.02]	0.51 (0.29–0.93) [0.03]
Some of the time	62 (9.5)	76 (6.5)	0.81 (0.47–1.41) [0.49]	0.71 (0.35–1.46) [0.36]
Most of the time	153 (23.5)	239 (20.3)	0.64 (0.40–1.05) [0.08]	0.55 (0.29–1.05) [0.07]
All of the time	393 (60.3)	819 (69.6)	0.49 (0.31–0.78) [<0.01]	0.44 (0.24–0.82) [<0.01]

Abbreviation: Ref = referent group.

* Trained interviewers administered a structured telephone-based questionnaire and asked participants to indicate whether they attended indoor public spaces during the 2 weeks before seeking a SARS-CoV-2 test. Participants who indicated attending these settings were further asked to specify whether they typically wore a face mask or respirator all, most, some, or none of the time while in these settings.

† Conditional logistic regression models were used to estimate the unadjusted odds of mask use by type of face mask or respirator worn in indoor public settings during the 2 weeks before testing. Models included matching strata defined by (for the period before June 15, 2021) the reopening tier of California in the county of residence and the week of SARS-CoV-2 testing.

§ Conditional logistic regression models were used to estimate the odds of face mask or respirator use in indoor public settings during the 2 weeks before testing, adjusting for COVID-19 vaccination status, household income, race/ethnicity, age group, sex, state region, and county population density. All models included matching strata defined by (for the period before June 15, 2021) the reopening tier of California in the county of residence, and the week of SARS-CoV-2 testing. To understand the effects of masking in community settings, this analysis was restricted to a subset of persons who did not indicate a known or suspected exposure to a SARS-CoV-2 case within 14 days of seeking a SARS-CoV-2 test. Adjusted models used a complete case analysis (454 case-participants and 789 control-participants). A sensitivity analysis using multiple imputation of missing covariate values obtained results similar to those reported in the table: adjusted odds ratios were 0.54 (95% CI = 0.33–0.89) for any mask use, 0.44 (95% CI = 0.27–0.73) for mask use all of the time, 0.62 (95% CI = 0.37–1.04) for mask use most of the time, and 0.77 (95% CI = 0.43–1.40) for mask use some of the time. An additional sensitivity analysis was conducted with additional adjustment for the reasons for SARS-CoV-2 testing as listed in Table 1 (experiencing symptoms, testing required for medical procedure, routine screening through work or school, pre-travel test, just wanted to see if I was infected, test required for admission to an event or gathering). The adjusted odds ratio was 0.42 (95% CI = 0.20–0.89) for any mask use as compared to no mask use upon additional adjustment for testing indications.

TABLE 3. Types of face mask or respirator worn in indoor public settings among persons with positive or negative SARS-CoV-2 test results — California, September–December 2021

	SARS-CoV-2 infection status, no. (%)		Odds ratio (95% CI)	
Mask type*	Positive (case-participant) N = 259	Negative (control-participant) N = 275	Unadjusted† [p-value]	Adjusted§ [p-value]
None (Ref)	24 (9.3)	11 (4.0)	—	—
Cloth mask	112 (43.2)	104 (37.8)	0.50 (0.23–1.06) [0.07]	0.44 (0.17–1.17) [0.10]
Surgical mask	113 (43.6)	139 (50.5)	0.28 (0.18–0.81) [0.01]	0.34 (0.13–0.90) [0.03]
N95/KN95 respirator	10 (3.9)	21 (7.6)	0.22 (0.08–0.62) [<0.01]	0.17 (0.05–0.64) [<0.01]

Abbreviation: Ref = referent group.

* Trained interviewers administered a structured telephone-based questionnaire and asked participants enrolled after September 9, 2021, to identify the type of face covering typically worn in indoor public settings during the 2 weeks before seeking a SARS-CoV-2 test. Participants who indicated typically wearing multiple different mask types were categorized as wearing either a cloth mask (if they reported cloth mask use) or a surgical mask (if they didn't report cloth mask use).

† Conditional logistic regression models were used to estimate the unadjusted odds of mask use by type of face mask or respirator worn in indoor public settings during the 2 weeks before testing. Models included matching strata defined by the week of SARS-CoV-2 testing.

§ This analysis was not restricted to persons with no self-reported known or suspected SARS-CoV-2 contact given that this secondary analysis was underpowered upon exclusion of these participants (N = 316) because adjusted models did not converge. Instead, models adjusted for history of known or suspected contact as a covariate. In a sensitivity analysis restricting to participants who did not report known or suspected contact (N = 316), conditional logistic regression models were used to estimate that the unadjusted odds ratios of face mask use by type of face mask with matching strata defined by the week of SARS-CoV-2 testing: 0.13 (95% CI = 0.03–0.61), 0.32 (95% CI = 0.12–0.89), and 0.36 (95% CI = 0.13–1.00) for N95/KN95 respirators, surgical masks, or cloth masks, respectively, relative to no face mask or respirator use.

use of a clinical endpoint of SARS-CoV-2 test result, and applicability to a general population sample.

The findings in this report are subject to at least eight limitations. First, this study did not account for other preventive behaviors that could influence risk for acquiring infection, including adherence to physical distancing recommendations. In addition, generalizability of this study is limited to persons seeking SARS-CoV-2 testing and who were willing to participate in a telephone interview, who might otherwise exercise other protective behaviors. Second, this analysis relied on an aggregate estimate of self-reported face mask or respirator use across, for some participants, multiple indoor public locations. However, the study was designed to minimize recall bias by enrolling both case- and control-participants within a 48-hour window of receiving a SARS-CoV-2 test result. Third, small strata limited the ability to differentiate between types of cloth masks or participants who wore different types of face masks in differing settings, and also resulted in wider CIs and statistical nonsignificance for some estimates that were suggestive of a protective effect. Fourth, estimates do not account for face mask or respirator fit or the correctness of face mask or respirator wearing;

Summary

What is already known about this topic?

Face masks or respirators (N95/KN95s) effectively filter virus-sized particles in laboratory settings. The real-world effectiveness of face coverings to prevent acquisition of SARS-CoV-2 infection has not been widely studied.

What is added by this report?

Consistent use of a face mask or respirator in indoor public settings was associated with lower odds of a positive SARS-CoV-2 test result (adjusted odds ratio = 0.44). Use of respirators with higher filtration capacity was associated with the most protection, compared with no mask use.

What are the implications for public health practice?

In addition to being up to date with recommended COVID-19 vaccinations, consistently wearing a comfortable, well-fitting face mask or respirator in indoor public settings protects against acquisition of SARS-CoV-2 infection; a respirator offers the best protection.

assessing the effectiveness of face mask or respirator use under real-world conditions is nonetheless important for developing policy. Fifth, data collection occurred before the expansion of the SARS-CoV-2 B.1.1.529 (Omicron) variant, which is more transmissible than earlier variants. Sixth, face mask or respirator use was self-reported, which could introduce social desirability bias. Seventh, small strata limited the ability to account for reasons for testing in the adjusted analysis, which may be correlated with face mask or respirator use. Finally, this analysis does not account for potential differences in the intensity of exposures, which could vary by duration, ventilation system, and activity in each of the various indoor public settings visited.

The findings of this report reinforce that in addition to being up to date with recommended COVID-19 vaccinations, consistently wearing face masks or respirators while in indoor public settings protects against the acquisition of SARS-CoV-2 infection (*9*,*10*). This highlights the importance of improving access to high-quality masks to ensure access is not a barrier to use. Using a respirator offers the highest level of protection from acquisition of SARS-CoV-2 infection, although it is most important to wear a well-fitting mask or respirator that is comfortable and can be used consistently.

California COVID-19 Case-Control Study Team

Yasmine Abdulrahim, California Department of Public Health; Camilla M. Barbaduomo, California Department of Public Health; Miriam I. Bermejo, California Department of Public Health; Julia Cheunkarndee, California Department of Public Health; Adrian F. Cornejo, California Department of Public Health; Savannah Corredor, California Department of Public Health; Najla Dabbagh, California Department of Public Health; Zheng N. Dong, California Department of Public Health; Ashly Dyke, California Department of Public Health; Anna T. Fang, California Department of Public Health; Diana Felipe, California Department of Public Health; Paulina M. Frost, California Department of Public Health; Timothy Ho, California Department of Public Health; Mahsa H. Javadi, California Department of Public Health; Amandeep Kaur, California Department of Public Health; Amanda Lam, California Department of Public Health; Sophia S. Li, California Department of Public Health; Monique Miller, California Department of Public Health; Jessica Ni, California Department of Public Health; Hyemin Park, California Department of Public Health; Diana J. Poindexter, California Department of Public Health; Helia Samani, California Department of Public Health; Shrey Saretha, California Department of Public Health; Maya Spencer, California Department of Public Health; Michelle M. Spinosa, California Department of Public Health; Vivian H. Tran, California Department of Public Health; Nikolina Walas, California Department of Public Health; Christine Wan, California Department of Public Health; Erin Xavier California Department of Public Health.

Corresponding authors: Seema Jain, Seema.Jain@cdph.ca.gov; Kristin L. Andrejko, Kristin.Andrejko@cdph.ca.gov.

[1]Division of Epidemiology and Biostatistics, School of Public Health, University of California, Berkeley, California; [2]California Department of Public Health; [3]Division of Infectious Diseases & Vaccinology, School of Public Health, University of California, Berkeley, California; [4]Center for Computational Biology, College of Engineering, University of California, Berkeley, California.

All authors have completed and submitted the International Committee of Medical Journal Editors form for disclosure of potential conflicts of interest. Joseph A. Lewnard discloses receipt of research grants and consulting fees from Pfizer, Inc., unrelated to the current study. No other potential conflicts of interest were disclosed.

References

1. CDC. Science brief: community use of cloth masks to control the spread of SARS-CoV-2. Atlanta, GA: US Department of Health and Human Services, CDC; 2020. https://www.cdc.gov/coronavirus/2019-ncov/science/science-briefs/masking-science-sars-cov2.html
2. Pan J, Harb C, Leng W, Marr LC. Inward and outward effectiveness of cloth masks, a surgical mask, and a face shield. Aerosol Sci Technol 2021;55:718–33. https://doi.org/10.1080/02786826.2021.1890687
3. Brooks JT, Beezhold DH, Noti JD, et al. Maximizing fit for cloth and medical surgical masks to improve performance and reduce SARS-CoV-2 transmission and exposure, 2021. MMWR Morb Mortal Wkly Rep 2021;70:254–7. PMID:33600386 https://doi.org/10.15585/mmwr.mm7007e1
4. Howard J, Huang A, Li Z, et al. An evidence review of face masks against COVID-19. Proc Natl Acad Sci U S A 2021;118:e2014564118. PMID:33431650 https://doi.org/10.1073/pnas.2014564118
5. Lewnard JA, Patel MM, Jewell NP, et al. Theoretical framework for retrospective studies of the effectiveness of SARS-CoV-2 vaccines. Epidemiology 2021;32:508–17. PMID:34001753 https://doi.org/10.1097/EDE.0000000000001366
6. Brooks JT, Butler JC. Effectiveness of mask wearing to control community spread of SARS-CoV-2. JAMA 2021;325:998–9. PMID:33566056 https://doi.org/10.1001/jama.2021.1505
7. Chughtai AA, Seale H, Macintyre CR. Effectiveness of cloth masks for protection against severe acute respiratory syndrome coronavirus 2. Emerg Infect Dis 2020;26:e200948. PMID:32639930 https://doi.org/10.3201/eid2610.200948

8. Andrejko KL, Pry J, Myers JF, et al.; California COVID-19 Case-Control Study Team. Predictors of SARS-CoV-2 infection following high-risk exposure. Clin Infect Dis. Epub December 21, 2021. PMID:34932817 https://doi.org/10.1093/cid/ciab1040
9. California Department of Public Health. Guidance for the use of face masks. Sacramento, CA: California Department of Public Health. 2022. Accessed January 14, 2022. https://www.cdph.ca.gov/Programs/CID/DCDC/Pages/COVID-19/guidance-for-face-coverings.aspx
10. CDC. Use masks to slow the spread of COVID-19. Atlanta, GA: US Department of Health and Human Services, CDC; 2020. https://www.cdc.gov/coronavirus/2019-ncov/prevent-getting-sick/about-face-coverings.html

Readers who have difficulty accessing this PDF file may access the HTML file at https://www.cdc.gov/mmwr/volumes/71/wr/mm7106e1.htm?s_cid=mm7106e1_w. Address all inquiries about the *MMWR* Series, including material to be considered for publication, to Editor, *MMWR* Series, Mailstop V25-5, CDC, 1600 Clifton Rd., N.E., Atlanta, GA 30329-4027 or to mmwrq@cdc.gov.

ORIGINAL ARTICLE

Lifting Universal Masking in Schools — Covid-19 Incidence among Students and Staff

Tori L. Cowger, Ph.D., M.P.H., Eleanor J. Murray, Sc.D., M.P.H., Jaylen Clarke, M.Sc., Mary T. Bassett, M.D., M.P.H., Bisola O. Ojikutu, M.D., M.P.H., Sarimer M. Sánchez, M.D., M.P.H., Natalia Linos, Sc.D., and Kathryn T. Hall, Ph.D., M.P.H.

ABSTRACT

BACKGROUND

In February 2022, Massachusetts rescinded a statewide universal masking policy in public schools, and many Massachusetts school districts lifted masking requirements during the subsequent weeks. In the greater Boston area, only two school districts — the Boston and neighboring Chelsea districts — sustained masking requirements through June 2022. The staggered lifting of masking requirements provided an opportunity to examine the effect of universal masking policies on the incidence of coronavirus disease 2019 (Covid-19) in schools.

METHODS

We used a difference-in-differences analysis for staggered policy implementation to compare the incidence of Covid-19 among students and staff in school districts in the greater Boston area that lifted masking requirements with the incidence in districts that sustained masking requirements during the 2021–2022 school year. Characteristics of the school districts were also compared.

RESULTS

Before the statewide masking policy was rescinded, trends in the incidence of Covid-19 were similar across school districts. During the 15 weeks after the statewide masking policy was rescinded, the lifting of masking requirements was associated with an additional 44.9 cases per 1000 students and staff (95% confidence interval, 32.6 to 57.1), which corresponded to an estimated 11,901 cases and to 29.4% of the cases in all districts during that time. Districts that chose to sustain masking requirements longer tended to have school buildings that were older and in worse condition and to have more students per classroom than districts that chose to lift masking requirements earlier. In addition, these districts had higher percentages of low-income students, students with disabilities, and students who were English-language learners, as well as higher percentages of Black and Latinx students and staff. Our results support universal masking as an important strategy for reducing Covid-19 incidence in schools and loss of in-person school days. As such, we believe that universal masking may be especially useful for mitigating effects of structural racism in schools, including potential deepening of educational inequities.

CONCLUSIONS

Among school districts in the greater Boston area, the lifting of masking requirements was associated with an additional 44.9 Covid-19 cases per 1000 students and staff during the 15 weeks after the statewide masking policy was rescinded.

From the François–Xavier Bagnoud Center for Health and Human Rights, Harvard T.H. Chan School of Public Health (T.L.C., M.T.B., N.L.), the Boston Public Health Commission (T.L.C., E.J.M., J.C., B.O.O., S.M.S., K.T.H.), the Department of Epidemiology, School of Public Health, Boston University (E.J.M.), the Division of Infectious Diseases, Massachusetts General Hospital (B.O.O., S.M.S.), and Brigham and Women's Hospital and Harvard Medical School (B.O.O., K.T.H.) — all in Boston. Dr. Cowger can be contacted at vcowger@hsph.harvard.edu or at the François–Xavier Bagnoud Center for Health and Human Rights, Harvard T.H. Chan School of Public Health, 651 Huntington Ave., Boston, MA 02115.

This article was published on November 9, 2022, at NEJM.org.

DOI: 10.1056/NEJMoa2211029

The direct and indirect effects of the coronavirus disease 2019 (Covid-19) pandemic on children, their families, and surrounding communities have been substantial. By the end of February 2022, children and adolescents in the United States had a higher prevalence of infection with severe acute respiratory syndrome coronavirus 2 (SARS-CoV-2) than any other age group; children with Covid-19 are at risk for severe acute complications, death, and long-term sequelae (known as long Covid or post-Covid conditions).[1-4] Furthermore, by the end of September 2022, more than 265,000 children and adolescents in the United States had had a parent or caregiver die from Covid-19,[5,6] and the pandemic had caused substantial interruptions in school settings — including staffing shortages, closures, and missed school days — and had deepened educational inequities.[7,8] These effects have been disproportionately borne by groups already made vulnerable by historical and contemporary systems of oppression, including structural racism and settler colonialism.[9-11] Black, Latinx, and Indigenous children and adolescents are more likely to have had severe Covid-19, to have had a parent or caregiver die from Covid-19, and to be affected by worsening mental health and by educational disruptions than their White counterparts.[6,8,12,13]

During the Covid-19 pandemic, schools have become an important setting for implementing policies that minimize inequitable health, educational, social, and economic effects on children and their families. However, even before the pandemic, schools were not uniformly health-promoting environments. Chronic underinvestment in combination with structural racism codified in state-sanctioned historical and contemporary policies and practices (e.g., redlining, exclusionary zoning, disinvestment, and gentrification) eroded tax bases in some school districts and shaped the quality of public school infrastructure and associated environmental hazards.[10,14-19] These processes left school districts differentially equipped to respond to the Covid-19 pandemic and concentrated high-risk conditions, such as crowded classrooms and poor indoor air quality due to outdated or absent ventilation or filtration systems, in low-income and Black, Latinx, and Indigenous communities.[14,18,19]

Alongside other measures, universal masking with high-quality masks or respirators has been an important piece of a layered risk-mitigation strategy to reduce the transmission of SARS-CoV-2 in community and school settings below levels that have been observed with individual (optional) masking.[20-31] Massachusetts was among the 18 states plus Washington, DC, that had a universal masking policy in public schools during the 2021–2022 school year.[32] The Massachusetts Department of Elementary and Secondary Education (DESE) rescinded the statewide masking policy on February 28, 2022, in accordance with updated guidance from the Centers for Disease Control and Prevention (CDC), and many Massachusetts school districts lifted masking requirements during the subsequent weeks. In the greater Boston area, only two school districts — the Boston and neighboring Chelsea districts — sustained masking requirements through June 2022.

The staggered lifting of masking requirements provided an opportunity to examine the potential effect of universal masking policies in schools. Specifically, this study aimed to assess trends in the observed weekly incidence of Covid-19 according to the length of time that school districts sustained masking requirements; to compare the incidence of Covid-19 among students and staff in districts that lifted masking requirements with the incidence in districts that sustained masking requirements in a given reporting week in order to estimate the effect of lifting masking requirements; and to compare school-district characteristics in districts that chose to sustain masking requirements longer with the characteristics in districts that chose to lift masking requirements earlier.

METHODS

STUDY POPULATION

This study considered the 79 public, noncharter school districts in the greater Boston area, defined according to the U.S. Census Bureau as the New England city and town area of Boston–Cambridge–Newton (Fig. S1 in the Supplementary Appendix, available with the full text of this article at NEJM.org). Of these 79 school districts, 7 with unreliable or missing Covid-19 data were excluded (Table S1). The final sample included 72 school districts, which comprised 294,084 students and 46,530 staff during the study period. The study period was defined as the 40 calendar weeks of the 2021–2022 school year, which ended

on June 15, 2022 (the end of the last full reporting week in all districts).

INTERVENTION AND PRIMARY OUTCOME

The primary exposure variable was whether a school district lifted or sustained its masking requirement in each reporting week. For all school districts, masking requirements were in place from the start of the study period through February 28, 2022, when the statewide masking policy was rescinded. A school district was considered to have lifted its masking requirement in a given reporting week if the requirement had been lifted before the first day of the reporting week (reporting weeks start on Thursday). The primary outcome was the incidence of Covid-19 among students and staff, considered together and separately.

DATA SOURCES

For each school district, data regarding weekly Covid-19 cases, student enrollment, and staffing during the 2021–2022 school year were publicly available from the Massachusetts DESE.[33,34] Throughout the study period, DESE required standardized weekly reporting of all positive tests for Covid-19 among students and staff, regardless of symptoms, testing type or program (e.g., testing of symptomatic persons or pooled polymerase-chain-reaction testing), and testing location (community setting or school setting). Details regarding DESE reporting requirements are provided in the Supplementary Appendix. DESE strongly encouraged, and provided full funding for, school districts to opt in to standardized Covid-19 testing programs; 2311 Massachusetts schools (approximately 95%) participated in at least one such program. From 1 month before the statewide masking policy was rescinded through the end of the school year, statewide testing recommendations did not differ according to masking or vaccination status (Table S2).[35]

The dates during which masking requirements were in place for each school district were obtained from school-district websites or local news sources. For sensitivity analyses, data to be used for covariate adjustments, including data regarding Covid-19 indicators (i.e., measures of Covid-19 burden) according to city and town and Covid-19 vaccination coverage according to age, were publicly available from the Massachusetts Department of Public Health. For descriptive analyses, data regarding the distribution of students and staff according to sociodemographic characteristics and the distribution of students in populations selected and defined by DESE (low-income students, students with disabilities, and English-language learner [ELL] students) during the 2021–2022 school year were obtained from DESE.[34] In addition, data regarding building conditions and learning environment were obtained from the Massachusetts School Building Authority 2016–2017 school survey (most recent data).[36]

CONTRIBUTIONS

The first, second, and last authors wrote the first draft of the manuscript and vouch for the accuracy and completeness of the data and the fidelity of the study to the protocol, available at NEJM.org. All the authors reviewed and edited the draft and made the decision to submit the manuscript for publication. No external funding was received for this study.

STATISTICAL ANALYSIS

Trends in the observed incidence of Covid-19 (weekly Covid-19 cases per 1000 population) before the statewide masking policy was rescinded were compared with trends after the policy was rescinded according to the length of time that school districts sustained masking requirements. A difference-in-differences analysis for staggered policy implementation was used to compare the incidence of Covid-19 in school districts that lifted masking requirements with the incidence in districts that sustained masking requirements in a given reporting week (i.e., school districts that had not yet lifted masking requirements) in order to estimate the effect of lifting masking requirements.[37,38]

Difference-in-differences methods allow for the estimation of causal effects of policy changes enacted at the group level by comparing the change in the outcome over time in the intervention group with the change in the control group, under an assumption of parallel trends (i.e., in the absence of the intervention, outcomes in the intervention group and the control group would have remained parallel over time).[37,39] Unlike some observational methods, difference-in-differences methods are not biased by unmeasured time-invariant confounders or time-varying confounders with consistent trends across the intervention

and control groups; the absence of such bias strengthens causal inferences. In this analysis, the weekly and cumulative effects of lifting masking requirements during the 15 weeks after the statewide masking policy was rescinded were estimated with respect to the incidence of Covid-19 cases in school districts that lifted masking requirements (i.e., the average [mean] treatment effect among the treated). Details regarding the difference-in-differences analysis are provided in the Supplementary Appendix.

Several sensitivity analyses were performed: a formal test for parallel trends before masking requirements were lifted; adjustment for time-varying covariates, including Covid-19 indicators at the community level, vaccination coverage, and previous incidences of infection among students and staff; and an assessment of the potential effects of differences in testing definitions or programs across districts (Tables S3 and S4). In the main analysis, data for the weeks in which school districts did not report Covid-19 cases were corrected (these weeks were originally recorded as having zero cases), all school districts in the greater Boston area were included as comparison districts, and weighting according to school population size was performed to capture the effect of masking policies at the population level.

Finally, to provide insight into Covid-19 policy decisions in schools and their potential to exacerbate or mitigate inequities in Covid-19 incidence and educational outcomes, descriptive analyses were performed. The decision to sustain or lift masking requirements was assessed according to various school-district characteristics, including sociodemographic characteristics of the students and staff and physical characteristics of the learning environment.

RESULTS

PRIMARY ANALYSIS

Of the 72 school districts in the greater Boston area that were included in the study, only Boston Public Schools and Chelsea Public Schools sustained masking requirements throughout the study period (Fig. S2A). Of the remaining school districts, 46 districts (64%) lifted masking requirements in the first reporting week after the statewide masking policy was rescinded, 17 (24%) lifted masking in the second reporting week, and 7 (10%) lifted masking in the third reporting week (Fig. S2B). Cumulatively, 46 districts lifted masking requirements and 26 districts sustained masking requirements by the first reporting week after the policy was rescinded, 63 lifted and 9 sustained masking by the second reporting week, and 70 lifted and 2 sustained masking thereafter.

Before the statewide masking policy was rescinded, the trends in the incidence of Covid-19 observed in the Boston and Chelsea districts were similar to the trends in school districts that later lifted masking requirements. However, after the statewide masking policy was rescinded, the trends in the incidence of Covid-19 diverged, with a substantially higher incidence observed in school districts that lifted masking requirements than in school districts that sustained masking requirements. These trends were observed among students and staff overall (Fig. 1A), as well as among students alone (Fig. 1B) and among staff alone (Fig. 1C).

Figure 2 shows difference-in-differences estimates of additional weekly and cumulative Covid-19 cases associated with the lifting of masking requirements. Before masking requirements were lifted, difference-in-differences estimates were essentially zero, a finding that supports the assumption of parallel trends. After masking requirements were lifted, the lifting of masking requirements was consistently associated with additional Covid-19 cases. The effect was significant during 12 of the 15 weeks after masking requirements were lifted. Weekly estimates ranged from 1.4 additional cases per 1000 students and staff (95% confidence interval [CI], 0.6 to 2.3) in the first reporting week after masking requirements were lifted to 9.7 additional cases per 1000 students and staff (95% CI, 7.1 to 12.3) in the ninth reporting week.

The strength of the association between school masking policies and the incidence of Covid-19 in school districts varied according to the incidence of Covid-19 in surrounding communities; the strongest associations were observed during the weeks when the incidences in surrounding communities were highest (Figs. S3 and S4). The weekly effects that were observed among students and staff overall were similar to those observed among students alone and those observed among staff alone, with slightly greater effects observed among staff than among students.

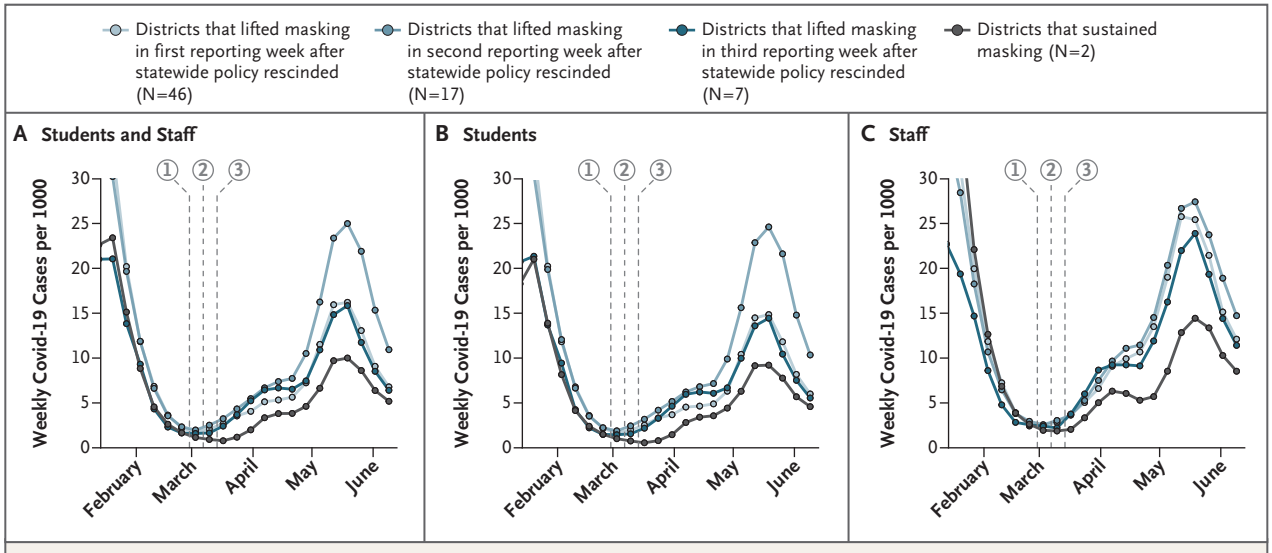

Figure 1. Incidence of Covid-19 in School Districts in the Greater Boston Area before and after the Statewide Masking Policy Was Rescinded.

The observed incidence of coronavirus disease 2019 (Covid-19) (weekly Covid-19 cases per 1000 population) among students and staff overall (Panel A), among students alone (Panel B), and among staff alone (Panel C) is shown for the 72 school districts in the greater Boston area that were included in the study. The greater Boston area was defined according to the U.S. Census Bureau as the New England city and town area of Boston–Cambridge–Newton. The Massachusetts Department of Elementary and Secondary Education rescinded the statewide masking policy on February 28, 2022. The incidence is shown according to whether the school district lifted its masking requirement in the first, second, or third reporting week after the statewide masking policy was rescinded or the district sustained its masking requirement. A school district was considered to have lifted its masking requirement in a given reporting week if the requirement had been lifted before the first day of the reporting week (reporting weeks start on Thursday). The dashed lines indicate the first (1), second (2), and third (3) school weeks (school weeks start on Monday) during which school districts lifted masking requirements. A total of 46 school districts lifted masking requirements during the first school week (starting on February 28, 2022) and in the first reporting week (starting on March 3, 2022) after the statewide masking policy was rescinded; 17 districts lifted masking requirements during the second school week (starting on March 7, 2022) and in the second reporting week (starting on March 10, 2022); 7 districts lifted masking requirements during the third school week (starting on March 14, 2022) and in the third reporting week (starting on March 17, 2022); and 2 districts sustained masking requirements. Data points are shown on the first day of the reporting week and represent 3-week trailing rolling averages to reduce statistical noise. Dates on the x axis are restricted to the period immediately before and after the statewide masking policy was rescinded.

In addition, the weekly effects were consistent with the cumulative effects.

Overall, the lifting of masking requirements was associated with an additional 44.9 Covid-19 cases per 1000 students and staff (95% CI, 32.6 to 57.1) during the 15 weeks after the statewide masking policy was rescinded (Table 1). This estimate corresponded to an additional 11,901 Covid-19 cases (95% CI, 8651 to 15,151), which accounted for 33.4% of the cases (95% CI, 24.3 to 42.5) in school districts that lifted masking requirements and for 29.4% of the cases (95% CI, 21.4 to 37.5) in all school districts during that period. The effect was more pronounced among staff. The lifting of masking requirements was associated with an additional 81.7 Covid-19 cases per 1000 staff (95% CI, 59.3 to 104.1) during the 15-week period, with these cases accounting for 40.4% of the cases (95% CI, 29.4 to 51.5) among staff in school districts that lifted masking requirements. Because persons who had a positive test for Covid-19 were instructed to isolate for at least 5 days, the additional cases translated to a minimum of approximately 17,500 missed school days for students and 6500 missed school days for staff during the 15-week period (Table S5).

SENSITIVITY ANALYSES

The results were shown to be robust in a range of sensitivity analyses, including analyses that assessed potential differences in testing programs and analyses that adjusted for Covid-19 indicators at the community level and vaccination coverage according to age (Fig. S5). Results of sensitivity

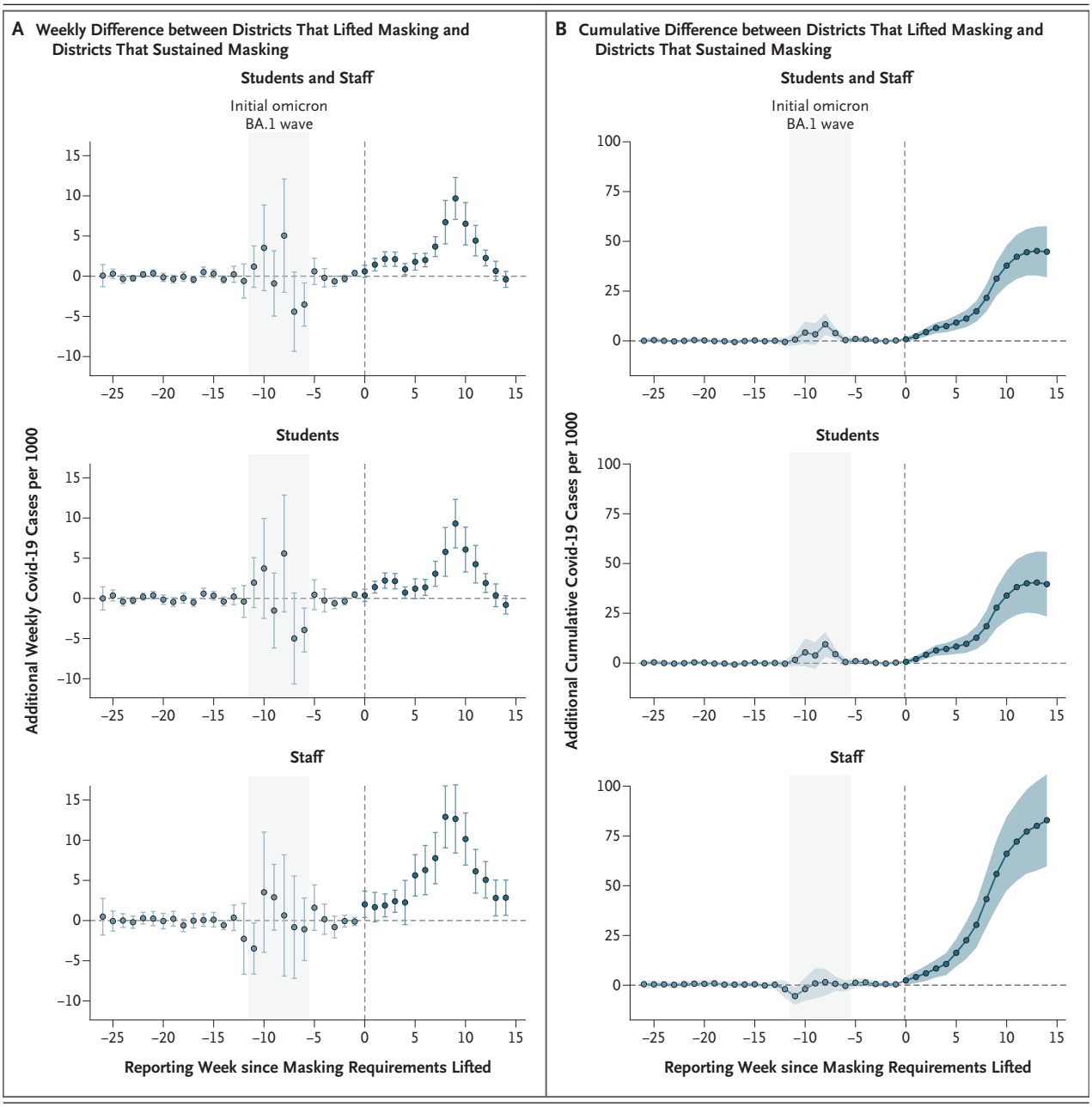

analyses are provided in the Supplementary Appendix.

DESCRIPTIVE ANALYSES

School districts that chose to sustain masking requirements longer had higher percentages of low-income students, students with disabilities, and ELL students (Fig. 3A), as well as higher percentages of Black and Latinx students (Fig. 3B) and Black and Latinx staff (Fig. 3C), than school districts that chose to lift masking requirements earlier. In addition, school districts that chose to sustain masking requirements longer tended to have school buildings that were older and in worse physical condition (e.g., with outdated or absent ventilation or filtration systems) and to have more students per classroom (Fig. 3D).

DISCUSSION

Schools are an important yet politically contested space in the Covid-19 response, which makes

Figure 2 (facing page). Difference-in-Differences Estimates of Additional Weekly and Cumulative Covid-19 Cases Associated with the Lifting of Masking Requirements.

Difference-in-differences models were used to estimate the difference in the change in the incidence of Covid-19 between school districts that lifted masking requirements and school districts that sustained masking requirements in each reporting week among students and staff overall, among students alone, and among staff alone, with estimates calculated on a weekly basis (Panel A) and on a cumulative basis (Panel B). I bars and blue shading indicate 95% confidence intervals for weekly and cumulative differences, respectively. Estimates are shown according to reporting weeks since masking requirements were lifted. Vertical dashed lines indicate the first reporting week in which masking requirements were lifted in each school district; because the reporting week in which masking requirements were lifted varied according to district, the vertical dashed lines represent different calendar weeks for different school districts, depending on when masking requirements were lifted. Values in light blue and dark blue show differences during the reporting weeks before and after masking requirements were lifted, respectively. Horizontal dashed lines correspond to no difference; values above the line show additional Covid-19 cases. Gray shading indicates the initial period of peak infection with the BA.1 subvariant of the B.1.1.529 (omicron) variant (December 2021 through January 2022). Details regarding the difference-in-differences analysis are provided in the Supplementary Appendix.

analyses such as this one particularly relevant to decision makers. We estimated that the lifting of masking requirements in school districts in the greater Boston area during March 2022 contributed an additional 45 Covid-19 cases per 1000 students and staff during the following 15-week period. Overall, this estimate corresponded to nearly 12,000 additional Covid-19 cases among students and staff, which accounted for one third of the cases in school districts that lifted masking requirements during that time and most likely translated to substantial loss of in-person school days.

We observed that the effect of school masking policies was greatest during the weeks when the background incidences of Covid-19 in surrounding cities and towns were highest, a finding that suggests that universal masking policies may be most effective when they are implemented before and throughout periods of high SARS-CoV-2 transmission. Under the CDC guidance at that time, as well as the updated guidance issued in August 2022, universal masking would not have been recommended until the incidences of Covid-19 in schools and surrounding communities were already nearing their peak (May 2022); by this time, a substantial proportion of the effects of masking polices that we observed had already accrued. As such, relying on lagging metrics such as CDC Covid-19 Community Levels and Covid-19 hospitalizations to inform school masking policies is most likely insufficient to prevent Covid-19 cases and loss of in-person school days, and policymakers might instead consider measures of community transmission (e.g., SARS-CoV-2 wastewater concentration or Covid-19 incidence) to inform such policies.

Understanding Covid-19 policy decisions requires attention to power and existing historical and sociopolitical contexts.[10,40] Structural racism and racial capitalism operate through multiple pathways, including higher levels of household crowding and employment in essential industries and lower levels of access to testing, vaccines, and treatment; these structural forces differentially concentrate the risk of both SARS-CoV-2 exposure and severe Covid-19 in low-income and Black, Latinx, and Indigenous communities.[9-11,18] In our study, school districts that chose to sustain masking requirements longer tended to have school buildings in worse physical condition and more students per classroom, and these districts had higher percentages of students and staff already made vulnerable by historical and contemporary systems of oppression (e.g., racism, capitalism, xenophobia, and ableism). In Boston and Chelsea, more than 80% of the students are Black, Latinx, or people of color, and these cities were among the Massachusetts cities and towns that were hit hardest by Covid-19. Students and families in these school districts have strongly advocated and organized for governmental action to increase Covid-19 protections in schools, emphasizing their role as essential workers, the risk to vulnerable family members, and the unequal consequences of missed work and school.[41,42] The decision in some school districts to sustain school masking policies longer may therefore reflect an understanding among parents and elected officials that structural racism is embedded in public policies and that policy decisions have the potential to rectify or reproduce health inequities.[10,14,16,40]

A growing body of work suggests that knowledge of differential conditions and inequitable effects may decrease support for Covid-19 pro-

Table 1. Cumulative Incidence of Covid-19 and Estimated Effect of Lifting Masking Requirements during the 15 Weeks after the Statewide Masking Policy Was Rescinded.*

Population†	Cumulative Covid-19 Cases during the 15-Week Period						Difference-in-Differences Estimates of Covid-19 Cases Associated with the Lifting of Masking Requirements during the 15-Week Period			
	All Districts		Districts That Lifted Masking Requirements		Districts That Sustained Masking Requirements		No. of Additional Cases per 1000 (95% CI)‡	No. of Additional Cases (95% CI)§	Percentage of Cases in Districts That Lifted Masking Requirements (95% CI)¶	Percentage of Cases in All Districts (95% CI)‖
	no. of cases	*no. of cases per 1000*	*no. of cases*	*no. of cases per 1000*	*no. of cases*	*no. of cases per 1000*				
Students and staff	40,416	119.8	35,651	134.4	4,766	66.1	44.9 (32.6–57.1)	11,901 (8651–15,151)	33.4 (24.3–42.5)	29.4 (21.4–37.5)
Students	32,198	110.6	28,524	124.1	3,674	60.0	39.9 (24.3–55.4)	9,168 (5594–12,743)	32.1 (19.6–44.7)	28.5 (17.4–39.6)
Staff	8,218	178.4	7,127	202.1	1,091	101.0	81.7 (59.3–104.1)	2,882 (2092–3673)	40.4 (29.4–51.5)	35.1 (25.5–44.7)

* The Massachusetts Department of Elementary and Secondary Education rescinded the statewide masking policy on February 28, 2022. Details regarding the difference-in-differences analysis are provided in the Supplementary Appendix. Covid-19 denotes coronavirus disease 2019.

† The study included a total of 340,614 students and staff (294,084 students and 46,530 staff) across 72 school districts. The number of districts that lifted masking requirements and the number of districts that sustained masking requirements varied according to reporting week; the mean population per week during the 15-week period was 265,173 students and staff (229,899 students and 35,274 staff) in districts that lifted masking requirements and was 72,053 students and staff (61,250 students and 10,803 staff) in districts that sustained masking requirements. The sum of these mean populations per week does not equal the total study population because of the exclusion of less than 1% of person-weeks (see the Supplementary Appendix).

‡ A difference-in-differences model was used to estimate the cumulative average treatment effect among the treated during the 15-week period. The number of additional Covid-19 cases per 1000 population that were associated with the lifting of masking requirements was estimated by calculating the difference between the observed number of Covid-19 cases per 1000 population in districts that lifted masking requirements and the expected number of Covid-19 cases per 1000 population if masking requirements had been sustained during the 15 weeks after the statewide masking policy was rescinded.

§ The number of additional Covid-19 cases that were associated with the lifting of masking requirements was estimated by multiplying the number of additional Covid-19 cases per 1000 population that were associated with the lifting of masking requirements (from the difference-in-differences model) by the mean population per 1000 in school districts that lifted masking requirements.

¶ The percentage of Covid-19 cases in school districts that lifted masking requirements that were associated with the lifting of masking requirements was estimated by dividing the number of additional Covid-19 cases per 1000 population that were associated with the lifting of masking requirements (from the difference-in-differences model) by the observed number of Covid-19 cases per 1000 population in school districts that lifted masking requirements.

‖ The percentage of Covid-19 cases in all school districts that were associated with the lifting of masking requirements was estimated by dividing the number of additional Covid-19 cases that were associated with the lifting of masking requirements by the observed number of Covid-19 cases in all school districts.

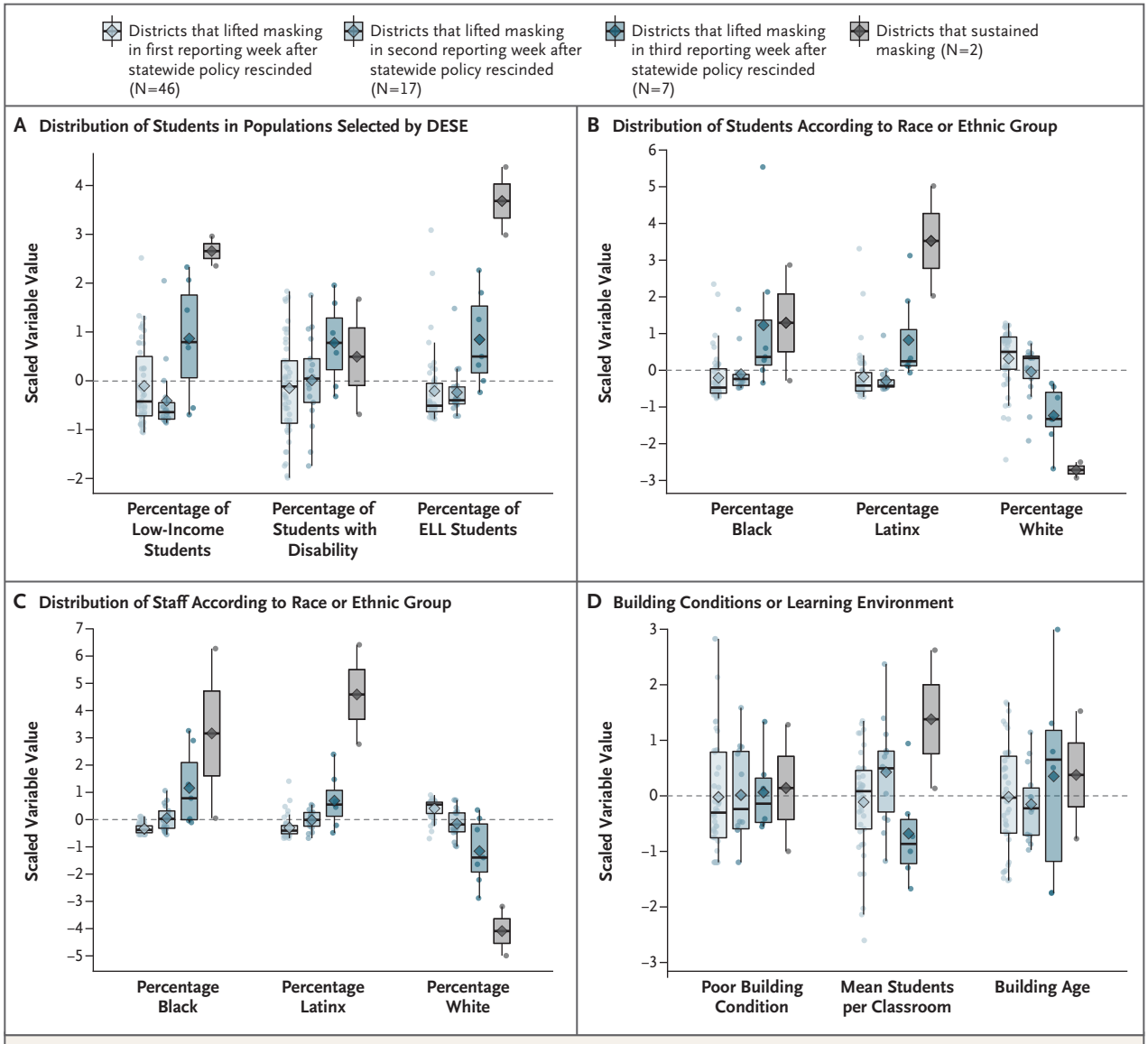

Figure 3. Characteristics of the School Districts.

Data regarding the following school-district characteristics are shown: distribution of students in populations selected and defined by the Massachusetts Department of Elementary and Secondary Education (DESE), including low-income students, students with disabilities, and English-language learner (ELL) students (Panel A); distribution of students according to race or ethnic group (Panel B); distribution of staff according to race or ethnic group (Panel C); and scores for building conditions and learning environment (Panel D). The data are shown in scaled variable values so that all variables can be depicted on the same scale; the scaled variable value reflects the difference from the mean value in standard deviations. Dashed lines indicate the mean value across all school districts. Dots indicate values for individual school districts. In the box plots, horizontal bars indicate the median value, boxes the interquartile range, whiskers the value 1.5 times the interquartile range, and diamonds the mean value. Data are plotted according to whether the school district had chosen to lift its masking requirement in the first, second, or third reporting week after the statewide masking policy was rescinded or the district had chosen to sustain its masking requirement. The data shown in Panels A, B, and C are for the 2021–2022 school year and were obtained from DESE.[34] The data shown in Panel D were obtained from the Massachusetts School Building Authority 2016–2017 school survey (most recent data).[36]

tections among systematically advantaged groups, whose relative position largely insulates them from Covid-19 harms, while simultaneously increasing support among groups that are directly affected by systems of oppression.[43-45] For example, in a randomized trial in which White persons were

assigned to receive information about structural causes of persistent Covid-19 inequities across racial or ethnic groups or to not receive such information, those who received the information were less likely to support Covid-19 prevention policies and were less likely to report individual concern about Covid-19 and empathy for the groups that were most affected.[45] In several studies and polls, Black and Latinx parents were more likely than White parents to support school masking requirements and less likely to have confidence that schools could operate safely without additional protections.[43,44,46] Failure to consider unequal baseline conditions and ongoing inequitable effects of Covid-19 policies risks further exacerbating inequities in Covid-19 incidence and educational outcomes.

Because universal masking policies in schools have been contentious, we anticipate several critiques. One such critique is that the benefits of universal masking in schools are outstripped by potential disruptions to teaching, learning, and social development. These effects warrant further rigorous evaluation; however, to date, there is no clear existing evidence that masking inhibits learning or harms development.[47,48] In addition, such effects might be considered alongside the spectrum of benefits of universal masking, including fewer missed school days and staffing shortages, reduced risk of illness for students and their families, and reduced economic hardship for caregivers, who might miss work if their child is sick or if they become ill themselves. For example, in Lexington, MA, a comparison district approximately 10 miles from Boston, mean student and staff absences due to Covid-19 during weeks when masking was optional were 50% higher than absences during previous weeks, when masking was required (see the Supplementary Appendix).

In addition, severe Covid-19 and post-Covid conditions remain substantial risks among school-age children. Like much of the United States, the greater Boston area has low Covid-19 vaccination coverage among children (only 53% of children 5 to 11 years of age had been fully vaccinated in Boston and Chelsea through October 2022, as compared with 67% in comparison districts), with substantial inequities according to race or ethnic group and socioeconomic status. Furthermore, we observed greater benefits of sustaining masking among staff, a finding that emphasizes that universal masking is an important component of comprehensive workplace protections for staff, who may be at a higher risk for severe Covid-19 than students. In addition, staff absences may be especially consequential for students who need additional educational supports and services, including ELL students and students with disabilities.

A second common critique is that there are alternative approaches to reducing transmission and severe disease, such as improved ventilation and increased vaccination coverage. Our findings show that the better ventilation and higher vaccination coverage in school districts that lifted masking requirements than in districts that sustained masking requirements were insufficient to prevent all Covid-19 cases in these schools. Therefore, although we cannot weigh the full spectrum of individual and societal implications of masking policies, our study highlights the important role of interim universal school masking policies in mitigating the effects of Covid-19 while longer-term, more sustainable policies are developed to increase vaccination uptake and improve learning environments.

A key strength of this study is our use of difference-in-differences methods with staggered dates of the lifting of masking requirements. Although there are some factors related to SARS-CoV-2 exposure that differed across school districts, difference-in-differences methods yield robust analyses in the context of sources of confounding that do not change over time (e.g., sociodemographic characteristics or building conditions) or do not coincide with the policy change of interest. In sensitivity analyses, the benefits of masking requirements persisted after we controlled for Covid-19 indicators at the community level, vaccination coverage, and previous incidence of infection. Furthermore, we found that school districts that lifted masking requirements were districts that would have been expected to have lower incidences of Covid-19 (on average, they had buildings in better physical condition and had higher vaccination coverage), which suggests that any residual confounding by Covid-19 risk would have led to underestimation of the harms of lifting masking requirements overall.

A limitation of this study is that we did not have data regarding Covid-19 testing in individual school districts. However, DESE ended the practice of required testing of only unmasked close

contacts in January 2022, and data from that "test-and-stay" program show that far too few schools continued with the program for it to explain our results. Under the most extreme assumptions, additional testing of unmasked close contacts could explain less than 7% of the estimated excess cases. Overall, our findings should be interpreted as the effect of universal masking policies and not as the effect of masking per se, since masks were still encouraged in most school settings. Despite this consideration, the effect of lifting masking requirements was substantial.

The winter wave of the B.1.1.529 (omicron) variant during the 2021–2022 school year will not be the final Covid-19 surge to affect students and staff, and ongoing efforts to address inequitable environmental risks and effects of Covid-19 in school settings are urgently needed. Our results support that universal masking with high-quality masks or respirators during periods of high community transmission is an important strategy for minimizing SARS-CoV-2 spread and loss of in-person school days. Our results also suggest that universal masking may be an important tool for mitigating the effects of structural racism in schools, including the differential risk of severe Covid-19, educational disruptions, and health and economic effects of secondary transmission to household members. School districts could use these findings to develop equitable mitigation plans in anticipation of a potential winter Covid-19 wave during the 2022–2023 school year, as well as clear decision thresholds for removing masks as the wave abates.

Disclosure forms provided by the authors are available with the full text of this article at NEJM.org.

We thank the Boston Public Schools staff and leadership and the nurses and team within Boston Public Schools Health Services for their role in protecting our Boston children and families; and Dr. Brigette Davis and Dr. Jourdyn Lawrence for their critical review and feedback on earlier drafts of this work.

REFERENCES

1. Clarke KEN, Jones JM, Deng Y, et al. Seroprevalence of infection-induced SARS-CoV-2 antibodies — United States, September 2021–February 2022. MMWR Morb Mortal Wkly Rep 2022;71:606-8.
2. Miller AD, Yousaf AR, Bornstein E, et al. Multisystem inflammatory syndrome in children (MIS-C) during SARS-CoV-2 delta and omicron variant circulation — United States, July 2021–January 2022. Clin Infect Dis 2022;75:Suppl 2:S303-S307.
3. Centers for Disease Control and Prevention. Long COVID or post-COVID conditions. September 1, 2022 (https://www.cdc.gov/coronavirus/2019-ncov/long-term-effects/index.html).
4. Kompaniyets L, Bull-Otterson L, Boehmer TK, et al. Post-COVID-19 symptoms and conditions among children and adolescents — United States, March 1, 2020–January 31, 2022. MMWR Morb Mortal Wkly Rep 2022;71:993-9.
5. Imperial College London. COVID-19 orphanhood. 2022 (https://imperialcollegelondon.github.io/orphanhood_calculator/#/country/United%20States%20of%20America).
6. Hillis SD, Blenkinsop A, Villaveces A, et al. COVID-19-associated orphanhood and caregiver death in the United States. Pediatrics 2021 October 7 (Epub ahead of print).
7. Parks SE, Zviedrite N, Budzyn SE, et al. COVID-19-related school closures and learning modality changes — United States, August 1–September 17, 2021. MMWR Morb Mortal Wkly Rep 2021;70:1374-6.
8. Nunez-Smith M, COVID-19 Health Equity Task Force. Presidential COVID-19 Health Equity Task Force — final report and recommendations. Department of Health and Human Services, October 2021 (https://www.minorityhealth.hhs.gov/assets/pdf/HETF_Report_508_102821_9am_508Team%20WIP11.pdf).
9. Laster Pirtle WN. Racial capitalism: a fundamental cause of novel coronavirus (COVID-19) pandemic inequities in the United States. Health Educ Behav 2020;47:504-8.
10. Bailey ZD, Moon JR. Racism and the political economy of COVID-19: will we continue to resurrect the past? J Health Polit Policy Law 2020;45:937-50.
11. Emerson MA, Montoya T. Confronting legacies of structural racism and settler colonialism to understand COVID-19 impacts on the Navajo Nation. Am J Public Health 2021;111:1465-9.
12. Shi DS, Whitaker M, Marks KJ, et al. Hospitalizations of children aged 5–11 years with laboratory-confirmed COVID-19 — COVID-NET, 14 States, March 2020–February 2022. MMWR Morb Mortal Wkly Rep 2022;71:574-81.
13. Xiao Y, Yip PS-F, Pathak J, Mann JJ. Association of social determinants of health and vaccinations with child mental health during the COVID-19 pandemic in the US. JAMA Psychiatry 2022;79:610-21.
14. Neal DE. Healthy schools: a major front in the fight for environmental justice. Environ Law 2008;38:473-93.
15. Wilson S, Hutson M, Mujahid M. How planning and zoning contribute to inequitable development, neighborhood health, and environmental injustice. Environ Justice 2008;1:211-6.
16. Bailey ZD, Krieger N, Agénor M, Graves J, Linos N, Bassett MT. Structural racism and health inequities in the USA: evidence and interventions. Lancet 2017;389:1453-63.
17. Bullard RD, Wright BH. Environmental justice for all: community perspectives on health and research needs. Toxicol Ind Health 1993;9:821-41.
18. Kitzmiller EM, Drake Rodriguez A. Addressing our nation's toxic school infrastructure in the wake of COVID-19. Educ Res 2022;51:88-92.
19. Pastor M Jr, Sadd JL, Morello-Frosch R. Who's minding the kids? Pollucion, public schools, and environmental justice in Los Angeles. Soc Sci Q 2002;83:263-80.
20. Wiens KE, Smith CP, Badillo-Goicoechea E, et al. In-person schooling and associated COVID-19 risk in the United States over spring semester 2021. Sci Adv 2022;8(16):eabm9128.
21. Lessler J, Grabowski MK, Grantz KH, et al. Household COVID-19 risk and in-person schooling. Science 2021;372:1092-7.
22. Gettings J, Czarnik M, Morris E, et al. Mask use and ventilation improvements to reduce COVID-19 incidence in elementary schools — Georgia, November 16–December 11, 2020. MMWR Morb Mortal Wkly Rep 2021;70:779-84.
23. Falk A, Benda A, Falk P, Steffen S, Wallace Z, Høeg TB. COVID-19 cases and transmission in 17 K–12 schools — Wood County, Wisconsin, August 31–November

29, 2020. MMWR Morb Mortal Wkly Rep 2021;70:136-40.
24. Boutzoukas AE, Zimmerman KO, Inkelas M, et al. School masking policies and secondary SARS-CoV-2 transmission. Pediatrics 2022;149(6):e2022056687.
25. Andrejko KL, Pry J, Myers JF, et al. Predictors of severe acute respiratory syndrome coronavirus 2 infection following high-risk exposure. Clin Infect Dis 2022; 75(1):e276-e288.
26. Andrejko KL, Pry JM, Myers JF, et al. Effectiveness of face mask or respirator use in indoor public settings for prevention of SARS-CoV-2 infection — California, February–December 2021. MMWR Morb Mortal Wkly Rep 2022;71:212-6.
27. Budzyn SE, Panaggio MJ, Parks SE, et al. Pediatric COVID-19 cases in counties with and without school mask requirements — United States, July 1–September 4, 2021. MMWR Morb Mortal Wkly Rep 2021;70:1377-8.
28. Jehn M, McCullough JM, Dale AP, et al. Association between K–12 school mask policies and school-associated COVID-19 outbreaks — Maricopa and Pima counties, Arizona, July–August 2021. MMWR Morb Mortal Wkly Rep 2021;70:1372-3.
29. Donovan CV, Rose C, Lewis KN, et al. SARS-CoV-2 incidence in K–12 school districts with mask-required versus mask-optional policies — Arkansas, August–October 2021. MMWR Morb Mortal Wkly Rep 2022;71:384-9.
30. Murray TS, Malik AA, Shafiq M, et al. Association of child masking with COVID-19-related closures in US child-care programs. JAMA Netw Open 2022; 5(1):e2141227.
31. Bagheri G, Thiede B, Hejazi B, Schlenczek O, Bodenschatz E. An upper bound on one-to-one exposure to infectious human respiratory particles. Proc Natl Acad Sci U S A 2021;118(49): e2110117118.
32. Decker S. Which states banned mask mandates in schools, and which required masks? EducationWeek. July 8, 2022 (updated date) (https://www.edweek.org/policy-politics/which-states-ban-mask-mandates-in-schools-and-which-require-masks/2021/08).
33. Massachusetts Department of Elementary and Secondary Education. Positive COVID-19 cases in schools. State Library of Massachusetts (https://archives.lib.state.ma.us/handle/2452/833423).
34. Massachusetts Department of Elementary and Secondary Education. School and district profiles — statewide reports (https://profiles.doe.mass.edu/state_report/).
35. Massachusetts Department of Elementary and Secondary Education. Memorandum: DESE/DPH protocols for responding to COVID-19 scenarios — SY 2021–22. State Library of Massachusetts, January 5, 2022 (https://archives.lib.state.ma.us/handle/2452/852221).
36. Massachusetts School Building Authority. 2016 School survey report. 2017 (https://www.massschoolbuildings.org/sites/default/files/edit-contentfiles/Programs/School_Survey/2016/MSBA%202016%20Survey%20Report_102417-FINAL.pdf).
37. Callaway B, Sant'Anna PHC. Difference-in-differences with multiple time periods. J Econom 2021;225:200-30.
38. Roth J, Sant'Anna PHC, Bilinski A, Poe J. What's trending in difference-in-differences? A synthesis of the recent econometrics literature. January 13, 2022 (http://arxiv.org/abs/2201.01194). preprint.
39. Wing C, Simon K, Bello-Gomez RA. Designing difference in difference studies: best practices for public health policy research. Annu Rev Public Health 2018; 39:453-69.
40. Michener J. Race, power, and policy: understanding state anti-eviction policies during COVID-19. Policy Soc 2022;41:231-46.
41. Bartlett J. Mass. health leaders call for stepped-up COVID plans for fall and winter. Boston Globe, August 22, 2022 (https://www.bostonglobe.com/2022/08/22/metro/mass-health-leaders-call-stepped-up-covid-plans-fall-winter/).
42. Daniel S. Students across city 'walk-out' to protest lack of Covid safety. Dorchester Reporter, January 20, 2022 (https://www.dotnews.com/2022/students-across-city-walk-out-protest-lack-covid-safety).
43. Cotto R Jr, Woulfin S. Choice with(out) equity? Family decisions of child return to urban schools in pandemic. JFDE 2021;4:42-63.
44. Gilbert LK, Strine TW, Szucs LE, et al. Racial and ethnic differences in parental attitudes and concerns about school reopening during the COVID-19 pandemic — United States, July 2020. MMWR Morb Mortal Wkly Rep 2020;69:1848-52.
45. Skinner-Dorkenoo AL, Sarmal A, Rogbeer KG, André CJ, Patel B, Cha L. Highlighting COVID-19 racial disparities can reduce support for safety precautions among White U.S. residents. Soc Sci Med 2022;301:114951.
46. Parr R. New K–12 parent poll: student mental health, academics pose challenge to Massachusetts schools COVID recovery plans. MassINC Polling Group, May 2, 2022 (https://www.massincpolling.com/the-topline/new-k-12-parent-poll-student-mental-health-academics-pose-challenge-to-massachusetts-schools-covid-recovery-plans).
47. Centers for Disease Control and Prevention. Science brief: community use of masks to control the spread of SARS-CoV-2. December 6, 2021 (https://www.cdc.gov/coronavirus/2019-ncov/science/science-briefs/masking-science-sars-cov2.html).
48. American Academy of Pediatrics, American Speech-Language-Hearing Association. Do masks delay speech and language development? Healthychildren.org, August 6, 2021 (https://web.archive.org/web/20220826213955/https://healthychildren.org/English/health-issues/conditions/COVID-19/Pages/Do-face-masks-interfere-with-language-development.aspx).

ADMINISTRATIVE REPORT: SCHOOL CLIMATE SURVEY

EDUCATION, POLICY AND OPERATIONS COMMITTEE

December 7, 2022

Purpose

To update Trustees on the results of the LDSB School Climate Survey.

Background

A school climate survey is required by the Ministry of Education as part of Policy/Program Memorandum 145 and provides feedback to each school about the degree to which students feel their school supports learning and positive behaviour, perceptions of safety and bullying, and how effectively the school promotes a safe and inclusive environment.

As part of our ongoing efforts to create and maintain safe, inclusive, and accepting schools, the LDSB undertakes a School Climate Survey every 2 years to gather input from students. In November 2021, the district conducted the School Climate Survey in class for students in grades 4-12.

Limestone DSB has been utilizing a school climate survey since 2008. In the past, Limestone utilized the Learning Bar's *Tell-Them-From-Me* (TTFM) tool, later rebranded as the *Our Schools* survey, to engage with students. This data would then be utilized by the school to support school-based initiatives focused on school climate and would be shared with the school community through a safe school team and/or school advisory councils. In 2021 LDSB decided to utilize a new platform, and this was the first iteration of the School Climate Survey that was built and written in-house. We have now started to use the survey tool, Qualtrics, to collect school climate data. Extensive consultation was needed prior to administering the most recent survey. Data from student voice sessions from previous years, and student voice projects, were used to inform the questions we asked, and the wording within each question. Similar to the past with TTFM, students, families, and staff had the opportunity to view the survey online in advance, alongside frequently asked questions that provided rationale for each question. The data team responded to each piece of feedback and included it in the Educator Guide available to staff in advance of the survey.

The School Climate Survey asked students for their opinion on key areas that research has shown to be important in understanding school climate, and that have an impact on student outcomes – with a focus on safety, well-being, relationships, and sense of belonging.

The survey is voluntary, and students could decide whether to complete the survey and/or skip any questions they did not want to answer. The survey was anonymous and confidential, and individual respondents were not identified. In advance, students and staff were offered definitions for more complex terms in multiple formats to support survey administration and students' comfort with the questions. It is made clear to everyone in the community that the results are intended to be utilized for school improvement purposes.

Reporting Tool

As indicated, Limestone began using Qualtrics to collect School Climate data in the most recent collection. Qualtrics is a powerful and intuitive survey software used globally by institutions such as hospitals, post-secondary institutions, and governments. Qualtrics is PHIPA and MFIPPA compliant. The software allows for visualizations and statistical analyses to be conducted within the application, and is highly customizable to meet the needs of different users. Access to data is restricted by role, and managed by members of the Data Team. School administrators can duplicate, filter, and share their data within their school teams and school advisory councils in interactive and engaging ways. It should also be noted that we used Qualtrics for the Student Equity Census.

Results and Status

In the most recent administration of the survey, 9855 students in grades 4 to 12 completed the survey (3330 students in grades 4-6, 2434 students in grades 7-8, and 4091 students in grades 9-12). School Climate data is designed to be used at the school level (rather than at the system level, like the Student Census). Throughout the fall of 2022, school administrators have received training and support in accessing, manipulating, and sharing this data to support their school planning. Administrators can access an online resource via Minds Online on data culture. In addition, administrators have been able to attend group drop-in sessions for support, and have had direct access to data team members' calendars to book appointments for discussion and assistance. Based on their learning and school level priorities, administrators have applied this data in several ways within schools. Additional details will be presented at the meeting.

Next Steps

Schools continue to utilize the data for school improvement purposes. This process requires the sharing of information with school staff, students, and the safe schools' team and/or school advisory council. The next administration of the school climate survey will be launched in the fall of 2023.

Recommendations

That this report be received for information.

Prepared by: Patty Gollogly, Associate Superintendent
Reviewed by: Krishna Burra, Director of Education

ADMINISTRATIVE REPORT: EQAO

EDUCATION, POLICY AND OPERATIONS COMMITTEE

December 7, 2022

Purpose

To provide trustees with a historical overview of the provincial EQAO assessments.

Background (Historical Programs)

In response to recommendations made by the Royal Commission on Learning in February 1995, the EQAO (Education Quality and Accountability Office) was legislated into creation. The first EQAO assessment was delivered in the 1996-1997 school year for all Grade 3 Ontario students. At that time, participating in the assessment comprised of performance tasks related to a particular theme, which required approximately 12 hours of testing over two weeks. Over the years, EQAO added assessments to develop an annually administered assessment program. The Grade 6 Assessment of Reading, Writing and Mathematics (administered at the end of the junior division) was introduced in 1998–1999, and required the same amount of class time as the Grade 3 test; the first Grade 9 Assessment of Mathematics (administered in the first year of secondary school) was conducted in 2000–2001; and the first Ontario Secondary School Literacy Test (OSSLT) (a literacy graduation requirement) was administered in 2002. Each of the secondary school assessments required about five hours of testing over two days.

Between 2005 and 2012, program reviews occurred which led to a reduction in the Primary and Junior testing time by half, to six hours. In addition, the name of the assessment was changed to Assessment of Reading, Writing and Mathematics, Primary Division (1-3) and Junior Division (4-6) in recognition that the entire primary and junior divisions were responsible for students' learning progress. The Grade 9 Assessment of Mathematics was also reduced by half to two hours, and the OSSLT was reduced by half, to two and a half hours, administered on one day.

This assessment model continued until 2018. EQAO undertook efforts to modernize the assessments in 2019. The assessment period was disrupted by the pandemic until field testing of the new

secondary assessments began in the 2020-2021 school year. EQAO was not relaunched in elementary until Spring, 2022.

In addition, during this period of disruption, new Mathematics curriculum was launched at the elementary and secondary level, and destreaming was introduced for Grade 9.

Current Status

Primary and Junior Assessments

In May and June, 2022, schools returned to administering the EQAO assessments. Students learning in person (and students learning remotely who wrote in person) participated in the assessments this past year. The administration of the assessment underwent some very significant, notable changes:

1) The assessment was delivered in an online model that differed from that of the prior paper-based assessments
2) Schools had a six-week time period to complete the assessment
3) The format of the assessment changed. Primary and Junior language components consisted of four sessions, and each session was designed to be completed within 15-35 minutes. The Mathematics component consisted of four stages in which students completed a total of 44 (primary)/48 (junior) questions. The mathematics component was an adaptive model which means that each stage adapts to provide students with questions based on how they performed on the previous stage. This means that students did not necessarily receive the same questions in the same order, at the same time.
4) All students had access to text-to-speech tools as well as the zoom in and zoom out function and an online highlighter.

Secondary Assessments

EQAO provided the Grade 9 Assessment of Mathematics and OSSLT in the form of a field test during the 2020-21 school year. Some grade 9 students participated in the voluntary mathematics assessment; however, some did not due to some technical challenges with the testing platform and the compressed timeline with the octomester schedule used that year. More students participated in the OSSLT field test as it is a graduation requirement and, if students were successful, then it counted toward completion of the graduation requirement. If students were not successful, it did not count.

During the 2021-22 school year, schools administered the new official versions of the EQAO Grade 9 Assessment of Mathematics and the OSSLT. Students learning in person (and students learning remotely who wrote in person) participated in the assessments this past year.

The administration of the assessment was different from past years and adapted based on the field tests from the previous year. There were several significant changes:

1) The assessments were delivered online, not in the form of paper-based assessments

2) Although students continued to write the Grade 9 Assessment of Mathematics as part of their Grade 9 Math course, the administration of the OSSLT changed from a school-wide event on one day with all eligible students writing at the same time to multi-day administration in smaller groups, scheduled and facilitated at each individual school within a larger flexible administration window of several weeks.

3) The Grade 9 Assessment of Mathematics uses a multi-stage computer adaptive testing model that adapts to the individual student's performance as the student progresses through the two sessions containing a total of 54 questions (e.g., drag and drop, drop-down menu, and single- and multiple-selection). The OSSLT also consisted of two sessions containing a total of 33 questions: 31 selected-response questions (e.g., multiple-choice, drag and drop, drop-down menu, checklist) and two open-response questions. Each session in the case of both assessments is designed to be completed in 60 minutes, and students must complete each session in one sitting. The sessions can be attempted one after the other, either back-to-back with a short break, or on two different dates and times. At the end of the two sessions, students are presented with a questionnaire that asks them about their attitudes and perceptions with respect to mathematics or literacy.

4) All students had access to text-to-speech tools as well as the zoom in and zoom out function, an online highlighter and calculator within the assessment platform.

5) Additional time with supervision to complete the assessment was available to all students, if needed.

Next Steps

Individual Student Reports will be sent home with Grade 3 and 6 students, and students who write the Grade 9 Assessment of Mathematics and OSSLT. The Grade 9 Assessment of Mathematics report indicates students' achievement on the assessment, while the OSSLT report provides the outcome deeming them "successful" or "not yet successful."

Administrators have been invited to participate in webinars hosted by EQAO, in order to review how to navigate the new EQAO assessment portal. Schools will use this data as one of many sources in order to determine student strengths and needs that will then drive planning and instruction. System

data will also be analyzed to plan for instructional supports and to differentiate support based on need. Additional information will be presented at the meeting.

Recommendations

That this report be received for information purposes.

Prepared by: Stephanie Sartor, Associate Superintendent, Steve Hedderson, Associate Superintendent, Alison McDonnell, Superintendent, Jessica Silver, Superintendent

Reviewed by: Krishna Burra, Director of Education

ADMINISTRATIVE REPORT: DIRECTOR'S ANNUAL REPORT 2021-2022
EDUCATION, POLICY AND OPERATIONS COMMITTEE

December 7, 2022

Purpose

To provide the Board of Trustees with information on the 2021-2022 Director's Annual Report.

Background

In compliance with the Education Act, the Limestone District School Board's 2021-2022 Director's Annual Report includes information on the Board's strategic goals and progress the Board has made against these goals in the previous year, and actions the Board is taking in those strategic priority areas where goals are not being met.

Current Status

In keeping with the requirements under the Education Act, the Director of Education must report annually on the board's multi-year strategic plan via the Director's Annual Report. In Limestone, the Director provides progress on the Board's strategic goals and actions twice a year, through a mid-year report in the spring and a year-end report in the fall.

The Strategic Plan Year-End Report is provided within the online Director's Annual Report, along with stories from the 2021-2022 school year that highlight some of the initiatives supporting the Board's strategic pillars of Wellness, Innovation, and Collaboration.

Review the report online at https://seeyourselfinlimestone.ca/directors-annual-report/ (effective November 30, 2022). The report will be submitted to the Ministry of Education in compliance with the January 31, 2023, deadline.

Recommendations

That this report be received for information.

Prepared by: Maddie Crothers, Communications Consultant

Reviewed by: Krishna Burra, Director of Education